STUDIES ON PROTON EMISSION FROM MEDIUM, HEAVY AND SUPERHEAVY NUCLEI

Thesis submitted to Bharathidasan University

in partial fulfillment of the requirements for the degree of

Doctor of Philosophy in Physics

Submitted by

SRINIVAS M G

(Ref. No. 06976/Ph. D-K3/Physics/PT/April 2019)

Part time Research Scholar in Physics
St. Joseph's College (Autonomous)
Tiruchirappalli

Under the guidance of

Supervisor

Dr. S. ALFRED CECIL RAJ
Associate Professor of Physics
St. Joseph's College (Autonomous)
Tiruchirappalli – 620 002
Tamilnadu

Co-Supervisor

Dr. H.C. MANJUNATHA
Associate Professor of Physics
Government College for Women
Kolar – 563 101
Karnataka

Department of Physics
St. Joseph's College (Autonomous)
(Affiliated to Bharathidasan University)
Tiruchirappalli-620 002

MAY 2022

Dr. S. Alfred Cecil Raj, M Sc., M.Phil., Ph.D.
Associate Professor
Department of Physics
St. Joseph's College (Autonomous)
Tiruchirappalli- 620 002

CERTIFICATE

This is to certify that the thesis entitled **"STUDIES ON PROTON EMISSION FROM MEDIUM, HEAVY AND SUPERHEAVY NUCLEI"** submitted to the Bharathidasan University, Tiruchirappalli in partial fulfillment of the requirements for the award of the degree of Doctor of Philosophy in Physics, is a bonafide record of the work done by **Srinivas M G** (Ref.No.06976/Ph.D.-K3/ Physics/PT/April 2019) from May 2019 to May 2022 under our supervision and guidance. This is an independent work on the part of the candidate under our guidance.

(Dr. S. Alfred Cecil Raj)
Supervisor

Place : Tiruchirappalli

Date :

Dr. H.C. Manjunatha, M Sc., M.Phil., Ph.D.
Associate Professor
Department of Physics
Govt. College for Women
Kolar - 563 101

CERTIFICATE

This is to certify that the thesis entitled **"STUDIES ON PROTON EMISSION FROM MEDIUM, HEAVY AND SUPERHEAVY NUCLEI"** submitted to the Bharathidasan University, Tiruchirappalli in partial fulfillment of the requirements for the award of the degree of Doctor of Philosophy in Physics, is a bonafide record of the work done by **SRINIVAS M G** (Ref.No.06976/Ph.D.-K3/ Physics/PT/April 2019) from May 2019 to May 2022 under my supervision and guidance. This is an independent work on the part of the candidate under my guidance.

(Dr. H.C. Manjunatha)
Co-Supervisor

Place : Kolar

Date :

DECLARATION

I hereby declare that the thesis entitled **"STUDIES ON PROTON EMISSION FROM MEDIUM, HEAVY AND SUPERHEAVY NUCLEI"** embodies the results of my research work carried out under the guidance and supervision of **Dr. S. Alfred Cecil Raj, M.Sc., M.Phil., Ph.D.** Supervisor, Associate Professor, Department of Physics, St. Joseph's College (Autonomous), Tiruchirappalli **& Dr. H.C. Manjunatha, M.Sc., M.Phil., Ph.D.** Co-Supervisor, Associate Professor, Department of Physics, Govt. College for Women, Kolar. I have not submitted the above thesis to any University for any Degree, Diploma, Fellowship or any other similar titles previously.

(SRINIVAS M G)

Place : Tiruchirappalli

Date :

Department of Physics
St. Joseph's College (Autonomous)
(Affiliated to Bharathidasan University)
Tiruchirappalli-620002

CERTIFICATE OF PLAGIARISM CHECK

1.	Name of the Research Scholar	**SRINIVAS. M. G** **(Ref. No. 06976/Ph. D-K3/Physics/PT/2019)**
2.	Course of study	Ph.D. Physics
3.	Title of the Thesis	**STUDIES ON PROTON EMISSION FROM MEDIUM, HEAVY AND SUPERHEAVY NUCLEI**
4.	Name of the Supervisor	**Dr. S. Alfred Cecil Raj, M.Sc., M.Phil., Ph.D.**
5	Name of the Co-Supervisor	**Dr. H.C. Manjunatha, M.Sc., M.Phil., Ph.D.**
6.	Department/Institution/ Research Centre	Department of Physics St. Joseph's College (Autonomous) Tiruchirapalli -620 002
7.	Acceptable Maximum Limit	10%
8.	Percentage of similarity of content identified	0%
9.	Software Used	Ouriginal
10.	Date of Verification	23.05.2022

Report on plagiarism check, item with % of similarity is attached.

Signature of the Co-Supervisor **Signature of the Supervisor**

Signature of the Candidate

Curiginal

Document Information

Analyzed document	SRINIVAS MG.pdf (D137587765)
Submitted	2022-05-23T07:05:00.0000000
Submitted by	Dorairajan
Submitter email	manavaidorai@gmail.com
Similarity	0%
Analysis address	manavaidorai.stjct@analysis.ouriginal.com

Sources included in the report

W URL: https://www.octa.net/ebusbook/RoutePDF/AmtrakSchedules.pdf
Fetched: 2021-05-24T23:06:32.5300000 3

ACKNOWLEDGEMENT

I would like to express my sincere gratitude to my Supervisor **Dr. S. Alfred Cecil Raj**, Associate Professor, Department of Physics, St. Joseph's College (Autonomous), Tiruchirappalli for his continuous support of my Ph.D. work. As my research Supervisor, the valuable guidance given during the course of this investigation helped me to complete my Ph.D. work successfully. I thank my Supervisor for the extended support and encouragement over these years.

With immense pleasure and a deep sense of gratitude, I wish to express my sincere thanks to my Co-Supervisor **Dr. H.C. Manjunatha,** Associate Professor, Department of Physics, Government College for Women, Kolar, without his motivation, continuous encouragement, and suggestions, this research would not have been successfully completed.

I would like to extend my special thanks to Doctoral Committee Members **Dr. A.J. Clement Lourduraj**, Assistant Professor, St. Joseph's College (Autonomous), Tiruchirappalli, and **Dr. J. Ebenezer**, Assistant Professor Department of Physics, Jamal Mohamed College (Autonomous), Tiruchirappalli, for their valuable and inspiring guidance which enabled me to bring out this research successfully.

I am grateful to **Rev. Dr. M. Arockiasamy Xavier S.J.,** Principal, St. Joseph's College (Autonomous), Tiruchirappalli for providing me with the facilities and many other resources needed for my research. I am extremely grateful to **Dr. N. Ravi,** HOD, and all the faculty members of the Department of Physics, St. Joseph's College (Autonomous), Tiruchirappalli for their consent, encouragement, and support in my research.

My sincere thanks to research colleagues **Dr. L. Seenappa, Dr. K.N. Sridhar, Dr. N. Sowmya, Prof. K.V. Sathish, Prof. G.R. Sridhara, Prof. N. Nagaraja, and Prof. Nagaraja. A.M. Dr. Y.S. Vidya and Prof. B. Chinnappa Reddy fellow researchers Mr. P.S. Damodara Gupta, Mr. N. Manjunath, Mr. R. Munirathnam, and Mr. B. Mahesh and Miss. S. Deepthi** for their cooperation, support, and encouragement during the research work.

My sincere thanks to the Principal, H.O.D, and faculties of the Physics department, Government College for Women, Kolar. I wish to extend my profound sense of gratitude to my family members and friends for all the sacrifices they made during my research and also for providing me with moral support and encouragement whenever required.

SRINIVAS M G

CONTENTS

List of Figures

List of Tables

ABSTRACT

A thorough study on one proton and two proton radioactivity is carried in the atomic number range $3 \leq Z \leq 126$ using well accepted Coulomb and proximity potential model (CPPM), effective liquid drop model(ELDM), generalized liquid drop model(GLDM) and modified generalised liquid drop model(MGLDM) models. The proton decay half-lives produced by these models are compared with the experiments. Predictive power of these models are assessed by evaluation of the mean squared error and it can be concluded that CPPM model produces proton decay half-lives close to experiments. Furthermore, we constructed semi empirical formula for one and two proton decay half-lives by including angular momentum term . The values produced by the present formula is also compared with experiments. Even though, identified one and two proton emitters along with half lives and decay energies are based on theory, further investigations requires comparison of these predicted half-lives with the other decay modes.

The competition between proton decay and other possible decay modes such as alpha decay, beta decay and spontaneous fission in Lanthanide, Actinide and Super heavy region to identify the dominant decay mode is studied. Also identified the proton emitters from medium, heavy and super heavy nuclei ie among Lanthanides, Actinides and super heavy region.

The proton decay half-lives in the lanthanide region (Z=58 to71) have been systematically studied using different proximity functions such as Prox. 13, Prox. 77, MP 77, Ng 80 and Bass 80. Though the experimental values are found to be in good agreement with the proximity function of Ng 80, we have constructed an empirical formula to calculate the half-lives of such proton-emitting lanthanides. The half life values produced by the present formula is compared with that of NG 80.

The half-lives of one-proton emitters in the actinide region (Z=89-103) are theoretically presented using the coulomb and proximity potential method. In the present work the calculated one-proton decay half-live values compare fairly well with the available experimental values. To check the Geiger Nuttal law for proton decay in actinide nuclei, logarithmic proton decay half-lives are plotted against 1/sqrt(Q). The competition of proton decay with different decay modes such as alpha decay and spontaneous fission are also studied. The one proton emitters in the actinide region are identified in the unexplored isotopes of actinide region which is not specified in the nuclear chart.

The proton radioactivity of heavy nuclei of atomic number range $72 < Z < 88$ is studied. The energy released during the proton decay (Q_P) and half-lives of proton decay are evaluated for heavy nuclei. The competition between different decay modes is studied by comparing the proton decay half lives with that of other decay modes such as alpha decay, β^+ and β^- decay. To check the Geiger-Nuttal law for proton decay, the logarithmic proton decay half-lives are plotted against $1/\sqrt{Q}$. The possible proton emitters of heavy nuclei corresponding in the atomic number range $72 < Z < 88$ are also highlighted.

The proton decay in almost all super heavy nuclei with atomic number Z=104-126 is studied by theoretically calculating the energy released during the proton decay (Q_P), penetration factor (P), normalisation factor (F) and half lives of proton decay, out of which proton decay is possible in few super heavy nuclei. The study of competition of proton decay with different decay modes of super heavy nuclei such as alpha decay and spontaneous fission reveals that proton decay is not dominant decay mode in the super heavy nuclei region. This means super heavy nuclei is stable against the proton decay.

The proton radioactivity half-lives in the atomic number range $53 \leq Z \leq 83$ is studied using macroscopic models such as Coulomb and Proximity potential model, effective liquid drop model (ELDM), Generalised liquid drop model (GLDM), Universal decay law for proton emission (UDLP), Gammow-like model (GLM) and Unified fission model (UFM). The proton decay half-lives produced by the macroscopic models are compared with that of microscopic models such as DDM3Y, JLM, M3Y+EX, R3Y+EX, SLy4, SRG, Skc and SkD. After detail analysis, it is found that among macroscopic models, UDLP and ELDM produces proton decay half-lives close to experiments. Furthermore, among microscopic models, DDM3Y produces proton decay half-lives close to the experiments. To study the proton decay process, microscopic approach is more appropriate than the macroscopic approach. We have also investigated the correct mass excess data which can be used in proton decay studies. Thus, Both UDLP and ELDM macroscopic models and DDM3Y microscopic model can be effectively used in the prediction of half-lives of unexplored proton emitters.

CHAPTER 1

Introduction

1.1 Introduction

Proton emission is a type of radioactive decay that occurs when a proton is released from a nucleus. After a beta decay, Proton emission can happen in a nucleus from highly excited states, known as beta-delayed proton emission, or from the ground state of highly proton-rich nuclei, which is comparable to alpha decay. During proton emission, a proton is emitted from the nucleus of an atom. An atom converts from one element to another when it loses a proton during proton emission. An atom of nitrogen (containing 7 protons) becomes an atom of carbon after undergoing proton emission (with 6 protons). The phenomenon of proton radioactivity has gained attention as an important tool for understanding the nuclear structure of nuclides far from the stability line[1]. Nuclear structure information such as shell structure and interaction among bound and unbound nuclear states may be extracted using proton radioactivity.[2]. Beyond beta stability, proton emission from the nuclear ground state is intended to yield information on nuclear masses and structure.[3].

1.2 Proton emission

Proton emission is one method through which unstable atoms might become more stable. A proton is simply released from a nucleus containing surplus protons in proton decay, a rare kind of

radioactive decay. Proton emission happens in the most proton-rich nuclides and after a positive beta decay from a nucleus's high-lying excited states. In proton decay, quantum tunnelling is also involved. Before a proton can be released, it must first pass through a potential barrier. The proton separation energy must be negative for a proton to exit a nucleus; as a result, the unbound proton tunnels out of the nucleus in a finite time. Some nuclei, such as ^{45}Fe, decay by double proton emission. When a nucleus undergoes proton decay , the atomic number and mass number of the daughter nucleus change by one, and she becomes a new element. The neutron drip line is distinguished by its location above the nuclei that may decay in this manner. In naturally occurring isotopes, proton emission is not seen. Nuclear reactions that use particle accelerators can produce proton radioactive isotopes. Protons are not produced by naturally occurring isotopes. The proton emission half-lives of spherical proton emitters were investigated using the unified fission model (UFM) in conjunction with the phenomenological attack frequency[4].

1.3 Theoretical studies

Nuclear structure and nuclear reaction research in unusual nuclei is now focusing on proton emission investigations. Theoretical ways for studying the characteristics of such nuclei utilising proton emission are discussed [5]. Delion et al., predicted a simple formula in proton decay processes that relates logarithmic half-life, modified by the centrifugal barrier along with the Coulomb parameter. [6]. Buck et al., investigated proton emission from heavy nuclei's ground states, employing a model of charged particle emission that has previously been shown to accurately describe unimpeded s-wave alpha and exotic decays in heavy nuclei [7]. Proton systematics were studied by Delion and Dumitrescu in terms of barrier penetration and formation likelihood. To do this, they used a parabolic dependency characterising the nuclear portion and a pure Coulomb potential to simulate the true proton-core interaction [8]. Sreeja and Balasubramaniam presented an em-

pirical formula for two-proton decay half-lives based on their publication of an empirical method for determining the logarithmic half-lives of one-proton emitters. For the two proton emitters, a four-parameter formula as a function of rotational momentum is provided and the findings of the effective liquid drop model were used to fit the formula's parameters (ELDM) [9].

Zdeb et al., explained proton emission using a model with basic phenomenological formalism, which is based on the Gamow theory for alpha decay and is expanded by incorporating the centrifugal factor [10]. Karny et al., used a unique approach of digital processing of overlapping recoil implantation and decay data to identify the fine structure in proton emission from ^{145}Tm [11]. Axelsson et al., investigated the two-proton emission in the decay of ^{31}Ar using the energy and angular distributions of the two protons [12]. Using an empirical method, Sreeja and Balasubramaniam revealed half-life estimates for one proton transition from ground state to isomeric states of 44 proton emitters [13]. Goncalves et al., calculated the half-lives for two-proton radioactivity of emitter nuclides using ELDM that has been successfully used to alpha decay, one-proton radioactivity, and cold fission processes. They used this method to calculate half-lives for many 2p-emitted nuclei and compared their findings to predictions from other models as well as existing data in the literature, focusing on the parent nuclei ^{16}Ne, ^{19}Mg, ^{45}Fe, ^{48}Ni, ^{54}Zn, and ^{67}Kr [14].

Ferreira et al., investigated the relationship between the half-lives for proton emission from deformed nuclei and the various single particle potentials that reflect typical nuclear structural attributes that have been published in the literature [15]. Using the effective liquid drop model of heavy-particle nuclei decay, Guzman et al., determined half-lives for proton emission from proton-rich nuclei [16]. Zhang Hong-Fei et al., computed the proton radioactivity half-lives of spherical proton emitters and suggested two formulae for the proton decay half-life of spherical proton emitters based on the experimental data available, and were able to successfully recreate the experimental half-lives [17].

Dong et al., [18] investigated theoretically the proton radioactivity half-lives of spherical proton emitters by determining the potential barriers preventing protons from being emitted in the quasi molecular shape path within a generalised liquid drop model. . Various theoretical methods to proton emission from spherical nuclei were examined by Sven Aberg et al., who derived decay widths that were found to be qualitatively insensitive to the parameters of the proton-nucleus potential [19]. Delion et al., explored proton decay from triaxially deformed nuclei ^{161}Re and ^{185}Bi by determining the decay width and angular distribution of the decaying particle, as well as their relationship to the triaxial deformation parameters [20].

Starting from a mean field HF potential and employing the Skyrme interaction, J. S. AlKhalili et al., outlined a two potential approach to one proton emission for the situation of spherical nuclei, resulting to an expanded 3D TPA model [21]. Bugrov and Kadmenskii derived an equation for the proton decay width of a deformed nucleus based on proton radioactivity theory, with many-particle effects taken into account [22]. Using the multiparticle theory of proton radioactivity, Kadmensky and Bugrov estimated the half-lives of ^{147}Tm, ^{147m}Tm, ^{150}Lu, and ^{151}Lu nuclei with regard to proton decay. In these computations, the deformation of decaying nuclei examined in the spherical model was taken into consideration [23]. Maglione et al.,[24] predicted precisely the proton decay half-lives $T_{1/2}$ from the nuclei $^{109}_{53}$I, $^{131}_{63}$Eu, and $^{141}_{67}$Ho assuming that the released proton travels in a distorted single particle Nilsson level.Delsanto et al.,[25] evaluated the proton separation energies, half-lives, and excitation energies of ^{69}Kr and ^{68}Se from beta-delayed proton emission.

Alavi et al., [26] used the WKB Method to calculate the proton radioactivity half-lives of 45 proton emitters and noticed a decline in the values of estimated half-lives employing the orientation angle dependent formalism . Baye et al.,[27] calculated the decay probability per second for the one-neutron halo nuclei ^{11}Be, ^{19}C, and ^{31}Ne. Feix and Hilf [28] computed the Decay widths of

nuclear proton emission from neutron-deficient odd-Z nuclei, $51 \leq Z \leq 71$, by the quasi-stationary model. Giusti et al., [29] developed the theoretical frame work of emission of two protons in electron induced reactions. Arumugam et al., [30] investigated the proton emission, gamma deformation, and the spin of the isomeric state of ^{141}Ho and revealed the proton deformations and other structural properties of exotic nuclei beyond the proton drip-line. Duarte et al., [31] used the Effective Liquid Drop Model (ELDM) to investigate the half-lives for proton emission, alpha decay, cluster radioactivity, and cold fission processes employing a combination of variable mass asymmetry shape description for mass transfer with Werner-Wheeler's inertia coefficient. Ferreira et al., [32] investigated proton radioactivity from spherical nuclei by using a self-consistent computation . Maglione and Ferreira computed precisely the half-lives of proton emission from the drip line nucleus ^{131}Eu to the first excited 2 + state of the daughter nucleus ^{130}Sm [33]. Santhosh and Indu Sukumaran used the Coulomb and proximity potential model for deformed nuclei (CPPMDN) to predict half-lives for proton emitters with $Z>50$ in the ground state and isomeric state [34].

Blank and Borge discussed certain features of beta-delayed decay modes, one- and two-proton radioactivity, and the experimental procedures to get a deeper understanding of the atomic nucleus' organisation [35]. Manjunatha et al., [36] proposed a new empirical formula for the mass excess of heavy and superheavy nuclei in the Z=96–129 range. In non-minimal SUSY SU (5) GUTs, Borut Bajc et al., computed the high and low scale threshold corrections to dimension-six proton decay operators [37]. Mukha et al., [38] discovered one and two-proton radioactivity in ^{94}Ag isomers with more than 21 high-spin isomers. Rykaczewski examined experimental data on proton-radioactive nuclei ^{131}Eu, ^{145}Tm, and ^{146}Tm, which included the finding of fine structure in proton emission and analyses of excited states in proton-emitting nuclei [39]. Denisov and Khudenko developed set of relations for evaluating the half-lives of alpha emitters [40].

Chang Xu et al., [41] evaluated the α-decay half-lives for the nuclei range Z$\geq$ 90 using the distorted version of the density-dependent cluster model. Yibin Qian et al., [42] evaluated proton decay half-lives using the modified two-potential method. Dongdong Ni et al., [43] developed, with some approximations, a generic formula of half-lives and decay energies for decay and cluster radioactivity directly determined from the WKB barrier penetration probability. Delion approximated the preformation amplitude for heavy cluster decays till ^{14}C emission by offering numerical findings for^{14}C emission and outlining the fission-like theory of emission processes based on the Two Center Shell Model[44]. Horia Hulubei et al., [45] determined the proton emission half-lives for Z $\geq$51 nuclei using a simple analytical model based on the WKB approximation for the barrier penetration probability, which incorporates centrifugal and overlapping effects in addition to electrostatic repulsion. Gerald Gilbert investigated the possibility of proton decay in the presence of topology-changing field configurations in euclidean quantum gravity[46]. Uusitalo et al., [47] discovered proton radioactivity from the closed neutron shell nucleus ^{155}Ta utilising the p4n fusion evaporation channel and a ^{58}Ni beam on a ^{102}Pd target.

Livingston et al., [48]discovered proton emission from the new isotope ^{146}Tm and identified two transitions at energies of 11195 keV and 11895 keV, corresponding to Q-values of 11275 keV and 11975 keV, respectively. Sonzogni et al., [49] detected fine structure in the ground-state proton radioactive decay of severely deformed ^{131}Eu. Dehghani and Alavi present two empirical formulae for proton decay half-lives which included nuclear deformation. [50]. On the basis of the real-energy continuum shell model, Rotureau et al., [51] developed a theory of two-proton radioactivity. Bogdanov et al., [52] investigated proton decay of the ground states (PDGS) of the nuclei ^{121}Pr and ^{117}La within the context of the many-particle proton radioactivity theory. Honkanen et al., [53] discovered beta-delayed emission of two protons in the decay of ^{26}P and estimated a two-proton summed energy group of 4.914 MeV to the decay to the ^{24}Mg ground

state after the superallowed beta-decay of ^{26}P. Fengzhu Xing et al.,[54] extended the unified fission model to explore two-proton radioactivity of nuclei's ground states, as well as two-proton radioactivity of excited states of ^{14}O, $^{17,18}Ne$, ^{22}Mg, ^{29}S, and ^{94}Ag. Balasubramanyamn and Arunachalam Calculated the half-lives of different spherical proton emitters using unified fission model [55].Oudih et al., [56]investigated the proton decay of spherical proton emitters from the ground and isomeric states in the WKB approximation by using the unified fission model with a Modified-Woods–Saxon (MWS) nuclear potential. In grand unified theories Rubakov detailed the theoretical studies of proton decay monopole catalysis. [57].

1.4 Experimental studies

In an experiment conducted at ISAC-TRIUMF, Ayyad et al., [58] reported delayed proton decay in ^{11}Be by directly quantifying the released protons and their energy distribution for the first time with the prototype Active Target Time Projection Chamber. Delion et al., [59]investigated the two-proton decay process using a basic technique based on scattering theory, assuming that the decaying nucleus is in a pairing state and that the two-particle wave function on the nuclear surface corresponds to the two protons travelling in time-reversed states. Jinter et al., [60] investigated the Proton emission from ^{150}Lu using Recoil Mass Spectrometer at Holifield Radioactive Ion Beam Facility. M.G. Procter et al., [61] used gamma-ray coincidence techniques to investigate proton emission from an oblate ^{151}Lu nucleus and determined the lifetime of the first excited state above the proton-emitting ground state using the recoil-distance Doppler-shift approach coupled with recoil-decay tagging. C.R.Bain et al., [62] investigated two proton emission by bombarding a radioactive beam of ^{13}N ions with a (CH2)n target to fill a narrow resonance in ^{14}O at 7.77 MeV.

^{54}Zn was discovered for the first time, and its decay via two-proton emission was seen for the first time.In an experiment at GANIL's SISSI/LISE3 facility, Blank et al., [63] made the first de-

tection of the nucleus ^{54}Zn in the quasi-fragmentation of a ^{58}Ni beam at 74.5 MeV/nucleon in a nat Ni target. Lund et al., [64] studied to the beta-delayed proton emission from ^{20}Mg at ISOLDE, CERN. Particle radioactivity was discovered in the closed neutron shell nucleus ^{155}Ta by Uusitalo et al., [65] by utilising a ^{58}Ni beam on a ^{102}Pd target in the p4n fusion evaporation channel. Canchel et al., [66]in a GANIL LISE3 experiment, produced radioactive ^{27}S isotopes by projectile fragmentation of a 95 AMeV ^{36}Ar primary beam and measured the half life and main decay branches of the isotope of interest by implanting in a silicon-detector telescope afterselection with the LISE3 separator.

Giovinazzo et al., [67] explored the decay of the proton drip line nucleus ^{45}Fe in an experiment at GANIL's SISSI-LISE3 facility. Bertram Blank and Marek loszajczak looked into the experimental findings that led to the discovery of two-proton radioactivity, as well as experimental investigations of two-proton emission from excitedstates inhabited by nuclear decay or inelastic processes [68]. Chong Qi et al., [69] described the systematics of proton decay half-lives and found that the proton formation probability is a relevant parameter for determining the mother nucleus's deformation property.

Raciti et al., [70] examined the decay of ^{18}Ne excited states via the simultaneous emission of two protons. ^{18}Ne nuclei, produced at the FRIBs facility of the Laboratori Nazionali del Sud (LNS). Coniglione et al., [71] explored the generation mechanism of high energetic protons in heavy ion reactions close to the Fermi energy in an experiment done with the MEDEA detector. Ludewigt et al., [72] investigated proton emission in α-induced reactions at 43 Mev nucleon. At energies E = 100 MeV and 172 MeV, inclusive proton spectra and proton-proton correlations were observed from + ^{58}Ni and + ^{197}Au reactions, respectively. Riisager et al., [73] experimentally studied beta -delayed proton emission from ^{11}Be nucleus using accelerator mass spectrometry on a sample taken at CERN's ISOLDE facility (AMS). Shi et al., [74] explored the β -delayed

two-proton (β 2 p) decay of ^{27}S utilising a cutting-edge silicon array and Clover-type HPGe detectors. Robinson et al., [75] by blasting a ^{96}Rn target with a 297-MeV ^{58}Ni beam, ^{150}Lu was created through the 1p3n fusion-evaporation channel, and evaporation residues were examined using the fragment mass analyzer at Argonne National Laboratory. Batchelder et al., [76] witnessed the proton emission from ^{145}Tm for the first time through the ^{92}Mo (^{58}Ni, p 4 n) reaction using Holifield Radioactive Ion Beam Facility Recoil Mass Spectrometer. Lis et al.,[77] explored the decay of ^{31}Ar, which was created by fragmentation of a ^{36}Ar beam at 880 MeV/nucleon.

Faux et al., [78] determined the half-life of ^{52}Ni and the energies of β-delayed protons released during the decay by fragmenting a ^{58}Ni beam at 68 MeV/nucleon on a nickel target using the LISE spectrometer at GANIL. Cable et al., [79] discovered beta-delayed two-proton radioactivity for the two nuclei ^{22}Al and ^{26}P, revealing that the major two-proton emission mechanism is a sequential process from Proton proton coincidence studies done at small and large angles. Sun Li-Jie et al., [80] examined beta-delayed proton decay mode by conducting a beta-delayed proton emission experiment using $^{36,37}Ca$ under a high-intensity continuous-beam mode provided by the Radioactive Ion Beam Line in Lanzhou.

Page et al., [81] detected proton radioactivity in ^{160}Re and ^{156}Ta by mass separating in flight evaporation residues from fusion reactions of 300 MeV ^{58}Ni ions with ^{106}Cd targets and implanting them onto a double-sided silicon strip detector. Ascher et al., [82] observed the two protons released in the decay of ^{54}Zn for the first time in a temporal projection chamber. Pomorski et al., [83] investigated the decay of the neutron-deficient ^{48}Ni using an image time-projection chamber that enabled the tracking of charged particle tracks. Azhari et al., [84] examined the proton-unbound nucleus ^{11}N using kinematic reconstruction of the released proton in conjunction with the remnant ^{10}C daughter nucleus.

The nuclei with decay energy greater than zero,that are above the drip line are proton unstable

and also they are proton rich nuclei [85]. Jackson et al., [86, 87] investigated proton radioactivity from the isomeric state of ^{53}Co. Till date, different nuclear decay modes such as α, $\beta^{\pm}$, electron capture, spontaneous fission, proton radioactivity, cluster radioactivity and many more have been identified both theoretically and experimentally. From past two decades an attention has also given for heavy particle radioactivity [88–90]. The two proton radioactivity was experimentally confirmed from the proton rich nuclei ^{48}Fe [91, 92].

Both microscopic approach and macroscopic studies have given insight into theoretical prediction of one and two proton-decay. The microscopic approaches such as two-potential approach with Skyrme-Hartree-Fock [93], DDM3Y and JLM [94, 95] real-energy continuum shell model (SMEC) [51], M3Y effective interaction [96], R3Y nucleon-nucleus interaction potential [97], Skyrme-Sly4 interaction [98], Hartree-Fock-Bogoliubov [99], similarity renormalization group (SRG) [100] and Skyrme force of SkC and SkD [93]. The skyrme interaction is an important phenomenon which explains the ground state properties of nuclei.

Further, the macroscopic models such as preformation cluster model by Gupta et al., [101], unified fission model [102], effective liquid drop model [14, 103], generalised liquid drop model [2], Coulomb and proximity potential model [104–108], Geiger Nuttal law [109] for proton decay and within WKB penetration probability [101, 110, 111] the proton half-lives were investigated. Routray et al., [112, 113] investigated proton decay half-lives in ^{113}Cs to ^{185}Bi nuclei. Chen et al., [109] proposed two-parameter formula for proton radioactivity using Geiger–Nuttall law. Using various proximity potentials earlier researchers [114] have studied proton decay within generalised liquid drop model.

The proton radioactivity has been experimentally observed in the fusion reaction of $^{58}Ni +^{96} Ru \rightarrow^{154} Hf$ [115]. Earlier researchers [116] have studied the formation probability in one proton radioactivity. Two proton nuclei ^{113}Cs and ^{109}I [117] is experimentally produced by bombarding

^{58}Ni and ^{54}Fe on ^{58}Ni beams. Mukha et al., [118] experimentally investigated one proton decay from the 21^{+} isomer state of ^{94}Ag in to ^{93}Pd nuclei. Later Aggarwal [119] theoretically proved the proton radioactivity of ^{94}Ag using macroscopic–microscopic approach which is in good agreement with the experimental value of Mukha et al., [118]. Further, Roeckl et al., [120] studied one and two proton radioactivity in ^{94}Ag. The proton radioactivity half-life of 17 seconds were experimentally observed when ^{53m}Co decays to ^{52}Fe [121]. Proton decay half-lives are investigated both in ground and isomeric states of the nuclei [122]. Poli et al., [123] experimentally measured proton and alpha decay half-lives from ^{185}Bi. Later, using self-consistent relativistic density functionals [32] proton radioactivity of odd-odd nuclei were studied. Within covariant density functional (CDF) theory [124, 125], the properties of proton emitters were investigated. Previous works [126–129] shows investigation of proton decay in actinides.

The present work investigates the half-lives of proton radioactivity using various macroscopic models such as Coulomb and proximity potential model (CPPM), effective liquid drop model (ELDM), generalised liquid drop model (GLDM), universal decay law for proton emission, Gammow-like model and unified fission model for proton radioactivity. The values produced using macroscopic models is compared with the different microscopic models available in literature.

The study of the radioactive decay is crucial importance for the further development of nuclear physics. Proton radioactivity studies are becoming important tool for nuclear structure [130]. Two-proton radioactivity is the emission of a pair of protons from a nuclear ground state. Giovinazzo et al., [92] studied the two proton radioactivity of ^{45}Fe and fragment-implantation events that correlate with radioactive decay events. Anguiano et al., [131] investigated the photo-emission of two protons from ^{12}C, ^{16}O and ^{40}Ca nuclei for the study of short range correlations. Raciti et al., [132] measured the emission of two protons from the decay of ^{18}Ne. Goldanskii [133] experimentally proposed one and two proton radioactivity for both odd and even atomic number. Mukha et al.,

[38, 134] observed one and two-proton radioactivity of more than 21 high-spin isomers in ^{94}Ag. Previous workers [135, 136] experimentally studied one and two proton radioactivity of ^{45}Fe and ^{54}Zn. The two-proton radioactivity was experimentally observed in ^{45}Fe [67, 91] and later in ^{19}Mg [137, 138], ^{48}Ni [83] and ^{54}Zn [63]. Davids et al., [139] identified the proton radioactivity from highly deformed nuclei(^{141}Ho and ^{131}Eu). Goigoux et al., [140] observed two proton emission for ^{67}Kr. The two proton radioactivity was experimentally observed [91, 115, 141, 142] in ^{58}Fe to ^{151}Lu.

Theoretically, many models have been used to predict one and two proton decay. Giusti et al.,[143] studied the two proton emission in electron induced reactions within the theoretical framework. Furthermore, the two proton decay was estimated in the region $18 < A < 68$ [144] by the quantum mechanical tunneling mechanism through a potential barrier. In addition, ELDM was also used to evaluate two proton radioactivity of nuclei of mass number $A < 70$ [145]. The proton decay process can be treated as quantum tunneling process which passes through a potential barrier like an α-decay, is evaluated using Wentzel–Kramers–Brillouin approximation method. Theoretical models of proton radioactivity from spherical nuclei can predict the systematics of proton decay and spectroscopic factors.

Dossat et al., [146] studied the decay of the two proton rich nuclei ^{45}Fe and ^{48}Ni. Cui [147] first extended the GLDM to study the two proton radioactivity half lives of the ground state of nuclei. Grigorenko et al., [148] studied the two proton radioactivity using the three body model. The investigation of proton radioactivity was carried out using several models such as density-dependent M3Y effective interaction [94, 149, 150], unified fission model [55, 102] , the Jeukenne, Lejeune and Mahaux (JLM) interaction [94], the cluster model [17], the CPPM for deformed nuclei [34], the deformed density-dependent model [151, 152], the Gamow-like model [10], the covariant density functional theory [153], the analytic formula [154], the distorted-wave Born ap-

proximation [19], the two-potential approach [19], and so on [7, 24, 155].

Most of the previous studies were focused on range of nuclei $22 \leq Z \leq 30$ [156–159]. Earlier researchers [107, 126, 127] have studied the proton radioactivity in the actinide and pre-actinide region. Spherical proton emitters were studied using the GLDM [18], one and two proton emitters [160] were identified in the Lanthanides and pre-actinide region. Half-lives in the heavy and superheavy region were evaluated using different theoretical models such as Modified Generalised Liquid Drop Model, Coulomb and Proximity Potential Model, and Effective Liquid Drop Model [110, 111, 161–169].

Royer et al., [170, 171] presented the GLDM which includes quasi molecular shapes and nuclear proximity energy. By adding different proximity potentials, pre-formation factor with isospin parameter, size of cluster and daughter nucleus and the modified pre-formation factor GLDM is modified and is referred as MGLDM [172–174].Goncalves and Duarte [175] introduced ELDM, a super asymmetric fission model, to analyse α-decay, proton emission, cluster radioactivity, and cold fission in a single framework. ELDM is validated by many experiments [31, 175–180].
Two proton radioactivity arises for element isotopes with substantial negative proton separation energies. Because these protons must tunnel through a combined Coulomb and orbital angular momentum barrier, their half-lives are very sensitive to proton energy and angular momentum.Proton emitters have shorter half-lives because they are far from stability. As a result, an effort was undertaken to investigate one and two proton radioactivity in the atomic number range $3 \leq Z \leq 126$ using well-known CPPM, ELDM, and MGLDM models. Furthermore, semi empirical formula was constructed for one and two proton decay half-lives.

Light and medium nuclei mostly show proton decay whereas lanthanides show the proton and β decay. Furthermore, heavy nuclei (Z = 72 - 88) show β^+ and β^- decay, actinides (Z= 89 - 103) and superheavy nuclei or transactinides decay through α particles. It is also predicted that

nuclei with Z $\geq$126 may undergo cluster decay / exotic decay [181]. The competition between decay modes depends sensitively on the Coulomb and centrifugal barriers. Proton radioactivity studies provide a unique insight into the structure of nuclei beyond the drip line limit [39]. Proton emission from long-lived excited states has been investigated since the 1970's in ^{53m}Co [86]. Subsequent discoveries of proton decay from ^{151}Lu [115], ^{113}Cs, ^{109}I [117] and eventually other exotic heavy isotopes like ^{117}La [182] and ^{135}Tb additional measurements.

The Lanthanide series includes 14 elements having atomic numbers from 58 to 71. The lanthanides and their analogs find importance in radiotherapy due to their physical properties physical half-life, type(s) of decay emission(s), energy of the emission, cost and availability, and specific activity [183]. Few studies have been devoted towards different decay modes of actinides, lanthanides and transactinides [107, 184–188]. Sridhara et al., [163] studied the cluster radioactivity in actinide nuclei. Quadrelli et al., [189] analyzed the quadratic decay observed for Ln(III) ionic radii and calculated bond distances and lanthanide atomic orbital expectation values. Nitscke et al., [190] identified a total of 24 new β - delayed proton precursors and several new decay branches in the region of 56 $<$ Z $<$ 72 and N $<$ 82 using OASIS online mass separator facility. Davids et al., [139] identified proton decay from ^{141}Ho and ^{131}Eu. Sowmya et al., [110] studied the competition between different decay modes such as binary, ternary, cluster radioactivity and alpha decay of Darmstadtium. Although different decay modes are explained for few series of actinide and the heavy elements, the lanthanide series yet to be explored. The presence of high coulomb barrier for heavy nuclei (Z $>$ 52), reduces the proton barrier penetration probability to the extent that proton decay taking place from the ground states of nuclei have measurable long half lives [107]. There are various methods to investigate the proton radioactivity such as the density – dependent M3Y effective interaction [94, 152], the Jeukenne-Lejeune-Mahaux (JLM) interaction [94], the unified fission model [55, 102], the generalized liquid drop model [18], the cluster

model [17], the deformed density model [10], the coulomb and proximity potential model [34], the covariant density functional theory [153] and so on. These nuclear proximity potentials provide the phenomenological potentials for nuclear reaction and structure including nuclear decay [191]. Santhosh et al., [34] explained the half life predictions for the proton emitters with Z $>$ 50 in the ground state and isomeric state using Coulomb and proximity potential model for the deformed nuclei. Dong et al., [192] studied the $\alpha-$decay using double-folding potentials from chiral effective field theory for the nuclei ^{104}Te.

The coulomb and nuclear proximity potential provides another simple and practical formalism to estimate the strength of the nuclear interactions during collision of heavy-ions. When two surfaces are approaching each other, approximately at a distance of 2–3 fm, an additional force due to the proximity of surfaces will appear which is called proximity potential [193]. There are adjustable parameters in various parts of the proximity formalism such as the radius parameter R, the surface energy coefficient and the universal function which lead to introduce different versions of the proximity potentials. Santhosh et al., [194] studied the Coulomb and proximity potential as interacting barrier for post-scission region and calculated half – life time for different modes of exotic decay treating parent and fragments as spheres and these values are compared with experimental data. Dutta et al., [195] performed a detailed comparative study of fusion barriers for asymmetric colliding nuclei using different versions of phenomenological proximity potential as well as other parameterizations within the proximity concept. From the detailed analysis of literature, it is found that, there is no systematic study of proton decay in the lanthanide region. The aim of the study is to predict the unexplored proton emitters in the lanthanide region.

Proton decay is rare type of decay which can exist in following ways, in high lying exited states of a nucleus after beta-decay or from ground state of very rich proton nuclei or nucleus with odd atomic numbers beyond proton drip line [196]. Buck et al., [7] investigated proton emission from

the ground state of heavy nuclei using charged particle emission model. Proton decay, half-life and branching ratio measurements aid in determining the angular momentum ℓ [197–199]. The spherical proton decay half-lives are studied using two potential approach, quasi-classical methods and distorted wave Born approximation (DWBA) [19]. Guzman et al., [16] investigated proton radioactivity in proton rich nuclei in heavy nuclei using effective liquid drop model(ELDM). Using CPPM (Coulomb and proximity model), Santhosh et al., [34] predicted proton decay half-lives in heavy nuclei $Z > 50$.

Under experimental approach Belli et al., [200] observed one proton decay and β^+-decay in Dysprosium using γ detector. Schardt et al., [201] studied beta delayed proton emission in Dysprosium. A microscopical variational method is developed resulting in a Hamiltonian for the non-adiabatical particle rotator model, where numerical calculations have been performed for the positive parity bands in the ^{157,159,161}Dy [202]. The ft-values for the Gamov-Teller β^+ decay of ^{148,146}Dy is calculated in the random phase approximation taking into account of interactions in particle-hole and particle-particle channels [203]. β^+-decay strength functions have been measured for the neutron-deficient isotopes of ^{149,151}Dy using self-consistent HF+RPA approach with Skyrme forces [204].

Earlier studies have shown detail analysis of proton radioactivity [107, 126, 127, 205]. Nuclear structural information can be extracted via proton radioactivity Dong et al., [18]. Many theoretical studies shows inclusion of different proximity potential and different theoretical models to evaluate half-lives [90, 111, 161, 173, 206, 207]. As a result of the thorough literature review, it is obvious that the sensitivity of experimental and theoretical approaches to proton decay in Dysprosium need improvement. As a result, we were inspired to investigate several decay modes in the current study such as β-decay, proton decay and α-decay half-lives of isotopes of Dysprosium in the mass number range $133 \leq A \leq 180$ and to determine the various decay modes of Dysprosium

nuclei.

In the energy domain of radioactivity, proton can be considered as a point charge having highest probability of being present in the parent nucleus. Gonclaves et al., [14] studied the two-proton radioactivity of nuclei of mass number $A < 70$ using the effective liquid drop model. Delion et al., [5] reviewed the theories of proton emission to analyse the properties of nuclear matter. Maglione et al., [24] analysed the proton emission half-lives from the deformed nuclei ^{109}I, ^{131}Eu and ^{141}Ho. Delsanto et al., [25] investigated the β-delayed proton emission of ^{69}Kr and ^{68}Se and extracted their proton separation energies, half-lives and excitation energies. Alavi et al., [26] calculated the proton radioactivity half-lives of 45 proton emitters by WKB Method and observed the decrease in values of calculated half-lives using the orientation angle dependent formalism. Raciti et al., [70] measured the emission of two protons from the decay of ^{18}Ne. Baye et al., [27] evaluated the decay probability per second for ^{11}Be, ^{19}C and ^{31}Ne one-neutron halo nuclei. Feix et al., [28] computed the decay widths of nuclear proton emission for Z=51 to 71 nuclei using Droplet Model. Anguiano et al., [208] investigated the photo-emission of two protons from the ^{12}C, ^{16}O and ^{40}Ca nuclei for the study of short range correlations. Coniglione et al., [71] explored high energy proton emission in heavy ion reactions close to the Fermi energy by investigating the production mechanism of energetic protons in an experiment performed with the MEDEA detector. Giusti et al., [29] developed the theoretical frame work of emission of two protons in electron induced reactions.

Ludewigt et al.,[72] studied the proton emission in α-induced reactions at 43 MeV nucleon. Guzman et al.,[16] analysed the proton emission from proton-rich nuclei and calculated the half-lives using the effective liquid drop model. Delion et al.,[6] proposed semi empirical formula for logarithmic half-lives of proton decay. Dong et al., [18] theoretically calculated the half-lives of proton emitters using generalized liquid drop model (GLDM) and WKB approximation. Maglione

et al., [209] studied the proton emission from ^{125}Pm and the behaviour of the half-lives were discussed as a function of deformation, spin of the decaying state, and energy of the emitted protons. Arumugam et al., [30] investigated the proton emission, gamma deformation, and the spin of the isomeric state of ^{141}Ho and revealed that proton deformations and other structural properties of exotic nuclei beyond the proton drip-line. Duarte et al., [31] explored the half-lives for proton emission, alpha decay, cluster radioactivity, and cold fission processes theoretically. Ferreira et al., [32] planned to study the proton radioactivity from spherical nuclei theoretically based on relativistic density functional derived from meson exchange and point coupling models. Ginter et al., [60] studied the proton emission from ^{150}Lu and new proton emitting state was observed. Delion et al., [20] investigated proton decay from tri-axially deformed nuclei ^{161}Re and ^{185}Bi and studied the dependence of angular distribution of decaying particle on triaxial deformation parameters. Earlier workers [15, 33, 67] studied one and two proton decay half-lives of ^{131}Eu, ^{45}Fe and also studied proton emission from the deformed nuclei. In the literature, different theortical approaches are availble [105–108, 161, 163–165, 169, 207, 210–215] to study different decay modes including proton decay.

Proton decay is one of the key predictions of various grand unified theories (GUTS) proposed in the 1970s, another major one being the existence of magnetic monopoles. Both concepts have been the focus of major experimental physics efforts since the early 1980s. The proton decay hypothesis was first formulated by Andrei Sakharov in 1967 [37]. During the year 1981 at GSI Darmstadt one proton (1P) ground decay was observed [216]. Half-lives of proton emission of nuclei such as ^{151}Lu, ^{53}Co and so on have been studied [196, 217]. Many theoretical models [7, 16, 19, 55, 150] have been made used to study 1P-decay. M.Pfutzner et al., [91] observed the decays of fine^{45}Fe atoms at the fragment separator of GSI. Bajc et al., [218] systematically studied proton decay in the minimal super symmetric SU(5) grand unified theory. Goldman and

Ross [219] predicted theoretical upper limit for proton decay. Two proton decay of ^{67}Kr is experimentally observed [140]. The life time of proton has been identified by earlier researchers [220]. Santosh and Indu sukumaran [34] theoretically predicted half-lives of proton emitters with the atomic number of $Z > 50$. The proton radioactivity has been studied using various proximity potentials [221]. Experimental evidence shows proton drip line of ^{45}Fe [67]. After bombardment of ^{92}Mo target nuclei with ^{50}C, Woods et al., [222] observed proton decay. Developmental theories of proton decay has been predicted by Maglione et al., [223]. Detail analysis of proton decay has been done by Rykaczewskiaet al.,[39]. Ferreira et al., [32] based on relativistic density functional theory, the proton radioactivity from spherical nuclei were studied.

Delion et al., [5] examined the characteristics of nuclear matter by reviewing proton emission hypotheses. Recent literature [107, 126, 129] also predicts proton emitters in the atomic number range $72 < Z < 88$ and actinides. Many theoretical studies shows the prediction of possible decay mode in the superheavy region [161, 164, 165, 213]. Hence, in the present work we made an attempt to study one proton radioactivity of Tantalum using different models such as Coulomb and proximity potential model(CPPM), effective liquid drop model (ELDM) and modified generalised liquid drop model (MGLDM).

During the last two decades, significant progress has been made in the experimental investigation of processes leading to superheavy nuclei, their decay properties and structure. The most stable superheavies are anticipated to be positioned along the β-stability line, which is unreachable by fusion reactions with stable beams. The literature studies shows the competition between different decay modes [173, 205]. The proton decay half-lives of lanthanides and actinides were studied [107, 111, 161, 224]. Qian et al., [225] systematically studied α-decay half-lives of heavy and superheavy elements. Tan et al., [226] investigated the β^+ decays of some medium-mass nuclei.

Many theoretical models have been proposed to explore the half-lives of spherical and deformed nuclei. Earlier workers [164] have studied different decay modes of superheavy nuclei. Hence, in the present work we have examined possible decay modes such as proton decay using Coulomb and Proximity potential Model (CPPM), $\beta^{\pm}$-decay and an alpha decay are evaluated using semi-empirical relations in the isotopes of Bismuth.

Protons may be thought of as a point charge with the highest chance of being present in the parent nucleus in the energy domain of radioactivity.For both odd and even atomic numbers, Goldanskii [85]predicted one and two proton radioactivity in the mid-1960s. Mukha et al [38, 134] reported one- and two-proton radioactivity in ^{94}Ag in over 21 high-spin isomers. Routray et al., [112] used Yukawa effective interaction to calculate the half-lives of proton radioactivity. Deng et al., [221] investigated proton radio activity, α decay, and heavy particle radioactivity using various proximity potentials. At the RIKEN Nishina Center in 2015, prior researcher [227] evaluated proton radioactivity in ^{67}Kr. Two-proton radioactivity in ^{45}Fe was explored experimentally by Giovinazzo et al., [228] by the use of silicon detectors.Previous research [135, 136] looked at ^{45}Fe and ^{54}Zn radioactivity at one and two proton levels.

The systematics of proton decay and spectroscopic effects can be predicted using theoretical proton radioactivity models from spherical nuclei [229]. Santhosh et al., [34] used the Coulomb Proximity Potential Model for deformed nuclei to predict proton radioactivity in nuclei with $Z > 50$. Using the newly constructed velocity separator SHIP, which was created at GSI, Darmstadt, the researchers [230] identified proton active nucleus outside the proton drip line. The proton decay of ^{108}I was discovered experimentally by Auranen et al., [231]. Alavi et al., [26] used the WKB approach to calculate proton decay half-lives. Previously, researches [232, 233] revealed about proton decay emission in actinides and alkaline metals . Pfutzner et al., [234] investigated the proton emission phenomena of odd Z nuclei and discovered extensive structural data. The two-

proton radioactivity was experimentally observed in ^{45}Fe [67, 91], and later in ^{19}Mg [137, 138], ^{48}Ni [83], and ^{54}Zn [63]. The proton radioactivity was experimentally detected by Jackson [86] in 1970 by detecting proton emission from ^{53}Co to the ground state of ^{52}Fe. Many theoretical models for studying the half-lives of spherical and deformed nuclei have been proposed since then. [69, 122, 223, 235–239]. Previously, researchers [108, 161, 164, 165, 169]used various proximity potentials to evaluate the half-lives of superheavy nuclei. The search for proton emission nuclei will lead to the determination of nuclear stability in proton-rich nuclei. Although proton emission is a challenging process, the simplified way of one proton overcoming the coulomb barrier will illustrate the process quite well.Proton emissions have the lowest coulomb potential and the least decreased mass when compared to the other decay types. According to the literature, a comprehensive investigation of one-proton decay half-lives in the actinide area is necessary. The study of proton decay half-lives in the actinide area is the major goal of this research. Proton radioactivity was studied using the coulomb and proximity potential models, which have been used for alpha and cluster decay for many years. The study predicts that in future experiments, proton unstable nuclei close or outside the proton drip line would be detected. The half-lives of proton emitters in the actinide region that had not yet been observed experimentally are predicted.

The nuclei beyond the proton drip line with Q_p >0 are the one with proton unstable and also exhibit exotic decay modes. The understanding of the proton decay is important to study the nuclear structure. The exotic nuclei exists away from the stability. The binding energy of protons above the drip line gradually decreases and hence one-proton and two proton decay is predicted. Brown [240] studied two proton decay in Z=22-28 in the ground state. Goldanskii [85] for the first time studied the one proton and two proton decay for odd and even atomic number. Janecke [241] studied the emission of protons from the light nuclei ^{12,13}O, ^{21}Mg and ^{24,32}Si. The spherical proton and deformed proton emitters were investigated in lanthanides and transition metals. Previous

workers [63, 67, 83, 86, 91, 135–138, 227, 228, 231] experimentally observed one and two proton decay in proton rich nuclei. There are several theoretical models [38, 112, 134], studied one proton and two proton activity in light nuclei.

Using different proximity potentials previous workers [34, 221, 229] studied proton activity in the light nuclei. The emission of heavy particles such as one proton, one neutron, two protons, two neutrons and alpha particle emission takes place when the nuclei are proton rich, neutron rich and very heavy nuclei. Successively many theoretical models [69, 122, 223, 235–239] were presented to study the half-lives of spherical and deformed nuclei. Dobaczewski and Nazarewicz [232] studied two-proton stability in doubly magic nuclei ^{100}Sn using self-consistent Skyrme-Hartree-Fock-Bogoliubov theory. Olsen et al., [233, 233] investigated two-proton decay in even-even nuclei and also studied competition between proton decay and alpha decay. Poenaru et al., [242] measured half-lives and branching ratios for ^{12}C, ^{16}O and ^{28}Si and proton and neutron rich nuclei with Z=56-64.

The observations of proton decay is quite recent, they are several approaches to study this proton decay process, such as distorted-wave Born approximation [19], the study of effective interaction by the density dependent M3Y (DDM3Y) [94, 150]. The construction of proton nucleus potential by Jeukenne, Lejeune and Mahaux (JLM) applied to finite nuclei in the Local Density Approximation [55], the unified fission model [5], the coupled-channels approach [16] and also generalized liquid drop models [18, 243, 244]. Earlier workers [108, 111, 161, 164, 165, 169, 210, 213, 245] studied half-lives of spontaneous fission, ternary fission, cluster decay and alpha decay in the superheavy region using different proximity potentials. Faestermann [117] experimentally observed proton decay half-lives and proton energies in ^{113}Cs and ^{109}I. Sellin [246] experimentally measured proton decay half-lives in ^{150}Lu, ^{151}Lu and ^{147}Tm. Page et al., [247] reported proton emitter ^{112}Cs with the half-life of $500\pm100\mu$s. Livingston [248] experimentally ob-

served proton emission from the ^{146}Tm. The two proton radioactivity [63, 67, 83, 91, 137, 138] was experimentally observed ^{45}Fe, ^{19}Mg, ^{48}Ni and ^{54}Zn. In the year 1970, Jackson [86] confirmed proton radioactivity from the proton emitter ^{53}Co.

The proton radioactivity is applied for nuclear astrophysics. In the nuclear astrophysics, the process of two-proton radiation capture process is considered, which is important for extremely high densities and temperatures. The example of such an astrophysical environment is the sources of gamma bursts related with the explosive burning of deposited hydrogen on the surface of neutron stars. Previous workers [249–251] explained the astrophysical applications of the two-proton radioactivity.

From the available literature, the study on one proton emission in the actinide region is required. The study on the proton decay not only provides information about the drip line, but also provides spectroscopic information on the unpaired proton not substantial in its orbit. Hence, in the present work we want to emphasize on the possible proton emitters in the actinide region and also prediction of half-lives in the same region. The main objective is to systematically study one proton decay half-lives of spherical and deformed nuclei in the actinide region.

A Systematic study of proton decay in superheavy elements Goncalves et al., [145] studied two-proton radioactivity of nuclei of mass number $A < 70$ using the effective liquid drop model. Delion et al., [252] reviewed the theories of proton emission to analyse the properties of nuclear matter. Maglione et al., [253] analyzed the proton emission from the some deformed nuclei. Santo et al., [254] investigated the β-delayed proton emission of ^{69}Kr and ^{68}Se and extracted their proton separation energies, half lives and excitation energies. Alavi et al., [255] calculated the proton radioactivity half-lives of 45 proton emitters by WKB Method and observed the decrease in values of calculated half lives using the orientation angle dependent formalism. Raciti et al., [132] measured the emission of two protons from the decay of ^{18}Ne excited states. Baye and Tursuno [256]

studied that a proton is emitted during β decay of one neutron halo nuclei. Feix and Hilf [257] computed the decay widths of proton emission for Z=51 to 71 nuclei using droplet model potentials and spectroscopic data from shell model considerations. Anguiano et al., [131] investigated the photo-emission of two protons from the ^{12}C, ^{16}O and ^{40}Ca nuclei for the study of short range correlations. Coniglione et al., [258] explored high energy proton emission in heavy ion reactions close to the Fermi energy by investigating the production mechanism of energetic protons in an experiment performed with the MEDEA detector.

Giusti and Pacati [143] developed the theoretical frame work of emission of two protons in electron induced reactions. Ludewigt et al. [259] studied the proton emission in alpha induced reactions at 43 MeV nucleon. Guzman et.al. [260] analyzed the proton emission from proton-rich nuclei and calculated the half lives using the effective liquid drop model. Delion et al. [261] also studied the proton emission. Dong et al [2] theoretically calculated the half lives of proton emitters using generalized liquid drop model (GLDM) and WKB approximation. Maglione and Ferreira [262] studied the proton emission from ^{125}Pm and the behaviour of the half lives were discussed as a function of deformation, spin of the decaying state, and energy of the emitted protons. Arumugam et al., [263] investigated the proton emission , gamma deformation, and the spin of the isomeric state of ^{141}Ho and revealed that proton emission measurements could be a precise tool to probe triaxial deformations and other structural properties of exotic nuclei beyond the proton drip-line. DUARTE et al., [264] studied the half-lives for proton emission, alpha decay, cluster radioactivity, and cold fission processes theoretically. Ferreira et al., [265] also studied the proton radioactivity from spherical nuclei theoretically based on relativistic density functional derived from meson exchange and point coupling models. Also previous researchers studied on the decay modes[107, 111, 126, 129, 163, 181, 207, 207, 266–270]. From study of literature survey, it reveals that there is a lack of study on proton emission from superheavy nuclei. Superheavy

nuclei is unstable and it decay through different decay modes. Hence the present work studies the systematics of proton emission from superheavy nuclei.

In the line of stability, the excess protons still adequately bound to the nucleus with the nuclear forces, hence direct emission of proton is not possible. However, while beyond the line of stability the protons are no longer bound by the nuclear forces. In order to study the proton emission beyond the stability line Conclaves et al., [14] studied two-proton radioactivity in the mass number $A < 70$ using liquid drop model. Earlier [6, 24] studied proton emission from the deformed nuclei. One proton, two proton, β decay [25–28, 70] were studied using droplet model and WKB approximation. Giusti et al., [29] established theoretical frame work for the emission of two protons in electron induced reactions. Using generalized liquid drop model and WKB approximation, Dong et al., [18] theoretically studied proton decay half-lives of spherical proton emitters.

Previous workers [29, 72] theoretically studied half-lives of proton radioactivity. Earlier workers [108, 161, 164, 165, 169] were studied ternary fission, binary fission, cluster radioactivity and alpha decay in the superheavy region using different proximity functions. From the available literature, it is essential to study the proton radioactivity in the Dubnium. Hence, in the present work first attempt was made to study proton radioactivity in the isotopes of Dubnium.

1.5 Objectives of research work

- Construction of semi empirical formula for proton decay half-lives in the complete range of medium, heavy and superheavy nuclei region.
- A detail study of proton radioactivity using effective liquid drop model (ELDM), generalized liquid drop model (GLDM) and modified generalised liquid drop model (MGLDM) models.
- To identify the dominant decay mode by comparing proton decay with other decay modes such as alpha decay, beta decay, and spontaneous fission in Lanthanide, Actinide and Super-

heavy region.

- Identification of new proton emitters among the Lanthanides, Actinides, heavy and Super-heavy nuclei.

- The comparison of proton decay half-lives calculated using macroscopic models with that of the microscopic models.

CHAPTER 2

Semi empirical formula for proton radioactivity half lives

2.1 Construction of Semi-empirical formula for one and two proton decay

The knowledge of accurate Q-values helps to analyse the 1p and 2p radioactivity in the atomic number region $3 \leq Z \leq 126$. In order to evaluate the Q-values, the mass excess values available in the literature [271] are taken. The Q-values of 2p and 1p radioactivity are selected in such way that the $Q_{2p,1p} > 0$.

The selection of angular momentum and centrifugal barrier is more important in proton decay. The effect of reduced mass is smaller when compared to angular momentum and the proton, in most instances, has a non-vanishing angular momentum.. The values of angular momentum accompanying with the one and two proton radioactivity is deduced from the spin and conservation laws as described. In addition one and two proton decay half-lives are compared with that of $\beta^{\pm}$-decay [107], α-decay [161] and spontaneous fission [107]. Among these different decay modes, the possible decay modes were compared and finally predicted pure one and two proton emitters.

However, the different microscopic and macroscopic models such as folding model analysis [96], relativistic mean field approach [96], modified preformed cluster model [272], effective liquid drop model [14] in which either preformation probability is taken as unity or majority of the cases in which the effect of spectroscopic factor were not considered. It is also evident from the literature that the MGLDM was used to evaluate cluster-decay [273], alpha-decay [274] and heavy

particle radioactivity [90] but not for proton-decay half-lives. Even though, spectroscopic factor is an important key factor and it is model dependent, but these macroscopic models also predicts half-lives close to experimental values. The significant correlation between log$T_{1/2}$ values of α-decay and amount of energy released (Q) was successfully explained by Geiger and Nuttall [275]. Also tried to construct the semi empirical formula for one proton radio activities using the Geiger-Nuttall law.

Proton decay half lives are evaluated using well accepted models such as MGLDM [274], ELDM [239] and CPPM [276]. Even-though, all the three models have its own physical significance in reproducing the experimental half-lives more accurately and precisely but, CPPM half-lives are considered for construction of semi empirical formula. Since, the standard deviation obtained using CPPM model is smaller when compared to MGLDM and ELDM models i.e the half-lives predicted using CPPM are in close agreement with that of experiments. Hence, it is appropriate to consider the CPPM half-lives to fit a semi-empirical formulae. As a consequence, half-lives obtained using CPPM in an unexplored nuclei may also predict the half-lives more accurately. In this view, we have considered half-lives produced by CPPM. The logarithmic half-lives of 1P radioactivity as a function of atomic number of daughter nuclei, angular momentum and amount of energy released and it is as follows;

$$logT_{1/2}(1P) \propto f(Z_D, \ell, Q) \tag{2.1}$$

The function $f(Z_D, \ell, Q)$ is evaluated by studying the variation of $logT_{1/2}(1P)$ as a function of $f(Z_D, \ell, Q)$. To derive suitable empirical formula for logarithmic half-lives of 1P radioactivity, it is assumed that $logT_{1/2}(1P)$ is directly proportional to Z_D^x and inversely proportional to $\sqrt{Q}$ and

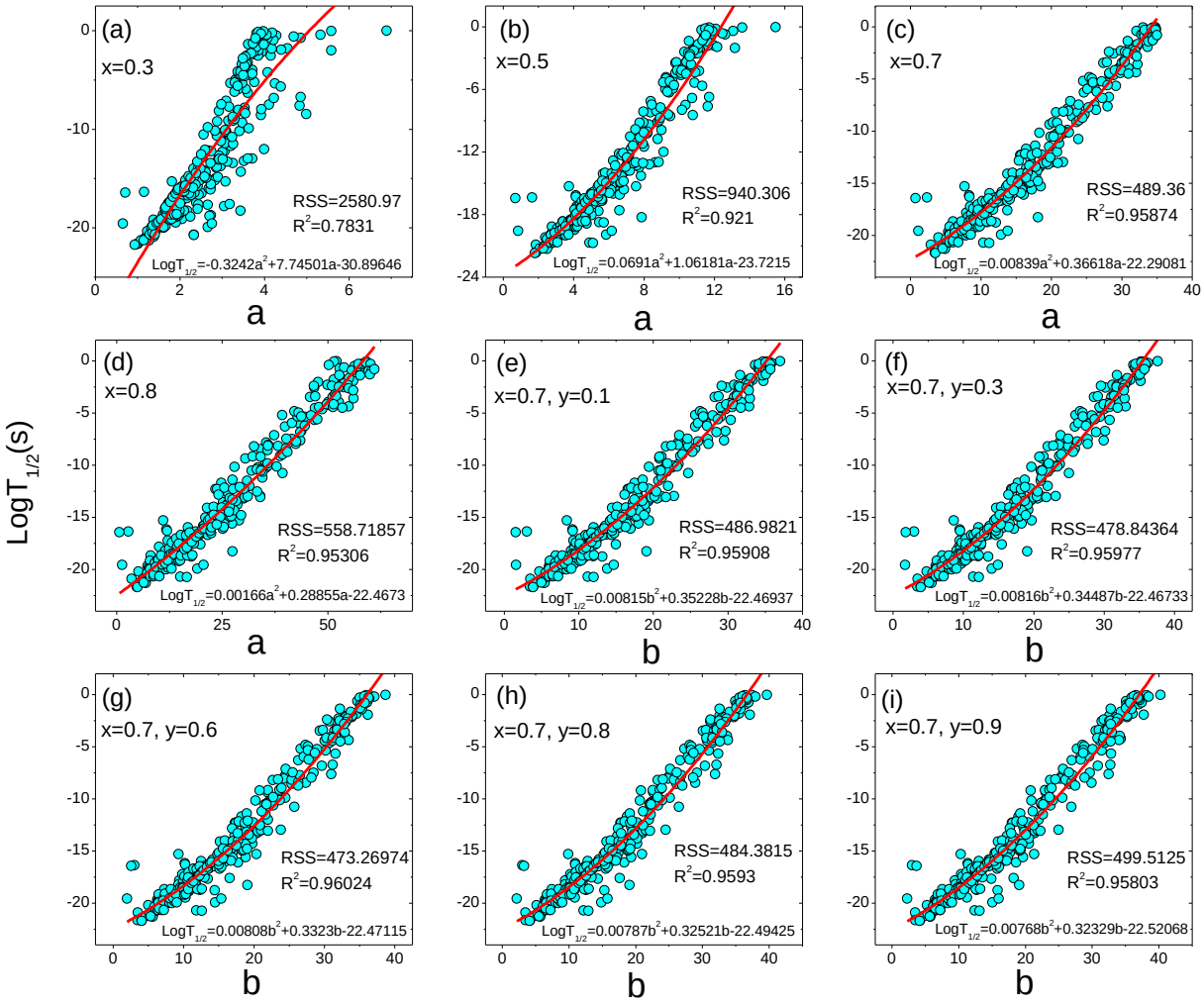

Fig. 2.1 (a-d): The variation of $\log T_{1/2}$ during one proton radioactivity as a function of a where $Z_D^x/\sqrt{Q}$. **(e)-(i)**: The variation of $\log T_{1/2}$ during one proton radioactivity as a function of b where $(Z_D^{0.7} + \ell^y)/\sqrt{Q}$.

it is as follows;

$$logT_{1/2}(1P) = f(Z_D^x/\sqrt{Q}) \tag{2.2}$$

We tried many functions such as $A_1a + A_2/a^2 + A_3$, $A_1a + A_2a/(a - A_3)$, $A_1/a + A_2 + A_3/a^2$, $A_1ln(a - A_2) + A_3$, $A_1exp^{A_2}/(a - A_3lna)$, $A_1ln(a) + A_2$, $\frac{1}{(A_1lnZ+A_2)}$ and polynomial functions such as $A_4a^4 + A_3a^3 + A_2a^2 + A_1a + A_0$. Among all the studied functions, we have considered polynomial function whose residual sum of squares (RSS) is minimum value and coefficient of determination is $R^2 \approx 1$. The figure 2.1(a) to (d) shows the variation of $\log T_{1/2}$ of the one

proton emission with $Z_D^x/\sqrt{Q}$ for different values of x=0.3, 0.5, 0.7 and 0.8 respectively. Among the studied functions, the function with $x = 0.7$ shows smaller RSS and larger R^2 value. The effect of angular momentum plays a major role in the proton decay and from the literature [13, 109, 180] many empirical relations included the effect of angular momentum. The inclusion of angular momentum significantly effect the RSS and R^2 value. Dehghani and Alavi [277] has also shown that the inclusion of deformation, angular momentum and Q-values reduces the rms value. Hence, in order to obtain accurate half-lives, the angular momentum is included in the fitting of the semi-empirical formulae. Later by keeping $X = 0.7$, the effect of angular momentum included by considering the $(Z_D^{0.7} + \ell^y)/\sqrt{Q}$. The maximum value of coefficient of determination $R^2 = 0.96024$ is observed when $y = 0.6$. The final constructed semi empirical formula for one proton radioactivity is as follows;

$$logT_{1/2}(1P) = 0.00808\left(\frac{Z_D^{0.7} + \ell^{0.6}}{\sqrt{Q}}\right)^2 + 0.3323\left(\frac{Z_D^{0.7} + \ell^{0.6}}{\sqrt{Q}}\right) - 22.47115 \qquad (2.3)$$

where Z_D, ℓ and Q are the atomic number of daughter nuclei, angular momentum and amount of energy released during one proton decay respectively.

To obtain further insight into systematics of two proton radioactivity, an attempt was made to construct semi empirical formula similar to one proton radioactivity by including the effects of atomic number, Q-values and angular momentum. The figure 2.2 (a) to (i) shows the variation of log$T_{1/2}$ of two proton radioactivity with $a = Z_D^x/\sqrt{Q}$. The remaining layers of the same figure 2.2(g) to (i) depicts the variation of log$T_{1/2}$ with $b = (Z_D^x + \ell^y)/\sqrt{Q}$. From this study, it is observed that the variation of log$T_{1/2}$ with $(Z_D^x + \ell^y)/\sqrt{Q}$ is found to be more systematic at x=0.7 and y=0.01 and it is shown in the figure 2.2(g). The constructed semi empirical formula having

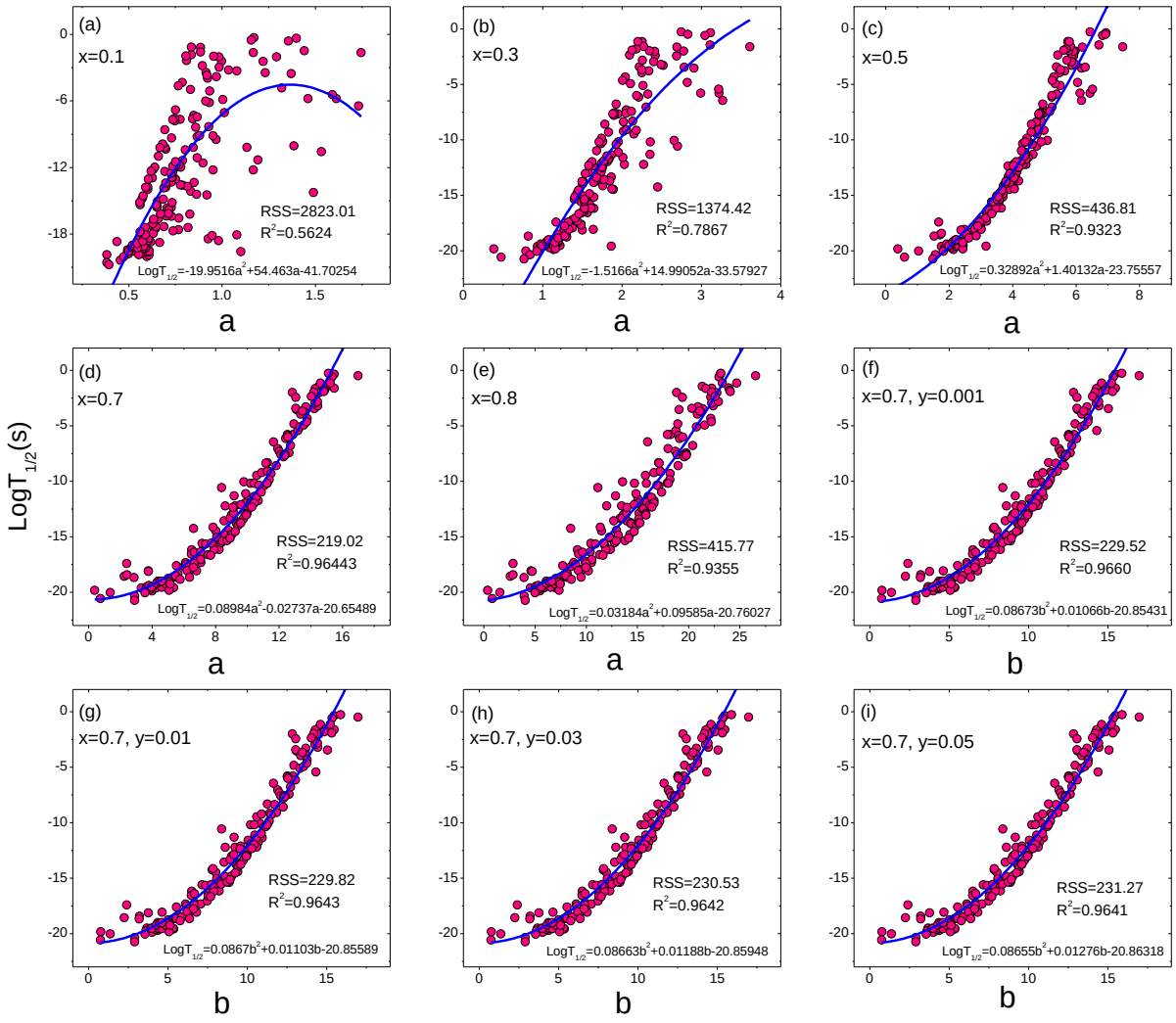

Fig. 2.2 (a)-(e):The variation of $\log T_{1/2}$ during two proton radioactivity as a function of $a = Z_D^x/\sqrt{Q}$. **(f)-(i)**: The variation of $\log T_{1/2}$ during one two radioactivity as a function of $b = (Z_D^{0.7} + \ell^y)/\sqrt{Q}$

maximum R^2 and minimum RSS for the two proton radioactivity is expressed as;

$$logT_{1/2}(2P) = 0.08673\left(\frac{Z_D^{0.7} + \ell^{0.001}}{\sqrt{Q}}\right)^2 + 0.01066\left(\frac{Z_D^{0.7} + \ell^{0.001}}{\sqrt{Q}}\right) - 20.85431 \qquad (2.4)$$

where Z_D, ℓ and Q are the atomic number of daughter nuclei, angular momentum and amount of energy released during two proton decay respectively.

1p and 2p radioactivity half-lives are evaluated for the nuclei whose experimental values are accessible using the proposed semi empirical formulae defined in the equations 2.3 and 2.4.

Table 2.1 Comparison of calculated half-lives with the different models.

Reaction	Q(MeV)	l_{min}	$LogT_{1/2}(s)$	
			PF	Models
$^{6}Be \rightarrow^{4} He$	1.372	0	-20.67	-19.97 [145]
$^{7}B \rightarrow^{5} Li$	1.42	0	-20.55	-19.55[145]
$^{8}C \rightarrow^{6} Be$	2.111	0	-20.55	-19.62[145]
$^{10}N \rightarrow^{8} B$	1.3	1	-19.70	-17.64[145]
$^{12}O \rightarrow^{10} C$	1.638	0	-20.17	-18.27[145]
$^{16}Ne \rightarrow^{14} O$	1.401	0	-19.68	-16.60[145]
$^{12}O \rightarrow^{10} C$	1.82	0	-20.24	-19.46[147]
$^{12}O \rightarrow^{10} C$	1.79	0	-20.23	-19.43[147]
$^{12}O \rightarrow^{10} C$	1.8	0	-20.23	-19.44[147]

To test the predictive power of the constructed semi-empirical formula, we have evaluated the mean squared error. The evaluated mean squared error in predicting the half-lives corresponds to 1p and 2p radio activities are 0.75 and 0.53 respectively. Further, the values obtained from the present work is compared with that of two proton radioactivity available in literature for which semi-empirical fit is adopted and it is tabulated in table 2.1. The half-lives obtained from present formulae are nearly equal to the values proposed by the previous models. However, a change in the magnitude of two to three order has been observed from the present semi-empirical formulae. The values produced by the present semi-empirical formula is compared with that of experiments.

The table 2.2 shows the comparision of one proton radioactivity half lives produced by the present formula with that of experiments. From this comparision it is observed that the present formula sucessfully produces experimental half lives.

The table 2.3 shows the comparision of two proton radioactivity half lives produced by the present formula with that of experiments. The present formula also sucessfully produces two proton radioactivity half lives which are close to the experiments.

Table 2.2 Comparison of 1P decay logarithmic half lives obtained using present formula (PF) with that of experiments[109].

Reaction	Q_{1P}	$J_i \rightarrow J_f$	ℓ	$logT_{1/2}(s)$	
				Exp	PF
^{146}Tm$\rightarrow^{145}$Er	0.891	$1^+ \rightarrow 1/2^+\#$	0	-0.81	-0.30$\pm$0.63
$^{146}Tm^m \rightarrow^{145} Er^m$	1.001	$5^- \rightarrow 11/2^-\#$	0	-1.12	-1.60$\pm$0.42
$^{150}Lu^m \rightarrow^{149} Yb$	1.291	$1^+, 2^+ \rightarrow 1/2^+$	0	-4.4	-3.47$\pm$0.21
$^{157}Ta \rightarrow^{156} Hf$	0.941	$1/2^+ \rightarrow 0^+$	0	-0.53	-0.32$\pm$0.39
$^{160}Re \rightarrow^{159} W$	1.271	$4^- \rightarrow 7/2^-\#$	0	-3.16	-2.73$\pm$0.13
$^{161}Re \rightarrow^{160} W$	1.201	$1/2^+ \rightarrow 0^+$	0	-3.36	-2.22$\pm$0.34
$^{167}Ir \rightarrow^{166} Os$	1.071	$1/2^+ \rightarrow 0^+$	0	-1.13	-0.64$\pm$0.43
$^{171}Au \rightarrow^{170} Pt$	1.448	$1/2^+ \rightarrow 0^+$	0	-4.65	-3.12$\pm$0.32
$^{176}Tl \rightarrow^{175} Hg$	1.261	$3^-, 4^-, 5^- \rightarrow 7/2^-$	0	-2.21	-1.64$\pm$0.25
$^{177}Tl \rightarrow^{176} Hg$	1.155	$1/2^+ \rightarrow 0^+$	0	-1.18	-0.68$\pm$0.42
$^{185}Bi^m \rightarrow^{184} Pb$	1.607	$1/2^+ \rightarrow 0^+$	0	-4.19	-3.45$\pm$0.17
$^{147}Tm^m \rightarrow^{146} Er$	1.12	$3/2^+ \rightarrow 0^+$	2	-3.44	-2.70$\pm$0.21
$^{151}Lu^m \rightarrow^{150} Yb$	1.291	$3/2^+ \rightarrow 0^+$	2	-4.78	-2.67$\pm$0.44
$^{156}Ta \rightarrow^{155} Hf$	1.021	$2^- \rightarrow 7/2^-\#$	2	-0.83	-0.68$\pm$0.18
$^{166}Ir \rightarrow^{165} Os$	1.161	$2^- \rightarrow 7/2^-$	2	-0.84	-0.48$\pm$0.42
$^{170}Au \rightarrow^{169} Pt$	1.471	$2^- \rightarrow 7/2^-$	2	-3.49	-2.55$\pm$0.26
$^{145}Tm \rightarrow^{144} Er$	1.741	$11/2^- \rightarrow 0^+$	5	-5.5	-5.0$\pm$0.09
$^{147}Tm \rightarrow^{146} Er$	1.059	$11/2^- \rightarrow 0^+$	5	0.57	0.28$\pm$50
$^{155}Ta \rightarrow^{154} Hf$	1.451	$11/2^- \rightarrow 0^+$	5	-2.49	-3.30$\pm$0.32
$^{156}Ta^m \rightarrow^{155} Hf$	1.111	$9^+ \rightarrow 7/2^-\#$	5	0.92	0.81$\pm$0.11
$^{161}Re^m \rightarrow^{160} W$	1.321	$11/2^- \rightarrow 0^+$	5	-0.68	-0.26$\pm$0.61
$^{165}Ir^m \rightarrow^{164} Os$	1.721	$11/2^- \rightarrow 0^+$	5	-3.43	-4.00$\pm$0.16
$^{166}Ir^m \rightarrow^{165} Os$	1.331	$9^+ \rightarrow 7/2^-$	5	-0.09	‘ -1.94$\pm$2.0
$^{167}Ir^m \rightarrow^{166} Os$	1.246	$11/2^- \rightarrow 0^+$	5	0.78	0.54$\pm$0.3
$^{170}Au^m \rightarrow^{169} Pt$	1.751	$9^+ \rightarrow 7/2^-$	5	-2.97	-3.88$\pm$0.30
$^{171}Au^m \rightarrow^{170} Pt$	1.702	$11/2^- \rightarrow 0^+$	5	-2.59	-3.70$\pm$0.42
$^{177}Tl^m \rightarrow^{176} Hg$	1.962	$11/2^- \rightarrow 0^+$	5	-3.46	-4.3$\pm$0.24

Table 2.3 Comparison of 2P decay logarithmic half lives obtained using present formula (PF) with that of experiments [145]

Reaction	Q_{2P}	$J_i \rightarrow J_f$	ℓ	$logT_{1/2}(s)$	
				Exp	PF
$^{6}Be \rightarrow^{4} He$	1.371	$0^+ \rightarrow 0^+$	0	-19.51	-20.48$\pm$0.04
$^{12}O \rightarrow^{10} C$	1.79	$0^+ \rightarrow 0^+$	0	-20.31	-20.04$\pm$0.01
$^{16}Ne \rightarrow^{14} O$	1.4	$0^+ \rightarrow 0^+$	0	-19.58	-19.82$\pm$0.01
$^{19}Mg \rightarrow^{17} Ne$	0.75	$1/2^-\# \rightarrow 1/2^-$	0	-11.4	-13.42$\pm$0.17
$^{45}Fe \rightarrow^{43} Cr$	1.14	$3/2^+\# \rightarrow 3/2^+$	0	-2.07	-3.82$\pm$0.84
$^{48}Ni \rightarrow^{46} Fe$	1.29	$0^+ \rightarrow 0^+$	0	-2.52	-4.06$\pm$0.61
$^{54}Zn \rightarrow^{52} Ni$	1.48	$0^+ \rightarrow 0^+$	0	-2.43	-4.16$\pm$0.71
$^{67}Kr \rightarrow^{65} Se$	1.69	$3/2^- \rightarrow 3/2^-\#$	0	-1.7	-2.18$\pm$0.28

CHAPTER 3

Study of Proton radioactivity using Theoritical models

3.1 Theory

A detail study is carried on one and two proton radioactivity using well accepted theoretical models such as MGLDM, CPPM and ELDM.

3.1.1 Modified Generalized Liquid Drop Model (MGLDM)

For a deformed nucleus, total energy is the sum of the volume energy E_v, surface energy E_S, coulomb energy E_C, proximity energy E_P and centrifugal energy E_ℓ and it is given by;

$$E = E_v + E_s + E_c + E_P + E_\ell \tag{3.1}$$

For the deformed nuclei, the volume E_v, surface E_S and coulomb E_C energies are given by;

$$E_v = -15.494(1 - 1.8I^2)AMeV \tag{3.2}$$

$$E_s = 17.9439[(1 - 2.6I_1^2)A_1^{2/3} + (1 - 2.6I_2^2)A_2^{2/3}]MeV \tag{3.3}$$

$$E_c = 0.6e^2(Z^2/R_0) \times 0.5 \int (V(\theta)/V_0)(R(\theta)/R_0)^3 sin(\theta) d\theta MeV \tag{3.4}$$

where I is the relative neutron excess, $R(0)$ is the effective sharp radius, V(θ) is the electrostatic potential at the surface and V_0 is the surface potential of the sphere. When the nuclei are far apart then above equations are written as;

$$E_v = -15.494(1 - 1.8I_1^2)A_1 + (1 - 1.8I_2^2)A_2 \;\; MeV \tag{3.5}$$

here A_1 is the daughter nuclei and A_2 is the one/two proton mass number.

$$E_s = 17.9439(1 - 2.6I_1^2)A_1^{2/3} + (1 - 2.6I_2^2)A_2^{2/3} \;\; MeV \tag{3.6}$$

$$E_c = 0.6e^2(Z_1^2/R_1) + 0.6e^2(Z_2^2/R_2) + e^2 Z_1 Z_2/r MeV \tag{3.7}$$

Here A_i, Z_i, R_i, I_i(1,2) and r are mass number, atomic number, radii of daughter nuclei and one/two protons relative neutron excess of the daughter nuclei and distance between the mass centres respectively. The centrifugal energy E_ℓ of the emitted proton is expressed as;

$$E_\ell(r) = \frac{\hbar^2}{2\mu} \frac{\ell(\ell+1)}{r^2} MeV \tag{3.8}$$

where $\mu = \frac{A_1 A2}{A_1 + A_2}$, r and ℓ are the reduced mass, separation distance between two nuclei and angular momentum, respectively. The selection rule for proton decay [109] is as follows;

$$J_p = J_d + J_{p^\ell} \tag{3.9}$$

$$\pi_p = \pi_d \pi_{p^\ell} (-1)^\ell \tag{3.10}$$

where J_p, π_p, J_d, π_d, J_{p^ℓ} and π_{p^ℓ} are spin and parity values of the parent, daughter and outgoing one/two proton respectively. The proton has a non zero value of spin and positive parity, therefore the minimal value of angular momentum at the proton transition is expressed as

$$\ell_{min} = \begin{cases} \Delta_j \quad for\ \ even\ \ \Delta_j\ \ and\ \ \pi_p = \pi_d \\ \Delta_j + 1 \quad for\ \ even\ \ \Delta_j\ \ and\ \ \pi_p \neq \pi_d \\ \Delta_j \quad for\ \ odd\ \ \Delta_j\ \ and\ \ \pi_p \neq \pi_d \\ \Delta_j + 1 \quad for\ \ odd\ \ \Delta_j\ \ and\ \ \pi_p = \pi_d \end{cases} \tag{3.11}$$

where $\Delta_j = |J_p - J_d - J_{p^\ell}|$. The proximity function is evaluated as described in the literature[278] and it is expressed as;

$$\Phi(\epsilon) = \begin{cases} -1.7817 + 0.9270\epsilon + 0.143\epsilon^2 & for\ \ \epsilon \leq 0.0; \\ -1.7817 + 0.9270\epsilon + 0.0169\epsilon^2 - 0.05148\epsilon^3 & for\ \ 0 \leq \epsilon \leq 1.9475; \\ -4.41 exp\left(\frac{-\epsilon}{0.7176}\right) & for\ \epsilon \geq 1.9475 \end{cases} \tag{3.12}$$

The proton decay half-lives is evaluated using the probability of penetration and it is evaluated using the WKB integration;

$$P = exp\left[-\frac{2}{\hbar}\int_{R_{in}}^{R_{out}} \sqrt{2B(r)E(r) - E(sphere)}\right] \tag{3.13}$$

here $E(r)$ is evaluated as explained in equation (3.1) and $E(sphere) = Q$ is the amount of energy released during one and two proton radioactivity. R_{in} and R_{out} are the classical turning points

and are evaluated using the following conditions $V(r = R_{in}) = V(r = R_{out}) = Q$ and μ is the reduced mass of the daughter and one or two protons. Both one and two proton decay half-lives [34] were evaluated as follows;

$$T_{1/2} = \frac{ln2}{\nu P} \tag{3.14}$$

where ν is the assault frequency of proton against potential energy barrier. $\nu = \frac{41}{hA^{1/3}}$.

3.1.2 **Coulomb and Proximity Potential Model (CPPM)**

The total interacting potential is the sum of Coulomb potential, proximity potential and centrifugal potential and it is evaluated as;

$$V(R) = V_N(R) + V_c(R) + \frac{\ell(\ell+1)}{2\mu \times R^2} \tag{3.15}$$

Here ℓ and μ are the angular momentum and reduced mass of the emitted one or two proton and daughter nuclei respectively. The Coulomb potential is evaluated using the following expression;

$$V_c(R) = \frac{Z_1 Z_2 e^2}{r} \tag{3.16}$$

In above equation, Z_1 and Z_2 are the atomic numbers of daughter and emitted proton. The nuclear potential [279] is given by;

$$V_N\,(R) = 4\pi\gamma\bar{R}\Phi(s) \tag{3.17}$$

here the mean curvature radius is $\bar{R} = \frac{C_1 C_2}{C_1 + C_2}$ and C_i is the centre of matter radii and it is evaluated as follows;

$$C_i = c_i + \frac{N_i}{A_i} t_i (i = 1, 2) \tag{3.18}$$

here c_i is the half density radius of charge distribution is evaluated as follows;

$$c_i = R_{00i} \left(1 - \frac{7b^2}{R_{00i}^2} - \frac{49b^4}{8R_{00i}^4} \right) (i = 1, 2) \tag{3.19}$$

where R_{00i} is the nuclear charge radius;

$$R_{00i} = 1.256 A_i^{1/3} \left(1 - 0.202 \left(\frac{A_i - 2Z_i}{A_i} \right) \right) \tag{3.20}$$

and neutron skin t_i of nucleus is evaluated as follows;

$$t_i = \frac{3}{2} r_o \left[\frac{JI_i - \frac{1}{12} g Z_i A_i^{-1/3}}{Q + \frac{9}{4} A_i^{-1/3}} \right] (i = 1, 2) \tag{3.21}$$

with $r_0 = 1.14$fm, $J = 32.65$ MeV is the nuclear symmetric energy coefficient, $g = 0.757895$ MeV, $Q = 35.4$ MeV is the neutron skin stiffness coefficient and surface energy co-efficient γ is evaluated as follows;

$$\gamma = \frac{1}{4\pi r_o^2} \left[18.63 - Q \frac{(t_1^2 + t_2^2)}{2r_o^2} \right] \tag{3.22}$$

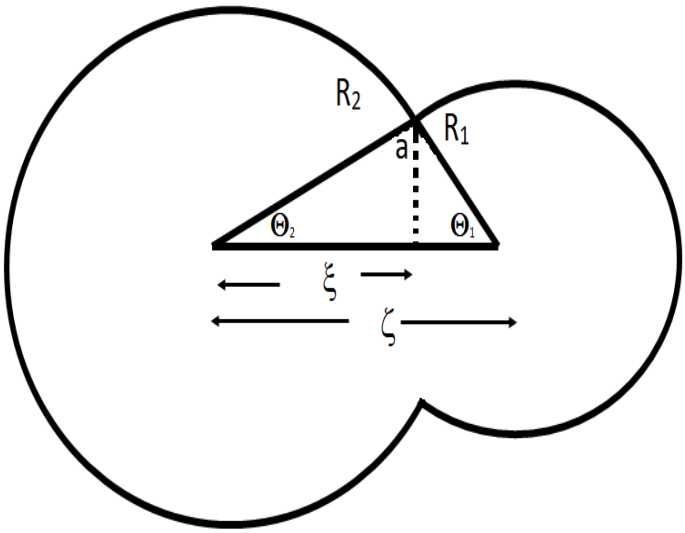

Fig. 3.1 Schematic presentation of molecular phase of the di-nuclear system. [14, 176]

The universal function in nuclear potential is given by

$$\Phi(\xi) = \begin{cases} -0.1353 + \sum_{n=0}^{5} \left[\frac{c_n}{(n+1)}\right] (2.5-\xi)^{n+1} \\ -0.0955 \exp\left(\frac{2.75-\xi}{0.7176}\right) \end{cases}$$

Here $\chi = (r - C_1 - C_2)/b$ and the width parameter $b \approx 1$. The different values of c_n constant are $c_0 = -0.1886$, $c_1 = 0.2628$, $c_2 = -0.15216$, $c_3 = -0.04562$, $c_4 = 0.069136$ and $c_5 = -0.011454$. The penetration probability P and half-lives are evaluated as explained in section 3.1.1.

3.1.3 **Effective Liquid Drop Model(ELDM)**

The ELDM [14, 176] is based on a calculation of Coulomb and surface energies. The electrostatic energy is expressed as;

$$V_c = \frac{8\pi}{9} a^5 \epsilon(\theta_2, \theta_2) \rho_c \tag{3.23}$$

where ρ_c is the initial charge density, $\epsilon(\theta_1, \theta_2)$ is a function of the angular variables, and a is the

radius of the sharp neck. The surface potential energy reads as;

$$V_s = \sigma_{eff}(S_{1p/2P} + S_D) \tag{3.24}$$

where $S_{1p/2P}$ is the surface area of the one and two proton nuclei and S_D denote the area of the surface of the daughter nuclei as follows;

$$S_{1p/2p} = 2\pi R_{1p/2p}(R_{1p/2p} + \zeta + \xi) \tag{3.25}$$

$$S_D = 2\pi R_D(R_D + \xi) \tag{3.26}$$

The centrifugal potential energy V_ℓ is written as;

$$V_\ell = \frac{\ell(\ell+1)\hbar^2}{2\mu\zeta^2} \tag{3.27}$$

here $\mu = \frac{A_1 A_2}{A_1 + A_2}$ where A_1 is the mass number of daughter nuclei and A_2 is the mass number of one or two proton. ℓ is the angular momentum and ζ is the distance between geometrical centers. The term $\hbar$ is the reduced planck's constant. The effective total potential energy is calculated as follows;

$$V = V_c + V_s + V_\ell \tag{3.28}$$

The penetrability factor P is expressed as;

$$P = exp\left[-\frac{2}{\hbar}\int_{\zeta_0}^{\zeta_c}\sqrt{2\mu[V(\zeta) - Q]}d\zeta\right] \tag{3.29}$$

The limit of integration are $\zeta_0 = R_P - R_{1p/2p}$ and $\zeta_c = Z_{1p/2p}Z_D e^2/Q$. The half-life of one and two proton radioactivity is evaluated as follows;

$$T_{1/2} = \frac{ln2}{\lambda_0 P} \tag{3.30}$$

where, $\lambda_0 = 4.96 \times 10^{19}$ [145]

3.2 Results

The half-lives of one and two proton radioactivity are studied using the CPPM, ELDM, MGLDM and semi-empirical theoretical formalism for macroscopic models is explained in the theory section and semi-empirical formula construction is explained in chapter 2. The half-lives calculated using macroscopic models such as CPPM, MGLDM and ELDM are compared with the experiments. Standard deviation produced by each model is also tabulated in table 3.1. The Q-values are evaluated using the mass excess data available in the literature [36, 270, 271, 280]. The one and two proton radioactivity is energetically feasible when the Q-values are positive and it is expressed as;

Table 3.1 A tabulation of standard deviation obtained for one and two proton decay logarithmic half-lives using CPPM, ELDM and MGLDM with that of available experiments.

Type of Decay	N	Standard deviation		
		CPPM	ELDM	MGLDM
1P	27	1.40	1.77	1.80
2P	08	0.42	0.76	1.24

$$Q_{1p} = \Delta M_P - \Delta M(A-1, Z-1) - m_p \tag{3.31}$$

$$Q_{2p} = \Delta M_P - \Delta M(A-2, Z-2) - m_2 p \tag{3.32}$$

here ΔM_P is the mass excess of parent nuclei, $\Delta M(A-1, Z-1)$ and $\Delta M(A-2, Z-2)$

Table 3.2 Comparison of 1P decay logarithmic half lives obtained using CPPM, ELDM, MGLDM and present formula (PF) with that of experiments.

Reaction	Q_{1P}	$J_i \rightarrow J_f$	ℓ	$logT_{1/2}(s)$				
				Exp	CPPM	ELDM	MGLDM	PF
$^{146}Tm \rightarrow^{145} Er$	0.891	$1^+ \rightarrow 1/2^+\#$	0	-0.81	-0.25±0.67	-0.71±0.12	-1.55±0.91	-0.30±0.63
$^{146}Tm^m \rightarrow^{145} Er^m$	1.001	$5^- \rightarrow 11/2^-\#$	0	-1.12	-1.41±0.26	-1.34±0.19	-2.34±1.08	-1.60±0.42
$^{150}Lu^m \rightarrow^{149} Yb$	1.291	$1^+, 2^+ \rightarrow 1/2^+$	0	-4.4	-4.4±0	-4.25±0.03	-4.91±0.11	-3.47±0.21
$^{157}Ta \rightarrow^{156} Hf$	0.941	$1/2^+ \rightarrow 0^+$	0	-0.53	-0.35±0.34	-0.58±0.09	-1.06±1	-0.32±0.39
$^{160}Re \rightarrow^{159} W$	1.271	$4^- \rightarrow 7/2^-\#$	0	-3.16	-3.05±0.03	-3.1±0.01	-3.24±0.02	-2.73±0.13
$^{161}Re \rightarrow^{160} W$	1.201	$1/2^+ \rightarrow 0^+$	0	-3.36	-3.48±0.03	-3.55±0.05	-3.07±0.08	-2.22±0.34
$^{167}Ir \rightarrow^{166} Os$	1.071	$1/2^+ \rightarrow 0^+$	0	-1.13	-1.12±0	-1.18±0.04	-1.29±0.14	-0.64±0.43
$^{171}Au \rightarrow^{170} Pt$	1.448	$1/2^+ \rightarrow 0^+$	0	-4.65	-4.48±0.03	-4.25±0.08	-4.15±0.10	-3.12±0.32
$^{176}Tl \rightarrow^{175} Hg$	1.261	$3^-, 4^-, 5^- \rightarrow 7/2^-$	0	-2.21	-2.5±0.13	-2.52±0.14	-2.01±0.09	-1.64±0.25
$^{177}Tl \rightarrow^{176} Hg$	1.155	$1/2^+ \rightarrow 0^+$	0	-1.18	-1.11±0.05	-2.38±1.01	-1.07±0.09	-0.68±0.42
$^{185}Bi^m \rightarrow^{184} Pb$	1.607	$1/2^+ \rightarrow 0^+$	0	-4.19	-4.13±0.01	-4.23±0.02	-4.45±0.06	-3.45±0.17
$^{147}Tm^m \rightarrow^{146} Er$	1.12	$3/2^+ \rightarrow 0^+$	2	-3.44	-3.17±0.07	-3.55±0.03	-3.35±0.02	-2.70±0.21
$^{151}Lu^m \rightarrow^{150} Yb$	1.291	$3/2^+ \rightarrow 0^+$	2	-4.78	-4.55±0.04	-4.21±0.11	-4.44±0.07	-2.67±0.44
$^{156}Ta \rightarrow^{155} Hf$	1.021	$2^- \rightarrow 7/2^-\#$	2	-0.83	-0.55±0.33	-0.5±0.39	-0.85±0.02	-0.68±0.18
$^{166}Ir \rightarrow^{165} Os$	1.161	$2^- \rightarrow 7/2^-$	2	-0.84	-0.62±0.26	-0.71±0.15	-0.87±0.03	-0.48±0.42
$^{170}Au \rightarrow^{169} Pt$	1.471	$2^- \rightarrow 7/2^-$	2	-3.49	-3.55±0.01	-3.21±0.08	-3.4±0.02	-2.55±0.26
$^{145}Tm \rightarrow^{144} Er$	1.741	$11/2^- \rightarrow 0^+$	5	-5.5	-5.55±0.01	-5.58±0.01	-5.25±0.04	-5.0±0.09
$^{147}Tm \rightarrow^{146} Er$	1.059	$11/2^- \rightarrow 0^+$	5	0.57	0.12±0.79	0.36±0.36	0.56±0.01	0.28±50
$^{155}Ta \rightarrow^{154} Hf$	1.451	$11/2^- \rightarrow 0^+$	5	-2.49	-2.4±0.03	-2.68±0.07	-2.12±0.14	-3.30±0.32
$^{156}Ta^m \rightarrow^{155} Hf$	1.111	$9^+ \rightarrow 7/2^-\#$	5	0.92	0.57±0.38	1.01±0.09	0.93±0.01	0.81±0.11
$^{161}Re^m \rightarrow^{160} W$	1.321	$11/2^- \rightarrow 0^+$	5	-0.68	-0.62±0.08	-0.25±0.63	-0.52±0.23	-0.26±0.61
$^{165}Ir^m \rightarrow^{164} Os$	1.721	$11/2^- \rightarrow 0^+$	5	-3.43	-3.74±0.09	-3.36±0.02	-3.49±0.01	-4.00±0.16
$^{166}Ir^m \rightarrow^{165} Os$	1.331	$9^+ \rightarrow 7/2^-$	5	-0.09	-0.21±1.3	-0.23±1.5	-0.21±1.3	-1.94±2.0
$^{167}Ir^m \rightarrow^{166} Os$	1.246	$11/2^- \rightarrow 0^+$	5	0.78	0.76±0.02	0.46±0.41	0.72±0.07	0.54±0.3
$^{170}Au^m \rightarrow^{169} Pt$	1.751	$9^+ \rightarrow 7/2^-$	5	-2.97	-2.65±0.10	-2.26±0.23	-2.97±0	-3.88±0.30
$^{171}Au^m \rightarrow^{170} Pt$	1.702	$11/2^- \rightarrow 0^+$	5	-2.59	-2.28±0.11	-2.18±0.15	-2.6±0.01	-3.70±0.42
$^{177}Tl^m \rightarrow^{176} Hg$	1.962	$11/2^- \rightarrow 0^+$	5	-3.46	-3.73±0.07	-3.44±0.01	-3.75±0.08	-4.3±0.24

are the mass excess of daughter nuclei during one and two proton, m_p and m_{2p} are masses of one and two proton emission respectively. From this analysis, it is observed that around 306 nuclei are energetically feasible for one proton radioactivity in the atomic number region $3 \leq Z \leq 126$. Among this, 29 one proton emitters are experimentally observed and these are listed in table 3.2. Remaining 277 one proton emitters are newly identified and it is tabulated along with their half-lives and decay energy in table 3.3 and 3.4. Even-though, around 277 proton emitters with positive Q-value were identified but comparison of logarithmic half-lives with other decay modes such as β^+-decay, β^--decay, electron capture and alpha-decay may result in most dominant decay mode. Hence, table 3.3 and 3.4 only gives the prediction of one proton logarithmic half-lives.

Furthermore, around 182 nuclei are energetically feasible for two proton radioactivity in the

Table 3.3 Tabulation of one proton radioactivity in the atomic number range $4 \leq Z \leq 43$ using theoretical models such as CPPM, ELDM, MGLDM and semi-empirical formula (PF).

Reaction	Q_{1p} (MeV)	l_{min}	$LogT_{1/2}(s)$				Reaction	Q_{1p} (MeV)	l_{min}	$LogT_{1/2}(s)$			
			CPPM	ELDM	MGLDM	PF				CPPM	ELDM	MGLDM	PF
$^{5}Be \rightarrow ^{4} Li$	5.384	3	-19.57	-19.85	-18.85	-21.78	$^{51}Zn \rightarrow ^{50} Cu$	2.621	3	-17.04	-16.39	-16.51	-17.96
$^{7}B \rightarrow ^{6} Be$	2.204	1	-16.37	-19.85	-20.46	-17.38	$^{52}Zn \rightarrow ^{51} Cu$	1.951	3	-20.73	-16.06	-15.12	-19.98
$^{10}N \rightarrow ^{9} C$	2.601	1	-20.90	-19.85	-20.53	-21.20	$^{53}Zn \rightarrow ^{52} Cu$	1.518	3	-19.92	-15.82	-15.20	-18.97
$^{12}O \rightarrow ^{11} N$	0.455	1	-17.82	-17.49	-17.23	-18.62	$^{53}Ga \rightarrow ^{52} Zn$	5.431	1	-20.66	-17.56	-20.85	-19.63
$^{14}F \rightarrow ^{13} O$	2.257	2	-20.21	-19.55	-18.85	-20.60	$^{54}Ga \rightarrow ^{53} Zn$	4.171	1	-19.99	-18.78	-20.15	-19.12
$^{19}Mg \rightarrow ^{18} Na$	1.561	2	-18.66	-17.44	-18.11	-19.62	$^{55}Ga \rightarrow ^{54} Zn$	3.958	1	-19.83	-18.67	-20.01	-18.96
$^{23}P \rightarrow ^{22} Si$	6.207	0	-21.63	-19.85	-20.90	-21.21	$^{56}Ga \rightarrow ^{55} Zn$	2.893	1	-18.75	-18.36	-18.87	-18.18
$^{24}S \rightarrow ^{23} P$	2.791	2	-19.67	-17.00	-19.37	-20.06	$^{57}Ga \rightarrow ^{56} Zn$	2.538	1	-18.25	-18.22	-18.36	-17.76
$^{25}S \rightarrow ^{24} P$	4.114	2	-20.91	-19.34	-20.38	-20.47	$^{58}Ga \rightarrow ^{57} Zn$	1.525	1	-15.83	-15.45	-15.86	-15.93
$^{25}Cl \rightarrow ^{24} S$	6.991	2	-21.66	-19.85	-20.96	-20.98	$^{55}Ge \rightarrow ^{54} Ga$	2.541	3	-16.69	-18.29	-17.02	-17.60
$^{26}Cl \rightarrow ^{25} S$	3.621	2	-20.90	-18.87	-19.91	-20.27	$^{56}Ge \rightarrow ^{55} Ga$	1.381	3	-15.02	-15.44	-13.77	-15.25
$^{27}Cl \rightarrow ^{26} S$	6.031	2	-21.27	-19.85	-20.89	-20.77	$^{57}Ge \rightarrow ^{56} Ga$	1.472	3	-19.56	-17.93	-14.17	-18.44
$^{28}Cl \rightarrow ^{27} S$	1.725	2	-19.11	-17.84	-17.80	-18.92	$^{57}As \rightarrow ^{56} Ge$	5.351	3	-19.54	-18.91	-19.23	-19.26
$^{27}Ar \rightarrow ^{26} Cl$	3.111	2	-19.79	-16.66	-19.37	-20.01	$^{58}As \rightarrow ^{57} Ge$	4.161	3	-18.70	-18.54	-18.27	-18.70
$^{29}Ar \rightarrow ^{28} Cl$	1.564	2	-18.25	-17.62	-17.49	-18.60	$^{59}As \rightarrow ^{58} Ge$	3.945	3	-18.49	-18.43	-18.07	-18.53
$^{29}K \rightarrow ^{28} Ar$	8.531	2	-21.71	-19.85	-21.04	-20.99	$^{60}As \rightarrow ^{59} Ge$	3.312	3	-17.81	-18.22	-17.35	-18.03
$^{30}K \rightarrow ^{29} Ar$	5.381	2	-21.05	-19.57	-20.84	-20.52	$^{61}As \rightarrow ^{60} Ge$	2.427	3	-16.40	-17.94	-17.19	-17.04
$^{31}K \rightarrow ^{30} Ar$	4.788	2	-21.31	-17.91	-20.60	-20.34	$^{62}As \rightarrow ^{61} Ge$	1.476	1	-15.20	-15.03	-15.24	-15.40
$^{32}K \rightarrow ^{31} Ar$	1.836	2	-18.21	-17.49	-17.81	-18.68	$^{59}Se \rightarrow ^{58} As$	2.321	3	-15.98	-15.47	-16.09	-17.03
$^{30}Ca \rightarrow ^{29} K$	4.021	2	-20.29	-16.82	-19.97	-20.17	$^{60}Se \rightarrow ^{59} As$	1.241	3	-12.29	-12.26	-13.17	-13.29
$^{31}Ca \rightarrow ^{30} K$	3.391	2	-19.50	-18.18	-19.53	-19.88	$^{61}Se \rightarrow ^{60} As$	1.14	3	-11.71	-11.14	-13.30	-13.70
$^{32}Ca \rightarrow ^{31} K$	1.381	2	-17.44	-15.19	-16.44	-17.98	$^{62}Se \rightarrow ^{61} As$	0.993	3	-14.30	-11.99	-12.32	-12.74
$^{33}Ca \rightarrow ^{32} K$	1.073	2	-18.72	-17.01	-15.41	-17.11	$^{63}Se \rightarrow ^{62} As$	0.745	1	-12.01	-10.79	-11.54	-11.26
$^{32}Sc \rightarrow ^{31} Ca$	4.701	3	-20.73	-17.12	-19.36	-20.18	$^{61}Br \rightarrow ^{60} Se$	5.281	3	-19.42	-18.66	-19.08	-19.06
$^{33}Sc \rightarrow ^{32} Ca$	6.111	3	-21.26	-19.66	-20.03	-20.45	$^{62}Br \rightarrow ^{61} Se$	4.871	3	-19.13	-18.50	-18.78	-18.86
$^{34}Sc \rightarrow ^{33} Ca$	4.301	3	-19.17	-16.71	-19.17	-19.96	$^{63}Br \rightarrow ^{62} Se$	4.061	3	-18.45	-18.22	-18.05	-18.39
$^{35}Sc \rightarrow ^{34} Ca$	4.608	3	-19.89	-18.62	-19.27	-20.01	$^{64}Br \rightarrow ^{63} Se$	3.041	1	-18.48	-17.90	-18.61	-17.83
$^{36}Sc \rightarrow ^{35} Ca$	2.007	3	-17.24	-17.67	-17.09	-18.40	$^{65}Br \rightarrow ^{64} Se$	2.651	3	-16.57	-17.74	-18.01	-17.06
$^{34}Ti \rightarrow ^{33} Sc$	1.931	5	-16.18	-17.15	-18.02	-18.23	$^{66}Br \rightarrow ^{65} Se$	2.05	1	-16.65	-17.55	-17.95	-16.41
$^{35}Ti \rightarrow ^{34} Sc$	1.981	5	-16.31	-17.65	-18.14	-18.21	$^{63}Kr \rightarrow ^{62} Br$	2.361	3	-16.46	-17.74	-17.30	-16.81
$^{36}Ti \rightarrow ^{35} Sc$	1.191	5	-17.65	-16.71	-15.83	-16.54	$^{64}Kr \rightarrow ^{63} Br$	1.331	3	-12.31	-14.59	-13.93	-17.12
$^{37}Ti \rightarrow ^{36} Sc$	1.443	3	-17.63	-17.34	-18.49	-17.40	$^{65}Kr \rightarrow ^{64} Br$	1.031	1	-18.27	-14.41	-13.50	-13.18
$^{36}V \rightarrow ^{35} Ti$	5.611	3	-20.33	-18.90	-19.70	-20.22	$^{66}Rb \rightarrow ^{65} Kr$	4.691	1	-19.93	-18.20	-20.12	-18.80
$^{37}V \rightarrow ^{36} Ti$	4.891	3	-19.98	-17.58	-19.31	-20.00	$^{67}Rb \rightarrow ^{66} Kr$	4.331	3	-18.55	-18.05	-18.18	-18.36
$^{38}V \rightarrow ^{37} Ti$	3.921	3	-19.36	-17.81	-18.64	-19.61	$^{68}Rb \rightarrow ^{67} Kr$	3.381	1	-18.70	-17.73	-18.84	-17.90
$^{39}V \rightarrow ^{38} Ti$	3.47	3	-19.05	-15.30	-18.26	-19.34	$^{69}Rb \rightarrow ^{68} Kr$	3.181	3	-18.24	-17.64	-18.63	-17.40
$^{40}V \rightarrow ^{39} Ti$	1.541	1	-18.08	-16.54	-17.54	-17.69	$^{70}Rb \rightarrow ^{69} Kr$	1.766	3	-16.00	-17.21	-15.61	-15.06
$^{38}Cr \rightarrow ^{37} V$	2.651	5	-15.31	-15.83	-18.79	-16.67	$^{68}Sr \rightarrow ^{67} Rb$	1.071	3	-10.18	-14.06	-11.86	-12.45
$^{39}Cr \rightarrow ^{38} V$	2.181	3	-18.01	-16.78	-19.47	-18.36	$^{69}Sr \rightarrow ^{68} Rb$	0.911	1	-12.99	-13.95	-10.28	-11.83
$^{40}Cr \rightarrow ^{39} V$	0.891	5	-17.59	-13.16	-13.44	-16.54	$^{70}Y \rightarrow ^{69} Sr$	4.041	1	-19.20	-17.75	-19.35	-18.27
$^{40}Mn \rightarrow ^{39} Cr$	5.461	3	-20.65	-16.56	-19.57	-20.01	$^{71}Y \rightarrow ^{70} Sr$	3.941	1	-19.12	-17.68	-19.26	-18.16
$^{41}Mn \rightarrow ^{40} Cr$	4.791	3	-20.68	-17.93	-19.18	-19.78	$^{72}Y \rightarrow ^{71} Sr$	2.781	1	-16.97	-17.30	-17.65	-17.08
$^{42}Mn \rightarrow ^{41} Cr$	3.851	1	-19.10	-17.85	-20.35	-19.58	$^{73}Y \rightarrow ^{72} Sr$	2.771	1	-17.01	-17.26	-17.64	-17.00
$^{43}Mn \rightarrow ^{42} Cr$	1.741	3	-20.70	-16.25	-18.59	-19.75	$^{74}Y \rightarrow ^{73} Sr$	1.06	1	-13.21	-13.60	-11.31	-12.23
$^{42}Fe \rightarrow ^{41} Mn$	1.991	5	-16.42	-13.38	-17.43	-15.85	$^{72}Zr \rightarrow ^{71} Y$	1.541	1	-14.83	-16.94	-13.85	-14.65
$^{43}Fe \rightarrow ^{42} Mn$	1.861	1	-18.88	-16.22	-17.71	-17.96	$^{73}Zr \rightarrow ^{72} Y$	1.471	1	-13.56	-16.86	-13.54	-14.31
$^{44}Fe \rightarrow ^{43} Mn$	1.311	5	-18.78	-16.59	-15.72	-16.95	$^{74}Zr \rightarrow ^{73} Y$	0.421	1	-2.03	-2.03	-4.37	-3.05
$^{44}Co \rightarrow ^{43} Fe$	5.231	1	-20.49	-17.80	-20.83	-19.96	$^{74}Nb \rightarrow ^{73} Zr$	4.121	2	-18.67	-17.51	-18.60	-18.00
$^{45}Co \rightarrow ^{44} Fe$	3.811	3	-18.68	-17.49	-18.29	-19.18	$^{75}Nb \rightarrow ^{74} Zr$	4.481	4	-17.53	-17.58	-16.99	-17.99
$^{46}Co \rightarrow ^{45} Fe$	2.462	1	-18.55	-16.22	-18.71	-18.44	$^{76}Nb \rightarrow ^{75} Zr$	3.581	2	-18.07	-17.27	-17.96	-17.50
$^{47}Co \rightarrow ^{46} Fe$	2.659	3	-17.43	-17.47	-19.88	-18.27	$^{77}Nb \rightarrow ^{76} Zr$	3.321	4	-16.86	-17.13	-17.05	-16.98
$^{46}Ni \rightarrow ^{45} Co$	2.721	5	-19.46	-16.23	-18.61	-18.19	$^{78}Nb \rightarrow ^{77} Zr$	2.461	2	-16.45	-16.84	-16.39	-16.06
$^{47}Ni \rightarrow ^{46} Co$	1.581	1	-16.51	-16.37	-16.58	-17.11	$^{77}Mo \rightarrow ^{76} Nb$	1.271	2	-13.45	-10.01	-11.10	-13.76
$^{48}Ni \rightarrow ^{47} Co$	0.405	5	-8.45	-7.84	-8.04	-7.30	$^{78}Mo \rightarrow ^{77} Nb$	1.121	4	-9.36	-9.87	-10.28	-11.23
$^{48}Cu \rightarrow ^{47} Ni$	5.481	3	-19.77	-18.00	-19.46	-19.68	$^{79}Mo \rightarrow ^{78} Nb$	1.551	2	-13.77	-16.50	-12.69	-13.76
$^{49}Cu \rightarrow ^{48} Ni$	3.994	1	-19.97	-17.20	-20.15	-19.28	$^{82}Mo \rightarrow ^{81} Nb$	0.599	4	-7.62	-8.14	-5.27	-4.42
$^{50}Cu \rightarrow ^{49} Ni$	2.843	1	-18.89	-16.63	-19.00	-18.51	$^{79}Tc \rightarrow ^{78} Mo$	3.901	4	-16.72	-17.12	-18.38	-16.54
$^{51}Cu \rightarrow ^{50} Ni$	2.442	1	-18.32	-16.41	-18.44	-18.07	$^{80}Tc \rightarrow ^{79} Mo$	2.881	2	-16.73	-16.77	-16.54	-16.54

Table 3.4 Tabulation of one proton radioactivity in the atomic number range $43 \leq Z \leq 105$ using theoretical models such as CPPM, ELDM, MGLDM and semi-empirical formula (PF). Table 3.3 continued.

Reaction	Q_{1p} (MeV)	l_{min}	$LogT_{1/2}(s)$				Reaction	Q_{1p} (MeV)	l_{min}	$LogT_{1/2}(s)$			
			CPPM	ELDM	MGLDM	PF				CPPM	ELDM	MGLDM	PF
$^{81}Tc \rightarrow ^{80} Mo$	3.961	4	-18.67	-17.06	-16.24	-17.34	$^{115}Ce \rightarrow ^{114} La$	0.891	4	-5.67	-3.44	-4.21	-3.90
$^{82}Tc \rightarrow ^{81} Mo$	3.221	4	-16.37	-16.78	-17.45	-16.59	$^{115}Pr \rightarrow ^{114} Ce$	3.861	3	-15.95	-15.17	-17.70	-15.67
$^{83}Tc \rightarrow ^{82} Mo$	1.651	4	-12.69	-16.27	-13.23	-13.36	$^{116}Pr \rightarrow ^{115} Ce$	3.061	3	-15.62	-14.19	-16.20	-14.52
$^{84}Tc \rightarrow ^{83} Mo$	3.509	4	-17.52	-16.79	-17.91	-16.78	$^{117}Pr \rightarrow ^{116} Ce$	2.811	3	-13.99	-14.06	-15.61	-14.01
$^{81}Ru \rightarrow ^{80} Tc$	1.471	2	-11.41	-12.89	-13.76	-13.26	$^{118}Pr \rightarrow ^{117} Ce$	1.821	3	-10.23	-10.57	-12.00	-11.10
$^{82}Ru \rightarrow ^{81} Tc$	0.591	4	-6.74	-6.91	-4.75	-4.25	$^{119}Pr \rightarrow ^{118} Ce$	1.411	3	-8.15	-9.04	-9.46	-8.83
$^{83}Ru \rightarrow ^{82} Tc$	1.721	4	-13.90	-16.25	-13.35	-13.61	$^{118}Nd \rightarrow ^{117} Pr$	1.131	3	-7.96	-4.56	-6.66	-6.68
$^{84}Ru \rightarrow ^{83} Tc$	0.921	4	-8.57	-9.09	-7.92	-8.84	$^{120}Pm \rightarrow ^{119} Nd$	3.461	3	-14.96	-14.01	-14.65	-14.91
$^{86}Ru \rightarrow ^{85} Tc$	1.936	4	-16.10	-16.16	-14.23	-14.01	$^{121}Pm \rightarrow ^{120} Nd$	3.301	3	-15.94	-14.59	-14.31	-14.62
$^{83}Rh \rightarrow ^{82} Ru$	3.861	4	-16.47	-16.82	-18.17	-17.16	$^{122}Pm \rightarrow ^{121} Nd$	2.361	3	-12.25	-13.52	-11.62	-12.63
$^{84}Rh \rightarrow ^{83} Ru$	2.571	4	-14.09	-16.39	-15.93	-15.56	$^{123}Pm \rightarrow ^{122} Nd$	1.981	3	-10.41	-12.60	-10.03	-11.32
$^{85}Rh \rightarrow ^{84} Ru$	2.441	4	-15.76	-16.30	-15.61	-15.26	$^{123}Sm \rightarrow ^{122} Pm$	1.371	3	-6.30	-5.11	-5.91	-8.13
$^{86}Rh \rightarrow ^{85} Ru$	1.701	4	-13.18	-16.06	-13.09	-13.27	$^{125}Eu \rightarrow ^{124} Sm$	3.981	3	-15.71	-15.48	-15.43	-15.31
$^{87}Rh \rightarrow ^{86} Ru$	1.491	4	-13.30	-15.93	-12.07	-12.33	$^{126}Eu \rightarrow ^{125} Sm$	3.191	3	-14.45	-14.21	-15.32	-14.16
$^{88}Rh \rightarrow ^{87} Ru$	3.94	4	-18.62	-16.63	-18.32	-16.98	$^{127}Eu \rightarrow ^{126} Sm$	2.701	3	-12.10	-13.26	-14.02	-13.14
$^{90}Pd \rightarrow ^{89} Rh$	1.139	4	-12.97	-12.01	-11.17	-10.53	$^{128}Eu \rightarrow ^{127} Sm$	2.011	2	-13.06	-12.97	-10.63	-11.24
$^{89}Ag \rightarrow ^{88} Pd$	2.381	4	-14.30	-15.99	-16.72	-14.86	$^{129}Eu \rightarrow ^{128} Sm$	1.459	3	-8.39	-8.05	-6.42	-8.12
$^{90}Ag \rightarrow ^{89} Pd$	1.561	4	-15.30	-15.71	-13.68	-13.35	$^{128}Gd \rightarrow ^{127} Eu$	1.061	3	-2.55	-4.31	-2.43	-4.65
$^{91}Ag \rightarrow ^{90} Pd$	1.401	4	-11.51	-11.97	-12.80	-11.48	$^{130}Tb \rightarrow ^{129} Gd$	3.171	2	-13.29	-13.14	-14.27	-14.05
$^{92}Ag \rightarrow ^{91} Pd$	2.914	4	-16.69	-16.01	-17.95	-15.60	$^{131}Tb \rightarrow ^{130} Gd$	2.771	2	-14.80	-12.96	-13.18	-13.21
$^{92}In \rightarrow ^{91} Cd$	2.331	4	-12.84	-15.73	-14.77	-13.54	$^{132}Tb \rightarrow ^{131} Gd$	2.071	2	-10.39	-12.65	-10.52	-11.15
$^{93}In \rightarrow ^{92} Cd$	2.121	4	-12.15	-15.63	-14.10	-13.96	$^{133}Tb \rightarrow ^{132} Gd$	1.971	2	-10.23	-12.56	-10.04	-10.68
$^{94}In \rightarrow ^{93} Cd$	1.331	4	-8.21	-11.54	-10.23	-9.77	$^{136}Ho \rightarrow ^{135} Dy$	2.151	0	-11.21	-12.34	-11.36	-11.84
$^{95}In \rightarrow ^{94} Cd$	1.161	4	-9.90	-11.42	-8.92	-9.51	$^{137}Ho \rightarrow ^{136} Dy$	2.021	2	-10.08	-12.25	-9.90	-10.56
$^{97}Sb \rightarrow ^{96} Sn$	5.731	4	-18.06	-16.52	-19.62	-17.75	$^{141}Tm \rightarrow ^{140} Er$	2.331	0	-9.21	-12.00	-11.77	-10.04
$^{98}Sb \rightarrow ^{97} Sn$	5.011	4	-17.39	-16.21	-19.05	-17.31	$^{142}Tm \rightarrow ^{141} Er$	1.831	0	-9.13	-11.77	-9.28	-10.12
$^{99}Sb \rightarrow ^{98} Sn$	5.001	4	-17.39	-16.17	-19.05	-17.26	$^{143}Tm \rightarrow ^{142} Er$	1.801	0	-8.96	-10.43	-9.11	-9.89
$^{100}Sb \rightarrow ^{99} Sn$	2.58	4	-15.20	-15.30	-15.25	-14.51	$^{146}Lu \rightarrow ^{145} Yb$	2.401	5	-10.64	-11.65	-10.10	-10.74
$^{101}Sb \rightarrow ^{100} Sn$	2.891	4	-14.13	-15.35	-16.03	-15.01	$^{147}Lu \rightarrow ^{146} Yb$	2.081	5	-7.14	-10.16	-8.61	-9.46
$^{99}Te \rightarrow ^{98} Sb$	2.911	4	-14.01	-15.40	-15.93	-15.16	$^{148}Lu \rightarrow ^{147} Yb$	1.581	5	-5.94	-6.05	-5.42	-6.63
$^{100}Te \rightarrow ^{99} Sb$	1.911	4	-13.81	-15.03	-14.47	-12.78	$^{149}Lu \rightarrow ^{148} Yb$	1.919	5	-10.78	-9.99	-7.73	-8.55
$^{101}Te \rightarrow ^{100} Sb$	2.121	4	-15.60	-15.05	-15.28	-13.35	$^{151}Ta \rightarrow ^{150} Hf$	2.361	5	-8.14	-11.21	-7.55	-10.25
$^{102}Te \rightarrow ^{101} Sb$	1.281	4	-7.83	-10.75	-10.92	-9.56	$^{152}Ta \rightarrow ^{151} Hf$	1.781	5	-5.97	-8.67	-6.46	-7.54
$^{103}Te \rightarrow ^{102} Sb$	0.951	4	-7.51	-8.00	-7.79	-6.45	$^{153}Ta \rightarrow ^{152} Hf$	1.691	5	-5.34	-5.60	-5.84	-6.89
$^{101}I \rightarrow ^{100} Te$	5.731	4	-17.91	-16.22	-16.55	-17.60	$^{154}Ta \rightarrow ^{153} Hf$	1.233	5	-4.23	-5.28	-4.03	-2.85
$^{102}I \rightarrow ^{101} Te$	4.801	4	-17.01	-16.37	-19.93	-17.00	$^{155}Ta \rightarrow ^{154} Hf$	1.451	5	-2.4	-2.68	-2.12	-4.90
$^{103}I \rightarrow ^{102} Te$	5.141	4	-17.38	-16.45	-20.20	-17.19	$^{156}Re \rightarrow ^{155} W$	1.951	5	-8.74	-9.27	-7.17	-8.12
$^{104}I \rightarrow ^{103} Te$	3.901	4	-15.82	-16.00	-19.01	-16.15	$^{157}Re \rightarrow ^{156} W$	1.821	5	-4.83	-9.17	-6.35	-7.63
$^{105}I \rightarrow ^{104} Te$	3.601	4	-15.34	-15.28	-18.60	-15.77	$^{164}Ir \rightarrow ^{163} Os$	1.57	5	-4.52	-7.53	-4.06	-4.96
$^{106}I \rightarrow ^{105} Te$	2.76	4	-14.05	-14.95	-17.02	-14.47	$^{169}Au \rightarrow ^{168} Pt$	1.961	5	-4.98	-9.70	-6.53	-7.09
$^{107}I \rightarrow ^{106} Te$	2.405	4	-14.96	-14.78	-16.10	-13.65	$^{170}Au \rightarrow ^{169} Pt$	1.474	5	-2.29	-3.77	-2.75	-3.53
$^{103}Xe \rightarrow ^{102} I$	3.251	4	-16.52	-15.19	-17.91	-15.43	$^{173}Tl \rightarrow ^{172} Hg$	1.798	5	-3.45	-7.77	-5.03	-5.76
$^{104}Xe \rightarrow ^{103} I$	2.441	4	-14.45	-14.89	-16.04	-13.94	$^{175}Tl \rightarrow ^{174} Hg$	1.478	5	-2.39	-2.68	-2.36	-3.04
$^{105}Xe \rightarrow ^{104} I$	2.421	4	-14.22	-14.84	-15.99	-13.82	$^{178}Bi \rightarrow ^{177} Pb$	3.571	3	-12.54	-11.39	-13.94	-12.03
$^{106}Xe \rightarrow ^{105} I$	1.651	4	-9.15	-10.46	-12.91	-11.23	$^{179}Bi \rightarrow ^{178} Pb$	3.413	5	-10.53	-10.40	-12.05	-11.40
$^{107}Xe \rightarrow ^{106} I$	0.921	4	-6.84	-4.67	-7.07	-5.50	$^{180}Bi \rightarrow ^{179} Pb$	2.808	3	-10.14	-9.17	-11.59	-10.06
$^{106}Cs \rightarrow ^{105} Xe$	4.821	4	-16.86	-16.11	-19.85	-16.84	$^{181}Bi \rightarrow ^{180} Pb$	3.18	5	-9.82	-10.21	-11.37	-10.74
$^{107}Cs \rightarrow ^{106} Xe$	4.541	4	-16.53	-16.78	-19.60	-16.59	$^{182}Bi \rightarrow ^{181} Pb$	2.266	3	-7.73	-8.83	-9.22	-7.94
$^{108}Cs \rightarrow ^{107} Xe$	3.621	4	-15.15	-15.04	-18.46	-15.64	$^{183}Bi \rightarrow ^{182} Pb$	2.557	5	-7.47	-8.91	-9.04	-8.72
$^{109}Cs \rightarrow ^{108} Xe$	3.401	4	-14.76	-16.38	-18.11	-15.30	$^{184}At \rightarrow ^{183} Po$	2.101	3	-6.22	-8.49	-7.91	-6.99
$^{110}Cs \rightarrow ^{109} Xe$	1.981	4	-13.10	-14.39	-14.32	-12.20	$^{185}At \rightarrow ^{184} Po$	1.901	5	-3.40	-4.12	-5.01	-5.37
$^{111}Cs \rightarrow ^{110} Xe$	2.426	4	-12.30	-14.49	-15.91	-13.42	$^{189}Fr \rightarrow ^{188} Rn$	2.271	5	-5.33	-8.14	-6.95	-7.08
$^{108}Ba \rightarrow ^{107} Cs$	2.391	4	-14.91	-14.55	-15.64	-13.54	$^{190}Fr \rightarrow ^{189} Rn$	1.851	5	-4.62	-6.34	-4.25	-4.60
$^{109}Ba \rightarrow ^{108} Cs$	2.231	4	-13.43	-14.45	-15.11	-13.05	$^{191}Fr \rightarrow ^{190} Rn$	1.761	5	-3.92	-3.48	-3.56	-3.86
$^{110}Ba \rightarrow ^{109} Cs$	1.181	4	-5.21	-5.74	-9.13	-7.86	$^{195}Ac \rightarrow ^{194} Ra$	2.161	5	-5.24	-7.63	-5.97	-6.07
$^{111}Ba \rightarrow ^{110} Cs$	0.931	4	-5.37	-4.06	-6.74	-5.05	$^{200}Pa \rightarrow ^{199} Th$	2.111	1	-5.61	-7.22	-7.77	-6.29
$^{110}La \rightarrow ^{109} Ba$	4.421	4	-16.18	-16.54	-19.35	-16.35	$^{201}Pa \rightarrow ^{200} Th$	2.091	5	-4.43	-7.18	-5.18	-5.20
$^{111}La \rightarrow ^{110} Ba$	4.321	4	-16.05	-15.61	-19.25	-16.22	$^{213}Am \rightarrow ^{212} Pu$	1.951	3	-3.35	-3.46	-5.00	-3.72
$^{112}La \rightarrow ^{111} Ba$	3.791	4	-16.29	-15.39	-18.56	-15.63	$^{219}Bk \rightarrow ^{218} Cm$	2.231	3	-4.17	-6.05	-6.53	-4.97
$^{113}La \rightarrow ^{112} Ba$	3.071	4	-14.78	-14.48	-17.30	-14.59	$^{220}Bk \rightarrow ^{219} Cm$	1.841	3	-4.36	-4.71	-3.73	-3.30
$^{114}La \rightarrow ^{113} Ba$	1.891	4	-10.54	-14.02	-13.61	-11.54	$^{224}Es \rightarrow ^{223} Cf$	2.181	3	-4.44	-5.67	-5.84	-4.29
$^{115}La \rightarrow ^{114} Ba$	2.517	4	-14.34	-14.18	-15.92	-13.36	$^{225}Es \rightarrow ^{224} Cf$	2.181	3	-4.17	-5.65	-5.85	-4.22
$^{113}Ce \rightarrow ^{112} La$	1.971	4	-13.01	-14.04	-13.78	-11.92	$^{235}Lr \rightarrow ^{234} No$	2.161	3	-4.50	-4.95	-4.95	-3.30
$^{114}Ce \rightarrow ^{113} La$	1.491	4	-8.05	-9.48	-11.16	-9.63	$^{241}Db \rightarrow ^{240} Rf$	2.131	3	-2.63	-4.57	-2.43	-2.63

Table 3.5 Comparison of 2P decay logarithmic half lives obtained using CPPM, ELDM, MGLDM and present formula (PF) with that of experiments and theoretical data available in literature [160].

Reaction	Q_{2P}	$J_i \rightarrow J_f$	ℓ	$LogT_{1/2}$						
				Exp	CPPM	ELDM	MGLDM	PF	Direct [160]	Diproton [160]
$^{6}Be \rightarrow ^{4}He$	1.371	$0^+ \rightarrow 0^+$	0	-19.51	-19.573±0.003	-19.51±0	-20.135±0.3	-20.48±0.04	-	-
$^{12}O \rightarrow ^{10}C$	1.79	$0^+ \rightarrow 0^+$	0	-20.31	-20.035±0.01	-19.855±0.02	-19.861±0.02	-20.04±0.01	-	-
$^{16}Ne \rightarrow ^{14}O$	1.4	$0^+ \rightarrow 0^+$	0	-19.58	-19.171±0.02	-18.365±0.06	-18.205±0.07	-19.82±0.01	-	-
$^{19}Mg \rightarrow ^{17}Ne$	0.75	$1/2^-\# \rightarrow 1/2^-$	0	-11.4	-10.58±0.07	-12.889±0.13	-13.286±0.16	-13.42±0.17	-11.21	-10.91
$^{45}Fe \rightarrow ^{43}Cr$	1.14	$3/2^+\# \rightarrow 3/2^+$	0	-2.07	-1.971±0.04	-2.195±0.06	-4.687±1.26	-3.82±0.84	-2.96	-2.06
$^{48}Ni \rightarrow ^{46}Fe$	1.29	$0^+ \rightarrow 0^+$	0	-2.52	-2.018±0.19	-2.235±0.11	-4.649±0.84	-4.06±0.61	-2.17	-2.28
$^{54}Zn \rightarrow ^{52}Ni$	1.48	$0^+ \rightarrow 0^+$	0	-2.43	-2.452±0.01	-2.588±0.06	-5.19±1.13	-4.16±0.71	-3.00	-3.10
$^{67}Kr \rightarrow ^{65}Se$	1.69	$3/2^- \rightarrow 3/2^-\#$	0	-1.7	-1.659±0.02	-1.671±0.01	-2.877±0.69	-2.18±0.28	-	-

atomic number region $3 \leq Z \leq 65$. Eventually it is also observed that two proton radioactivity is not energetically feasible when $Z > 65$. Among these nuclei 8 two proton emitters are experimentally observed and it is tabulated in the table 3.5. We have also compared $\log T_{1/2}$ predicted from earlier researchers [160] for two proton decay using direct and diproton models. Remaining 174 two proton emitters are newly identified and tabulated along with their half-lives and decay energies in the table 3.6. Even-though, around 174 two proton emitters with positive Q-value were identified but comparison of logarithmic half-lives with other decay modes may result in most dominant decay mode. Hence, table 3.6 only gives the prediction of two-proton logarithmic half-lives. Even though, identified one and two proton emitters along with half lives and decay energies are based on theory, but it gives blueprint in the experiments of proton radioactivity and also comparison with other possible decay modes.

It can also be noticed from the experiment that the nuclei ^{45}Fe shows the half-life of $3.2^{+2.6}_{-1.0}$ms for the Q-value of 1.1 ± 0.1MeV[91]. Giovinazzo et al.,[67] experimentally observed decay energy spectrum at 1.14 ± 0.04MeV with the half-life of $4.7^{+3.4}_{-1.4}$ms. These experimentally observed 2p radioactivity was good agreement with the theoretically predicted half-lives [85, 281]. From these experimental values, The half-lives are obviously influenced by the decay energy. A small change in the value of decay energy results in the measurable change in the half-lives.

The one and two proton radioactivity half-lives studied using the well accepted theoretical models such as CPPM, ELDM and MGLDM are compared with that of available experiments.

Table 3.6 Tabulation of two proton radioactivity in the atomic number range $3 \leq Z \leq 65$ using theoretical models such as CPPM, ELDM, MGLDM and semi-empirical formula (PF).

Reaction	Q_{2p} (MeV)	l_{min}	$LogT_{1/2}(s)$				Reaction	Q_{2p} (MeV)	l_{min}	$LogT_{1/2}(s)$			
			CPPM	ELDM	MGLDM	PF				CPPM	ELDM	MGLDM	PF
$^{3}Li \rightarrow ^{1} H$	6.8	1	-19.85	-19.85	-19.85	-20.80	$^{62}Se \rightarrow ^{60} Ge$	3.42	0	-13.71	-15.38	-13.14	-12.92
$^{5}Be \rightarrow ^{3} He$	8.48	0	-20.58	-19.85	-20.92	-20.81	$^{63}Se \rightarrow ^{61} Ge$	2.22	0	-7.07	-7.91	-8.13	-8.38
$^{6}Be \rightarrow ^{4} He$	1.37	0	-18.59	-18.23	-20.13	-20.38	$^{61}Br \rightarrow ^{59} As$	6.52	0	-18.07	-16.43	-18.38	-16.77
$^{6}B \rightarrow ^{4} Li$	3.7	0	-20.02	-19.85	-19.87	-20.67	$^{63}Br \rightarrow ^{61} As$	5.05	0	-16.18	-17.01	-16.43	-15.54
$^{7}B \rightarrow ^{5} Li$	1.61	1	-18.44	-18.36	-19.9	-19.92	$^{64}Br \rightarrow ^{62} As$	3.78	0	-13.57	-15.28	-13.79	-13.34
$^{8}C \rightarrow ^{6} Be$	2.14	0	-17.41	-18.19	-20.28	-18.33	$^{65}Br \rightarrow ^{63} As$	2.53	0	-9.15	-9.36	-9.29	-9.40
$^{10}N \rightarrow ^{8} B$	1.3	2	-18.08	-18.11	-18.33	-18.93	$^{63}Kr \rightarrow ^{61} Se$	7.23	0	-17.79	-17.04	-18.96	-17.00
$^{12}O \rightarrow ^{10} C$	1.77	0	-18.13	-18.62	-19.83	-19.58	$^{64}Kr \rightarrow ^{62} Se$	5.39	0	-15.57	-17.01	-16.67	-15.57
$^{14}F \rightarrow ^{12} N$	0.74	3	-14.25	-15.98	-14.93	-15.51	$^{65}Kr \rightarrow ^{63} Se$	4.07	0	-13.04	-15.24	-14.14	-13.71
$^{16}Ne \rightarrow ^{14} O$	1.40	0	-19.58	-19.17	-18.36	-18.30	$^{66}Kr \rightarrow ^{64} Se$	2.66	0	-8.32	-9.17	-9.33	-9.72
$^{19}Mg \rightarrow ^{17} Ne$	0.75	0	-10.58	-12.89	-13.28	-12.65	$^{67}Kr \rightarrow ^{65} Se$	1.69	0	-1.66	-1.67	-2.87	-2.98
$^{23}P \rightarrow ^{21} Al$	4.96	2	-19.49	-19.5	-20.24	-19.25	$^{66}Rb \rightarrow ^{64} Br$	5.72	0	-16.67	-16.91	-16.91	-15.65
$^{24}S \rightarrow ^{22} Si$	8.99	0	-20.36	-19.85	-20.95	-20.09	$^{67}Rb \rightarrow ^{65} Br$	4.34	0	-13.33	-15.1	-14.43	-13.86
$^{25}S \rightarrow ^{23} Si$	5.05	0	-19.9	-19.38	-20.7	-19.42	$^{68}Rb \rightarrow ^{66} Br$	3.23	0	-10.19	-10.5	-11.26	-11.27
$^{26}S \rightarrow ^{24} Si$	0.63	0	-6.46	-8.19	-7.47	-8.95	$^{69}Rb \rightarrow ^{67} Br$	2.3	0	-5.88	-4.92	-6.87	-7.13
$^{25}Cl \rightarrow ^{23} P$	9.78	2	-18.69	-19.85	-20.98	-19.93	$^{68}Sr \rightarrow ^{66} Kr$	5.4	0	-15.05	-15.33	-16.15	-15.10
$^{26}Cl \rightarrow ^{24} P$	7.73	2	-19.61	-18.25	-20.88	-19.63	$^{69}Sr \rightarrow ^{67} Kr$	4.29	0	-12.88	-14.88	-13.99	-13.47
$^{27}Cl \rightarrow ^{25} P$	5.84	2	-19.72	-18.21	-20.58	-19.16	$^{70}Sr \rightarrow ^{68} Kr$	3.09	0	-9.23	-10.11	-10.26	-10.41
$^{28}Cl \rightarrow ^{26} P$	1	2	-10.06	-11.04	-10.14	-10.65	$^{71}Sr \rightarrow ^{69} Kr$	2	0	-3.3	-3.18	-4.27	-4.43
$^{27}Ar \rightarrow ^{25} S$	6.73	0	-19.52	-18.54	-20.82	-19.64	$^{70}Y \rightarrow ^{68} Rb$	4.95	0	-14.86	-14.94	-15.07	-14.31
$^{28}Ar \rightarrow ^{26} S$	5.26	0	-19.61	-19.19	-20.65	-19.23	$^{71}Y \rightarrow ^{69} Rb$	3.85	2	-11.98	-13.71	-11.79	-11.39
$^{29}Ar \rightarrow ^{27} S$	3.28	0	-17.62	-18.47	-18.64	-18.12	$^{72}Y \rightarrow ^{70} Rb$	3.02	2	-9.11	-8.27	-8.87	-8.57
$^{30}Ar \rightarrow ^{28} S$	1.43	0	-12.22	-13.72	-13.25	-14.32	$^{73}Y \rightarrow ^{71} Rb$	1.71	2	-0.29	-0.16	-0.42	-0.10
$^{29}K \rightarrow ^{27} Cl$	7.76	0	-19.77	-18.27	-20.88	-19.68	$^{72}Zr \rightarrow ^{70} Sr$	5.48	0	-15.56	-14.89	-15.75	-14.70
$^{30}K \rightarrow ^{28} Cl$	6.94	0	-19.55	-18.31	-20.84	-19.48	$^{73}Zr \rightarrow ^{71} Sr$	4.25	0	-12.11	-13.6	-13.19	-12.78
$^{31}K \rightarrow ^{29} Cl$	4.43	0	-18.76	-18.69	-19.81	-18.61	$^{74}Zr \rightarrow ^{72} Sr$	3.19	2	-8.38	-9.49	-9.14	-8.78
$^{32}K \rightarrow ^{30} Cl$	1.39	0	-11.32	-11.08	-12.36	-13.45	$^{74}Nb \rightarrow ^{72} Y$	5.59	1	-15.38	-14.71	-15.5	-13.95
$^{30}Ca \rightarrow ^{28} Ar$	12.55	0	-20.76	-19.85	-21.09	-20.08	$^{75}Nb \rightarrow ^{73} Y$	4.9	5	-12.36	-14.38	-11.51	-12.83
$^{31}Ca \rightarrow ^{29} Ar$	8.77	0	-20.06	-19.85	-20.94	-19.71	$^{76}Nb \rightarrow ^{74} Y$	3.8	1	-11.37	-9.44	-11.32	-10.33
$^{32}Ca \rightarrow ^{30} Ar$	6.16	0	-19.03	-19.17	-20.78	-19.16	$^{77}Nb \rightarrow ^{75} Y$	2.73	5	-6.16	-7.29	-4.14	-5.97
$^{33}Ca \rightarrow ^{31} Ar$	2.9	0	-16.2	-18.02	-17.3	-17.12	$^{77}Mo \rightarrow ^{75} Zr$	4.85	0	-13.8	-14.14	-13.99	-13.21
$^{34}Ca \rightarrow ^{32} Ar$	0.77	0	-5.8	-5.92	-6.03	-6.30	$^{78}Mo \rightarrow ^{76} Zr$	4.44	0	-12.88	-13.9	-12.99	-12.35
$^{32}Sc \rightarrow ^{30} K$	8.09	5	-19.41	-19.68	-19.93	-19.31	$^{79}Mo \rightarrow ^{77} Zr$	4.01	0	-11.73	-12.85	-11.82	-11.27
$^{33}Sc \rightarrow ^{31} K$	7.49	3	-19.54	-19.48	-20.37	-19.12	$^{79}Tc \rightarrow ^{77} Nb$	5.02	0	-13.85	-13.94	-14.02	-13.19
$^{34}Sc \rightarrow ^{32} K$	5.37	5	-19.55	-18.74	-19.07	-18.34	$^{80}Tc \rightarrow ^{78} Nb$	4.43	0	-12.51	-12.83	-12.6	-12.02
$^{35}Sc \rightarrow ^{33} K$	3.7	3	-17.71	-18.11	-17.6	-17.08	$^{81}Tc \rightarrow ^{79} Nb$	3.71	0	-10.42	-8.63	-10.45	-10.13
$^{36}Sc \rightarrow ^{34} K$	0.8	3	-5.44	-5.31	-4.26	-3.50	$^{81}Tc \rightarrow ^{79} Nb$	2.88	0	-6.03	-6.56	-7.0	-7.06
$^{34}Ti \rightarrow ^{32} Ca$	8.04	0	-19.55	-19.52	-20.9	-19.43	$^{83}Tc \rightarrow ^{81} Nb$	2.25	0	-3.22	-2.07	-3.16	-2.60
$^{35}Ti \rightarrow ^{33} Ca$	6.28	0	-19.56	-18.92	-20.63	-18.95	$^{81}Ru \rightarrow ^{79} Mo$	4.35	0	-11.96	-12.64	-11.99	-11.70
$^{36}Ti \rightarrow ^{34} Ca$	5.79	0	-19.25	-18.71	-20.34	-18.71	$^{82}Ru \rightarrow ^{80} Mo$	4.55	0	-12.49	-12.6	-12.56	-11.94
$^{37}Ti \rightarrow ^{35} Ca$	3.45	0	-16.57	-17.85	-17.65	-17.13	$^{83}Ru \rightarrow ^{81} Mo$	4.94	0	-13.42	-13.51	-13.58	-12.50
$^{38}Ti \rightarrow ^{36} Ca$	0.96	0	-5.81	-7.01	-6.04	-7.08	$^{84}Ru \rightarrow ^{82} Mo$	2.57	0	-3.81	-3.1	-4.75	-4.58
$^{36}V \rightarrow ^{34} Sc$	7.59	0	-19.21	-19.22	-20.87	-19.21	$^{85}Ru \rightarrow ^{83} Mo$	4.25	0	-11.75	-13.12	-11.83	-10.82
$^{37}V \rightarrow ^{35} Sc$	6.08	0	-19.25	-18.68	-20.35	-18.73	$^{86}Ru \rightarrow ^{84} Mo$	2.78	0	-5.11	-5.94	-6.06	-5.29
$^{38}V \rightarrow ^{36} Sc$	5.36	0	-18.7	-18.37	-19.77	-18.35	$^{83}Rh \rightarrow ^{81} Tc$	4.45	0	-11.89	-11.93	-11.91	-11.58
$^{39}V \rightarrow ^{37} Sc$	2.44	0	-14.48	-17.36	-14.72	-15.19	$^{84}Rh \rightarrow ^{82} Tc$	4.29	0	-11.47	-11.79	-11.49	-11.08
$^{40}V \rightarrow ^{38} Sc$	0.68	0	-1.64	-1.18	-0.8	-0.70	$^{85}Rh \rightarrow ^{83} Tc$	3.36	0	-7.3	-7.79	-8.27	-8.17
$^{38}Cr \rightarrow ^{36} Ti$	7.54	0	-19.07	-19.04	-20.87	-19.07	$^{86}Rh \rightarrow ^{84} Tc$	2.44	0	-2.42	-1.38	-3.36	-3.13
$^{39}Cr \rightarrow ^{37} Ti$	6.1	0	-19.09	-18.5	-20.17	-18.57	$^{87}Rh \rightarrow ^{85} Tc$	3.42	0	-7.62	-7.64	-8.59	-7.98
$^{40}Cr \rightarrow ^{38} Ti$	4.36	0	-17.34	-17.86	-18.43	-17.55	$^{88}Rh \rightarrow ^{86} Tc$	2.51	0	-2.98	-2.45	-3.93	-3.05
$^{41}Cr \rightarrow ^{39} Ti$	1.62	0	-10.19	-11.94	-10.4	-11.70	$^{86}Pd \rightarrow ^{84} Ru$	2.9	0	-3.44	-5.63	-5.58	-4.93
$^{40}Mn \rightarrow ^{38} V$	7.64	0	-19.01	-18.89	-20.88	-18.95	$^{89}Pd \rightarrow ^{87} Ru$	3.25	0	-7.44	-5.53	-7.39	-6.86
$^{41}Mn \rightarrow ^{39} V$	5.68	0	-18.56	-18.19	-19.62	-18.21	$^{90}Pd \rightarrow ^{88} Ru$	1.83	0	-0.51	-0.72	-0.65	-0.34
$^{42}Mn \rightarrow ^{40} V$	3.93	0	-16.41	-17.54	-17.46	-16.92	$^{88}Ag \rightarrow ^{86} Rh$	2.86	0	-3.95	-3.45	-4.87	-4.90
$^{42}Fe \rightarrow ^{40} Cr$	6.78	0	-19.85	-18.42	-20.3	-18.56	$^{91}Ag \rightarrow ^{89} Rh$	2.54	0	-2.03	-2.35	-2.97	-2.39
$^{43}Fe \rightarrow ^{41} Cr$	5.71	0	-18.37	-18	-19.44	-18.04	$^{90}Cd \rightarrow ^{88} Pd$	2.9	0	-3.68	-4.9	-4.61	-4.93
$^{44}Fe \rightarrow ^{42} Cr$	3.05	0	-14.15	-14.08	-15.19	-15.44	$^{92}In \rightarrow ^{90} Ag$	2.7	0	-1.98	-2.53	-2.91	-3.21
$^{45}Fe \rightarrow ^{43} Cr$	1.13	0	-3.554	-4.42	-4.61	-5.85	$^{97}Sb \rightarrow ^{95} In$	5.1	2	-10.37	-11.84	-11.18	-9.90
$^{44}Co \rightarrow ^{42} Mn$	7.09	0	-19.26	-18.35	-20.38	-18.50	$^{99}Te \rightarrow ^{97} Sn$	7.92	0	-15.37	-14.35	-16.53	-14.41
$^{45}Co \rightarrow ^{43} Mn$	5.12	0	-17.53	-17.62	-18.61	-17.50	$^{100}Te \rightarrow ^{98} Sn$	6.91	0	-13.99	-13.52	-15.09	-13.05
$^{46}Co \rightarrow ^{44} Mn$	2.35	0	-12.22	-11.68	-12.42	-13.37	$^{101}Te \rightarrow ^{99} Sn$	4.7	0	-9.33	-8.12	-10.28	-9.25
$^{47}Co \rightarrow ^{45} Mn$	1.23	0	-4.83	-5.26	-5.0	-6.19	$^{102}Te \rightarrow ^{100} Sn$	4.17	0	-7.66	-6.67	-8.6	-7.60
$^{46}Ni \rightarrow ^{44} Fe$	6.53	0	-18.65	-17.95	-19.76	-18.14	$^{101}I \rightarrow ^{99} Sb$	7.64	0	-14.8	-14.06	-15.96	-13.70
$^{47}Ni \rightarrow ^{45} Fe$	4.04	0	-15.6	-17.09	-16.65	-16.34	$^{102}I \rightarrow ^{100} Sb$	6.92	0	-13.76	-13.74	-14.84	-12.84
$^{48}Ni \rightarrow ^{46} Fe$	1.29	0	-2.02	-2.23	-4.65	-2.32	$^{103}I \rightarrow ^{101} Sb$	6.42	0	-12.94	-12.62	-13.98	-12.10
$^{49}Ni \rightarrow ^{47} Fe$	1.04	0	-1.47	-1.02	-1.57	-2.40	$^{105}I \rightarrow ^{103} Sb$	3.16	0	-2.84	-3.29	-3.76	-2.65
$^{48}Cu \rightarrow ^{46} Co$	7.06	2	-18.53	-17.93	-19.51	-17.80	$^{103}Xe \rightarrow ^{101} Te$	8.05	0	-15.15	-13.52	-16.27	-13.86
$^{49}Cu \rightarrow ^{47} Co$	4.39	2	-16.37	-17	-16.35	-15.83	$^{104}Xe \rightarrow ^{102} Te$	7.58	0	-14.55	-13.29	-15.68	-13.33
$^{50}Cu \rightarrow ^{48} Co$	2.91	2	-14.43	-14.46	-13.13	-13.09	$^{105}Xe \rightarrow ^{103} Te$	6.32	2	-12.21	-11.35	-13.05	-11.12
$^{51}Zn \rightarrow ^{49} Ni$	5.46	0	-17.94	-17.15	-18.28	-17.09	$^{106}Xe \rightarrow ^{104} Te$	5.25	0	-10.18	-10.9	-11.15	-9.72
$^{52}Zn \rightarrow ^{50} Ni$	4.39	0	-15.67	-16.71	-16.71	-16.05	$^{107}Xe \rightarrow ^{105} Te$	3.68	0	-4.96	-4.46	-5.88	-4.78
$^{53}Zn \rightarrow ^{51} Ni$	3.04	0	-13.35	-16.19	-13.57	-13.74	$^{106}Cs \rightarrow ^{104} I$	7.24	0	-13.78	-11.54	-14.84	-12.76
$^{54}Zn \rightarrow ^{52} Ni$	1.48	0	-2.45	-2.58	-5.19	-3.68	$^{107}Cs \rightarrow ^{105} I$	6.19	0	-11.99	-11.06	-12.97	-11.27
$^{53}Ga \rightarrow ^{51} Cu$	7.38	0	-18.85	-17.58	-19.94	-17.90	$^{108}Cs \rightarrow ^{106} I$	4.54	0	-7.81	-8.73	-8.75	-7.64
$^{54}Ga \rightarrow ^{52} Cu$	5.68	0	-17.23	-16.93	-18.41	-16.92	$^{109}Cs \rightarrow ^{107} I$	3.25	0	-1.17	-1.95	-3.31	-2.18
$^{55}Ga \rightarrow ^{53} Cu$	3.56	0	-13.59	-15.15	-14.64	-14.44	$^{108}Ba \rightarrow ^{106} Xe$	6.93	0	-13.05	-11.15	-14.08	-12.18
$^{56}Ga \rightarrow ^{54} Cu$	2.37	0	-9.47	-10.69	-10.56	-10.11	$^{109}Ba \rightarrow ^{107} Xe$	5.85	0	-10.99	-10.67	-11.96	-10.45
$^{57}Ga \rightarrow ^{55} Cu$	1.14	0	-0.37	-0.22	-0.45	-0.35	$^{110}Ba \rightarrow ^{108} Xe$	4.58	0	-7.59	-6.73	-8.53	-7.41
$^{55}Ge \rightarrow ^{53} Zn$	6.71	0	-18.06	-17.15	-19.21	-17.43	$^{110}La \rightarrow ^{108} Cs$	6.65	0	-12.33	-10.8	-13.31	-11.57
$^{56}Ge \rightarrow ^{54} Zn$	5.33	0	-17.34	-16.6	-17.65	-16.44	$^{111}La \rightarrow ^{109} Cs$	5.5	0	-9.88	-10.27	-10.82	-9.50
$^{57}Ge \rightarrow ^{55} Zn$	4.36	0	-15.82	-16.2	-16.09	-15.33	$^{112}La \rightarrow ^{110} Cs$	4.72	0	-7.68	-9.93	-8.63	-7.47
$^{58}Ge \rightarrow ^{56} Zn$	2.77	0	-11.59	-12.61	-11.79	-11.97	$^{113}La \rightarrow ^{111} Cs$	3.27	0	-1.6	-1.18	-2.42	-1.32
$^{59}Ge \rightarrow ^{57} Zn$	1.22	0	-0.6	-0.79	-0.66	-0.42	$^{113}Ce \rightarrow ^{111} Ba$	5.76	0	-10.21	-10.11	-11.16	-9.73
$^{57}As \rightarrow ^{55} Ga$	6.73	0	-18.65	-16.93	-19.06	-17.26	$^{114}Ce \rightarrow ^{112} Ba$	4.56	0	-6.8	-7.87	-7.74	-6.65
$^{58}As \rightarrow ^{56} Ga$	5.63	4	-17.06	-16.49	-18.25	-15.92	$^{115}Pr \rightarrow ^{113} La$	5.35	2	-8.6	-9.69	-9.3	-7.68
$^{59}As \rightarrow ^{57} Ga$	4.18	0	-15.16	-15.94	-15.4	-14.80	$^{118}Nd \rightarrow ^{116} Ce$	3.94	0	-2.36	-2.56	-4.43	-3.60
$^{60}As \rightarrow ^{58} Ga$	3	3	-11.13	-11.48	-12.21	-11.21	$^{120}Pm \rightarrow ^{118} Pr$	4.2	0	-4.34	-2.3	-5.15	-4.28
$^{61}As \rightarrow ^{59} Ga$	1.49	2	-3.47	-3.9	-2.33	-2.06	$^{123}Sm \rightarrow ^{121} Nd$	3.73	0	-1.83	-1.63	-2.58	-1.53
$^{59}Se \rightarrow ^{57} Ge$	6.48	0	-17.43	-16.64	-18.58	-16.93	$^{125}Eu \rightarrow ^{123} Pm$	4.46	0	-4.64	-3.01	-5.43	-4.32
$^{60}Se \rightarrow ^{58} Ge$	5.18	0	-16.62	-16.12	-16.89	-15.84	$^{128}Gd \rightarrow ^{126} Sm$	3.76	0	-1.16	-0.82	-1.88	-1.57
$^{61}Se \rightarrow ^{59} Ge$	4.45	0	-16.15	-15.8	-15.63	-14.90	$^{130}Tb \rightarrow ^{128} Eu$	4.06	2	-1.94	-2.03	-2.47	-0.96

Table 3.2 and 3.5 summarises the half-lives obtained using the three models with available experimental values for one proton decay mode. From this observation, it is clear that the values obtained using the CPPM model are close to the experiments than that of the other two models. However, quite discrepancy has seen in case of the parent nuclei ^{146}Tm, ^{147}Tm, ^{156}Ta and ^{166}Ir. Similarly, the half-lives obtained using ELDM and MGLDM models are also producing experimental values successfully. Moreover, for the nuclei ^{177}Tl, ^{161}Re and ^{167}Ir the deviation produced by the ELDM lager when compared to CPPM and MGLDM. ^{146}Tm and ^{157}Ta will have change in the order of one magnitude when compared to experimental values in case of MGLDM. The overall deviation may vary between one or two magnitude of order using the three models, which are with in the limit of experimental error. Similarly, comparison is extended to two proton decay and the same is listed in table 3.5. From this comparison, it is noticed that although the three models used in the present work are quite good in agreement with that of available experiments. The semi-empirical formulae for one and two proton decay half-lives were constructed based on the half-lives produced by present work. Among these three models, the proton decay half-lives produced by the CPPM are closer to the experiments than that of other two models. Eventually, we have used the proton decay half-lives produced by CPPM for the construction of semi-empirical formulae. The uncertainty of the model is also included in the error associated with this calculation.From the table it is inferred that the standard deviation is smaller for 1P and 2P in CPPM when compared to ELDM and MGLDM.

Eventually, to know the predictive power of CPPM, ELDM and MGLDM in producing the proton decay logarithmic half-lives, we have also evaluated the mean squared error. The sum of squared residuals(SSR= $\sum_{i=1}^{n} e_i^2$) are calculated. Further, the mean squared errors ($\sigma^2 = \frac{SSR}{n-2}$) is evaluated. The evaluated mean squared error for CPPM, ELDM and MGLDM in predicting the one proton decay logarithmic half lives are 0.06, 0.13 and 0.14 respectively. Similarly, the mean

squared error for CPPM, ELDM and MGLDM in predicting the two proton decay logarithmic half-lives are 0.19, 0.67 and 1.1 respectively. From this analysis, it can be concluded that CPPM model produces one proton and two proton decay half-lives values close to experiments than the other two models.

CHAPTER 4

Competition between different decay modes

New isotopes were explored by studying the competition between different decay modes such as alpha-decay, beta-decay, spontaneous fission and proton-decay. Thus the proton decay half-lives evaluated using the present work is compared with that of other decay modes. The decay mode which is having smaller half-life than the other decay modes is identified as dominant decay mode. Eventually by studying the competition between different decay modes new proton emitters were explored in the different regions such as lanthanides, heavy nuclei, actinides and superheavy nuclei.

4.1 Method of Calculation of half-lives

According to WKB approximation (Wentzel-Kramers-Brillouin) of the penetration probability P through the potential barrier were studied for the cluster and alpha decay by the following equation;

$$P = \exp\left\{-\frac{2}{\hbar}\int_{R_a}^{R_b}\sqrt{2\mu(V-Q}dr\right\} \tag{4.1}$$

Where V is the potential and it is calculated using the procedure explained in the chapter 3. where μ is the reduced mass of proton decay system, R_a and R_b are the inner and outer turning points

and these turning points were evaluated using following conditions;

$$V_T(R_a) = Q = V_T(R_b) \tag{4.2}$$

The alpha decay half-life is studied using following equation ;

$$T_{1/2} = \frac{\ln 2}{\lambda} = \frac{\ln 2}{vPS_p} \tag{4.3}$$

Where λ is decay constant and v is the assault frequency. S_p is the spectroscopic factor and it is model dependent and very sensitive to decay energy. It is also evident from the literature [282, 283] that the spectroscopic factors are assumed as one in proton decay half-life calculation while using the WKB approximation. In the present work, we have used WKB approximation and accurate recent mass excess values in the calculation of decay energies. Thus the spectroscopic factors are assumed to be one. E_v is the empirical vibration energy and it is evaluated using the following equations;

$$v = \frac{\omega}{2\pi} = \frac{2E_v}{h} \tag{4.4}$$

$$E_v = Q\left\{0.056 + 0.039\exp\left[\frac{4 - A_2}{2.5}\right]\right\} for A_2 \geq 4 \tag{4.5}$$

4.2 Results

4.2.1 Proton radioactivity of Lanthanides

4.2.1.1 Empirical formula

The variation of experimental $log(T_{1/2})$ of proton decay in the lanthanide region as a function of $Z_d/\sqrt{Q}$ is shown in the Fig.4.1. We have fitted empirical relation for experimental $log(T_{1/2})$

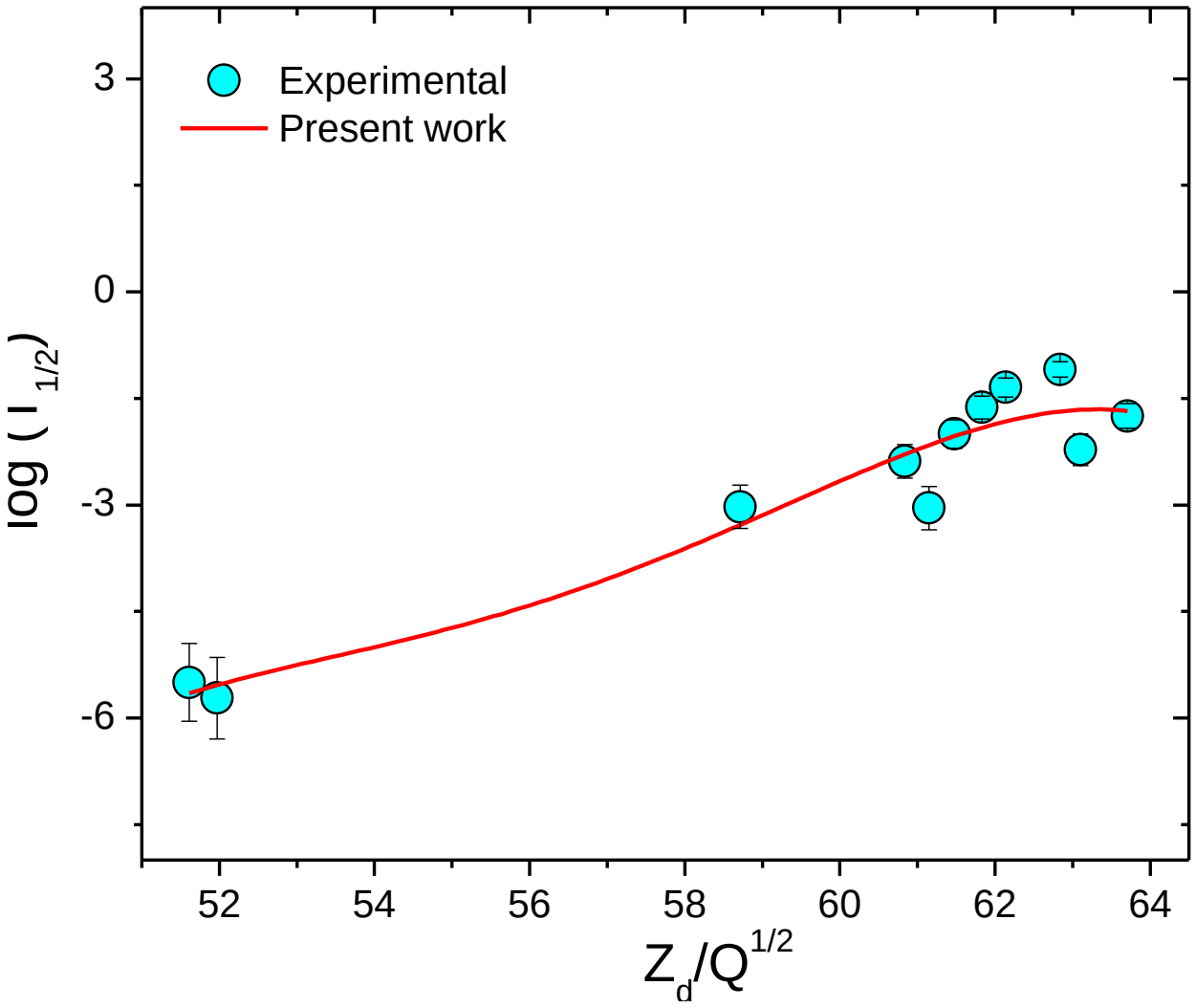

Fig. 4.1 Variation of experimental and present formula half lives as a function of $Z_d/\sqrt{Q}$.

in such a way that it should have maximum R^2 and minimum residual sum of squares. Hence, proposed empirical formula for $log(T_{1/2})$ of proton decay is given below; the half-lives for proton decay in the lanthanide region as a function of fissility parameter $Z_d/\sqrt{Q}$ is given by:

$$\log(T_{1/2}) = \sum_{i=0}^{i=4} A_i \left(\frac{Z_d}{\sqrt{Q}}\right)^i \tag{4.6}$$

Where Z_d is the atomic number of the daughter nuclei and Q is the decay energy. The fitting parameters A_0 , A_1, A_2, A_3 and A_4 are having the values -1.61, -20.82×10^{-2}, 71×10^{-4}, -8.18×10^{-5} and -3.11×10^{-7} $MeV^{1/2}$s respectively.

Table 4.1 The range of lanthanide isotopes having positive proton decay energy

Z	Range of mass number studied
57	110≤A≤119
58	113≤A≤115
59	115 ≤A≤123
60	118 ≤A≤119
61	120 ≤A≤128
62	123≤A≤125
63	125≤A≤135
64	128≤A≤130
65	130≤A≤139
66	133≤A≤135
67	136≤A≤143
68	138≤A≤139
69	141≤A≤149
70	143≤A≤147
71	146≤A≤155

4.2.1.2 **Results on proton radioactivity of Lanthanides**

The phenomenon of proton decay is treated as the transmission of the proton across a potential barrier developed due to combined effect of Coulombic and nuclear potential [236]. Experimentally 11 proton emitters were identified in the lanthanide region. We have studied the proton decay for lanthanide nuclei in which its decay energy (Q_p) is positive. In the present work, it is of first kind where we systematically explored the unexplored 24 proton decay emitters in the lanthanide region. These proton emitters having half-lives in terms of $1s - 1\mu s$. Generally, the half-lives of proton emitters nuclei have been determined by quantum-mechanical tunneling calculation through a potential barrier [284].

The universal function proposed by five different versions of Coulomb and nuclear proximity potentials such as Prox. 13, Prox. 77, MP 77, Ng 80 and Bass 80 are used to calculate the half lives of proton emitters in the lanthanide region for different isotopes of lanthanides. Table 4.1 gives the range of studied lanthanide isotopes having positive proton decay energy. In order to study

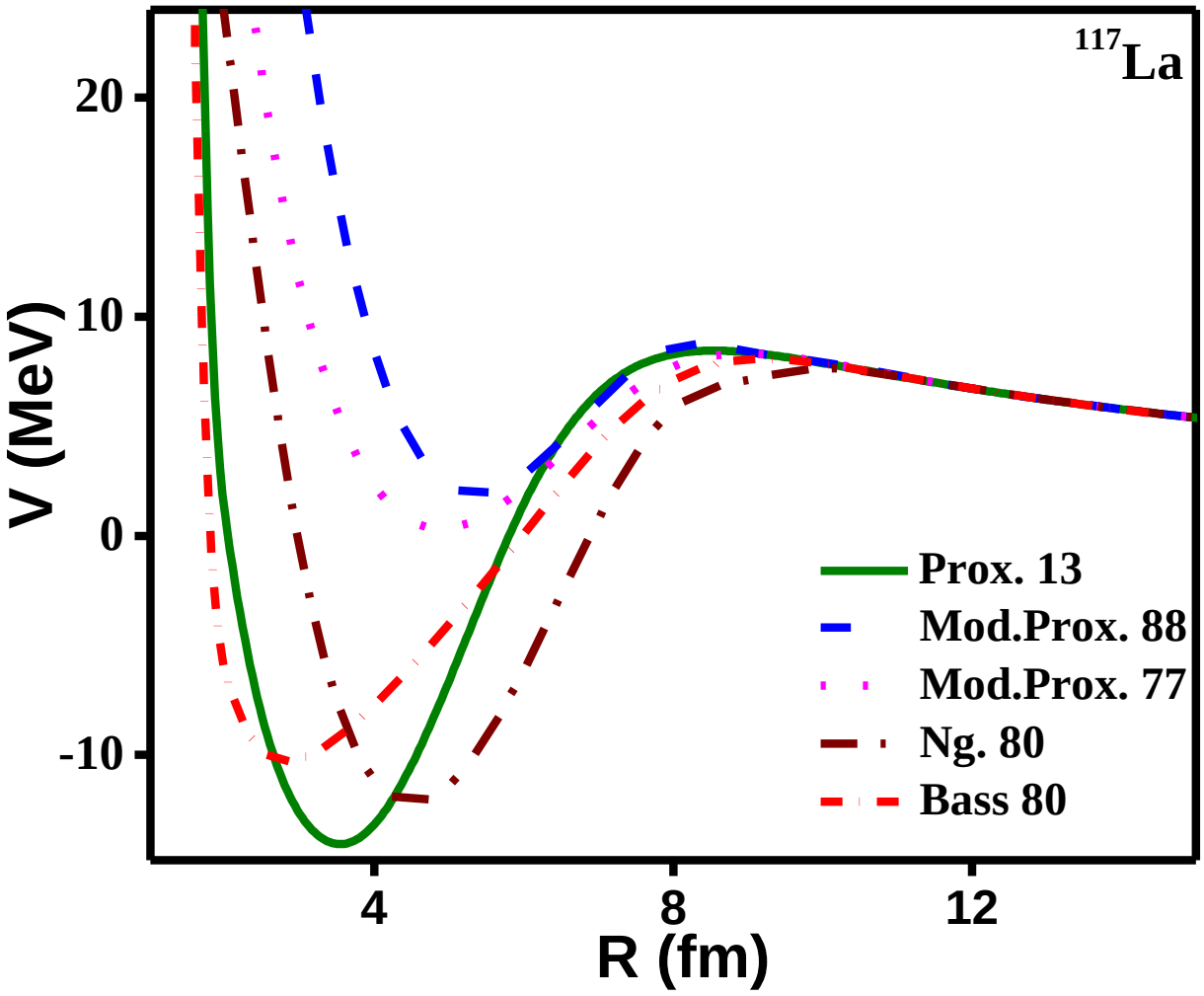

Fig. 4.2 Variation of potential energy as a function of R for different proximity potentials.

whether the shape of the potential leads to different half lives, the different proximity potentials are plotted as a function of R as shown in Fig. 4.2. X- axis corresponds to the distance between interacting nuclei and Y -axis corresponds to interacting potential. The area under the potential curve is directly proportional to the penetration probability. If the area under the potential curve is more, the probability of penetration is more which clearly indicates the short half life of the decay particle and vice versa. In the present study, from the Fig. 4.2, it is observed that, the area under the curve is found to be maximum for Bass 80 and then follows the order Prox. 13, Mod. Prox. 77, Prox. 77 and Ng 80.

The calculated proton decay half lives are compared with the experiments. The calculated

Table 4.2 Comparison of evaluated proton decay halflives using different proximity functions with that of the experiments

Proton emitter	Q_p MeV	$\log T_{1/2}(s)$						
		Expt	Ng. 80	Mp. 88	Mp. 77	Bass. 80	Prox. 13	Present formula
$^{111}La \rightarrow^{110} Ba$	4.321	-	-3.80	-6.96	-6.82	-17.94	-17.76	-3.51
$^{112}La \rightarrow^{111} Ba$	3.791	-	-3.62	-6.62	-6.46	-17.18	-17.03	-3.45
$^{113}La \rightarrow^{112} Ba$	3.071	-	-3.38	-5.85	-5.67	-15.86	-15.51	-3.35
$^{114}La \rightarrow^{113} Ba$	1.891	-	-3.13	-4.25	-4.00	-12.21	-12.07	-2.98
$^{115}La \rightarrow^{114} Ba$	2.517	-	-3.01	-5.19	-4.99	-14.51	-14.13	-3.21
$^{116}La \rightarrow^{115} Ba$	1.206	-	-2.77	-2.18	-1.89	-7.89	-7.76	-2.51
$^{117}La \rightarrow^{116} Ba$	0.803	-1.63	-2.58	-2.11	-2.43	-2.99	-2.92	-2.12
$^{118}La \rightarrow^{117} Ba$	0.378	-	-2.36	-2.33	-3.68	-2.00	-6.22	-2.13
$^{113}Ce \rightarrow^{112} La$	1.971	-	-3.45	-4.15	-3.88	-12.32	-11.94	-2.98
$^{114}Ce \rightarrow^{113} La$	1.491	-	-3.26	-2.91	-2.61	-9.76	-9.37	-2.71
$^{115}Ce \rightarrow^{114} La$	0.891	-	-3.06	-0.15	-0.79	-3.94	-3.55	-2.17
$^{115}Pr \rightarrow^{114} Ce$	3.861	-	-3.44	-6.58	-6.41	-17.03	-16.91	-3.43
$^{117}Pr \rightarrow^{116} Ce$	2.811	-	-3.00	-5.43	-5.24	-14.95	-14.61	-3.25
$^{119}Pr \rightarrow^{118} Ce$	1.411	-	-2.59	-2.74	-2.43	-8.98	-8.88	-2.61
$^{121}Pr \rightarrow^{120} Ce$	0.837	-2	-2.24	0.37	0.02	-2.80	-2.43	-2.11
$^{122}Pr \rightarrow^{121} Ce$	0.526	-	-2.05	3.44	3.79	1.11	4.00	-2.01
$^{123}Pr \rightarrow^{123} Ce$	0.209	-	-0.56	7.73	7.58	3.93	9.76	-0.46
$^{118}Nd \rightarrow^{117} Pr$	1.131	-	-2.89	-1.44	-1.11	-6.21	-6.15	-2.33
$^{119}Nd \rightarrow^{118} Pr$	0.741	-	-2.71	1.36	0.50	-0.93	-0.31	-2.01
$^{121}Pm \rightarrow^{120} Nd$	3.301	-	-2.70	-6.01	-5.82	-15.77	-15.69	-3.31
$^{123}Pm \rightarrow^{122} Nd$	1.981	-	-2.28	-4.09	-3.81	-11.78	-11.44	-2.89
$^{125}Pm \rightarrow^{124} Nd$	0.438	-	-1.85	5.48	6.15	2.47	6.45	-2.16
$^{127}Pm \rightarrow^{126} Nd$	0.545	-	-1.56	3.58	3.94	1.44	4.63	-2.01
$^{124}Sm \rightarrow^{123} Pm$	0.481	-	-2.16	5.08	5.12	2.35	6.02	-2.11
$^{129}Eu \rightarrow^{128} Sm$	1.459	-	-1.61	-2.47	-2.14	-8.31	-7.98	-2.49
$^{130}Eu \rightarrow^{129} Sm$	1.028	-3.05	-2.43	-0.31	-1.69	-4.14	-4.15	-2.15
$^{131}Eu \rightarrow^{130} Sm$	0.939	-1.75	-1.28	0.04	0.40	-2.94	-2.64	-2.10
$^{133}Eu \rightarrow^{132} Sm$	0.675	-	-0.96	2.53	3.81	0.63	1.84	-1.98
$^{135}Tb \rightarrow^{134} Gd$	0.524	-3.03	-2.91	-4.75	5.18	2.66	6.43	-2.11
$^{140}Ho \rightarrow^{139} Dy$	1.094	-2.23	-2.50	-0.36	0.06	-3.69	-3.44	-2.11
$^{141}Ho \rightarrow^{140} Dy$	1.176	-2.39	-2.35	-0.61	-2.01	-4.65	-4.72	-2.16
$^{144}Tm \rightarrow^{143} Er$	1.712	-5.73	-4.12	-6.34	-6.83	-4.11	-8.66	-5.53
$^{145}Tm \rightarrow^{144} Er$	1.736	-5.49	-5.07	-2.59	-1.24	-8.79	-8.84	-5.63
$^{150}Lu \rightarrow^{149} Yb$	1.27	-1.35	-1.10	-0.58	-2.28	-4.49	-4.61	-2.13
$^{151}Lu \rightarrow^{150} Yb$	1.241	-1.09	-1.78	-0.64	-0.22	-4.19	-3.99	-2.11

Table 4.3 Mean square error with respect to experiments for different proximity functions and proposed present formula

Proximity function	Ng. 80	MP. 88	MP. 77	Bass. 80	Prox. 13	Present formula
σ	1.23	1.52	1.64	1.82	2.12	1.60

Mean square error of different proximity functions with respect to experiments is shown in Table. 4.3. The sum of the squared residuals between the log($T_{1/2}$) of experimental and different proximity potentials ($SSR = \sum_{i=1}^{n} e_i^2$), where e_i is the i^{th} residual or difference and n is the number of data points. Mean square error with respect to experiments for different proximity functions and proposed present formula ($\sigma_\epsilon^2 = \frac{SSR}{n-2}$) are shown in Table. 4.3. From Table. 4.3, it is observed that the mean square error was found to be less for Ng 80 compared to other proximity potentials. The experimental values are found to be agree well with Ng 80 among the studied proximity functions. Thus, Ng 80 proximity potential was used to study the competition between different decay modes in the lanthanide region.

We have constructed new simple empirical relation to calculate the half life of proton emitters in the lanthanide region for different isotopes of lanthanides other than the above mentioned models. The constructed empirical formula is given in Eq. 4.6. The half-lives values produced with proximity function NG80 is close to the experiment. From the comparison of mean square error it shows that MP88 is better than the present empirical formula. Mean square error difference between Mp88 and Present Formula is 0.08 and it is almost negligible, means both methods used to calculate half lives will produce the almost same deviation. But, to calculate half lives using the MP88 proximity function involves many physical quantities. Whereas, the present formula produces the half lives with simple inputs of Z_d and Q values and this we may call pocket formula. So that the present formula is more advantageous than the MP88. The evaluated proton decay half-lives using present formula and different proximity functions along with the experiments are presented in the table 4.2. From this table, it is found that the present formula produces proton

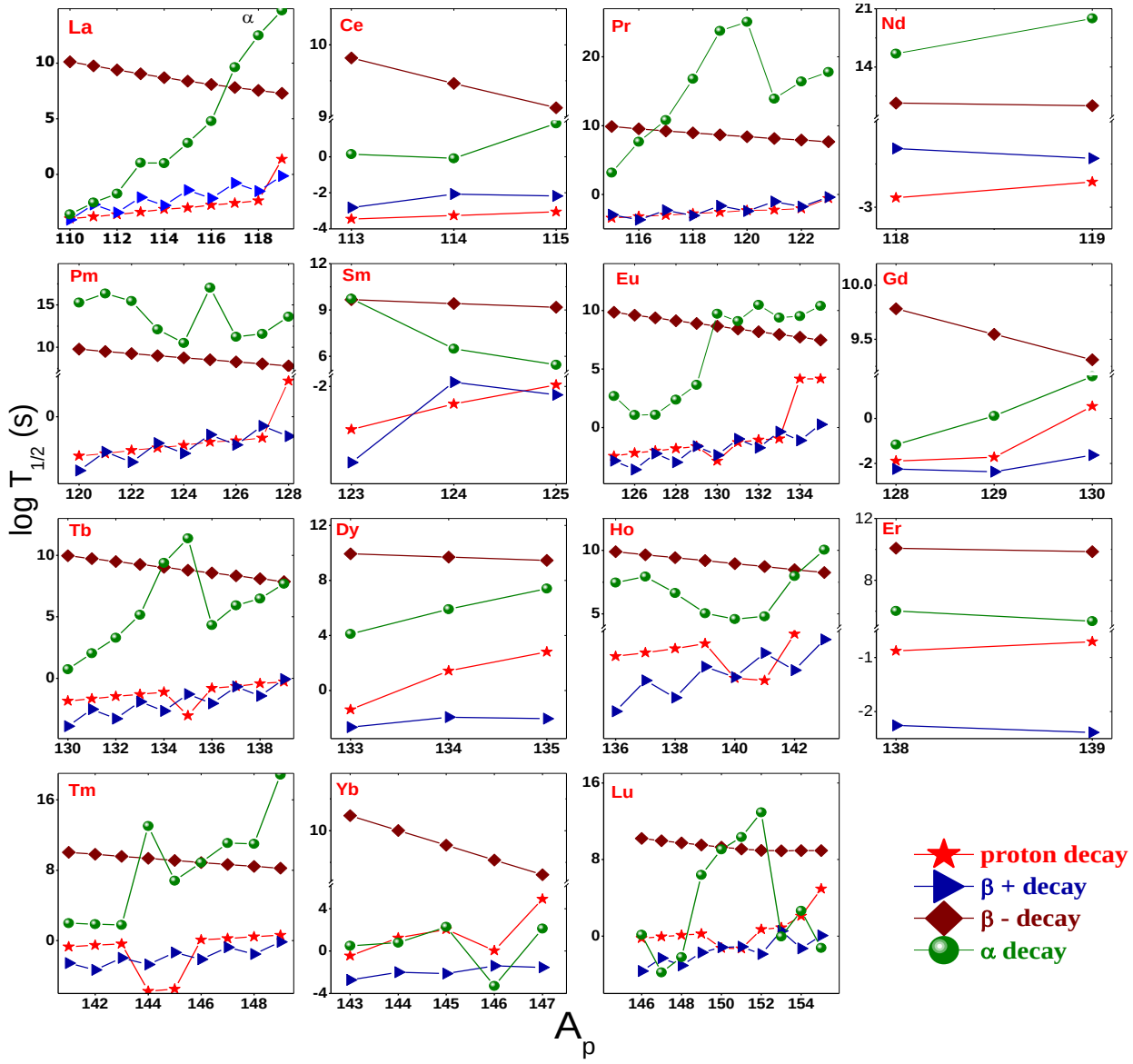

Fig. 4.3 Competition between different decay modes for lanthanide nuclei.

decay half lives close to the experiments. Proton decay energies are also presented in this table 4.2.

Dominant decay mode can be identified by studying the competition between the different possible decay modes such as alpha, β^+, β^-, Spontaneous fission (SF) and proton decay. We have also calculated the half lives of possible decay modes using the well established formulae available in the literature [alpha[285], β^+[286], β^- [286] and SF[287]. The competition between different decay modes in the studied lanthanide region is shown in Fig. 4.3. The decay mode which is

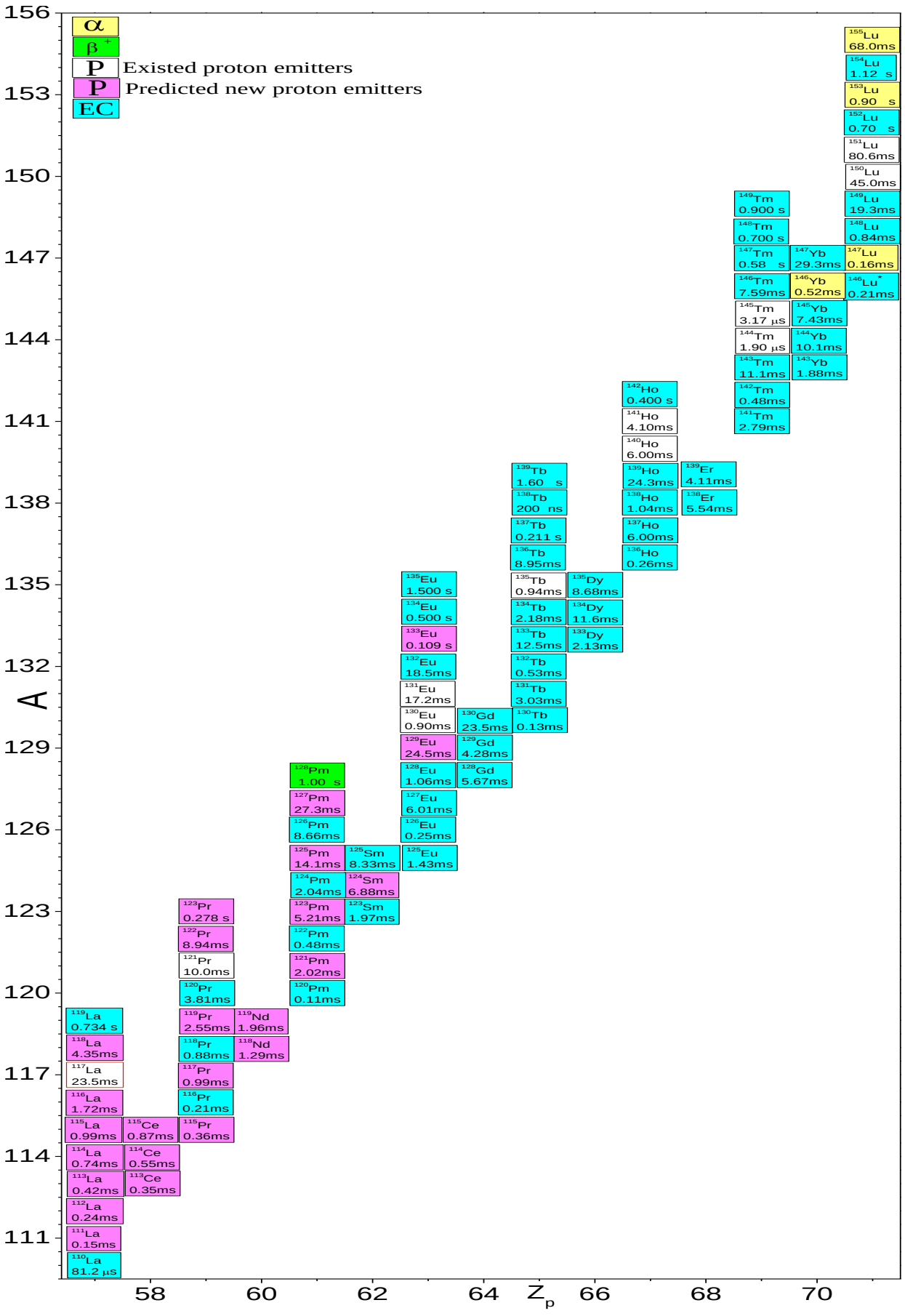

Fig. 4.4 Nuclide chart of Proton emitters in the lanthanide region.

having shorter half life among the possible decay modes will be identified as the dominant decay mode. The observation of Fig. 4.3 clearly indicates that some isotopes of lanthanides with atomic number ranging between 57 - 63 (La, Ce, Pr, Nd, Pm, Sm and Eu) are newly identified as proton emitters in the lanthanide region whereas the Gadollinium, Dysprosium and Erbium shows $\beta+$ decay as a dominant decay mode. In Terbium, Holmium, Thulium, even though maximum isotopes are β^+ decay emitters, few of them are proton decay emitters. In Ytterbium and Lutetium, few isotopes are β^+ decay emitters and few of them are α decay emitters. The newly identified 24 proton emitters in the lanthanide region are ^{111}La, ^{112}La, ^{113}La, ^{114}La, ^{115}La, ^{116}La, ^{118}La, ^{113}Ce, ^{114}Ce, ^{115}Ce, ^{115}Pr, ^{117}Pr, ^{119}Pr, ^{122}Pr, ^{123}Pr, ^{118}Nd, ^{119}Nd, ^{121}Pm, ^{123}Pm, ^{125}Pm, ^{127}Pm,^{124}Sm, ^{129}Eu, ^{133}Eu. The different α, β^+, existing proton emitters, nuclei with electron capture decay mode and the formula predicted new proton emitters are shown in the Nuclide chart (Fig. 4.4). The predicted new 24 proton emitters are highlighted in pink color, whereas α, β^+, electron capture and existing proton emitters are highlighted in yellow, green, aqua blue and brick red respectively.

4.2.1.3 **Systematics of proton radioactivity in Dysprosium**

The competing decay modes such as proton-radioactivity, β^+-decay, β^--decay and alpha decay were studied in the Dysprosium of mass number range $133 \leq A \leq 180$. The proton decay selection rule [109] is as follows;

$$J_p = J_d + J_{p^\ell} \tag{4.7}$$

$$\pi_p = \pi_d \pi_{p^\ell} (-1)^\ell \tag{4.8}$$

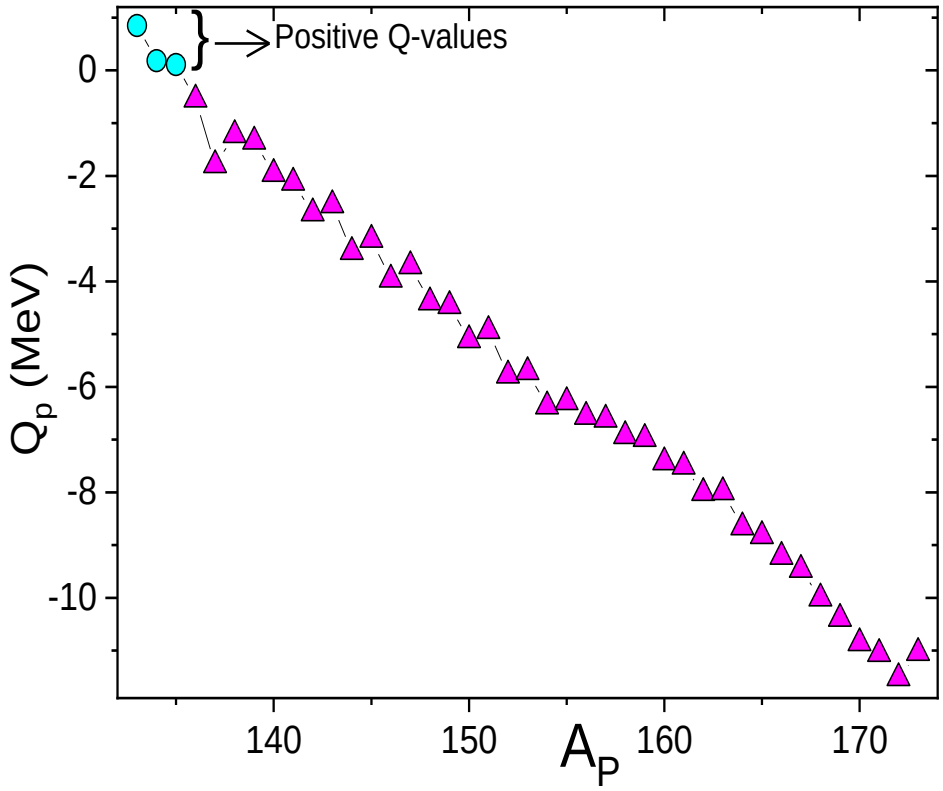

Fig. 4.5 The quantity of energy released during proton radioactivity and the mass number of Dysprosium parent nuclei.

where J_p, J_d and J_{p^ℓ} are the spin of parent, daughter and outgoing proton nuclei respectively. π_p, π_d and π_{p^ℓ} are parity of parent, daughter and outgoing proton respectively. The angular momentum for proton transition is evaluated using the ℓ_{min} as explained in literature [109]. Using recent mass excess values, the amount of energy released during proton radioactivity is calculated [288]. Wherever, recent mass excess values are not available, the mass excess values have been taken from the mass excess data [280]. The Q-value of one proton radioactivity can be calculated using the mass excess [288] and [280] values. When the Q-value is positive, i.e. Q>0, proton radioactivity is energetically possible. The graph 4.5 illustrates the relationship between the quantity of energy released during proton radioactivity and the mass number of parent nuclei. The amount of

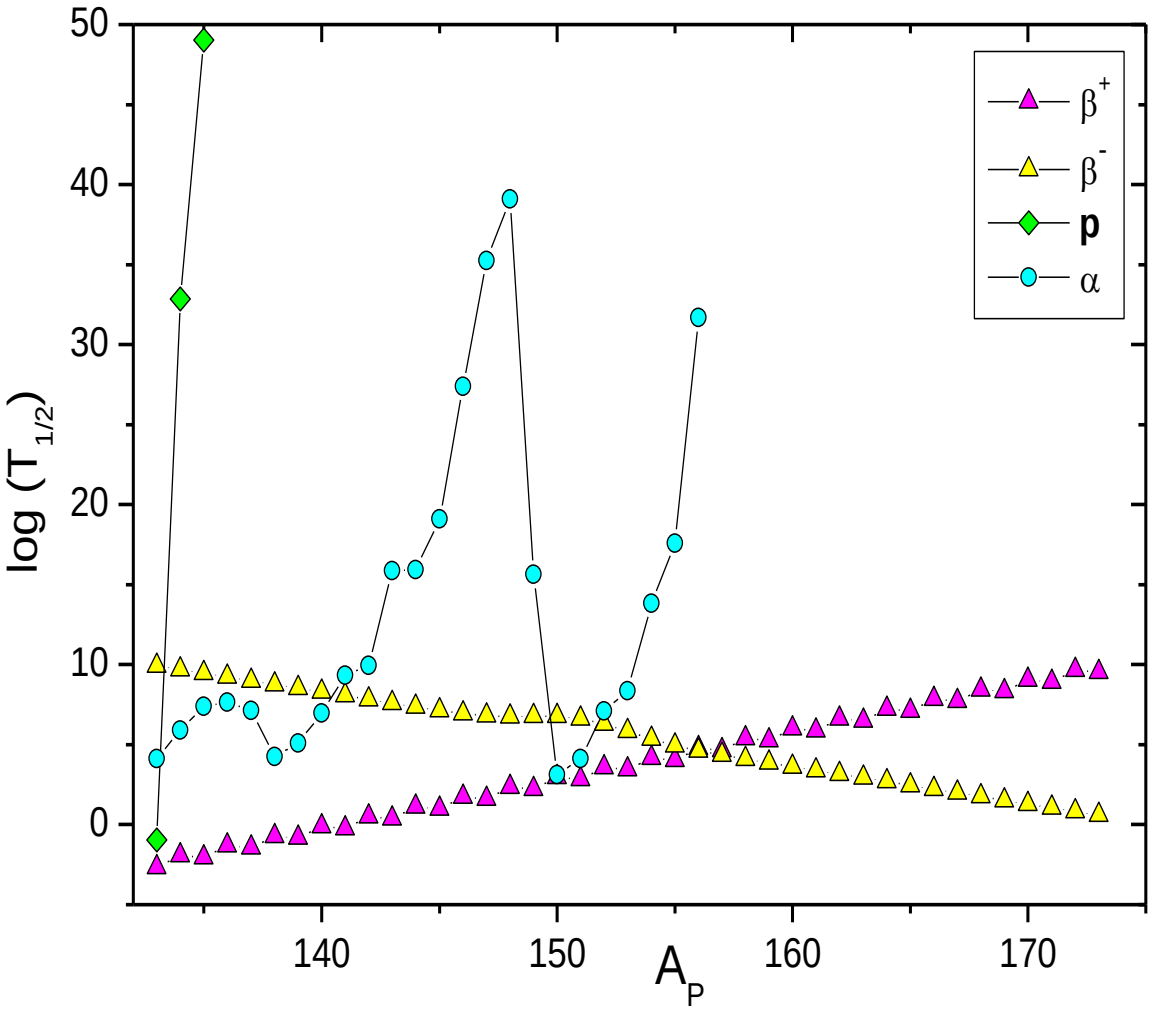

Fig. 4.6 Comparison of log$T_{1/2}$ of different decay modes such as $beta^{\pm}$, 1P, and α decay versus mass number of parent nuclei.

energy released gradually decreases as the mass number of parent nuclei increases. The Q-value is positive and proton radioactivity is energetically feasible for the isotope of $^{133-135}$Dy. Since, in addition to proton radioactivity, the competing decay modes such as β^--decay and β^+-decay and alpha decay have been evaluated as explained in theory section. The comparision of different competing decay modes such as β^-, $\beta+$, and α-decay with that of proton decay is studied and it is shown in figure 4.6.From the figure it is clear that β^+-decay is dominant in the isotopes of $^{133-149}$Dy, $^{151-154}$Dy, alpha decay is dominant in ^{150}Dy and again in $^{155-173}$Dy, β^--decay is dominant. Even though, there is less probability of proton radioactivity in isotopes of Dy but the

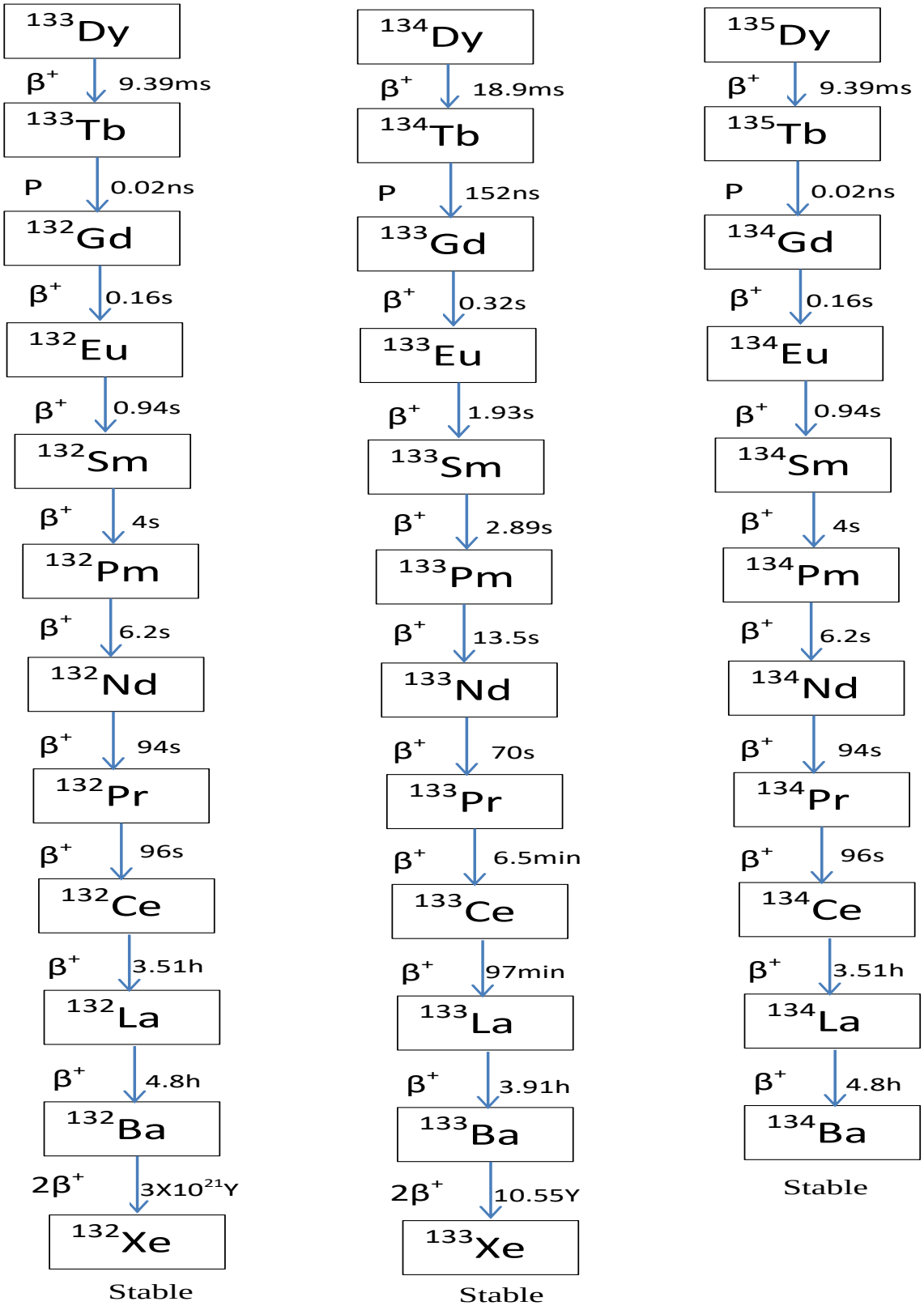

Fig. 4.7 Decay chains in the isotopes of $^{133-135}$Dy

Table 4.4 Identification of decay modes of $^{133-138}Dy$ and $^{177-180}Dy$

Nuclei	Q(MeV)	$logT_{1/2}$	Decay mode
^{133}Dy	13.48	-2.03	β^+
^{134}Dy	10.67	-1.72	β^+
^{135}Dy	12.03	-1.42	β^+
^{136}Dy	7.93	-1.11	β^+
^{137}Dy	9.50	-0.81	β^+
^{138}Dy	7.67	-0.50	β^+
^{177}Dy	7.17	-0.35	β^-
^{178}Dy	6.05	-0.58	β^-
^{179}Dy	7.78	-0.82	β^-
^{180}Dy	6.73	-1.05	β^-

positive Q-value in isotopes of $^{133-135}$Dy triggered us to analyse the decay chains of the same. The figure 4.7 shows the proton radioactivity of $^{133-135}$Tb. An isotope of ^{133}Dy doesn't sustain β^+-decay and it decays to ^{133}Tb within the half-life of 9.39ms, again ^{133}Tb undergoes proton decay within 0.02ns and converts to ^{132}Gd. Later, the ^{132}Gd follows series of β^+-decay up to ^{132}Xe and then it becomes stable. Similarly, the decay chains of ^{134}Dy and ^{135}Dy is also shown with the consisted decay chains until it reaches stable nuclei ^{133}Cs and ^{135}Ba respectively. The newly found isotopes of Dysprosium are shown in table 4.4. The decay modes of the newly identified isotopes of Dysprosium along with their decay energy and half-lives are also included. The newly discovered isotopes have decay energies ranging from 7MeV to 14MeV and half-lives ranging from miliseconds to seconds. These identified isotopes are first of its kind and may be useful in radiation physics.

4.2.2 **Proton radioactivity of heavy nuclei** ($72 \leq Z \leq 88$)

The amount of energy released during proton decay are studied using mass excess values available in the reference [36, 270, 289–291]. We have studied driving potential, penetration factor and half-lives of proton emission in the nuclei region $72 < Z < 88$ as explained in the theory section. The variation of amount of energy released during proton decay with the mass number of

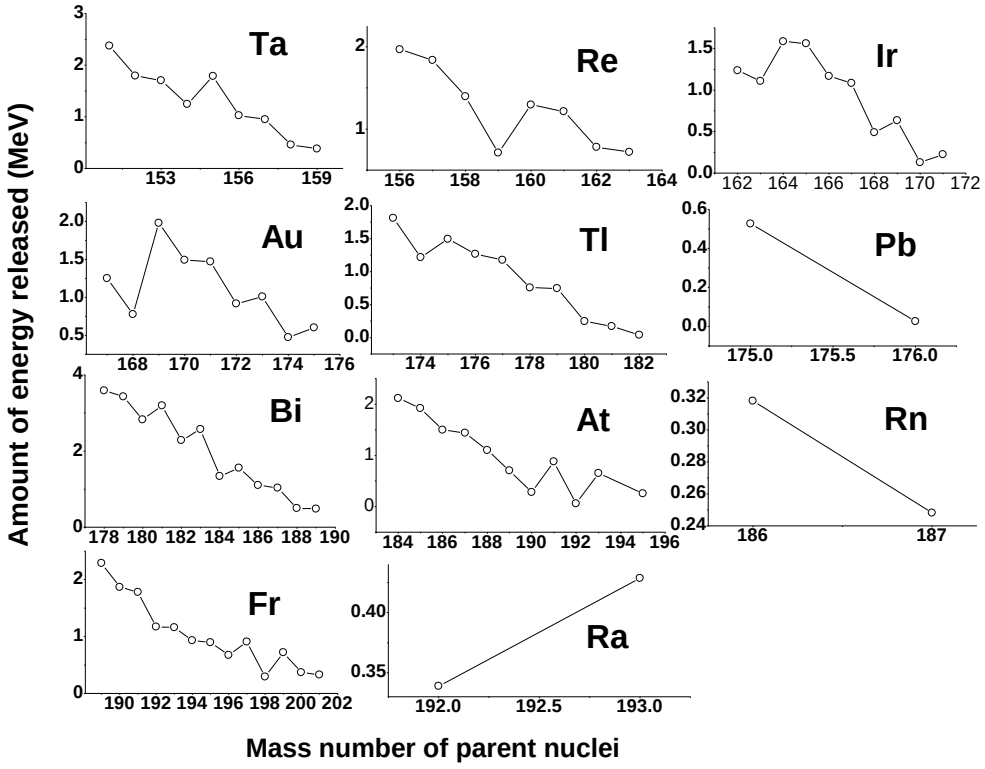

Fig. 4.8 A variation of amount of energy released during the proton emission in the nuclei region $72 < Z < 88$ with the mass number of parent nuclei.

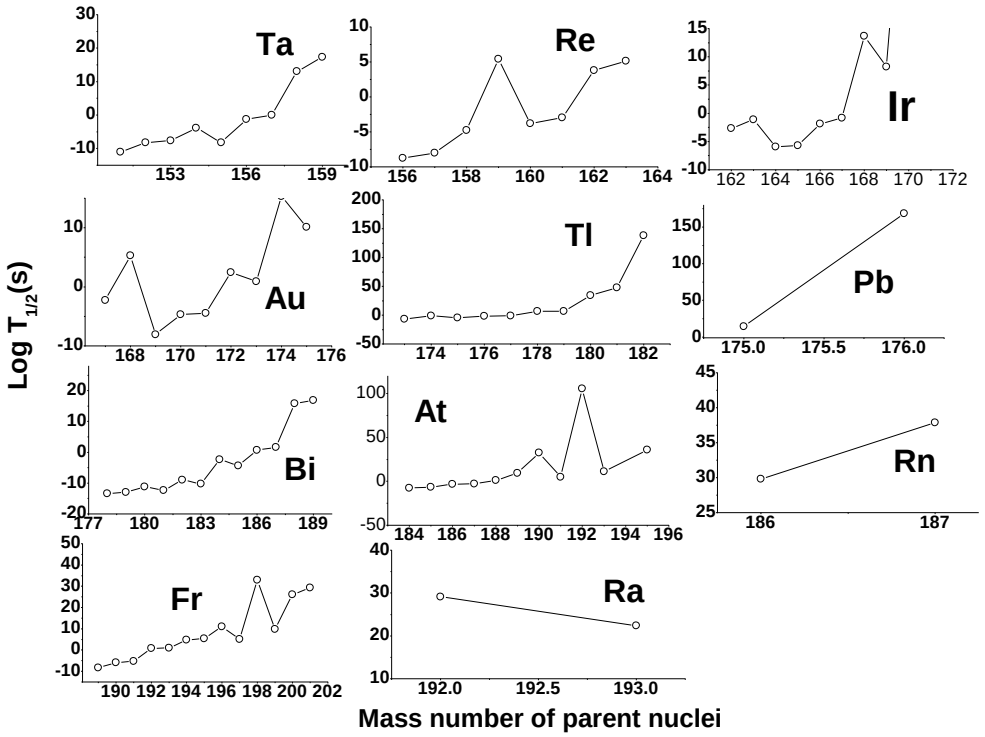

Fig. 4.9 A variation of logarithmic half-lives for the proton emission in the nuclei region $72 < Z < 88$ with the mass number of parent nuclei.

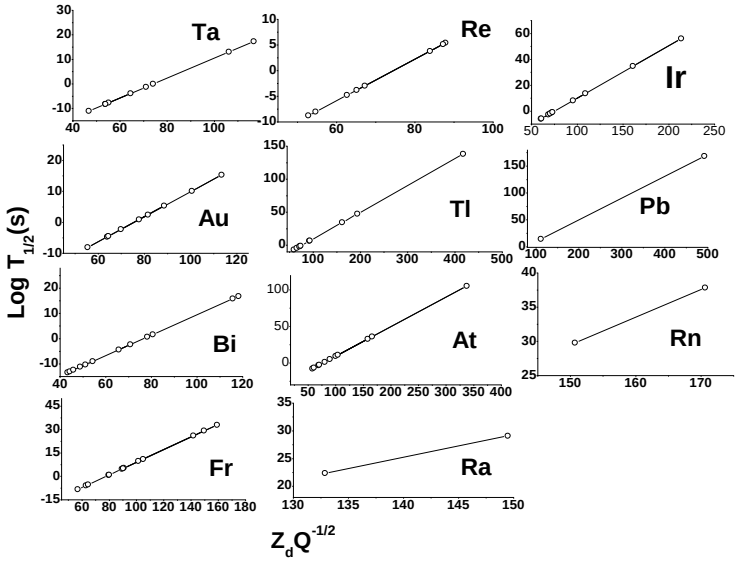

Fig. 4.10 A variation of logarithmic half-lives for the proton emission in the nuclei region $72 < Z < 88$ with the product of atomic number of daughter nuclei and amount of energy released during proton emission ($Z_dQ^{-1/2}$).

parent nuclei is as shown in figure 4.8. For the heavy nuclei Ta, Re, Ir, Au, Tl, Bi, At and Fr, the trend in the amount of energy released during the proton radioactivity is not unique, there is both increase and decrease in the decay energy and hence their half-lives. In case of Pb, Rn and Ra only two nuclei undergo proton radioactivity. In case of Pb and Rn, the decay energy of first nuclei is greater than that of second nuclei. Hence decay energy decreases. $T_{1/2}$ of first nuclei is smaller than $T_{1/2}$ of second nuclei. Hence half lives increases. In case of Ra the decay of first nuclei is less than that of second nuclei. Hence decay energy increases.$T_{1/2}$ of first nuclei is greater than of $T_{1/2}$ of second nuclei. Hence half lives decreases. Since only two proton emitters are identified in those elements, the trend of variation is difficult to predict. From the figure 4.10 we have observed linear variation of logarithmic half-lives with the $Z_dQ^{-1/2}$. We have also studied the competition between different decay modes such as alpha decay, β^+, β^- decay and proton decay. The half-lives corresponding to β^+-decay and β^--decay are evaluated using the semi empirical formula available in the literature [292, 293]. Alpha decay half-lives are evaluated using the procedure explained in the previous work [15]. The plot of different decay modes are as shown in figure 4.11

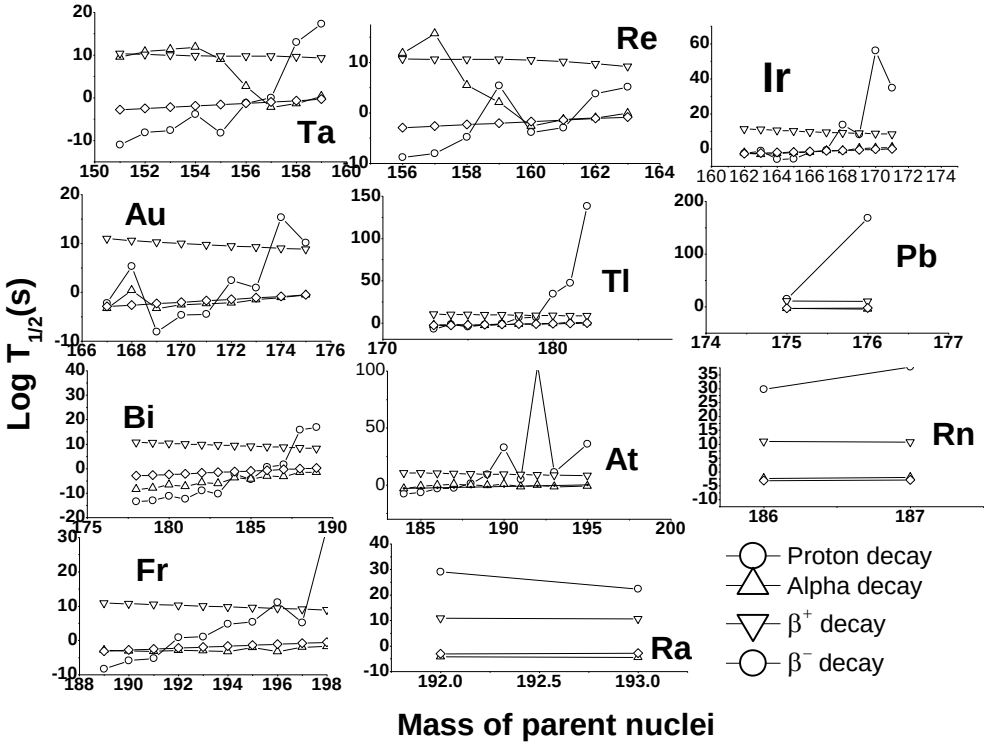

Fig. 4.11 A variation of logarithmic half-lives for the proton activity,alpha decay, β^+ and β^- decay as a function of mass number of the parent nuclei (A) .

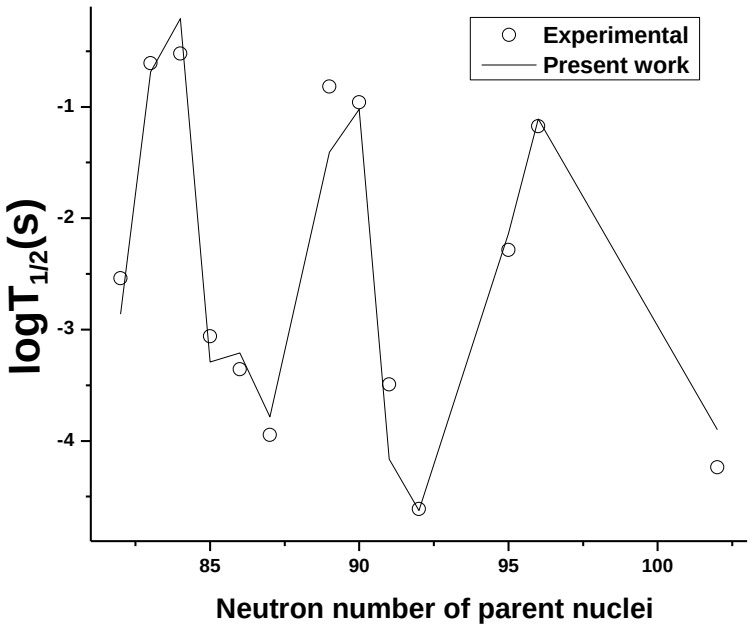

Fig. 4.12 A Comparison of logarithmic half -lives of proton radioactivity of present work with that of available experimental values

Table 4.5 Comparison of present work with experiments [5, 34, 35, 234] and available semi empirical formulae such as Hatsukawa et al.[294] and Gamow [10]

Parent nuclei	$Q_{exp.}$ (MeV)	$\log T_{1/2}$ [5, 34, 35, 234]	Q_{PW} (MeV)	ℓ	$\log T_{1/2}$		
					PW	Hatsukawa [294]	Gamow [10]
^{155}Ta	1.45	-2.54	1.79	5	-2.84	-2.38	-2.84
^{156}Ta	1.02	-0.61	1.03	2	-0.62	-6.74	-0.62
^{157}Ta	0.93	-0.52	0.95	0	-0.49	-7.28	-0.41
^{160}Re	1.27	-3.06	1.29	2	-2.29	-4.56	-3.36
^{161}Re	1.20	-3.36	1.21	0	-3.61	-5.05	-4.61
^{164}Ir	1.54	-3.95	1.58	5	-3.60	-2.29	2.40
^{166}Ir	1.15	-0.82	1.17	2	-0.87	-4.83	-3.40
^{167}Ir	1.07	-0.96	1.08	0	-1.02	-5.37	-1.32
^{170}Au	1.47	-3.49	1.49	2	-3.50	-2.24	1.15
^{171}Au	1.45	-4.61	1.47	0	-4.59	-2.35	2.19
^{176}Tl	1.27	-2.28	1.27	0	-2.36	-3.11	-2.36
^{177}Tl	1.16	-1.17	1.18	0	-1.18	-3.70	-2.84
^{185}Bi	1.53	-4.24	1.56	4	-4.12	-3.51	-3.93

and also highlighted possible proton emitters with the corresponding energies and half-lives in the atomic number range $72 < Z < 88$. To validate the present work, the proton emission half-lives produced by the present work are compared with that of experiments and available semi empirical formulae such as Hatsukawa et al. [294] and Gamow [10]. It is tabulated in table 4.5. We have also compared proton radioactivity logarithmic half-lives of present work with that of available experimental values and it is depicted in figure 4.12. From the figure 4.12 and the table 4.5, it is clearly observed that the present work is in close agreement with the experimental values.

4.2.2.1 **Proton radioactivity of Tantalum**

Using three models such as CPPM, ELDM and MGLDM, proton decay from the proton rich emitter Tantalum is studied. The 1P-decay is energetically possible only when Q-value of the reaction is positive. The decay energy is evaluated using the following equation;

$$Q = \delta M_P - (\delta M_d + \delta M_Z) + k(Z_P^{\epsilon} - Z_d^{\epsilon}) \tag{4.9}$$

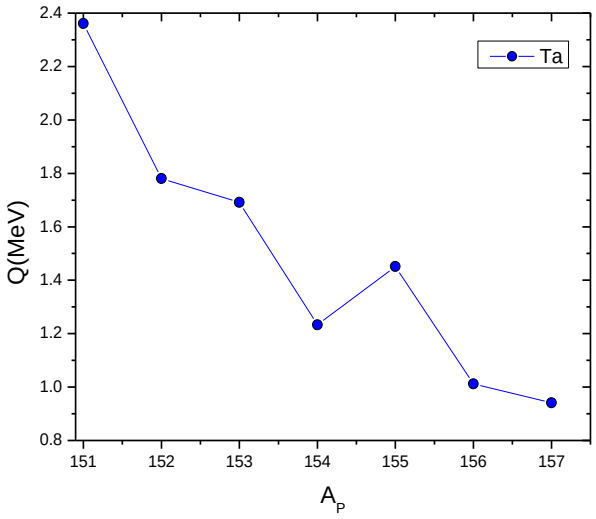

Fig. 4.13 A plot of Q-values during 1P- decay with the mass number of parent nuclei for the $^{151-157}$Ta nuclei.

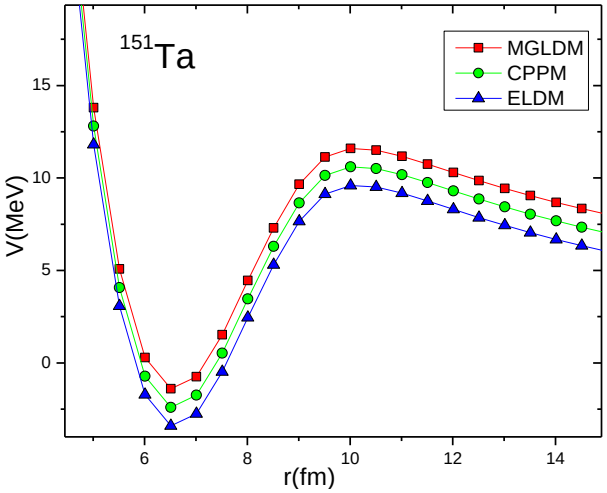

Fig. 4.14 Variation of total potential using three models such as CPPM, ELDM and MGLDM as function of separation distance in ^{151}Ta nuclei.

where δM_P is the is the mass excess of the parent nuclei, δM_d is the mass excess of the daughter nuclei and δM_Z is the mass excess of the emitted proton. The term $kZ^{\epsilon}_{P(d)}$ is the total binding energy of electrons in the parent or daughter nuclei. The value of k=13.6 eV and $\epsilon = 2.408$ for the nuclei $Z \leq 60$ and k=8.7 eV and $\epsilon = 2.517$ for the nuclei $Z > 60$. Figure 4.13 shows a plot of Q-values during 1P-decay with the mass number of parent nuclei. The minimum Q-value is observed in case of ^{157}Ta with 0.941 MeV and maximum is observed for ^{151}Ta with 2.361 MeV when compared to their neighboring one. Then, we have calculated total potential using

Table 4.6 Tabulation of $\log T_{1/2}$using three different models such as CPPM, ELDM and MGLDM for predicted proton emitters from $^{151-157}$Ta is compared to available experiments.

PN	DN	Q (MeV)	ℓ	exp.[34]	CPPM	ELDM	MGLDM
^{151}Ta	^{150}Hf	2.361	5	-	-11.21	-10.55	-10.18
^{152}Ta	^{151}Hf	1.781	5	-	-8.67	-7.46	-7.9
^{153}Ta	^{152}Hf	1.691	5	-	-5.6	-5.84	-7.43
^{154}Ta	^{153}Hf	1.233	5	-	-5.28	-4.03	-4.1
^{155}Ta	^{154}Hf	1.451	5	-2.49	-2.68	-2.12	-2.51
^{156}Ta	^{155}Hf	1.012	2	-0.83	-0.55	-0.5	-0.85
^{157}Ta	^{156}Hf	0.941	0	-0.53	-0.35	-0.58	-0.51

three models in nuclei $^{151-157}$Ta , the studied potential as function of separation distance is shown in figure 4.14.From the figure, the minimum potential is observed when the separation energy is 6.5fm. Then the potential gradually increases and area below the curve gives information on penetration probability. Later, the evaluated penetration probability and 1P-decay half-lives in $^{151-157}$Ta using three models and were tabulated in table 4.6. The evaluated $\log T_{1/2}$ value varies between -11.21s to -0.35s in case of CPPM. However, in case of ELDM it varies between -10.55s to -0.58s and in case of MGLDM the $\log T_{1/2}$ varies between -10.18s to -0.51s for the nuclei $^{151-157}$Ta. The values obtained using present work is compared with the available experimental value . The studied $\log T_{1/2}$ corresponding to $^{155-157}$Ta shows close agreement with the available experimental values. However, the value obtained using MGLDM produces experimental half-lives more accurately.

4.2.2.2 **Competition between different decay modes in Bismuth nuclei**

The proton decay half-lives are studied in the isotopes of heavy nuclei Bismuth (Bi) using CPPM with harmonic oscillator frequency. However, alpha-decay and $\beta^{\pm}$-decay half-lives are evaluated using semi-empirical relations. If the Q-value of the reaction in proton decay is positive, then the proton radioactivity is energetically feasible [224]. The mass excess values in order to evaluate Q-value of the reaction is taken by recent mass excess data available in literature [288].

Table 4.7 Prediction of logarithmic half-lives of β^--decay in the isotopes of heavy nuclei $^{220-244}$Bi

Parent Nuclei	$T_{1/2}$	Parent Nuclei	$T_{1/2}$
^{220}Bi	0.01	^{233}Bi	-0.55
^{221}Bi	0.79	^{234}Bi	-0.9
^{222}Bi	0.04	^{235}Bi	-0.71
^{223}Bi	0.42	^{236}Bi	-1.08
^{224}Bi	-0.14	^{237}Bi	-0.85
^{225}Bi	0.15	^{238}Bi	-1.16
^{226}Bi	-0.35	^{239}Bi	-0.94
^{227}Bi	-0.01	^{240}Bi	-1.22
^{228}Bi	-0.49	^{241}Bi	-1.01
^{229}Bi	-0.22	^{242}Bi	-1.28
^{230}Bi	-0.62	^{243}Bi	-1.33
^{231}Bi	-0.4	^{244}Bi	-1.59
^{232}Bi	-0.77		

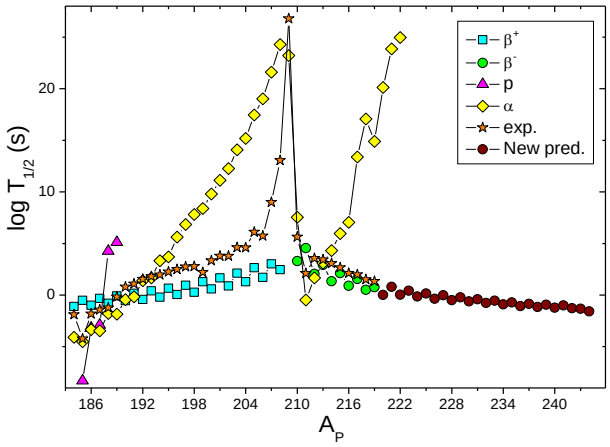

Fig. 4.15 A comparison of proton-decay, alpha-decay and beta-decay half-lives using CPPM and semi-empirical relations with that of available experiments.

The proton decay, alpha-decay and beta-decay half-lives obtained from the present work are compared with available experiments. The figure 4.15 shows comparison of proton, alpha and beta-decay half-lives using CPPM and semi-empirical relations with that of available experiments.

From this comparison it is observed that the nuclei $^{184,186-189}$Bi and $^{191,209,211-212}$Bi which possess alpha decay half-lives are in good agreement with the available experimental alpha decay half-lives. Similarly, the nuclei $^{190,192-208}$Bi, $^{210,213-244}$Bi and ^{185}Bi are having β^+, β^- and proton decay half-lives respectively are in close agreement with the available experimental values. the β^- -decay in the isotopes of heavy nuclei $^{220-244}$Bi shows shorter half-lives when compared to other

decay modes. Hence, the possible decay mode in heavy nuclei $^{220-244}$Bi is β^--decay only. The table 4.7 shows the predicted β^--decay half-lives in the heavy nuclei $^{220-244}$Bi. These predicted half-lives are in seconds to ms.

4.2.3 **Proton radioactivity of actinides** ($89 \leq Z \leq 103$)

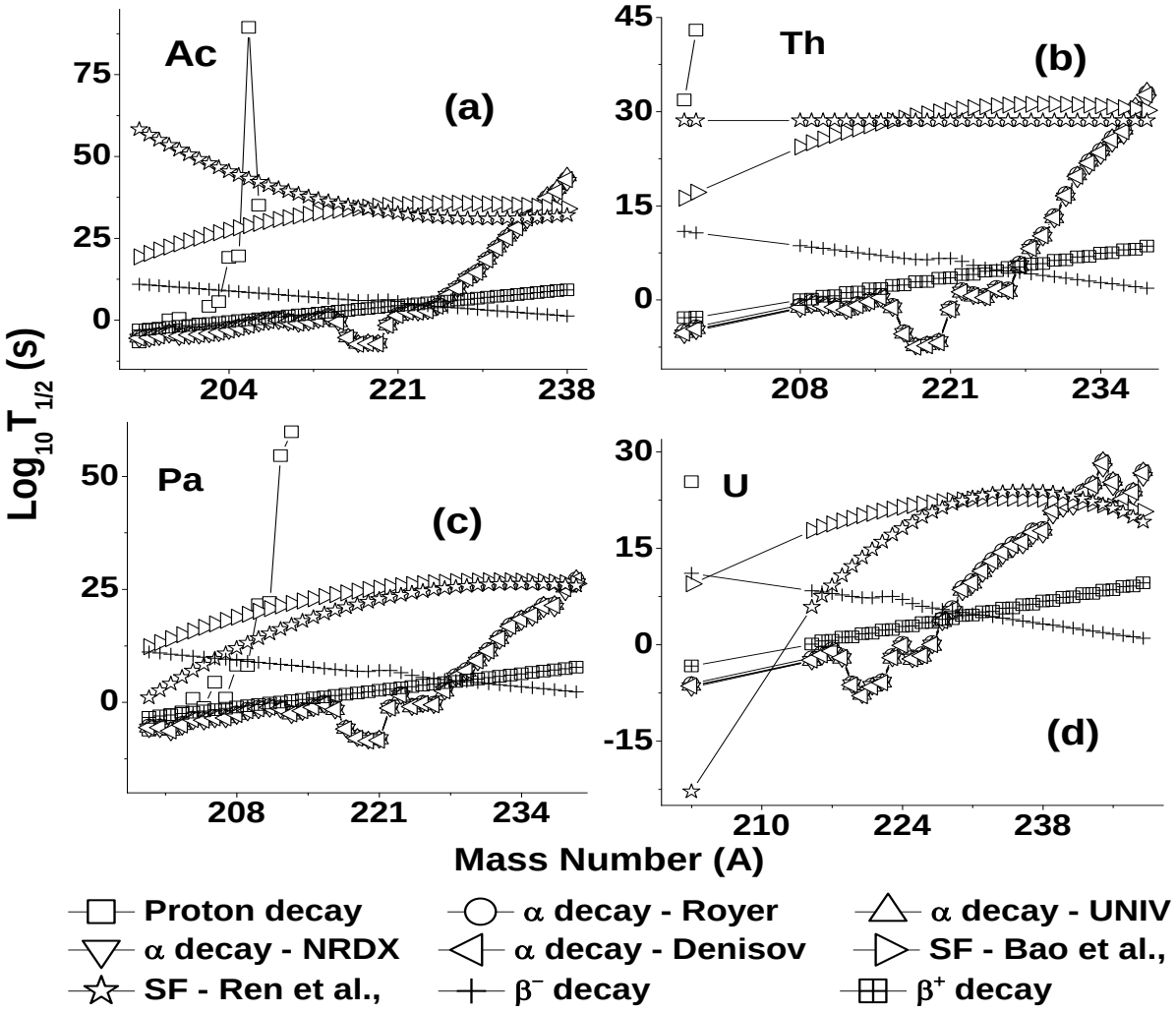

Fig. 4.16 Variation of log($T_{1/2}$) of proton activity, alpha decay, spontaneous fission and beta decay as a function of mass number of the parent nuclei (A).

Proton decay from rich proton emitters in the actinide region is studied using the Coulomb and proximity potential model(CPPM). The penetration probability and proton decay half-lives in the actinide region are calculated.logarithmic half-lives of alpha decay, spontaneous fission half-lives, β^- decay and β^+ decay half-lives are also studied. The comparison of log($T_{1/2}$) of proton

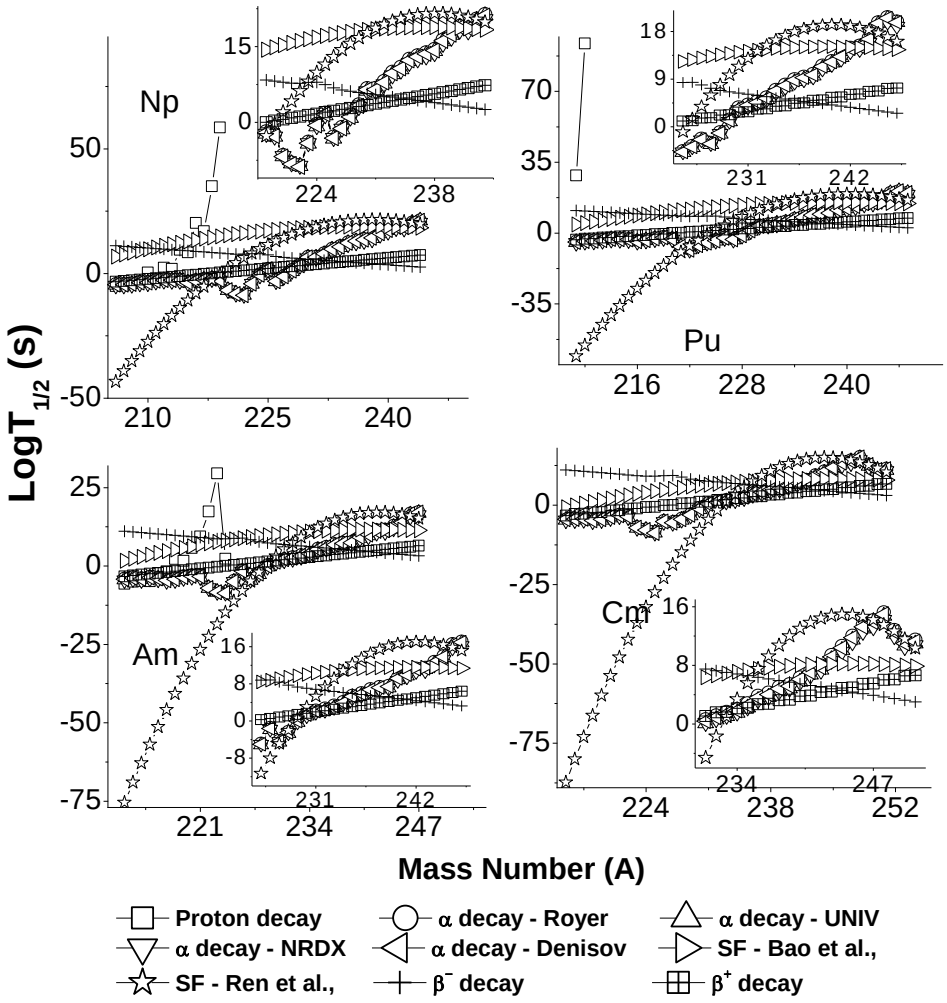

Fig. 4.17 Variation of log($T_{1/2}$) of proton activity, alpha decay, spontaneous fission and beta decay as a function of mass number of the parent nuclei (A).

decay with that of other decay modes such as alpha decay, spontaneous fission and beta decay as a function of mass number of parent nuclei is as presented in the figure 4.16. From the figure 4.16(a) it is observed that proton decay for Actinium (A_c) is energetically possible for the mass number of 195$<$ A $<$207. Figure 4.16(a) gives the comparison of proton decay with that of other decay modes such as alpha decay, spontaneous fission and beta decay. Similarly from the figure 4.16(b) for Th, proton decay is energetically possible in the mass number region 195$<$ A $<$207, from the figure. 4.16(c) for Pa, proton decay is energetically possible in the mass number region 200$<$ A $<$209 and 212$<$ A $<$213, and in figure 4.16(d) for U proton decay is energetically

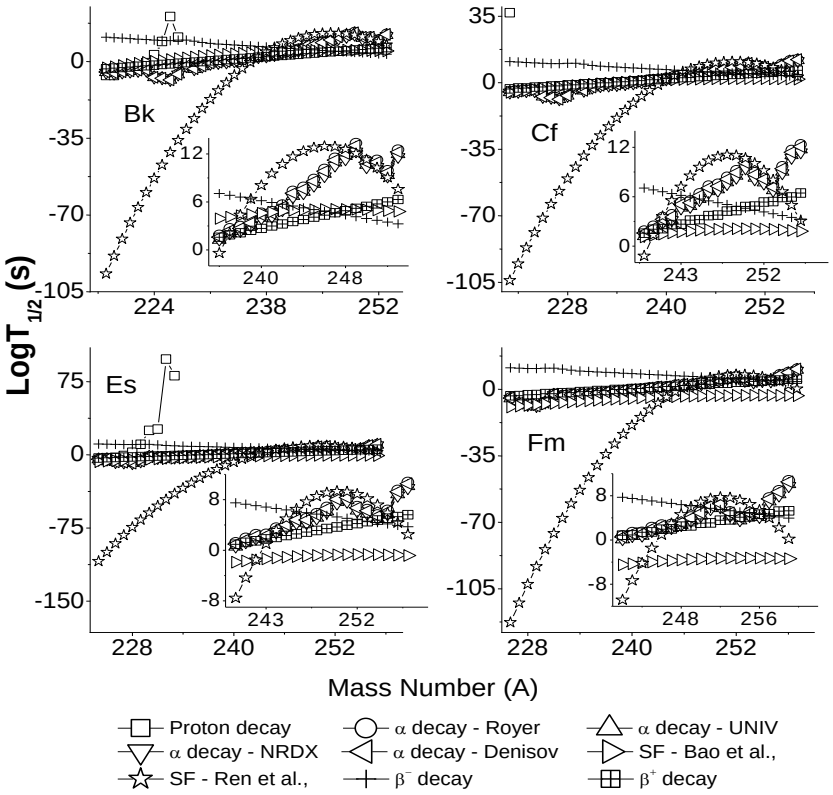

Fig. 4.18 Variation of log($T_{1/2}$) of proton activity, alpha decay, spontaneous fission and beta decay as a function of mass number of the parent nuclei (A).

Table 4.8 List of studied actinide nuclei for proton decay

Z	A-Range	A-Q+VE	A-Q-VE
89	195-293	195-207	208-293
90	198-296	198-199	200-296
91	200-300	200-209, 212-213	210-211, 214-300
92	203-303	203	204-303
93	206-306	206-217	218-306
94	209-309	209	210-309
95	212-313	212-224	225-313
96	215-316	215	216-316
97	218-319	218-227	228-319
98	221-322	221	222-322
99	224-326	224-231	232-326
100	226-329	-	226-329
101	229-332	229-239	240-332
102	232-335	232-233	234-335
103	235-339	235-243	244-339

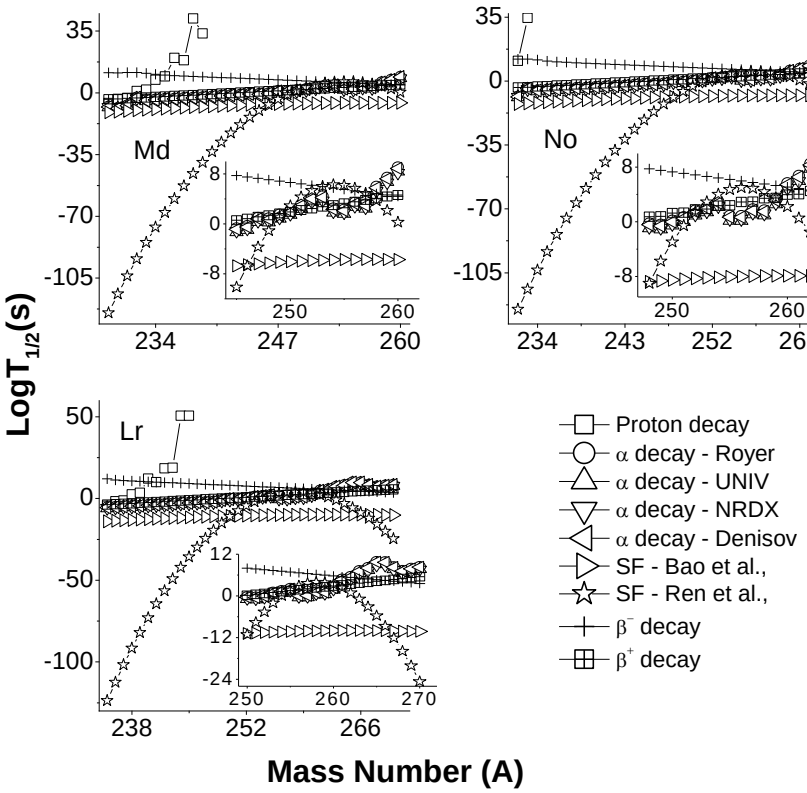

Fig. 4.19 Variation of log($T_{1/2}$) of proton activity, alpha decay, spontaneous fission and beta decay as a function of mass number of the parent nuclei (A).

possible in the mass number region 203.Similarly the figure 4.17-4.19 gives the comparison of proton decay with that of alpha decay, spontaneous fission and beta decay in the actinide region Z=93-103. The energetically favor proton emission is tabulated in table 4.8.

For better understanding of predictable decay modes, a graph is plotted with the logarithmic half-lives of different decay modes such as proton decay, spontaneous fission, alpha decay and beta decay half-lives and it is presented in figure 4.20. From the figure 4.20(a) it is observed that the ^{194}Ac is a proton emitter, alpha decay mode is observed in the mass number of range $^{195-209}$Ac and $^{211-224}$Ac, β^+ decay and β^- decay is energetically possible in the nuclei ^{210}Ac and $^{225-239}$Ac respectively. Similarly the decay modes for actinide nuclei with Z= 90-103 (Th-Lr) are shown in the figure 4.20. The predicted energy released during proton decay, penetration probability and half-lives for Z=89-103 and the results are tabulated in table 4.9. In order to predict the dominant

Table 4.9 Energy released, penetration factor and logarithmic half-lives for proton decay in actinide nuclei

Nuclei	Q	P	T	Nuclei	Q	P	T	Nuclei	Q	P	T
^{195}Ac	2.161	2.142×10^{-15}	1.892×10^{-7}	^{210}Np	1.301	5.444×10^{-24}	$7.631\times10^{+1}$	^{227}Bk	0.771	4.652×10^{-36}	$9.165\times10^{+13}$
^{196}Ac	1.591	1.396×10^{-19}	2.907×10^{-3}	^{211}Np	1.561	5.185×10^{-21}	8.025×10^{-2}	^{221}Cf	0.281	6.088×10^{-69}	$6.941\times10^{+46}$
^{197}Ac	1.591	1.391×10^{-19}	2.923×10^{-3}	^{212}Np	1.151	3.491×10^{-26}	$1.193\times10^{+4}$	^{224}Es	2.181	1.426×10^{-17}	2.976×10^{-5}
^{198}Ac	1.321	1.775×10^{-22}	2.294×10^{0}	^{213}Np	1.181	1.025×10^{-25}	$4.072\times10^{+3}$	^{225}Es	2.181	1.419×10^{-17}	2.995×10^{-5}
^{199}Ac	1.331	2.277×10^{-22}	1.791×10^{0}	^{214}Np	0.771	2.498×10^{-34}	$1.673\times10^{+12}$	^{226}Es	1.771	1.186×10^{-20}	3.589×10^{-2}
^{200}Ac	1.441	4.324×10^{-21}	9.452×10^{-2}	^{215}Np	0.811	3.254×10^{-33}	$1.286\times10^{+11}$	^{227}Es	1.541	6.434×10^{-23}	6.626×10^{0}
^{201}Ac	1.371	6.726×10^{-22}	6.087×10^{-1}	^{216}Np	0.471	4.977×10^{-47}	$8.426\times10^{+24}$	^{228}Es	1.251	1.236×10^{-26}	$3.454\times10^{+4}$
^{202}Ac	0.971	6.033×10^{-28}	$6.797\times10^{+5}$	^{217}Np	0.541	4.641×10^{-43}	$9.05\times10^{+20}$	^{229}Es	0.821	2.005×10^{-35}	$2.132\times10^{+13}$
^{203}Ac	1.018	4.688×10^{-27}	$8.762\times10^{+4}$	^{209}Pu	0.351	2.896×10^{-57}	$1.432\times10^{+35}$	^{230}Es	0.441	1.03×10^{-52}	$4.157\times10^{+30}$
^{204}Ac	0.595	1.424×10^{-38}	$2.889\times10^{+16}$	^{212}Am	2.051	1.838×10^{-17}	2.267×10^{-5}	^{231}Es	0.421	2.493×10^{-54}	$1.719\times10^{+32}$
^{205}Ac	0.707	1.575×10^{-34}	$2.616\times10^{+12}$	^{213}Am	1.951	3.465×10^{-18}	1.204×10^{-4}	^{229}Md	2.251	1.482×10^{-17}	2.883×10^{-5}
^{206}Ac	0.383	5.019×10^{-51}	$8.225\times10^{+28}$	^{214}Am	1.911	1.705×10^{-18}	2.451×10^{-4}	^{230}Md	1.921	6.453×10^{-20}	6.636×10^{-3}
^{207}Ac	0.277	4.149×10^{-62}	$9.965\times10^{+39}$	^{215}Am	1.931	2.449×10^{-18}	1.709×10^{-4}	^{231}Md	1.871	2.514×10^{-20}	1.705×10^{-2}
^{198}Th	0.291	2.163×10^{-56}	$1.883\times10^{+34}$	^{216}Am	1.601	3.564×10^{-21}	1.176×10^{-1}	^{232}Md	1.441	1.172×10^{-24}	$3.662\times10^{+2}$
^{199}Th	0.201	1.218×10^{-76}	$3.35\times10^{+54}$	^{217}Am	1.531	6.843×10^{-22}	6.138×10^{-1}	^{233}Md	1.381	1.935×10^{-25}	$2.222\times10^{+3}$
^{200}Pa	2.111	3.807×10^{-16}	1.073×10^{-6}	^{218}Am	1.191	3.191×10^{-26}	$1.318\times10^{+4}$	^{234}Md	1.001	8.656×10^{-32}	$4.975\times10^{+9}$
^{201}Pa	2.091	2.964×10^{-16}	1.381×10^{-6}	^{219}Am	1.231	1.29×10^{-25}	$3.264\times10^{+3}$	^{236}Md	0.911	7.3×10^{-34}	$5.909\times10^{+11}$
^{202}Pa	1.751	1.028×10^{-18}	3.988×10^{-4}	^{220}Am	0.971	3.403×10^{-30}	$1.24\times10^{+8}$	^{237}Md	0.561	2.862×10^{-46}	$1.509\times10^{+24}$
^{203}Pa	1.491	3.735×10^{-21}	1.099×10^{-1}	^{221}Am	0.801	2.486×10^{-34}	$1.7\times10^{+12}$	^{238}Md	0.591	9.869×10^{-45}	$4.383\times10^{+22}$
^{204}Pa	1.221	1.868×10^{-24}	$2.202\times10^{+2}$	^{222}Am	0.551	1.326×10^{-43}	$3.189\times10^{+21}$	^{239}Md	0.251	2.607×10^{-76}	$1.661\times10^{+54}$
^{205}Pa	1.391	2.895×10^{-22}	1.423×10^{0}	^{223}Am	0.341	5.349×10^{-59}	$7.923\times10^{+36}$	^{232}No	0.831	2.217×10^{-36}	$1.936\times10^{+14}$
^{206}Pa	0.981	1.738×10^{-28}	$2.375\times10^{+6}$	^{224}Am	1.181	2.105×10^{-26}	$2.016\times10^{+4}$	^{233}No	0.331	6.422×10^{-65}	$6.697\times10^{+42}$
^{207}Pa	1.221	1.842×10^{-24}	$2.244\times10^{+2}$	^{215}Cm	0.221	8.665×10^{-78}	$4.832\times10^{+55}$	^{235}Lr	2.161	1.317×10^{-18}	3.273×10^{-4}
^{208}Pa	0.801	1.222×10^{-32}	$3.388\times10^{+10}$	^{218}Bk	2.241	1.015×10^{-16}	4.142×10^{-6}	^{236}Lr	1.781	1.25×10^{-21}	3.455×10^{-1}
^{209}Pa	0.801	1.215×10^{-32}	$3.412\times10^{+10}$	^{219}Bk	2.231	8.983×10^{-17}	$4.69\times10^{+6}$	^{237}Lr	1.731	4.252×10^{-22}	1.017×10^{0}
^{212}Pa	0.42	3.479×10^{-49}	$1.197\times10^{+27}$	^{220}Bk	1.841	$1.507\text{x}1019\times10^{-}$	2.799×10^{-3}	^{238}Lr	1.361	2.602×10^{-26}	$1.66\times10^{+4}$
^{213}Pa	0.283	4.874×10^{-14}	8.563×10^{-9}	^{221}Bk	1.871	2.73×10^{-19}	1.547×10^{-3}	^{239}Lr	1.281	1.766×10^{-27}	$2.455\times10^{+5}$
^{203}U	0.381	3.469×10^{-53}	$1.184\times10^{+31}$	^{222}Bk	1.611	1.288×10^{-21}	3.283×10^{-1}	^{240}Lr	0.811	2.142×10^{-37}	$2.027\times10^{+15}$
^{206}Np	1.911	5.525×10^{-18}	7.471×10^{-5}	^{223}Bk	1.461	2.993×10^{-23}	$1.416\times10^{+1}$	^{241}Lr	0.901	6.58×10^{-35}	$6.61\times10^{+12}$
^{207}Np	1.881	3.226×10^{-18}	1.281×10^{-4}	^{224}Bk	1.171	3.263×10^{-27}	$1.3\times10^{+5}$	^{242}Lr	0.611	8.46×10^{-45}	$5.149\times10^{+22}$
^{208}Np	1.751	3.04×10^{-19}	1.362×10^{-3}	^{225}Bk	0.841	4.615×10^{-34}	$9.21\times10^{+11}$	^{243}Lr	0.601	2.884×10^{-45}	$1.512\times10^{+23}$
^{209}Np	1.691	8.868×10^{-20}	4.677×10^{-3}	^{226}Bk	0.501	1.852×10^{-47}	$2.298\times10^{+25}$				

decay mode in the atomic number range Z=89-103, branching ratios are calculated. The branching ratio of proton decay to alpha decay is defined as,

$$BR = \frac{\lambda_P}{\lambda_{\alpha/SF/\beta^+/\beta^-}} \tag{4.10}$$

Where λ_p is the decay constant corresponding to proton emission and $\lambda_{\alpha/SF/\beta^+/\beta^-}$ is the decay constant corresponding to alpha decay, spontaneous fission, β^+ decay and β^- decay respectively. The variation of branching ratios of proton decay with respect to the alpha decay (NRDX), SF (Bao et al.,), beta (minus) decay and beta (plus) decay as a function mass number of the nuclei is as shown in figure 4.21.From the figure 4.21(a) it is observed that the branching ratio of $\lambda_p/\lambda_{\alpha/\beta^+}$ values are higher in the mass number range $^{194-197}$Ac and gradually decreases with increase in mass number range above $^{197-207}$Ac. The branching ratio of $\lambda_p/\lambda_{sf/\beta^-}$ val-

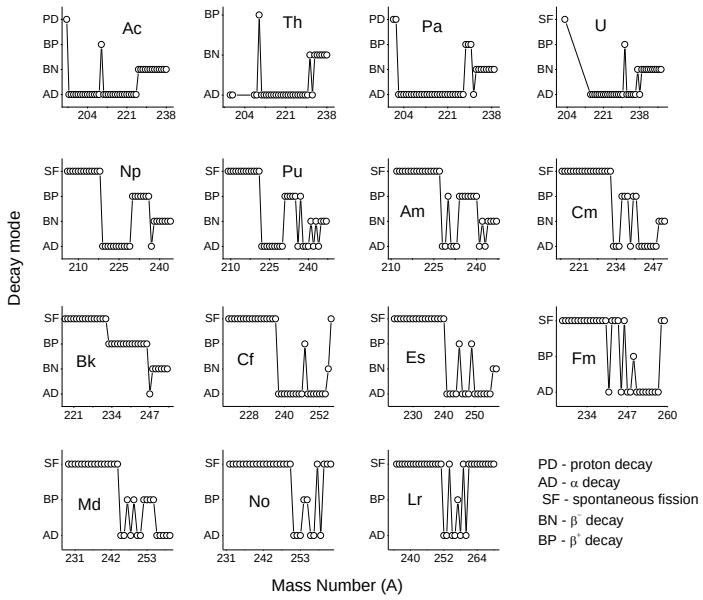

Fig. 4.20 Variation of decay modes such as proton activity, alpha decay, spontaneous fission, beta plus decay and beta minus decay as a function of mass number of the parent nuclei (A).

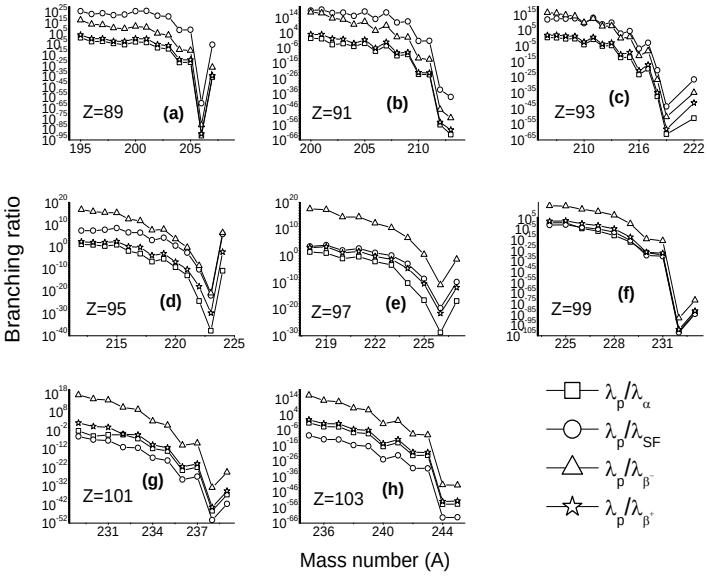

Fig. 4.21 A variation of branching ratios of proton decay to the alpha decay (NRDX), SF (Bao et al., [295]), beta (minus) decay and beta (plus) decay as a function mass number of the nuclei.

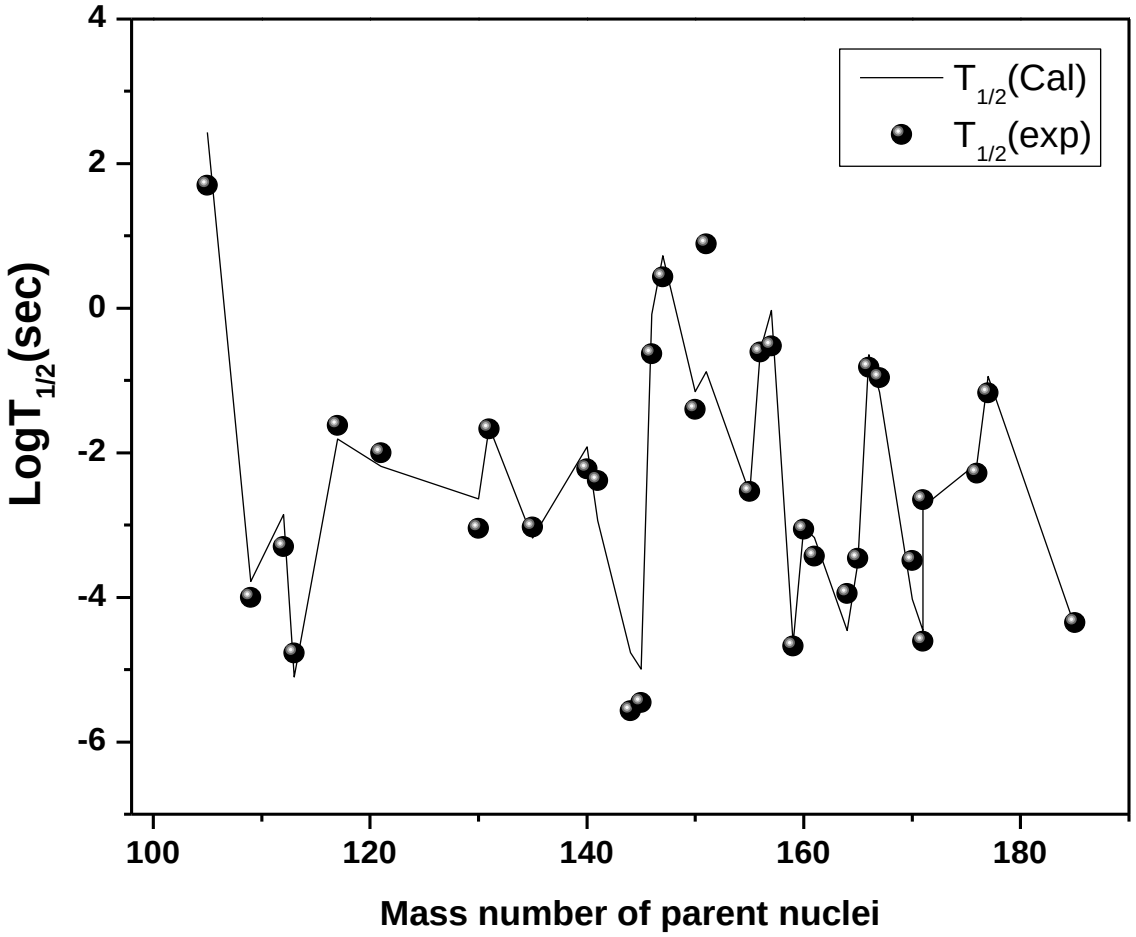

Fig. 4.22 The variation of calculated logarithmic half-lives of proton decay of different mass number of proton emitters with the available experimental values [6, 34, 35, 115, 117, 198, 216, 234, 246–248, 296–303] in the actinide range.

ues are higher in the mass number range $^{194-203}$Ac and decreases with increase in mass number range $^{204-207}$Ac. Similarly from the figure 4.21(b) to 4.21(h) it is observed that the values of branching ratios gradually decreases with increase in mass number. The figure 4.22 denotes the variation of calculated logarithmic half-lives with the available experimental values [6, 34, 35, 115, 117, 198, 216, 234, 246–248, 296–303]. The continuous line represents the calculated logarithmic half-lives and dots represents the experimental logarithmic half-lives values of proton emitters . Table 4.10 also lists the experimental half-live values, energy released during the proton decay and calculated half-lives of proton emitters. From the figure 4.22 and table 4.10 it is

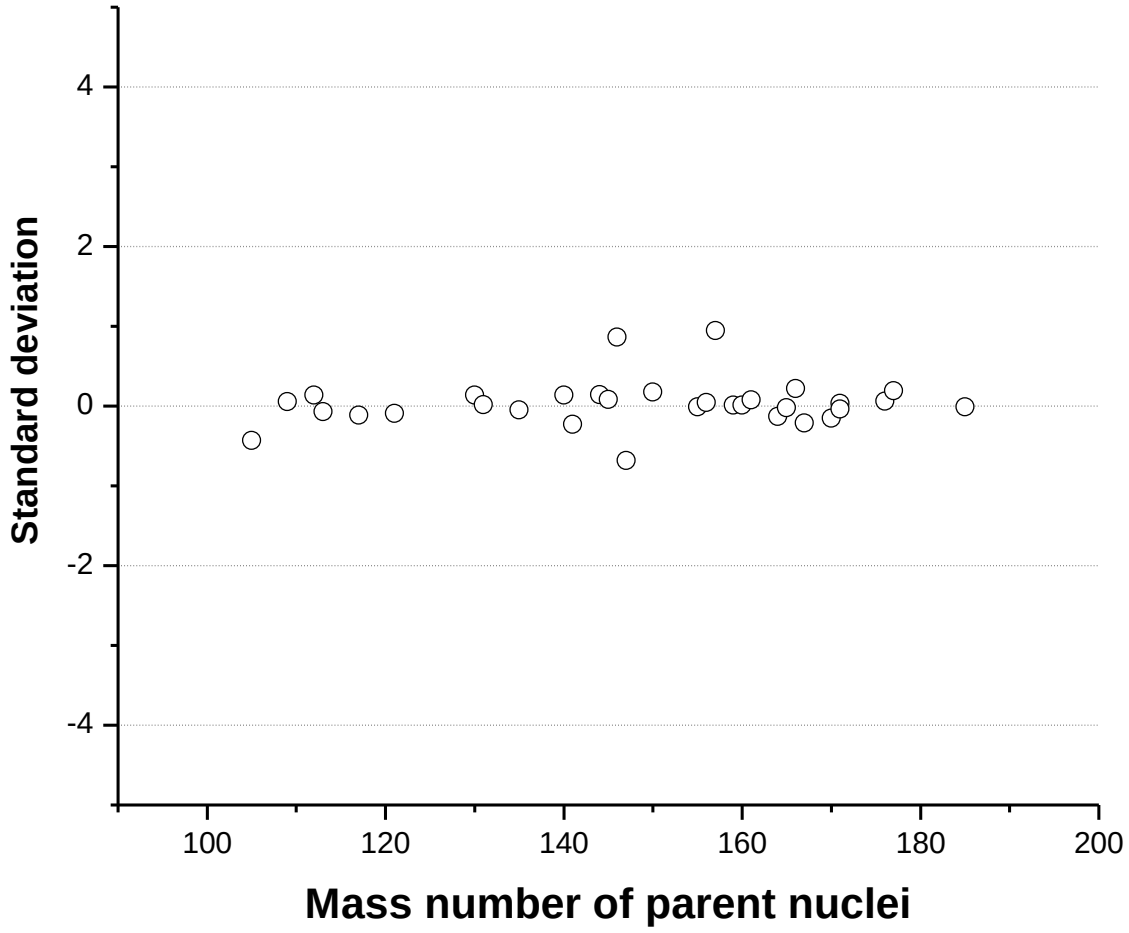

Fig. 4.23 A standard deviation of proton decay from the experimental values with that of mass number of parent nuclei.

Table 4.10 The comparison of calculated half-lives with the experimental values [6, 34, 35, 115, 117, 198, 216, 234, 246–248, 296–303].

Isotopes	β_2	β_4	ℓ	$\log 1/2$(exp.)	Ref.	Isotopes	β_2	β_4	ℓ	$\log 1/2$(exp.)	Ref.
^{105}Sb	0.081	0.051	2	1.7	[296]	^{155}Ta	0.008	0	5	-2.538	[6, 34, 35, 198, 234]
^{109}I	0.16	0.06	2	-4	[117, 246, 297]	^{156}Ta	-0.053	0.001	2	-0.609	[6, 34, 35, 198, 234]
^{112}Cs	0.208	0.067	2	-3.3	[247]	^{157}Ta	0.045	0.001	0	-0.523	[6, 34, 35, 198, 234]
^{113}Cs	0.207	0.052	2	-4.77	[247, 297]	^{159}Re	0.053	-0.007	5	-4.678	[6, 34, 35, 198, 234]
^{117}La	0.29	0.1	2	-1.623	[6, 34, 35, 198, 234]	^{160}Re	0.08	0.002	2	-3.06	[300]
^{121}Pr	0.318	0.075	2	-2	[6, 34, 35, 198, 234]	^{161}Re	0.08	-0.006	3	-3.43	[301]
^{130}Eu	0.331	0	2	-3.046	[6, 34, 35, 198, 234]	^{164}Ir	0.089	-0.006	5	-3.947	[6, 34, 35, 198, 234]
^{131}Eu	0.331	0	2	-1.67	[6, 34, 35, 198, 234]	^{165}Ir	0.099	-0.012	5	-3.46	[302]
^{135}Tb	0.325	-0.046	3	-3.027	[6, 34, 35, 198, 234]	^{166}Ir	0.107	-0.004	2	-0.82	[302]
^{140}Ho	0.297	-0.07	3	-2.222	[6, 34, 35, 198, 234]	^{167}Ir	0.116	-0.011	0	-0.96	[302]
^{141}Ho	0.286	-0.063	3	-2.387	[6, 34, 35, 198, 234]	^{170}Au	-0.096	-0.012	2	-3.493	[6, 34, 35, 198, 234]
^{144}Tm	0.258	-0.077	5	-5.569	[6, 34, 35, 198, 234]	^{171}Au	-0.105	-0.011	0	-4.611	[6, 34, 35, 198, 234]
^{145}Tm	0.249	-0.078	5	-5.456	[6, 34, 35, 198, 234]	^{171}Au	-0.105	-0.011	4	-2.65	[302]
^{146}Tm	-0.199	-0.038	5	-0.63	[248]	^{176}Tl	-0.053	-0.007	0	-2.284	[6, 34, 35, 198, 234]
^{147}Tm	-0.19	-0.04	5	0.43	[216, 246, 298]	^{177}Tl	-0.053	-0.007	0	-1.174	[6, 34, 35, 198, 234]
^{150}Lu	-0.164	-0.05	5	-1.4	[246, 299]	^{185}Bi	-0.052	0.016	0	-4.35	[303]
^{151}Lu	-0.156	-0.045	5	0.89	[115, 246]						

Table 4.11 Standard deviation of proton decay half-lives in the nuclei region Z=51-83.

n	Parent	σ
21	o-o	1.09065
12	o-e	0.879551

observed that the calculated half lives of proton emitters are in good agreement with the experimental values [6, 34, 35, 115, 117, 198, 216, 234, 246–248, 296–303]. The standard deviation of calculated proton decay half lives with the experimental values is studied. The standard deviation of present work with the experimental values is presented in figure 4.23. The standard root mean square deviation of calculated logarithmic half-lives are evaluated using the following equation:

$$\sigma = \left\{ \sum_{i=1}^{n} \left[\log_{10} \left(T_{cal} / T_{\exp} \right) \right]^2 / (n-1) \right\}^{1/2} \tag{4.11}$$

The overall standard deviation of proton decay half-lives in the odd-odd nuclei are observed to be 1.09065 and for odd-even were observed to be 0.879551 and are tabulated in table 4.11. From the predictions of proton decay in the atomic nuclei range Z=51-83, it is observed that our calculations are in good agreement with the experimental values. Hence forth, we have predicted half-lives of proton decay in the actinide region.

4.2.4 **Systematics of actinides**

The proton decay rates are sensitive to amount of energy released (Q_p) and the orbital angular momentum of the emitted proton. The total interacting potential which is a sum of Coulomb, proximity and angular potential is studied as explained in the theory. During the proton emission, the ground state to ground state transitions has zero angular momentum $\ell = 0$. Thus the effects of angular potential in case of proton emission is neglected and the deformed nuclei is also considered in the present work. The penetration probability is evaluated using WKB approximation and studied logarithmic half-lives of proton decay in the actinide region. The amount of energy

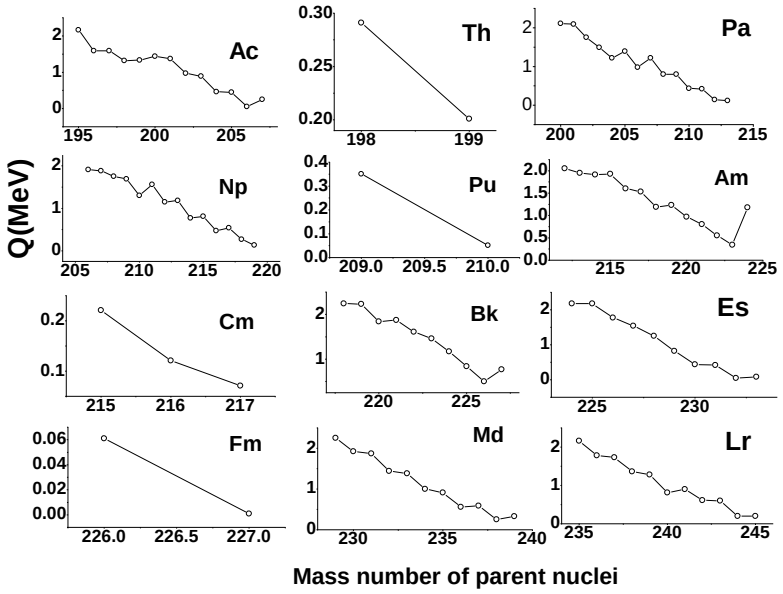

Fig. 4.24 The variation of amount of energy released during proton decay with the mass number of parent nuclei in the actinide region.

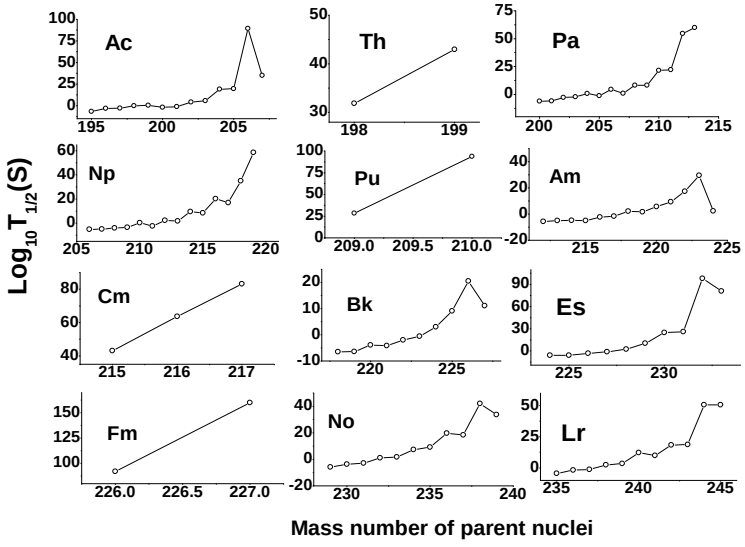

Fig. 4.25 The variation of logarithmic half-lives of proton decay with the mass number of parent nuclei in the actinide region.

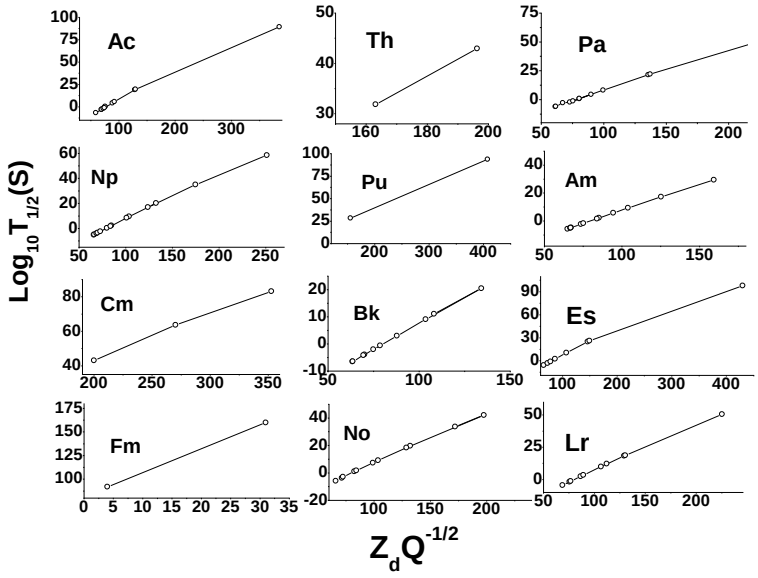

Fig. 4.26 Variation of logarithmic half-lives of proton decay with the product of $Z_dQ^{-1/2}$ in the actinide region.

Table 4.12 Proton decay half-lives, penetration factor and amount of energy released during proton decay in actinides.

Nuclei	Q (MeV)	Penetration factor	$\log T_{1/2}(s)$
^{195}Ac	2.161	2.14×10^{-15}	1.89×10^{-7}
^{200}Pa	2.111	3.8×10^{-16}	1.07×10^{-6}
^{206}Np	1.911	5.52×10^{-18}	1.47×10^{-5}
^{212}Am	2.051	1.83×10^{-17}	2.26×10^{-5}
^{218}Bk	2.241	1.01×10^{-16}	4.14×10^{-6}
^{224}Es	2.181	1.42×10^{-17}	2.97×10^{-5}
^{229}Md	2.251	1.48×10^{-17}	2.88×10^{-5}
^{235}Lr	2.161	1.31×10^{-18}	3.27×10^{-4}

released during proton decay as function of mass number of parent nuclei in the actinide region as shown in figure 4.24. From the figure it is observed that the amount of energy released during proton decay gradually decreases with the increase in mass number of parent nuclei.

The studied logarithmic half-lives of proton decay in the actinide region is plotted as function of the mass number of parent nuclei is presented in figure 4.25. The figure indicates that the logarithmic half-lives increases with increase in mass number of parent nuclei. The half-lives values are of the order of 10^{-6} to 10^{-4} S for the actinides ^{195}Ac, ^{200}Pa, ^{206}Np, ^{212}Am, ^{218}Bk,

Table 4.13 A comparison of logarithmic half-lives of proton decay with Royer, Univ, NRDX, Denisov and Bao.

Parent Nuclei	$\log T_{1/2}$(s)						Decay Mode	Parent Nuclei	$\log T_{1/2}$(s)						Decay Mode
	Proton	Sf	α-decay						Proton	Sf	α-decay				
		Bao	Royer	UNIV	NRDX	Denisov				Bao	Royer	UNIV	NRDX	Denisov	
^{195}Ac	-6.723	19.285	1.9019	1.389	1.0527	1.4794	p	^{219}Am	3.5138	5.7441	8.3273	7.6976	7.1848	7.9916	p
^{196}Ac	-2.536	20.325	4.1825	3.6576	3.281	3.7588	p	^{220}Am	8.0934	6.2466	9.6523	9.0362	8.4594	9.3163	p
^{197}Ac	-2.53	21.33	4.161	3.637	3.283	3.739	p	^{221}Am	12.231	6.7266	10.5613	9.9572	9.3406	10.2256	sf
^{198}Ac	0.3608	22.3023	5.3396	4.8169	4.4464	4.9171	p	^{222}Am	21.504	7.184	11.9864	11.4037	10.7102	11.6503	sf
^{199}Ac	0.2533	23.2399	5.2725	4.751	4.4043	4.8513	p	^{223}Am	36.899	7.6186	13.2599	12.6999	11.9365	12.9237	sf
^{200}Ac	-1.0245	24.1421	4.7543	4.234	3.9256	4.3348	p	^{224}Am	4.3046	8.0304	8.4788	7.8558	7.4335	8.1488	p
^{201}Ac	-0.2156	25.0094	5.0479	4.5289	4.2323	4.6293	p	^{215}Cm	55.684	-0.757	14.7612	14.1951	13.0602	14.4243	sf
^{202}Ac	5.8323	25.8415	6.9328	6.4209	6.0791	6.5134	p	^{218}Bk	-5.3828	-3.0072	4.7539	4.0643	3.6171	4.442	p
^{203}Ac	4.9426	26.6385	6.6779	6.1659	5.855	6.26	p	^{219}Bk	-5.3288	-2.467	4.774	4.0855	3.6571	4.4633	p
^{204}Ac	16.461	27.4004	8.8704	8.3763	7.9999	8.4513	α	^{220}Bk	-2.5529	-1.9435	6.41	5.7228	5.2133	6.0987	p
^{205}Ac	12.42	28.1272	8.2391	7.7403	7.4114	7.8219	α	^{221}Bk	-2.8104	-1.4371	6.2571	5.5707	5.0908	5.9472	p
^{206}Ac	28.92	28.8189	10.038	9.5593	9.1753	9.6197	α	^{222}Bk	-0.4836	-0.9482	7.4155	6.7345	6.1991	7.1056	sf
^{207}Ac	39.985	29.4757	10.65	10.18	9.79	10.2318	α	^{223}Bk	1.1511	-0.4774	8.1082	7.4325	6.8702	7.7987	sf
^{198}Th	34.275	16.1819	11.31	10.813	10.1	10.8917	α	^{224}Bk	5.1142	-0.0248	9.5409	8.8787	8.2362	9.231	sf
^{199}Th	54.525	17.1443	11.845	11.357	10.641	11.4272	α	^{225}Bk	11.964	0.4093	11.307	10.6676	9.9153	10.9964	sf
^{200}Pa	-5.9691	12.2615	2.9029	2.341	1.9651	2.5071	p	^{226}Bk	25.362	0.8245	13.297	12.6906	11.805	12.9856	sf
^{201}Pa	-5.8597	13.1791	2.96	2.3991	2.0424	2.5654	p	^{227}Bk	13.962	1.2206	11.666	11.0339	10.2944	11.3574	sf
^{202}Pa	-3.3992	14.068	4.3279	3.7624	3.3775	3.933	p	^{221}Cf	46.841	-5.1307	15.364	14.767	13.5179	15.0549	sf
^{203}Pa	-0.9587	14.9279	5.4434	4.8786	4.4705	5.0485	p	^{224}Es	-4.5262	-7.1242	5.7952	5.0641	4.5505	5.5104	sf
^{204}Pa	2.3428	15.7583	6.679	6.119	5.679	6.284	p	^{225}Es	-4.5235	-6.6849	5.7749	5.0449	4.5523	5.4914	sf
^{205}Pa	0.1534	16.5588	5.8572	5.2957	4.9125	5.4643	p	^{226}Es	-1.445	-6.2589	7.5555	6.8314	6.2318	7.2712	sf
^{206}Pa	6.3757	17.3293	7.8264	7.2758	6.8254	7.4327	p	^{227}Es	0.8213	-5.8467	8.6204	7.9043	7.2448	8.3362	sf
^{207}Pa	2.3511	18.0696	6.6162	6.0597	5.6857	6.2249	p	^{228}Es	4.5384	-5.4488	10.0548	9.3534	8.6021	9.7703	sf
^{208}Pa	10.53	18.7794	8.726	8.1856	7.734	8.3337	α	^{229}Es	13.329	-5.0656	12.393	11.7244	10.8019	12.1071	sf
^{209}Pa	10.533	19.4586	8.7054	8.1659	7.7364	8.3143	α	^{230}Es	30.619	-4.6974	14.6914	14.0653	12.9649	14.4042	sf
^{212}Pa	27.078	21.3128	10.794	10.281	9.8076	10.4027	α	^{231}Es	32.236	-4.3445	14.8004	14.1776	13.0875	14.5144	sf
^{213}Pa	-8.0673	21.8698	11.6	11.1	10.61	11.213	α	^{229}Md	-4.54	-11.0676	6.3166	5.5442	4.9712	6.0582	sf
^{203}U	31.073	9.436	11.764	11.23	10.42	11.3731	α	^{230}Md	-2.1781	-10.7089	7.7399	6.9732	6.3081	7.4812	sf
^{206}Np	-4.1266	6.7169	4.5136	3.9048	3.4685	4.1449	p	^{231}Md	-1.7682	-10.3599	7.9478	7.1833	6.5207	7.69	sf
^{207}Np	-3.8922	7.4948	4.6184	4.0107	3.5904	4.2508	p	^{232}Md	2.5638	-10.0213	9.9984	9.2518	8.4382	9.7396	sf
^{208}Np	-2.8658	8.2485	5.1529	4.546	4.1214	4.786	p	^{233}Md	3.3468	-9.6935	10.2843	9.5419	8.7231	10.0264	sf
^{209}Np	-2.33	8.9775	5.3939	4.7883	4.373	5.0279	p	^{234}Md	9.6969	-9.3769	12.309	11.5948	10.6168	12.0501	sf
^{210}Np	1.8826	9.6813	7.1678	6.5688	6.0847	6.8012	p	^{235}Md	11.772	-9.0719	12.8028	12.0975	11.0941	12.5445	sf
^{211}Np	-1.0955	10.3596	5.9324	5.3299	4.9296	5.5683	p	^{236}Md	24.179	-8.779	14.9003	14.2344	13.0556	14.6409	sf
^{212}Np	4.0769	11.0122	7.8628	7.2705	6.7906	7.4977	p	^{237}Md	22.642	-8.4983	14.6912	14.0222	12.8826	14.4333	sf
^{213}Np	3.6098	11.6388	7.6927	7.1005	6.6504	7.3291	p	^{238}Md	54.221	-8.2302	16.915	16.295	14.9613	16.6559	sf
^{214}Np	12.224	12.2391	9.8169	9.2454	8.6965	9.4522	α	^{239}Md	42.18	-7.975	16.3479	18.4435	21.3829	16.0906	sf
^{215}Np	11.11	12.8132	9.5771	9.004	8.4897	9.2138	α	^{232}No	14.287	-12.61	13.8567	13.1417	11.8994	13.6041	sf
^{216}Np	24.926	13.3607	11.5	10.95	10.34	11.1356	α	^{233}No	42.826	-12.2943	17.0247	16.3769	14.8403	16.77	sf
^{217}Np	20.957	13.8818	11.065	10.516	9.951	10.702	α	^{235}Lr	-3.485	-14.0132	7.5036	6.6935	6.0196	7.2718	sf
^{209}Pu	35.156	4.1089	12.929	12.374	11.439	12.5655	α	^{236}Lr	-0.4616	-13.7382	9.222	8.4237	7.6179	8.9895	sf
^{212}Am	-4.6445	1.6163	4.7376	4.0882	3.6407	4.3973	p	^{237}Lr	0.0075	-13.4702	9.442	8.6467	7.8401	9.2105	sf
^{213}Am	-3.9192	2.2689	5.1358	4.487	4.0386	4.7962	p	^{238}Lr	4.2212	-13.2097	11.2859	10.512	9.5541	11.0536	sf
^{214}Am	-3.6105	2.9012	5.2852	4.6376	4.2014	4.9467	p	^{239}Lr	5.3901	-12.9572	11.6911	10.9237	9.9465	11.4596	sf
^{215}Am	-3.7671	3.5128	5.1793	4.5329	4.1226	4.8422	p	^{240}Lr	15.307	-12.7131	14.3468	13.6242	12.4066	14.1136	sf
^{216}Am	-0.9294	4.1033	6.616	5.9729	5.5024	6.2785	p	^{241}Lr	12.82	-12.4779	13.7897	13.0578	11.9148	13.5583	sf
^{217}Am	-0.212	4.6721	6.919	6.2783	5.8103	6.5824	p	^{242}Lr	22.712	-12.2519	15.5493	14.8527	13.5519	15.3172	sf
^{218}Am	4.12	5.2192	8.5489	7.9199	7.3731	8.2118	p	^{243}Lr	23.179	-12.0354	15.5979	14.8991	13.6128	15.3628	sf

Table 4.14 The comparison of calculated half-lives with the experimental values [117, 246, 247],[6, 34, 35, 115, 198, 216, 234, 248, 296–303].

Parent	daughter	l	logt-pw	log $T_{1/2}$-exp	ref	parent	Daughter	l	logt-pw	log $T_{1/2}$-exp	ref
^{105}Sb	^{101}In	2	2.43	1.70	[296]	^{155}Ta	^{151}Lu	5	-2.56	-2.54	[6, 34, 35, 198, 234]
^{109}I	^{105}Sb	2	-3.78	-4.00	[117, 246, 297]	^{156}Ta	^{152}Lu	2	-0.58	-0.61	[6, 34, 35, 198, 234]
^{112}Cs	^{108}I	2	-2.86	-3.30	[247]	^{157}Ta	^{153}Lu	0	-0.03	-0.52	[6, 34, 35, 198, 234]
^{113}Cs	^{109}I	2	-5.10	-4.77	[247, 297]	^{159}Re	^{155}Ta	5	-4.64	-4.68	[6, 34, 35, 198, 234]
^{117}La	^{113}Cs	2	-1.81	-1.62	[6, 34, 35, 198, 234]	^{160}Re	^{156}Ta	2	-3.03	-3.06	[300]
^{121}Pr	^{117}La	2	-2.19	-2.00	[6, 34, 35, 198, 234]	^{161}Re	^{157}Ta	3	-3.17	-3.43	[301]
^{130}Eu	^{126}Pm	2	-2.64	-3.05	[6, 34, 35, 198, 234]	^{164}Ir	^{160}Re	5	-4.46	-3.95	[6, 34, 35, 198, 234]
^{131}Eu	^{127}Pm	2	-1.64	-1.67	[6, 34, 35, 198, 234]	^{165}Ir	^{161}Re	5	-3.53	-3.46	[302]
^{135}Tb	^{131}Eu	3	-3.18	-3.03	[6, 34, 35, 198, 234]	^{166}Ir	^{162}Re	2	-0.64	-0.82	[302]
^{140}Ho	^{136}Tb	3	-1.92	-2.22	[6, 34, 35, 198, 234]	^{167}Ir	^{163}Re	0	-1.16	-0.96	[302]
^{141}Ho	^{137}Tb	3	-2.94	-2.39	[6, 34, 35, 198, 234]	^{170}Au	^{166}Ir	2	-4.03	-3.49	[6, 34, 35, 198, 234]
^{144}Tm	^{140}Ho	5	-4.77	-5.57	[6, 34, 35, 198, 234]	^{171}Au	^{167}Ir	0	-4.46	-4.61	[6, 34, 35, 198, 234]
^{145}Tm	^{141}Ho	5	-5.00	-5.46	[6, 34, 35, 198, 234]	^{171}Au	^{167}Ir	4	-2.75	-2.65	[302]
^{146}Tm	^{142}Ho	5	-0.09	-0.63	[248]	^{176}Tl	^{172}Au	0	-2.15	-2.28	[6, 34, 35, 198, 234]
^{147}Tm	^{143}Ho	5	0.72	0.43	[246, 296, 297]	^{177}Tl	^{173}Au	0	-0.95	-1.17	[6, 34, 35, 198, 234]
^{150}Lu	^{146}Tm	5	-1.15	-1.40	[246, 299]	^{185}Bi	^{181}Tl	0	-4.40	-4.35	[303]
^{151}Lu	^{147}Tm	5	-0.88	0.89	[246, 299]						

^{224}Es, ^{229}Md and ^{235}Lr and the corresponding values of Q(MeV), penetration factor and half-lives are tabulated in table 4.12. Hence proton decay is favourably observed in the actinides such as ^{195}Ac, ^{200}Pa, ^{206}Np, ^{212}Am, ^{218}Bk, ^{224}Es, ^{229}Md and ^{235}Lr. The logarithmic half-lives of proton decay are plotted against the product of $Z_dQ^{-1/2}$ in the actinide region and is as shown in figure 4.26. From the figure it is observed that there is a linear variation in half-lives with the product of $Z_dQ^{-1/2}$. The logarithmic half-lives of proton decay with that of alpha decay are also compared. (Royer81[304], Univ82[305], NRDX83[43], Denisov84[40]) and spontaneous fission (Bao85[295]) and are tabulated in table 4.13. From the table it is clear that the predicted isotopes such as $^{195-203}$Ac, $^{200-207}$Pa, $^{212-220,224}$Am, and $^{218-221}$Bk are having less half-lives compared to alpha decay and spontaneous fission decay mode. The dominant decay mode is identified and specified in the actinide region Z=89-103 in the corresponding table. Due to non-availability of experimental values in the actinide region, the predictive power is tested by comparing the available experimental values with the present work and it is tabulated in table 4.14. From the table it is observed that studied values obtained from the present work agrees well with the available experimental values.

4.2.5 **Proton radioactivity of superheavy nuclei (**$104 \leq Z \leq 126$**)**

The energy released during the proton decay (Q) is calculated using the difference of mass excess values available in the literature. The experimental mass excess values are used [306]. For those nuclei, where experimental mass excess was unavailable, recent theoretical values are used

Table 4.15 List of studied superheavy nuclei for proton decay

Z	Mass number (A)	Mass Number Q_p positive	Z	Mass number (A)	Mass Number Q_p positive	Z	Mass number (A)	Mass Number Q_p positive
104	240-339	240	112	262-339	262-265	120	287-339	287-292
105	241-339	241-251	113	266-339	266-276	121	290-339	290-303
106	244-339	240-243	114	269-339	269-271	122	294-339	294-299
107	247-339	247-257	115	272-339	272-280,291	123	297-339	297-309
108	250-339	250-253	116	275-339	275-279	124	300-339	3,00,301
109	253-339	253-263	117	278-339	278-287,291	125	303-339	303-315
110	256-339	256-261	118	281-339	281-285	126	306-339	308-329
111	259-339	259-267	119	284-339	284-296			

[36, 307]. List of studied superheavy nuclei for proton decay is given in the table 4.15. In this table , the nuclei for which proton decay is possible are highlighted . The nuclei highlighted in this table are important proton emitters in the superheavy nuclei region. The energy released during the proton decay (Q_P), penetration factor (P), normalisation factor (F) and logarithmic half-lives for proton decay in superheavy nuclei is also given in the table 4.16 and 4.17.

To study the competition between different decay modes, the alpha decay half-lives and spontaneous fission half-lives are also calculated. Alpha decay half-lives are evaluated using the semi empirical relations such as Royer[308], UNIV[309], NRDX[310] and Denisov[311]. Spontaneous fission half-lives are evaluated using semi empirical formula [312]. Figure 4.27 shows the competition between different decay modes such as proton decay, spontaneous fission and alpha decay for superheavy elements. From the detail study of comparison among the different decay modes, it is observed that proton decay half-lives in the superheavy region is greater than that of alpha decay. For most of the superheavy nuclei proton decay half lives are greater than that of spontaneous fission.

Table 4.16 Energy released, penetration factor, normalisation factor and logarithmic half-lives for proton decay in superheavy nuclei

Nuclei	Q (MeV)	Penetration factor	Normalization factor	$\log T_{1/2}$ (s)	Nuclei	Q (MeV)	Penetration factor	Normalization factor	$\log T_{1/2}$ (s)
^{240}Rf	0.011	6.29×10^{-48}	7.56×10^{-02}	25.96	^{257}Ds	0.561	2.03×10^{-43}	7.48×10^{-02}	21.46
^{241}Db	2.131	5.45×10^{-21}	7.82×10^{-02}	-0.99	^{258}Ds	0.321	3.6×10^{-46}	7.43×10^{-02}	24.21
^{242}Db	1.711	1.48×10^{-24}	7.75×10^{-02}	2.58	^{259}Ds	0.241	4.98×10^{-47}	7.4×10^{-02}	25.08
^{243}Db	1.691	1.04×10^{-24}	7.72×10^{-02}	2.74	^{260}Ds	0.001	1.85×10^{-49}	7.36×10^{-02}	27.51
^{244}Db	1.341	4.5×10^{-29}	7.65×10^{-02}	7.1	^{262}Ds	0.011	2.29×10^{-49}	7.34×10^{-02}	27.42
^{245}Db	1.331	3.15×10^{-29}	7.63×10^{-02}	7.26	^{259}Rg	2.301	3.1×10^{-21}	7.66×10^{-02}	-0.73
^{246}Db	0.961	4.92×10^{-36}	7.56×10^{-02}	14.07	^{260}Rg	2.021	2.31×10^{-23}	7.61×10^{-02}	1.4
^{247}Db	0.941	1.95×10^{-36}	7.54×10^{-02}	14.47	^{261}Rg	1.961	5.64×10^{-24}	7.58×10^{-02}	2.01
^{248}Db	0.531	1.84×10^{-42}	7.47×10^{-02}	20.5	^{262}Rg	1.601	1.86×10^{-27}	7.52×10^{-02}	5.5
^{249}Db	0.501	7.78×10^{-43}	7.45×10^{-02}	20.88	^{263}Rg	1.591	1.51×10^{-27}	7.5×10^{-02}	5.59
^{250}Db	0.121	4.38×10^{-47}	7.39×10^{-02}	25.13	^{264}Rg	1.251	1.82×10^{-32}	7.44×10^{-02}	10.51
^{251}Db	0.091	2.12×10^{-47}	7.37×10^{-02}	25.45	^{265}Rg	1.231	9.59×10^{-33}	7.42×10^{-02}	10.79
^{244}Sg	0.241	5.08×10^{-46}	7.58×10^{-02}	24.06	^{266}Rg	0.851	6.92×10^{-40}	7.36×10^{-02}	17.93
^{245}Sg	0.421	5.13×10^{-44}	7.57×10^{-02}	22.05	^{267}Rg	0.731	1.41×10^{-41}	7.33×10^{-02}	19.63
^{246}Sg	0.071	8.37×10^{-48}	7.51×10^{-02}	25.84	^{262}Cn	0.691	2.44×10^{-42}	7.46×10^{-02}	20.38
^{247}Sg	0.021	2.6×10^{-48}	7.48×10^{-02}	26.35	^{263}Cn	0.711	4.38×10^{-42}	7.44×10^{-02}	20.13
^{247}Bh	1.881	1.34×10^{-23}	7.73×10^{-02}	1.63	^{264}Cn	0.391	6.57×10^{-46}	7.39×10^{-02}	23.96
^{248}Bh	1.761	1.13×10^{-24}	7.69×10^{-02}	2.7	^{265}Cn	0.321	1.12×10^{-46}	7.37×10^{-02}	24.72
^{249}Bh	1.701	4.02×10^{-25}	7.66×10^{-02}	3.15	^{266}Nh	2.251	2.71×10^{-22}	7.58×10^{-02}	0.33
^{250}Bh	1.341	9.7×10^{-30}	7.6×10^{-02}	7.77	^{267}Nh	2.151	5.04×10^{-23}	7.55×10^{-02}	1.06
^{251}Bh	1.161	1.17×10^{-32}	7.55×10^{-02}	10.69	^{268}Nh	1.751	1.42×10^{-26}	7.49×10^{-02}	4.61
^{252}Bh	0.771	7.75×10^{-40}	7.49×10^{-02}	17.88	^{269}Nh	1.681	2.79×10^{-27}	7.46×10^{-02}	5.32
^{253}Bh	0.861	1.74×10^{-38}	7.48×10^{-02}	16.53	^{270}Nh	1.321	4.65×10^{-32}	7.41×10^{-02}	10.1
^{254}Bh	0.511	3×10^{-43}	7.42×10^{-02}	21.29	^{271}Nh	1.251	4.34×10^{-33}	7.38×10^{-02}	11.14
^{255}Bh	0.391	1.17×10^{-44}	7.39×10^{-02}	22.71	^{272}Nh	0.921	1.94×10^{-39}	7.33×10^{-02}	17.49
^{256}Bh	0.101	8.89×10^{-48}	7.34×10^{-02}	25.83	^{273}Nh	0.881	4.69×10^{-40}	7.31×10^{-02}	18.11
^{257}Bh	0.091	6.94×10^{-48}	7.32×10^{-02}	25.94	^{274}Nh	0.521	9.75×10^{-45}	7.26×10^{-02}	22.79
^{250}Hs	0.521	2.32×10^{-43}	7.55×10^{-02}	21.4	^{275}Nh	0.551	2.16×10^{-44}	7.24×10^{-02}	22.45
^{251}Hs	0.521	2.29×10^{-43}	7.53×10^{-02}	21.4	^{276}Nh	0.101	3.15×10^{-49}	7.18×10^{-02}	27.29
^{252}Hs	0.261	2.57×10^{-46}	7.48×10^{-02}	24.36	^{269}Fl	0.651	2.13×10^{-43}	7.39×10^{-02}	21.45
^{253}Hs	0.241	1.56×10^{-46}	7.45×10^{-02}	24.58	^{270}Fl	0.271	1.08×10^{-47}	7.34×10^{-02}	25.74
^{253}Mt	2.211	1.92×10^{-21}	7.7×10^{-02}	-0.53	^{271}Fl	0.261	8.42×10^{-48}	7.32×10^{-02}	25.85
^{254}Mt	1.851	1.83×10^{-24}	7.64×10^{-02}	2.5	^{272}Mc	1.981	5.97×10^{-25}	7.51×10^{-02}	2.99
^{255}Mt	1.931	1.15×10^{-23}	7.63×10^{-02}	1.7	^{273}Mc	1.941	2.72×10^{-25}	7.48×10^{-02}	3.33
^{256}Mt	1.611	7.6×10^{-27}	7.57×10^{-02}	4.88	^{274}Mc	1.651	4.7×10^{-28}	7.43×10^{-02}	6.1
^{257}Mt	1.431	5.41×10^{-29}	7.53×10^{-02}	7.03	^{275}Mc	1.611	1.02×10^{-28}	7.41×10^{-02}	6.76
^{258}Mt	1.091	9.34×10^{-35}	7.47×10^{-02}	12.8	^{276}Mc	1.221	1.95×10^{-34}	7.36×10^{-02}	12.49
^{259}Mt	1.051	1.63×10^{-35}	7.45×10^{-02}	13.56	^{277}Mc	1.191	6.44×10^{-35}	7.33×10^{-02}	12.97
^{260}Mt	0.701	2.12×10^{-41}	7.39×10^{-02}	19.45	^{278}Mc	0.861	6.09×10^{-41}	7.29×10^{-02}	18.99
^{261}Mt	0.661	6.23×10^{-42}	7.37×10^{-02}	19.98	^{279}Mc	0.181	6.86×10^{-49}	7.21×10^{-02}	26.95
^{262}Mt	0.481	3.77×10^{-44}	7.33×10^{-02}	22.2	^{280}Mc	0.061	4.45×10^{-50}	7.18×10^{-02}	28.14
^{263}Mt	0.371	2.06×10^{-45}	7.3×10^{-02}	23.46	^{275}Lv	0.691	1.91×10^{-43}	7.36×10^{-02}	21.49
^{256}Ds	0.581	3.6×10^{-43}	7.5×10^{-02}	21.21	^{276}Lv	0.371	3.96×10^{-47}	7.31×10^{-02}	25.18

Table 4.17 Energy released, penetration factor, normalisation factor and logarithmic half-lives for proton decay in superheavy nuclei

Nuclei	Q (MeV)	Penetration factor	Normalization factor	$\log T_{1/2}$ (s)	Nuclei	Q (MeV)	Penetration factor	Normalization factor	$\log T_{1/2}$ (s)
^{277}Lv	0.351	2.39×10^{-47}	7.29×10^{-02}	25.4	$^{298}121$	0.831	4.28×10^{-43}	7.16×10^{-02}	21.16
^{278}Lv	0.011	9.3×10^{-51}	7.24×10^{-02}	28.81	$^{299}121$	0.741	3.02×10^{-44}	7.13×10^{-02}	22.31
^{279}Lv	0.001	7.37×10^{-51}	7.22×10^{-02}	28.92	$^{300}121$	0.401	4.15×10^{-48}	7.09×10^{-02}	26.17
^{278}Ts	1.961	1.23×10^{-25}	7.46×10^{-02}	3.68	$^{301}121$	0.331	7.66×10^{-49}	7.07×10^{-02}	26.91
^{279}Ts	1.591	1.52×10^{-29}	7.41×10^{-02}	7.59	$^{302}121$	0.091	3.25×10^{-51}	7.04×10^{-02}	29.28
^{280}Ts	1.681	2.62×10^{-28}	7.4×10^{-02}	6.35	$^{303}121$	0.091	3.19×10^{-51}	7.02×10^{-02}	29.29
^{281}Ts	1.391	3.58×10^{-32}	7.35×10^{-02}	10.22	$^{294}122$	0.481	1.94×10^{-47}	7.21×10^{-02}	25.5
^{282}Ts	1.011	3.03×10^{-39}	7.3×10^{-02}	17.3	$^{295}122$	0.531	6.69×10^{-47}	7.2×10^{-02}	24.96
^{283}Ts	1.021	4.4×10^{-39}	7.28×10^{-02}	17.14	$^{296}122$	0.311	3.14×10^{-49}	7.17×10^{-02}	27.29
^{284}Ts	0.661	4×10^{-44}	7.23×10^{-02}	22.18	$^{297}122$	0.511	3.91×10^{-47}	7.17×10^{-02}	25.19
^{285}Ts	0.641	2.26×10^{-44}	7.21×10^{-02}	22.43	$^{298}122$	0.041	7.28×10^{-52}	7.11×10^{-02}	29.93
^{286}Ts	0.331	7.63×10^{-48}	7.17×10^{-02}	25.9	$^{299}122$	0.101	2.62×10^{-51}	7.11×10^{-02}	29.37
^{287}Ts	0.261	1.42×10^{-48}	7.15×10^{-02}	26.64	$^{297}123$	2.031	1.38×10^{-26}	7.34×10^{-02}	4.64
^{281}Og	0.691	5.47×10^{-44}	7.32×10^{-02}	22.04	$^{298}123$	1.881	4.21×10^{-28}	7.31×10^{-02}	6.15
^{282}Og	0.301	2.36×10^{-48}	7.26×10^{-02}	26.41	$^{299}123$	1.791	6.53×10^{-29}	7.29×10^{-02}	6.96
^{283}Og	0.391	2.04×10^{-47}	7.25×10^{-02}	25.47	$^{300}123$	1.431	1.1×10^{-33}	7.24×10^{-02}	11.74
^{284}Og	0.011	3.23×10^{-51}	7.2×10^{-02}	29.28	$^{301}124$	1.311	1.21×10^{-35}	7.21×10^{-02}	13.7
^{285}Og	0.041	6.11×10^{-51}	7.19×10^{-02}	29	$^{302}125$	0.871	4.07×10^{-43}	7.16×10^{-02}	21.18
$^{284}119$	2.001	7.96×10^{-26}	7.43×10^{-02}	3.87	$^{303}123$	0.371	6.91×10^{-49}	7.1×10^{-02}	26.95
$^{285}119$	2.091	4.82×10^{-25}	7.42×10^{-02}	3.09	$^{304}123$	1.021	5.25×10^{-41}	7.15×10^{-02}	19.07
$^{286}119$	1.681	4.64×10^{-29}	7.36×10^{-02}	7.11	$^{305}123$	0.991	1.82×10^{-41}	7.13×10^{-02}	19.53
$^{287}119$	1.421	2.43×10^{-32}	7.32×10^{-02}	10.39	$^{306}123$	0.691	2.15×10^{-45}	7.09×10^{-02}	23.46
$^{288}119$	1.171	8.18×10^{-37}	7.28×10^{-02}	14.87	$^{307}123$	0.711	3.66×10^{-45}	7.08×10^{-02}	23.23
$^{289}119$	1.311	4.14×10^{-34}	7.28×10^{-02}	12.16	$^{308}123$	0.381	8.03×10^{-49}	7.04×10^{-02}	26.89
$^{290}119$	0.941	5.62×10^{-41}	7.23×10^{-02}	19.03	$^{309}123$	0.321	1.92×10^{-49}	7.02×10^{-02}	27.51
$^{291}119$	0.661	1.15×10^{-44}	7.18×10^{-02}	22.73	$^{300}124$	0.801	2.94×10^{-44}	7.21×10^{-02}	22.32
$^{292}119$	0.531	3.52×10^{-46}	7.16×10^{-02}	24.24	$^{301}124$	0.621	2.1×10^{-46}	7.18×10^{-02}	24.46
$^{293}119$	0.361	4.99×10^{-48}	7.13×10^{-02}	26.09	$^{303}125$	1.391	7.81×10^{-35}	7.25×10^{-02}	12.89
$^{295}119$	0.081	7.72×10^{-51}	7.08×10^{-02}	28.9	$^{304}125$	1.151	2.04×10^{-39}	7.22×10^{-02}	17.47
$^{296}119$	0.011	1.65×10^{-51}	7.06×10^{-02}	29.57	$^{305}125$	1.051	4.02×10^{-41}	7.19×10^{-02}	19.18
$^{287}120$	0.641	4.03×10^{-45}	7.28×10^{-02}	23.17	$^{306}125$	4.651	2.12×10^{-14}	7.53×10^{-02}	-7.56
$^{288}120$	0.491	7.88×10^{-47}	7.25×10^{-02}	24.88	$^{307}125$	1.951	5.77×10^{-28}	7.25×10^{-02}	6.02
$^{289}120$	0.541	2.78×10^{-46}	7.23×10^{-02}	24.34	$^{308}125$	1.731	2.47×10^{-30}	7.21×10^{-02}	8.39
$^{291}120$	0.181	4.68×10^{-50}	7.17×10^{-02}	28.12	$^{309}125$	1.721	1.87×10^{-30}	7.2×10^{-02}	8.51
$^{292}120$	0.011	1.09×10^{-51}	7.14×10^{-02}	29.75	$^{310}125$	1.271	5.13×10^{-37}	7.14×10^{-02}	15.08
$^{290}121$	2.021	3.61×10^{-26}	7.39×10^{-02}	4.22	$^{311}125$	1.361	1.77×10^{-35}	7.14×10^{-02}	13.54
$^{291}121$	1.981	1.81×10^{-26}	7.37×10^{-02}	4.52	$^{312}125$	0.721	1.44×10^{-45}	7.07×10^{-02}	23.63
$^{292}121$	1.581	9.49×10^{-31}	7.32×10^{-02}	8.8	$^{313}125$	0.571	2.76×10^{-47}	7.04×10^{-02}	25.35
$^{293}121$	1.561	3.91×10^{-31}	7.3×10^{-02}	9.19	$^{314}125$	0.211	5.37×10^{-51}	7×10^{-02}	29.07
$^{294}121$	1.411	2.48×10^{-33}	7.27×10^{-02}	11.39	$^{315}125$	0.151	1.4×10^{-51}	6.98×10^{-02}	29.65
$^{295}121$	1.571	7.27×10^{-31}	7.27×10^{-02}	8.92	$^{308}126$	0.721	8.91×10^{-46}	7.15×10^{-02}	23.84
$^{296}121$	1.271	1.25×10^{-35}	7.23×10^{-02}	13.69	$^{309}126$	0.661	1.77×10^{-46}	7.13×10^{-02}	24.54
$^{297}121$	1.031	3.22×10^{-40}	7.19×10^{-02}	18.28	$^{310}126$	0.071	1.7×10^{-52}	7.06×10^{-02}	30.56

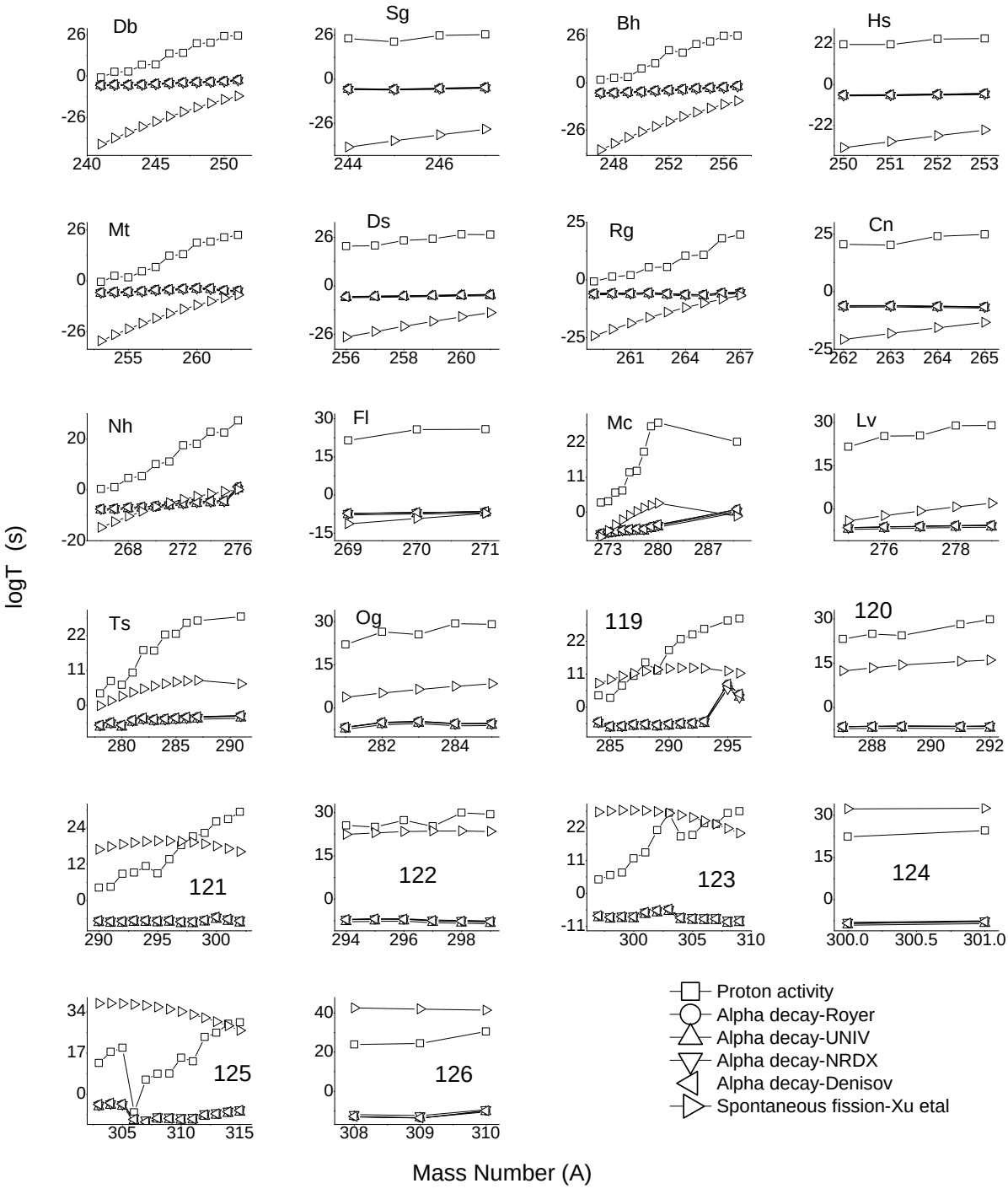

Fig. 4.27 Competition between different decay modes such as proton decay, spontaneous fission and alpha decay for superheavy elements.

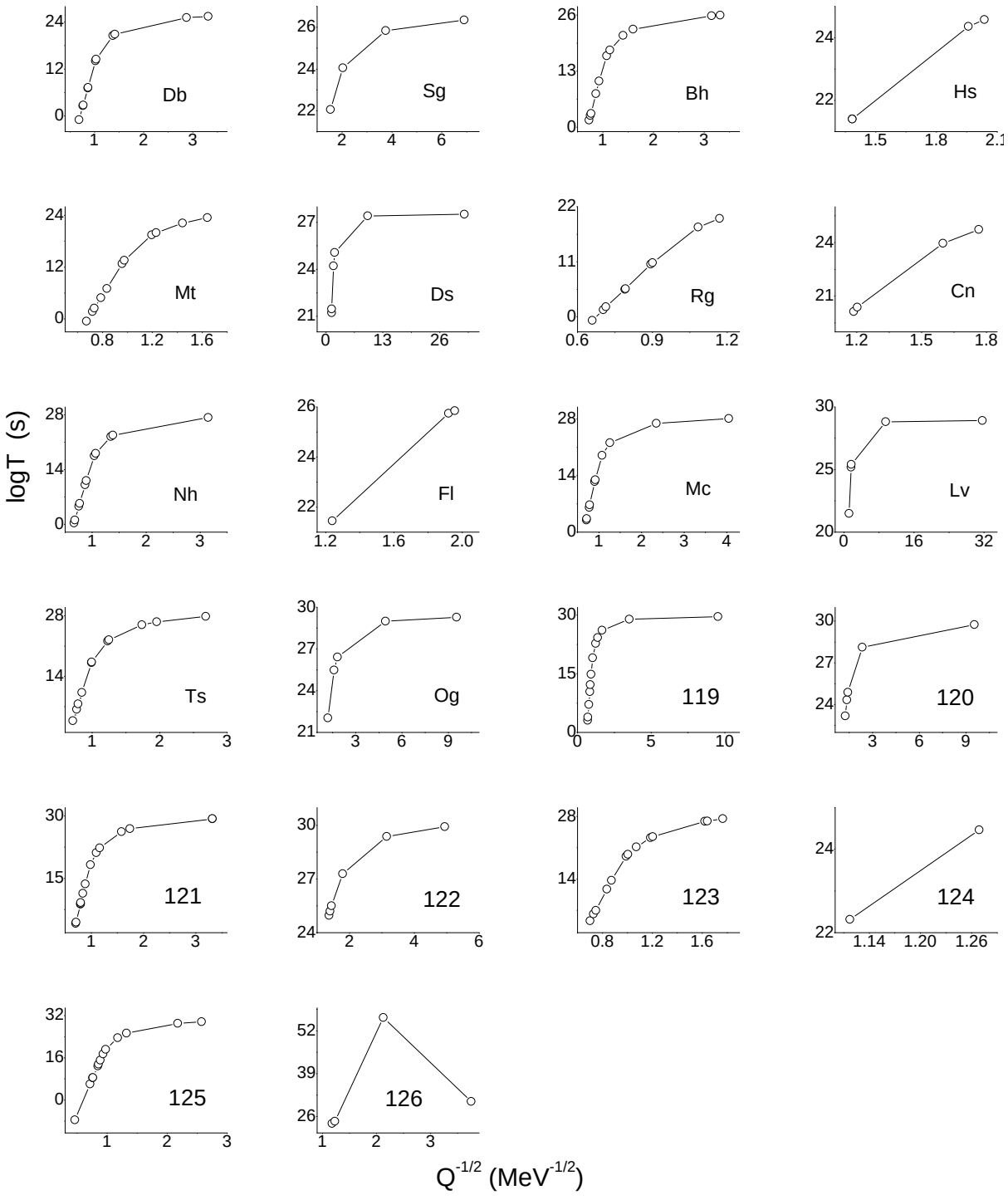

Fig. 4.28 Variation of logarithmic proton decay half-lives versus $1/\sqrt{Q}$

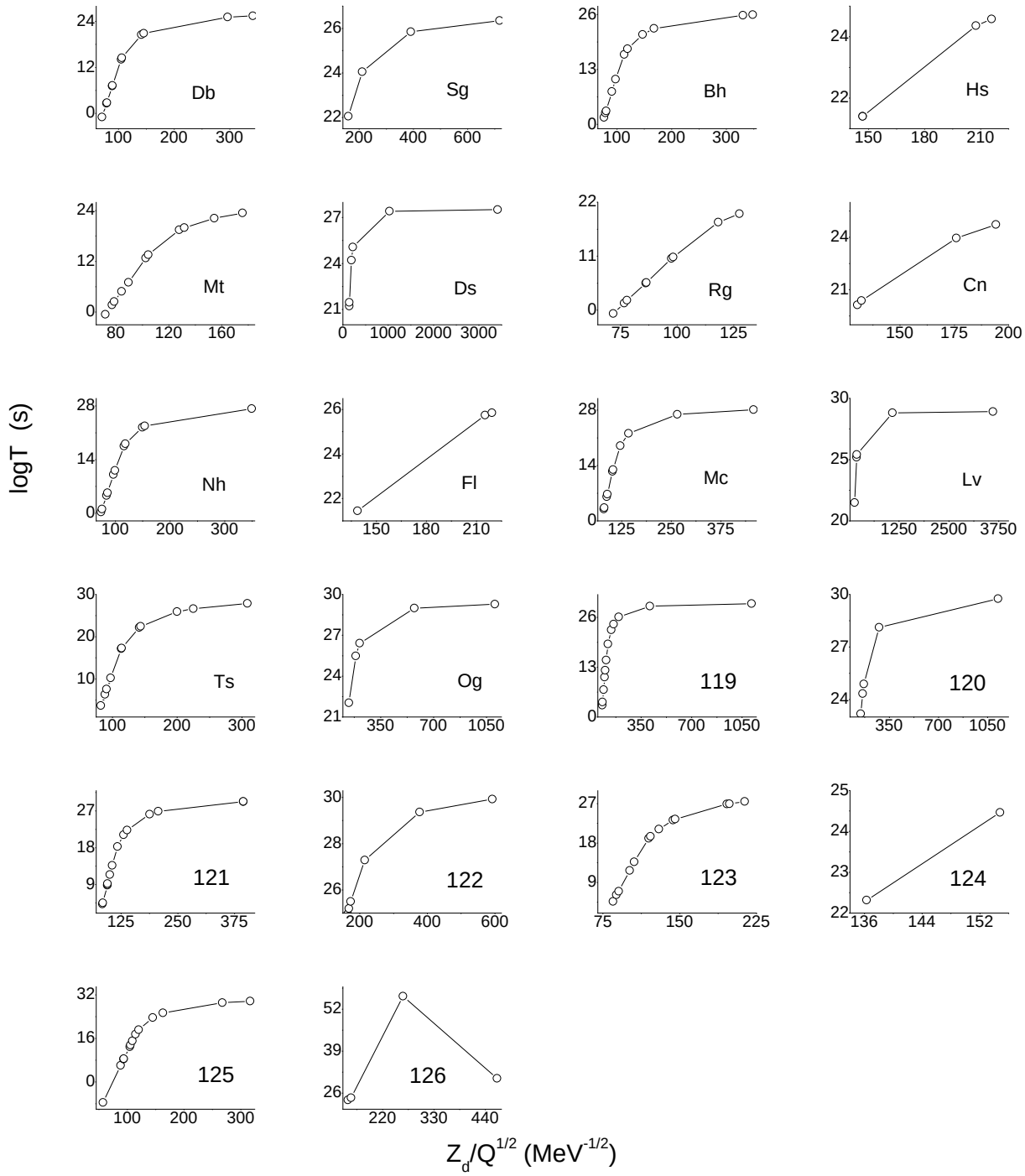

Fig. 4.29 Variation of logarithmic proton decay half-lives versus $Z_d/\sqrt{Q}$

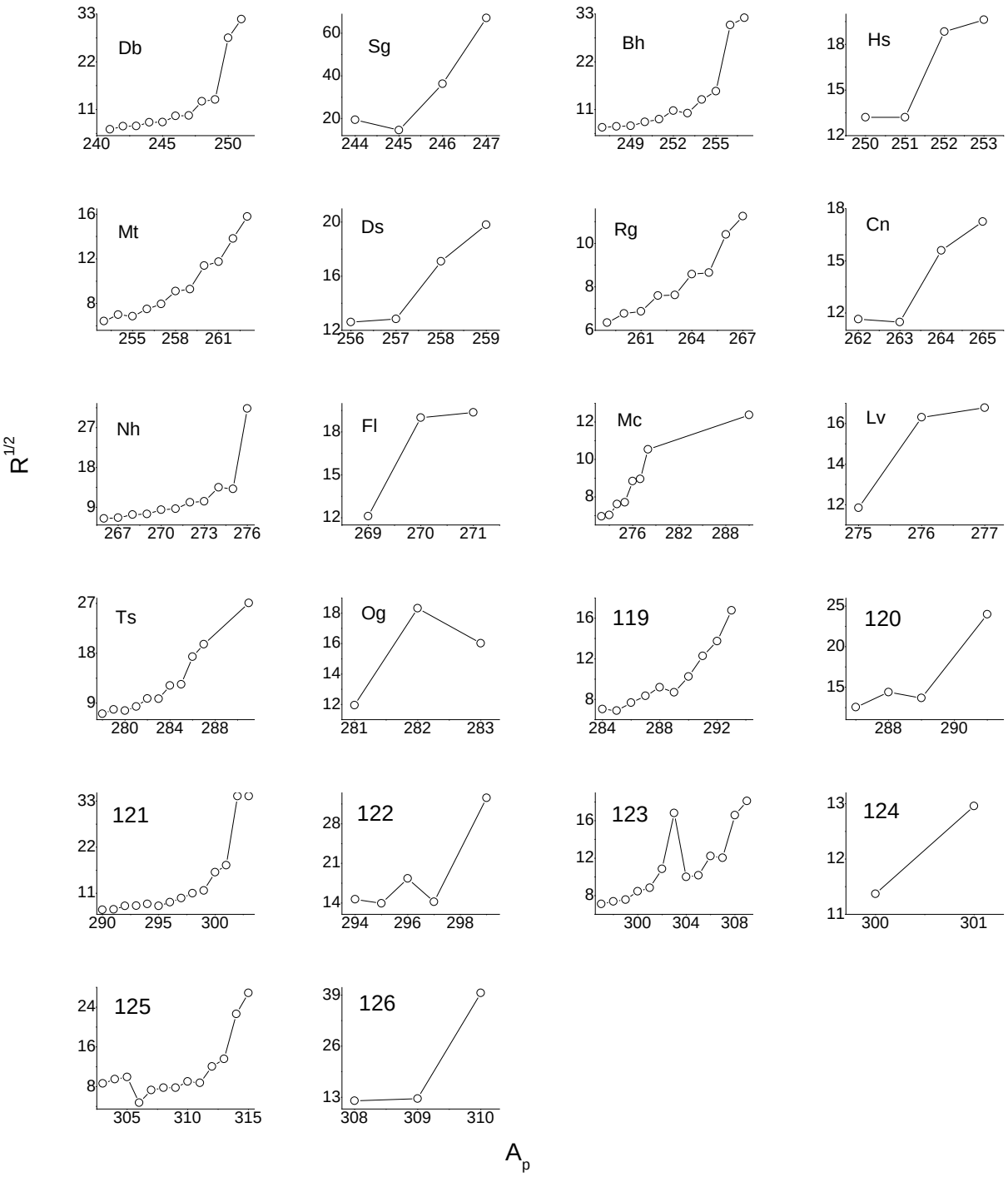

Fig. 4.30 Variation of $\sqrt{R}$ against mass number of the parent nuclei A

To check the Geiger-Nuttal law for proton decay in superheavy nuclei, the logarithmic proton decay half-lives versus $1/\sqrt{(Q)}$ are plotted. From this variation, it is found that proton decay half-lives do not vary linearly with $1/\sqrt{(Q)}$. Figure 4.29 shows the variation of logarithmic proton decay half-lives with $Z_d/\sqrt{(Q)}$ and it is found that proton decay half-lives do not vary linearly with $Z_d/\sqrt{(Q)}$ also. This fact clearly indicates that proton decay do not follows Geiger-Nuttal law.

The nuclear charge radii is possible to derive from the proton decay half-lives. The nuclear charge radii are evaluated using the semi-empirical relation explained in the literature [313]. Figure 4.30 shows the variation of $\sqrt{R}$ against mass number of the parent nuclei. From this variation it is observed that nuclear charge radii of superheavy nuclei does not varies systematically with mass number of parent nuclei.

The Proton decay in almost all superheavy nuclei with atomic number Z=104-126 is studied and it is listed in table 4.15. Proton decay half-lives are also longer than that of other decay modes. The competition of proton decay with different decay modes such as alpha decay and spontaneous fission reveals that proton decay is not dominant decay mode in the superheavy nuclei region. This means superheavy nuclei including Dubnium is stable against the proton decay.

4.2.5.1 **systematics of proton radioactivity of Dubnium**

The amount of energy released during one proton radioactivity is studied using the mass excess values available in the literature [164, 280]. The penetration factor (P), normalization factor (F) and logarithmic half-lives for proton decay in the heavy nuclei of $^{241-251}$Db is studied. The spontaneous fission half-lives and alpha decay half-lives of the heavy nuclei of $^{241-251}$Db is also studied. The comparison of the proton decay with the spontaneous fission and alpha decay half-lives are as shown in figure 4.31. From the figure it is observed that the spontaneous fission half-lives are

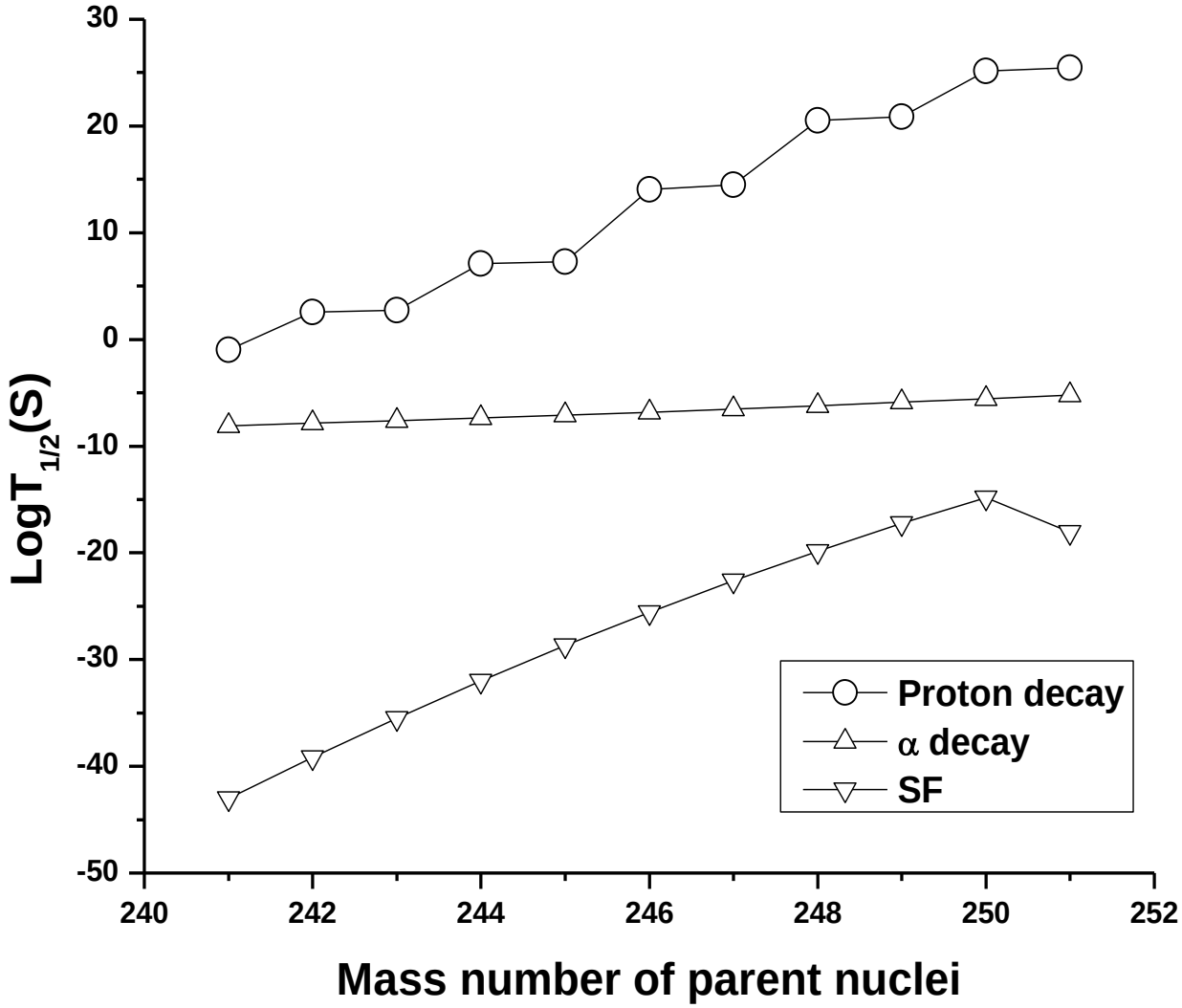

Fig. 4.31 The variation of logarithmic half-lives of the proton decay, spontaneous fission and alpha decay with the mass number of parent nuclei

smaller compared to proton and alpha decay.

The figure 4.32(a) explains the variation of amount of energy released with the mass number of parent nuclei and it decreases with increase in the mass number of parent nuclei, 4.32(b), 4.32(c) represents the penetration probability and normalization factor with the mass number of parent nuclei and both decreases with the increase in mass number of parent nuclei and 4.32(d) depicts the variation of logarithmic half lives with the product of atomic number and energy released during proton decay.

The proton decay in the heavy nuclei $^{241-251}$Db is studied. From the figure 4.31 and 4.32 it

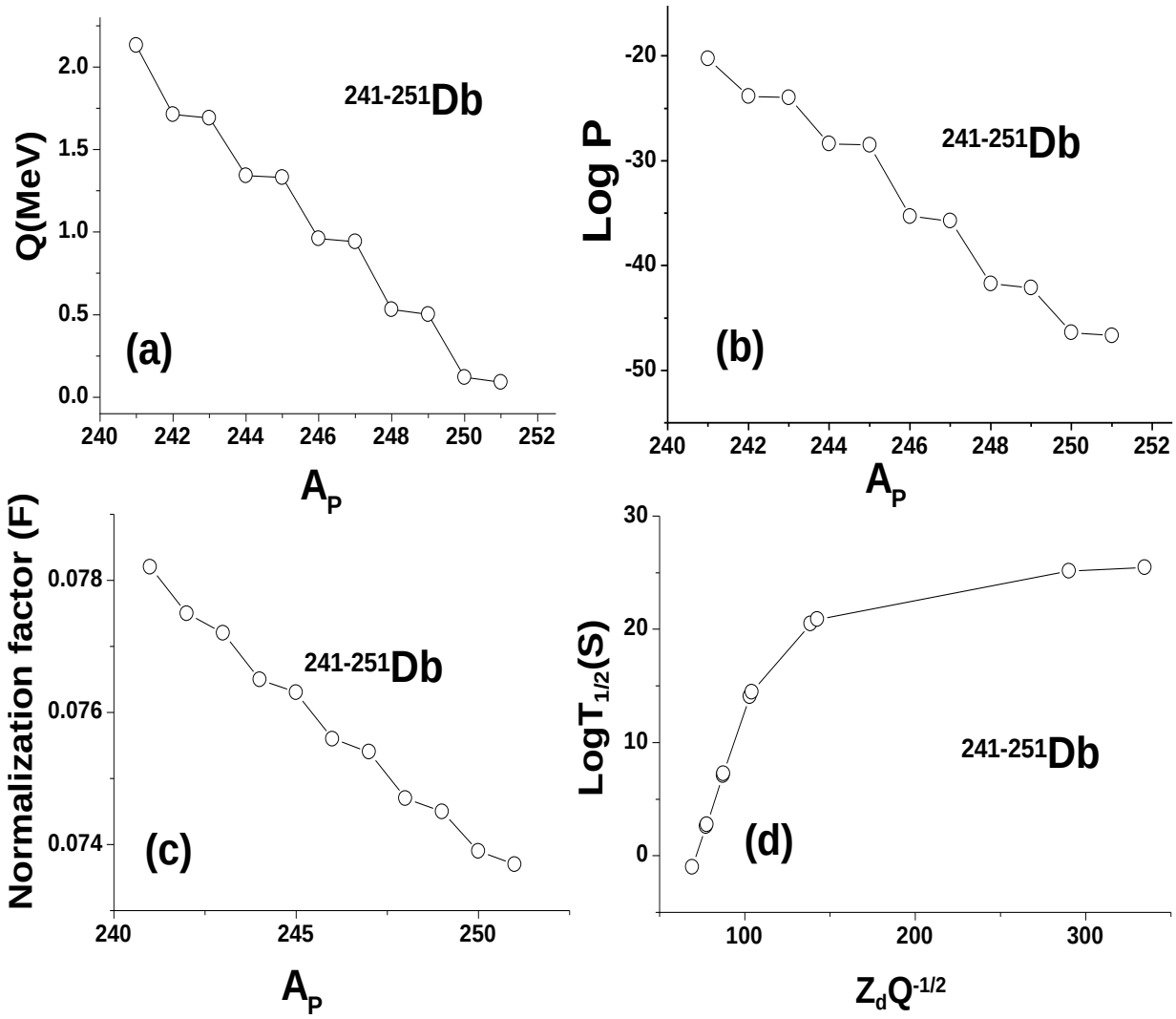

Fig. 4.32 The variation of amount of energy released, penetration probability and normalization factor with the mass number of parent nuclei and the variation of logarithmic half-lives with the product of atomic number and energy released during proton decay.

is observed that the proton decay half-lives are also longer than that of spontaneous fission and alpha decay. The competition of proton decay with different decay modes such as alpha decay and spontaneous fission reveals that proton decay is not dominant decay mode in the heavy nuclei $^{241-251}$Db.

CHAPTER 5

Comparison of present work with Microscopic models

5.1 Theory of Macroscopic models

To validate the present work, the values evaluated by the macroscopic models are compared with that of microscopic models. Brief explanation of CPPM, MGLDM and ELDM were explained in chapter 3. Eventually the other models such as GLDM, UDLP, GLM and UFM are explained below.

5.1.1 Generalized Liquid Drop Model (GLDM)

Royer et al., [170, 171] presented the Generalized Liquid Drop Model, which incorporates nuclear proximity energy and quasi molecular structures.The macroscopic energy terms including the surface, volume, Coulomb and proximity energies during an evaluation of proton decay half-lives [2] is expressed as;

$$E = E_v + E_s + E_c + E_{Prox} + E_\ell \tag{5.1}$$

The volume (E_v), surface (E_s) and coulomb energies (E_c) are given by;

$$E_v = -15.494(1 - 1.8I^2)A \;\; MeV \tag{5.2}$$

$$E_s = 17.9439(1 - 2.6I^2)A^{2/3}\frac{S}{4\pi R_0^2} \;\; MeV \tag{5.3}$$

$$E_c = 0.6e^2(Z^2/R_0) \times 0.5 \tag{5.4}$$
$$\int (V(\theta)/V_0)(R(\theta)/R_0)^3 sin(\theta)d\theta \;\; MeV$$

V_0 is the surface potential of the sphere and $V(\theta)$ is the electrostatic potential at the surface. For post-session region, the total potential and half-lives are evaluated as explained in the literature [2].

5.1.2 universal decay law for proton emission (UDLP)

The universal decay law for proton emission [116] is evaluated as follows;

$$logT_{1/2} = a\chi' + b\rho' + d\ell(\ell+1)/\rho' + c \tag{5.5}$$

The values of a, b, c and d are taken from the table 1 of reference [116]. In equation 5.5 the term $\rho = \sqrt{AZ_pZ_d(A_d^{1/3} + A_p^{1/3})}$, $\chi' = A^{1/2}Z_pZ_dQ_p^{-1/2}$ and $A = A_dA_p/(A_d + A_p)$. In case of one proton radioactivity $Z_p = A_p = 1$.

5.1.3 Gamow-like model for Proton decay (GLM)

As similar to an alpha and cluster radioactivity, proton decay is also understood by quantum tunneling through one-dimensional barrier [10]. The potential energy for Gamow like model is

evaluated as follows;

$$V(r) = \begin{cases} -V_0 & 0 \leq r \leq R_{in} \\ \\ V_C(r) + V_\ell(R) & r > R_{in} \end{cases} \tag{5.6}$$

The Coulomb potential is given by;

$$V_C(r) = \frac{Z_p Z_d e^2}{r} \tag{5.7}$$

and the centrifugal potential is given by

$$V_\ell(r) = \frac{\hbar^2 \ell(\ell+1)}{2\mu r^2} \tag{5.8}$$

where ℓ is the angular momentum and μ is the reduced mass. The penetration probability evaluated using boundary conditions and estimation of proton decay half-lives using Nilsson potential is carried out using the set of equations given in reference [10].

5.1.4 **Unified Fission model for Proton decay (UFM)**

The unified fission model uses mainly two conditions with $r \geq R_1 + R_2$ and $r < R_1 + R_2$. The term $V(r)$ is a polynomial function with R_0 as a radius of parent nuclei, R_1 and R_2 are the radii of daughter and emitted proton nucleus respectively. The term R_i is given by;

$$R_i = (1.28A_i^{1/3} - 0.76 + 0.8A_i^{-1/3})fm, \quad i = 0, 1, 2 \tag{5.9}$$

The total potential is evaluated as follows;

$$V(r) = \begin{cases} a_0 + a_1 r + a_2 r^2 \quad for \;\; R_0 \leq r \leq R_1 + R_2 \\ \\ V_P(r) + V_\ell(r) + \frac{Z_1 Z_2 e^2}{r} \quad for \;\; r \geq R_1 + R_2 \end{cases} \tag{5.10}$$

here Z_1 and Z_2 are the atomic number of daughter and emitted particle respectively. In the above equation, the coefficient a_0, a_1 and a_2 are evaluated using boundary conditions;

a) At $r = R_0 = R_{in}$, V(r)=Q

b) At $r = R_1 + R_2, V(r) = V(R_1 + R_2)$

c) At $r = R_1 + R_2, \frac{dV(r)}{dr} = \frac{dV(R_1+R_2)}{dr}$.

The penetration probability is evaluated using WKB integral and boundary conditions are evaluated as explained in detail in literature [102]. The half-lives are evaluated by $T_P = ln2/\nu_0 P$, here ν_0 is the assualt frequency [102].

5.2 Results

The main objective of the present work is to carry out comparative study of different macroscopic models such as CPPM [314], ELDM [14, 175], GLDM [170, 171], UDLP [116], GLM [10] and UFM [102] used to evaluate proton decay half-lives with that of microscopic models such as DDM3Y [94, 95], JLM [51], M3Y+EX [96], R3Y+EX [97], SLy4[98], SRG [100], Skc and SkD [93]. Also to determine which macroscopic model and microscopic model can give minimum value of statistical treatments in elucidation of experimental data.

The Q-values play a major role in the evaluation of half-lives. A small change in the value of 0.1MeV changes the half-life value of the magnitude of one to two order. Since, the sensitivity of half-lives depends on Q-values, the selection of exact Q-value is more important. Hence, the predictive power of the different models such as Lublin–Strasbourg drop model (LSD) [315], Fi-

Table 5.1 Tabulation of rms and average value ($\bar{\delta}$) for mass excess produced by different theoretical models.

Model	rms	δ
LSD	0.608	-0.027
FRDM	0.654	-0.059
FRDM12	0.579	-0.01
TF	0.649	0.027
HFB21	0.572	0.03
GHFB	0.789	-0.103
DZ	0.394	-0.032
KTUY	0.701	-0.058
INM	0.362	-0.011
WS3+	0.248	-0.008
WS4+	0.17	0

nite Range Droplet Model (FRDM) [290], Finite Range Liquid Droplet Model (FRLDM) [316], Thomas–Fermi model (TF) [317], HFB21 [318], D1MGogny forces (GHFB) [319], Duflo and Zuker (DZ) [320], Koura et al., (KTUY) [321], Nayak and Satpathy (INM) [322], WS3+ [323] and WS4+ [323] were studied in detail by previous researchers [324]. They also investigated the ability of the above nuclear mass models to predict experimental mass excess values. The accuracy of the different mass models were evaluated using root mean square and average values of the discrepancies is as follows;

$$rms^2 = \frac{1}{N_{nucl}} \sum_{i=1}^{N_{nucl}} (m_{th} - m_{exp})^2 \tag{5.11}$$

and

$$\bar{\delta} = \frac{1}{N_{nucl}} \sum_{i=1}^{N_{nucl}} (m_{th} - m_{exp}) \tag{5.12}$$

The values of rms, $\bar{\delta}$ and number of nuclei considered along with the mass model were extracted from the table A of reference [324]. The consolidated values from the table A of previous reference is tabulated in table 5.1. The two most recent Chinese versions i.e WS3+ and WS4+ achieve

the highest accuracy. However, in the present calculations we have considered experimental mass excess values available in literature and wherever experimental data is not available we have considered theoretical mass excess values from WS4+.

Table 5.2 The comparison logarithm half-lives of proton radioactivity produced by different macroscopic models CPPM, ELDM, UDLP, GLM and UFM with that of experiments [325] along with decay energies and angular momentum.

Parent nuclei	ℓ	Q_{exp}	$logT_{1/2}$						
			exp	CPPM	ELDM	GLDM	UDLP	GLM	UFM
^{109}I	2	0.83	-3.99	-4.77	-5.64	-4.58	-3.76	-4.86	-5.44
^{112}Cs	2	0.82	-3.31	-2.56	-2.23	-2.41	-2.88	-2.31	-2.91
^{113}Cs	2	0.98	-4.78	-5.10	-3.52	-4.22	-5.04	-9.02	-9.61
^{117}La	2	0.82	-1.61	-4.64	-3.25	-4.64	-2.06	0.01	-0.60
^{121}Pr	2	0.91	-3.05	-4.56	-4.86	-4.21	-2.50	-1.88	-2.18
^{130}EU	2	1.03	-1.58	-3.68	-3.96	-5.59	-2.81	-3.25	-3.87
^{131}EU	2	0.95	-2.99	-3.16	-3.86	-5.26	-1.75	0.05	-0.57
^{135}Tb	3	1.19	-3.03	-2.86	-3.85	-3.75	-3.24	-7.60	-8.21
^{140}Ho	3	1.11	-2.22	-2.64	-3.56	-4.25	-1.64	-2.79	-3.43
^{141}Ho	3	1.19	-2.39	-2.94	-2.12	-1.98	-2.64	-5.89	-6.52
^{144}Tm	5	1.73	-5.57	-4.28	-2.58	-3.68	-5.22	-8.32	-8.93
^{145}Tm	5	1.75	-1.92	-2.58	-2.68	-2.16	-1.39	-8.90	-9.50
^{146}Tm	5	1.21	-1.18	-1.28	-2.54	-2.62	-1.20	-4.80	-5.43
^{147}Tm	5	1.07	0.59	-0.88	-0.78	-1.02	0.36	0.49	-0.15
^{150}Lu	5	1.28	-1.18	-1.81	-3.44	-2.99	-1.32	-5.81	-6.45
^{151}Lu	5	1.25	-0.89	-1.92	-2.58	-3.58	-1.05	-4.90	-5.54
^{155}Ta	5	1.79	-4.92	-4.03	-3.51	-4.87	-4.64	-7.27	-7.89
^{156}Ta	2	1.03	-0.62	-1.64	-1.62	-1.95	-0.84	6.07	5.41
^{157}Ta	0	0.95	-0.52	-0.09	-1.25	-0.98	-0.43	2.14	5.48
^{159}Re	5	1.84	-4.68	-4.40	-4.54	-3.39	-4.42	-6.82	-1.44
^{160}Re	2	1.28	-3.05	-4.46	-4.76	-5.28	-3.19	-2.40	-3.05
^{161}Re	0	1.21	-3.43	-3.03	-2.70	-3.11	-3.21	0.11	-0.54
^{164}Ir	5	1.84	0.59	0.72	0.35	0.57	-3.99	-5.98	-6.60
^{165}Ir	5	1.73	-3.47	-3.17	-2.62	-3.32	-3.28	-3.64	-4.27
^{166}Ir	2	1.17	-0.82	-0.64	-0.76	-1.10	-1.23	-3.42	-2.76
^{167}Ir	0	1.08	-0.96	-2.15	-1.38	-1.87	-0.93	6.97	6.31
^{170}Au	5	1.49	-4.01	-0.58	-2.28	-0.64	-3.92	-6.18	-6.83
^{171}Au	0	1.47	-4.77	2.43	-3.56	1.83	-4.42	-5.38	-6.03
^{176}Tl	0	1.28	-2.28	-1.16	-0.35	-1.07	-1.88	2.69	2.02
^{177}Tl	0	1.18	-1.17	-0.95	-0.39	-1.05	-0.73	6.61	5.94
^{185}Bi	0	1.62	-4.23	-0.03	0.46	-0.17	-4.51	-7.10	-7.76

The proton radioactivity half-lives of parent nuclei in the atomic number range $53 \leq Z \leq$

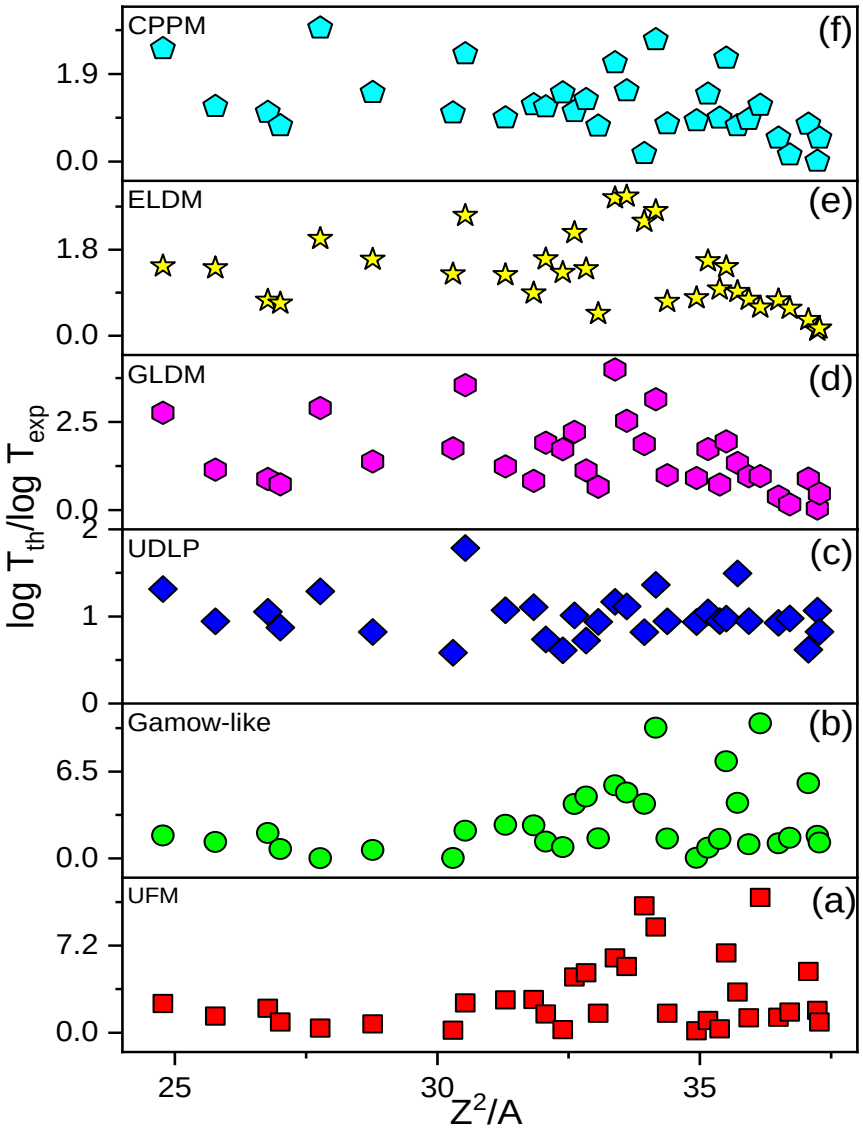

Fig. 5.1 Deviations between macroscopic models such as UFM,GLM,UDLP,GLDM,ELDM and CPPM with that of experimental logarithmic half-lives of proton radioactivity from ^{109}I to ^{209}Bi as a function of Z^2/A.

83 are studied using macroscopic models such as CPPM, ELDM, UDLP, GLM and UFM as explained in the section 5.1. The experimental half-lives of proton radioactivity is extracted from latest nuclear data [325]. For an instance, in case of ^{109}I nuclei different theoretical macroscopic models have been employed in order to evaluate its proton decay half-lives. The angular momentum is evaluated using spin-parity selection rules with; The selection rule for proton decay [109]

is as follows;

$$J_p = J_d + J_{p^\ell} \tag{5.13}$$

and

$$\pi_p = \pi_d \pi_{p^\ell} (-1)^\ell \tag{5.14}$$

where J_p, π_p, J_d, π_d, J_{p^ℓ} and π_{p^ℓ} are spin and parity values of the parent, daughter and outgoing proton particle respectively. Among 32 proton emitters available in literature, the nuclei ^{105}Sb is emitted because it is no longer a proton emitter [326, 327]. Hence, around 31 proton emitters are evaluated using macroscopic theoretical models such as CPPM, ELDM, UDLP, GLM and UFM. The proton decay half-lives obtained using these macroscopic models are tabulated in table 5.2. The closure look of the table gives an insight in to the logarithmic half-lives produced by each model. For an instance the nuclei ^{109}I whose experimental log$T_{1/2}$ value is -3.987 [94] when $\ell = 2$. From the comparison between experimental and macroscopic models it is clear that UDLP produces close value when compared to other models studied if we adopt experimental Q-value of 0.829MeV. Similarly, in all other cases we have also observed closer reproduction of experimental proton decay half-lives. These striking results are due to the coefficients (a-d) which were used to fit available experimental data. Since, the UDLP is good enough to reproduce the experimental value with root mean square deviation (σ) of 0.93, however beyond atomic number range $53 \leq Z \leq 83$ one should require a model which can effectively reproduce the experimental data as well as prediction of new proton emitter. In this aspect, the ELDM model closely reproduces the experimental data within an error of σ=1.61 and also effectively predicts logarithmic half-lives in the unexplored isotopes.

In order to give intuitive comparisons of the experimental proton decay half-lives with the cal-

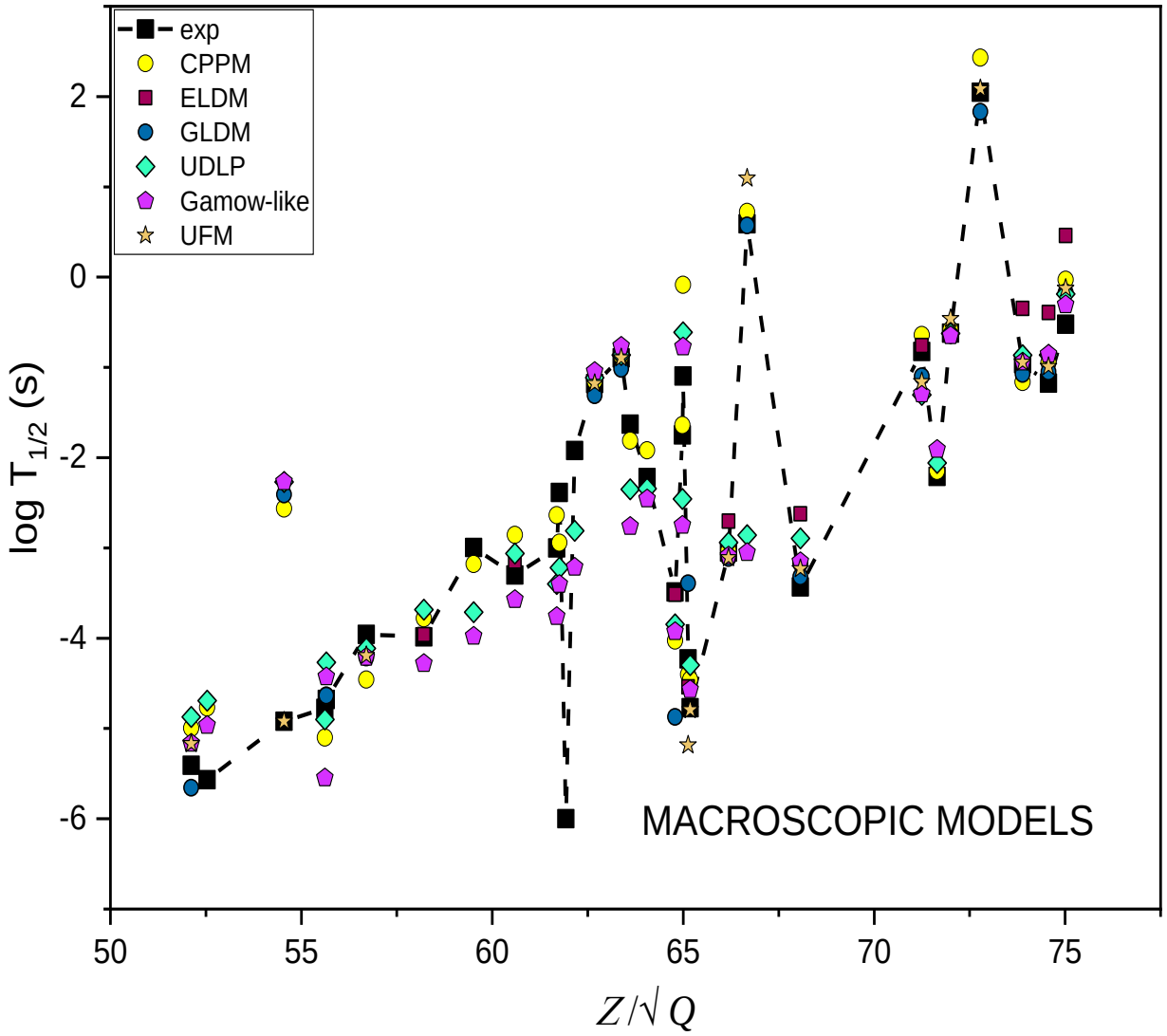

Fig. 5.2 Comparison of proton decay half-lives produced by macroscopic models such as CPPM, ELDM, GLDM, UDLP, GLM and UFM with that of experiments for various $Z/\sqrt{Q}$ values.

culated values, the deviations calulated using various macroscopic models such as GLDM, CPPM, ELDM, UDLP, GLM and UFM with that of experimental logarithmic half-lives of proton radioactivity from ^{109}I to ^{209}Bi as a function of Z^2/A are presented and is shown in figure 5.1(a-f). From these figures, it is clear that the proton radioactivity half-lives calculated using GLM and UFM are significantly different with the large value of up to 8. For the same experimental data, the models such as CPPM, ELDM and GLDM produces the deviation up to 2. However, the UDLP produces the deviation nearly equal to 1 in majority of cases. The logarithmic half-lives and the experi-

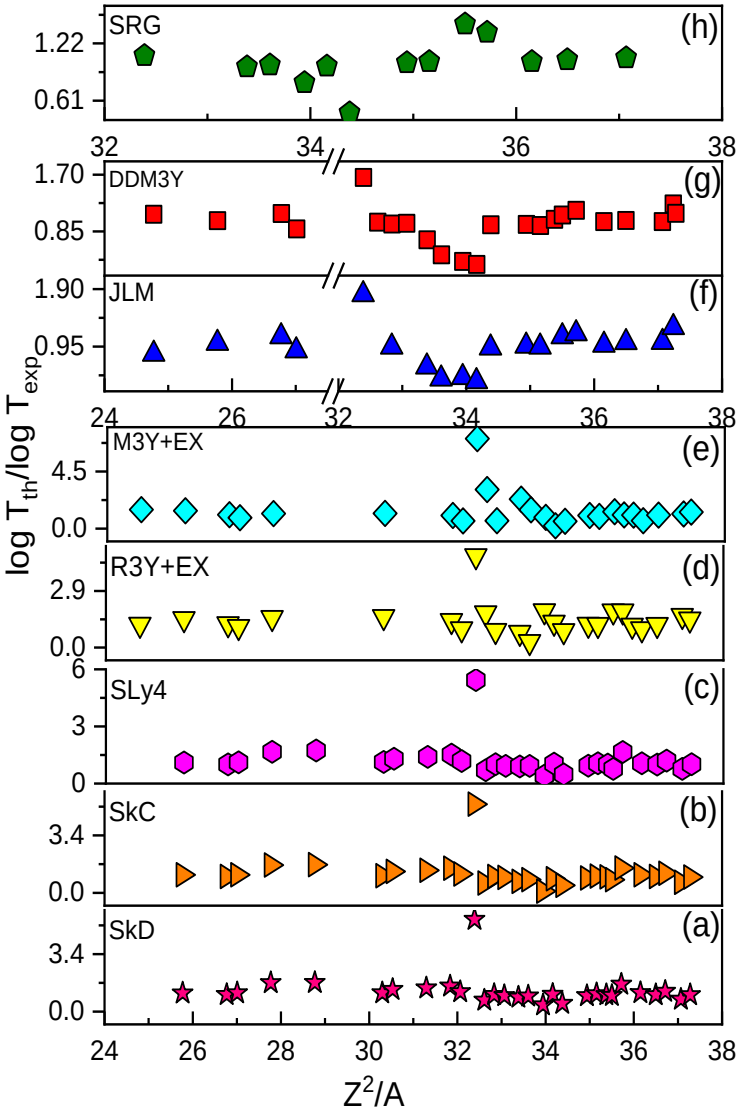

Fig. 5.3 Deviation between microscopic models such as DDM3Y [94, 95], JLM [51], M3Y+EX [96], R3Y+EX [97], SLy4[98], SRG[100], Skc and SkD [93] with that of experimental logarithmic half-lives of proton radioactivity from The nuclei ^{109}I to ^{209}Bi for various Z^2/A values.

mental values are plotted as function of $Z/\sqrt{Q}$ using different macroscopic models is as shown in figure 5.2. The closer look of the figure reveals that both ELDM and UDLP models achieve high accuracy of half-lives when compared to other macroscopic models such as CPPM, GLDM, GLM and UFM.

Furthermore, an information is gathered regarding proton decay half-lives produced using microscopic models such as DDM3Y [94, 95], JLM [51], M3Y+EX [96], R3Y+EX [97], SLy4[98], SRG [100], Skc and SkD [93]. A plot of $\log T_{th}/\log T_{exp}$ using microscopic models as a function

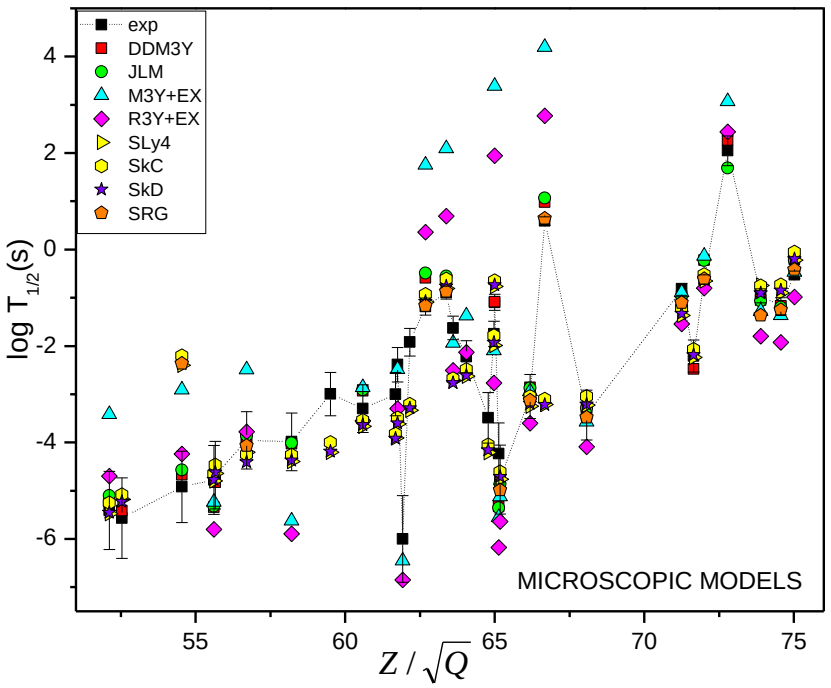

Fig. 5.4 Comparison of proton decay half-lives produced by microscopic models such as DDM3Y, JLM, M3Y+EX, R3Y+EX, SLy4, SRG, Skc and SkD with that of experiments for various $Z/\sqrt{Q}$ values.

of Z^2/A is presented in figure 5.3(a-h). One can see that the results obtained using microscopic models are in good agreement with the experimental values in majority of the cases. In some cases, even the microscopic models deviate from the experimental data. For an example in case of ^{147}Tm the final outcome is off by a factor of 3 and above in all investigated microscopic models. Similarly, in case of ^{156}Ta nuclei the results of JLM and DDM3Y are lowered by an order of one. The SRG shows deviation up to 1 in case of ^{167}Ir. Further, in all other cases, the experimental values are well reproduced in by a microscopic models. Eventually, the plot of log$T_{1/2}$ as function of $Z/\sqrt{Q}$ using the data extracted from different microscopic models are shown in figure 5.4. One can observe from the figure that there are large deviations in case of M3Y+EX and R3Y+Ex when compared to other microscopic models. This is not to say that these two models provide the worst results. But comparatively, M3Y+EX and R3Y+Ex produces large deviation than that of other microscopic models investigated.

Table 5.3 The root mean square error (RMSE) and root mean square deviations (σ) of the calculations from macroscopic models such as CPPM, ELDM, GLDM, UDLP, GLM and UFM with respect to the experimental data and microscopic models such as DDM3Y, JLM, M3Y+EX, R3Y+EX, SLy4, SRG, Skc and SkD with that of experiments.

Model	RMSE	σ
DDM3Y	0.35	0.5
JLM	0.41	0.59
M3Y+EX	1.19	1.06
R3Y+EX	1.19	0.98
SLy4	1.01	0.77
SkC	0.99	0.77
SkD	1.01	0.77
SRG	0.69	0.55
CPPM	2.21	1.24
ELDM	1.93	1.26
GLDM	2.71	1.43
UDLP	0.91	0.68
GAMOW	3.47	1.68
UFM	3.7	1.76

The root mean square error (RMSE) and root mean square deviation (σ) between the macroscopic, microscopic and experimental are given by;

$$RMSE = \sqrt{\frac{1}{N}\sum log\left(\frac{T_{th}}{T_{exp}}\right)^2} \tag{5.15}$$

and

$$\sigma = \sqrt{\frac{1}{N}\sum_{i=1}^{N}\left(log(T^{exp}) - log(T^{th})\right)^2} \tag{5.16}$$

where N is the number of nuclei considered to evaluate proton decay half-lives using microscopic and macroscopic models. The quantified deviations are tabulated in table 5.3. From the table it is clearly seen that RMSE and σ are smaller for the UDLP model. Since, the UDLP model is depended on coefficients which were fitted by taking an experimental proton decay half-lives. Applicability of UDLP beyond $53 \leq Z \leq 83$ is not known clearly. Hence the other possibility

is the ELDM with 1.93 and 1.26 of RMSE and σ respectively. Hence, during the prediction of proton decay half-lives ELDM macroscopic model is more effective in the unexplored region. Similarly, DDM3Y and JLM microscopic models effectively produces proton decay half-lives with less deviation with respect to experiments than that of other microscopic models investigated.

CHAPTER 6

Summary

6.1 Semi-empirical formula for one and two proton radioactivity

A thorough study on one proton and two proton radioactivity is carried in the atomic number range $3 \leq Z \leq 126$ using well accepted Coulomb and proximity potential model (CPPM), effective liquid drop model(ELDM), generalized liquid drop model(GLDM) and modified generalised liquid drop model(MGLDM) models. semi empirical formula for one and two proton decay half-lives is constructed by including angular momentum term . The values produced by the present formula is also compared with experiments. Around 241 and 174 energetically feasible one and two proton emitters were identified in the atomic number range $3 \leq Z \leq 126$.

6.2 Verification of Geiger-Nuttall law for Proton Radioactivity.

In order to construct a empirical relation, we have considered logarithmic half-lives of proton decay available in the reference [328] and [277] as a function of $Z_D/\sqrt{Q}$ and it is as follows;

$$\log T_{1/2} = f\left(\frac{Z_D^n}{\sqrt{Q}}\right) \tag{6.1}$$

From the study of logarithmic half-lives of proton decay as a function of $Z_D/\sqrt{Q}$, we have observed the systematic variation as shown in figure 6.1. The search was made to parameterize the

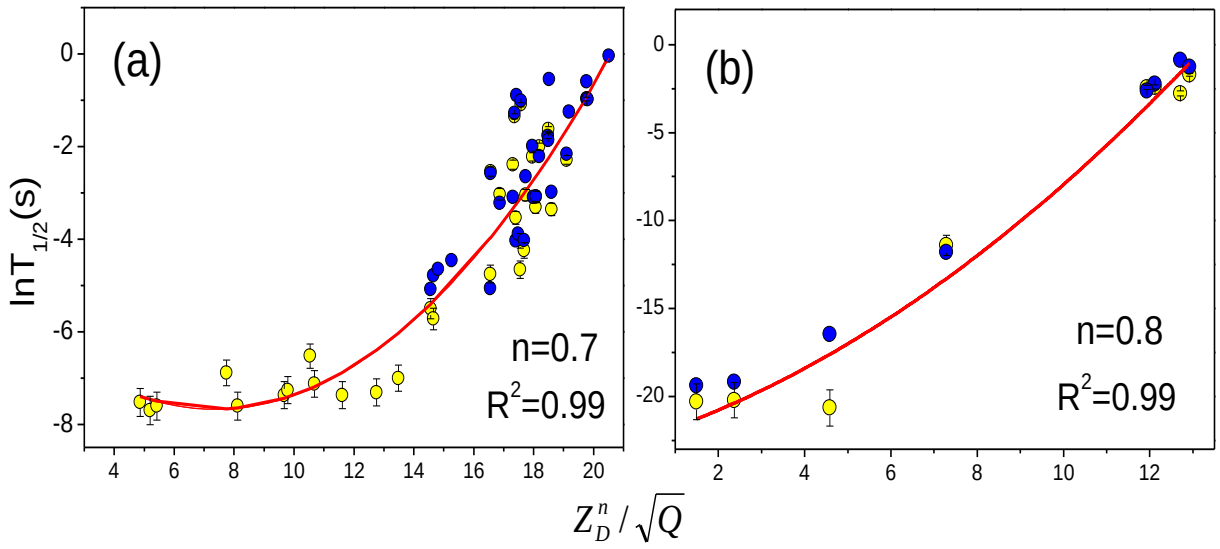

Fig. 6.1 Variation of logarithmic half lives as function of $Z_d^n/Q^{1/2}$. (a) One proton decay - Yellow circles represents the data corresponds to experiments [271], the blue colour circles represents the values produced by previous formula [277] and continues red line represents values obtained from the present formula and (b) Two proton decay- Yellow circles represents the two proton decay half-lives corresponds to experiments [271], blue colour circles represents the values produced by previous formula [329] and continues red line represents values obtained from the present formula.

logarithmic half-lives of one proton decay and 2-proton decay. We have tried different functions such as $a(Z_D/\sqrt{Q})+b$, $a\ln(Z_D/\sqrt{Q})+b$, $\frac{1}{a(Z_D/\sqrt{Q})+b}$, $aexp^{(Z_D/\sqrt{Q})}+b$, $aexp\frac{b}{(Z_D/\sqrt{Q})}$ and polynomial functions to fit the available experimental values of one and two proton decay. Among different equations mentioned above, we have considered a second order polynomial equation whose residual sum of squares(RSS) are nearly equal to 1. The plot of logarithmic half-lives with the $Z_D/\sqrt{Q}$ is shown in the figure 6.1. Finally the constructed semi-empirical formulae for the one and two proton decay based on Geiger Nuttall law is as follows;

$$\log T_{1/2}^{P} = a \times \left(\frac{Z_D^n}{\sqrt{Q}}\right)^2 + b \times \left(\frac{Z_D^n}{\sqrt{Q}}\right) + c \tag{6.2}$$

Where a, b and c are the fitting parameter and the coefficients corresponding to these values were tabulated in table 6.1.

Table 6.1 The index "n" and fitting coefficients a, b and c of one and two proton decay.

Decay type	range	n	a	b	c
1P	$5 \leq Z \leq 83$	0.7	0.04405	-0.65101	-5.26603
2P	$4 \leq Z \leq 36$	0.8	0.06954	0.76778	-22.58463

6.3 Studies on Proton radioactivity using Macroscopic models

A thorough study on one proton and two proton radioactivity is carried in the atomic number range $3 \leq Z \leq 126$ using well accepted Coulomb and proximity potential model (CPPM), effective liquid drop model(ELDM), generalized liquid drop model(GLDM) and modified generalised liquid drop model(MGLDM) models. The proton decay half-lives produced by these models are compared with the experiments. Predictive power of these models are assessed by evaluation of the mean squared error. Present work is validated by comparing with experiments. Among the studied three models, CPPM model produces proton decay half-lives close to experiments than the other two models.

6.4 Proton radioactivity in Lanthanides ($57 \leq Z \leq 71$)

The proton decay half-lives in the lanthanide region have been systematically studied using different proximity functions such as Prox. 13, Prox. 77, MP 77, Ng 80 and Bass 80. Though the experimental values are found to be in good agreement with the proximity function of Ng 80, empirical formula to calculate the half-lives of such proton-emitting lanthanides is developed. The half-lives values produced by the present formula is compared with that of NG 80. The present formula produces the half lives with simple inputs of Z_d and Q values and hence it may called as pocket formula.

The competition between the evaluated proton decay half-lives with other competent decay modes such as alpha, β^+, β^-, spontaneous fission and proton decay are also studied.Eventually,

24 new proton decay emitters in the Lanthanide region are identified. Newly identified proton emitters find application in radiation therapy.

The proton radioactivity in Dysprosium isotopes have been examined using effective liquid drop model. Proton radioactivity is energetically feasible in the isotopes Dysprosium from ^{133}Dy to ^{135}Dy. The different decay modes such as $beta^-$-decay, $beta^+$-decay, and α decay are evaluated in the isotopes of $^{133-173}$Dy. The half-lives against proton decay have been compared to competing decay modes such as $beta^-$-decay, $beta^+$-decay, and α decay. In the isotopes of $^{133-149}$Dy and $^{151-154}$Dy β^+-decay is dominant. In ^{150}Dy, α-decay is dominant, whereas $beta^-$-decay is dominating in $^{155-173}$Dy. The decay chains of $^{133-135}$Dy were investigated. The detail investigations of $^{133-135}$Dy shows that the probability of observing proton radioactivity when $^{133-135}$Tb is converted to $^{132-134}$Gd with the half-life of order of nanoseconds. Further, these identified proton emitters may find useful in the field of diagnosis and radiotherapy.

6.5 Proton radioactivity of Heavy nuclei ($72 \leq Z \leq 88$)

The proton radioactivity of heavy nuclei of atomic number range $72 < Z < 88$ is studied. The energy released during the proton decay (Q_P), and half-lives of proton decay are calculated. The competition between different decay modes is studied, by comparing the proton decay half lives with that of other decay modes such as alpha decay, beta decay, and spontaneous fission. To check the Geiger-Nuttal law for proton decay, the logarithmic proton decay half-lives are plotted against $1/\sqrt{Q}$. Also the possible proton emitters are also highlighted with the corresponding energies and half-lives in the atomic number range $72 < Z < 88$.

Using different models such as Coulomb and proximity potential model, effective liquid drop model and modified generalised liquid drop model, 1P-radioactivity of Tantalum is studied. The decay constant(λ) and half-lives($T_{1/2}$) of $^{151-157}$Ta were predicted.

The calculated half-lives from the present work are compared with the available experiments. The decay energy is feasible for the nuclei $^{151-157}$Ta. The identified 1P-radioactivity of $^{151-157}$Ta along with half-lives and decay energies plays an important role in the future experiments and may find useful applications in radiotherapy and diagnosis.

The different decay modes such as proton decay, beta-decay and an alpha decay have been evaluated using CPPM and semi-empirical relations in the isotopes of Bismuth. The values obtained from the present work were comparable with the experiments. Around 9 α emitters, one proton emitter, 18 β^+ emitters and 33 β^- emitters were identified. Among the β^- emitters, around 25 new emitters from ^{220}Bi to ^{244}Bi were newly identified. These identified new β^- emitters are useful in the field of radiotherapy.

6.6 **Proton radioactivity of Actinide nuclei** ($89 \leq Z \leq 103$)

The one-proton emission in the actinide region from Z=89-103 is theoretically studied . The half-lives of one-proton emitters in the actinide region are presented using the coulomb and proximity potential method. One-proton decay half-lives of present study have shown good agreement with the available experimental values.The studied proton decay half-lives are compared with that of other decay modes such as alpha decay, spontaneous fission and beta decay.

The proton emitters in the actinide region have been identified. The prediction of the new proton emitters in the actinide region are having measurable half-lives can be retrieved in future with developing experimental techniques.

The systematics of one proton decay in the actinide region through the study of energy released, penetration probability and logarithmic half-lives in the actinide region is studied. The studied half-lives of present work is compared with the different decay modes such as alpha decay and spontaneous fission. The possible proton emitters with the corresponding energies and half-

lives in the actinide region are identified. The possible proton emitters in the actinide region are $^{195-203}$Ac, $^{200-207}$Pa, $^{212-220,224}$Am, and $^{218-221}$Bk. The proton emitters in the unexplored isotopes of actinide region have been identified which is not specified in the nuclear chart.

6.7 Proton radioactivity of Superheavy nuclei ($104 \leq Z \leq 126$)

The proton decay in almost all superheavy nuclei with atomic number Z=104-126 is studied, out of which proton decay is possible in few superheavy nuclei . We have calculated the energy released during the proton decay (Q_P), penetration factor (P), normalisation factor (F) and half-lives of proton decay . Proton decay half-lives are also longer than that of other decay modes such as alpha decay and spontaneous fission. The competition of proton decay with different decay modes reveals that proton decay is not dominant decay mode in the superheavy nuclei region. This means superheavy nuclei is stable against the proton decay.

The proton radioactivity of Dubnium is studied. The amount of energy released during the proton decay, penetration probability, normalization factor and logarithmic half-lives in the superheavy nuclei of $^{241-251}$Db is calculated . The Proton decay half lives of Dubnium are compared with the spontaneous fission and alpha decay. From the results it can be concluded that the superheavy nuclei of $^{241-251}$Db are having half-lives greater than the spontaneous fission and alpha decay. Hence, the superheavy nuclei$^{241-251}$Db is stable against the proton decay.

6.8 Scope of research work

The prediction of the new proton emitters in the actinide region having measurable half-lives can be retrieved in future with developing experimental techniques. Proton therapy is a type of radiation used to treat cancer. Proton therapy sends positively charged atomic particles called protons [330]. Proton therapy is used to treat breast cancer [331, 332], brain cancer [333], head and neck cancer [334] and hepatocellular carcinoma of a liver tissue [335, 336]. Radio nuclides with different energy ranges up to 5 MeV are used in the radiotherapy [336, 337]. The identified new proton emitters having decay energy between 0.378 - 4.321 KeV which clearly suggests that the proton emitters identified in the lanthanide region might find application in radiation therapy. There is a need to make progress in preclinical proton radiation biology to give accessible data to medical physicists and practicing radiation oncologists. Proton radioactivity studies are becoming important tool for nuclear structure.

References

[1] N. Teruya, S. B. Duarte, and M. M. N. Rodrigues. Nonlocality effect in the tunneling of one-proton radioactivity. *Phys. Rev. C*, 93:024606, Feb 2016.

[2] J. M. Dong, H. F. Zhang, and G. Royer. Proton radioactivity within a generalized liquid drop model. *Phys. Rev. C*, 79:054330, May 2009.

[3] R. J. Tighe, D. M. Moltz, J. C. Batchelder, T. J. Ognibene, M. W. Rowe, and Joseph Cerny. Evidence for the ground-state proton decay of $^{105}\mathrm{Sb}$. *Phys. Rev. C*, 49:R2871–R2874, Jun 1994.

[4] Dong Jian-Min, Zhang Hong-Fei, Zuo Wei, and Li Jun-Qing. Unified fission model for proton emission. *Chinese Physics C*, 34(2):182–185, jan 2010.

[5] D.S. Delion, R.J. Liotta, and Ramon Wyss. Theories of proton emission. *Physics reports*, 424(3):113–174, 2006.

[6] D.S. Delion, R.J. Liotta, and Ramon Wyss. Systematics of proton emission. *Physical review letters*, 96(7):072501, 2006.

[7] B. Buck, A.C. Merchant, and S.M. Perez. Ground state proton emission from heavy nuclei. *Physical Review C*, 45(4):1688, 1992.

[8] D.S. Delion and A. Dumitrescu. Universal proton emission systematics. *Physical Review C*, 103(5):054325, 2021.

[9] I. Sreeja and M. Balasubramaniam. An empirical formula for the half-lives of exotic two-proton emission. *The European Physical Journal A*, 55(3):1–10, 2019.

[10] A. Zdeb, M. Warda, C.M. Petrache, and K. Pomorski. Proton emission half-lives within a gamow-like model. *The European Physical Journal A*, 52(10):1–6, 2016.

[11] M. Karny, R.K. Grzywacz, J.C. Batchelder, C.R. Bingham, C.J. Gross, K. Hagino, J.H. Hamilton, Z. Janas, W.D. Kulp, J.W. McConnell, et al. Fine structure in proton emission from t 145 m discovered with digital signal processing. *Physical review letters*, 90(1):012502, 2003.

[12] L. Axelsson, J. Äystö, U.C. Bergmann, M.J.G. Borge, L.M. Fraile, H.O.U. Fynbo, A. Honkanen, P. Hornshøj, A. Jokinen, B. Jonson, I. Martel, I. Mukha, T. Nilsson, G. Nyman, B. Petersen, K. Riisager, M.H. Smedberg, and O. Tengblad. Two-proton emission in the decay of 31ar. *Nuclear Physics A*, 628(3):345–362, 1998.

[13] I. Sreeja and M. Balasubramaniam. An empirical formula for the half-lives of ground state and isomeric state one proton emission. *The European Physical Journal A*, 54(6):1–9, 2018.

[14] M. Goncalves, N. Teruya, O.A.P. Tavares, and S.B. Duarte. Two-proton emission half-lives in the effective liquid drop model. *Physics Letters B*, 774:14–19, 2017.

[15] L.S. Ferreira, E. Maglione, and D.E.P. Fernandes. Dependence of the decay widths for proton emission on the single particle potential. *Physical Review C*, 65(2):024323, 2002.

[16] F. Guzman, M. Goncalves, O.A.P. Tavares, S.B. Duarte, F. Garcia, and O. Rodriguez. Proton radioactivity from proton-rich nuclei. *Physical Review C*, 59(5):R2339, 1999.

[17] Zhang Hong-Fei, Dong Jian-Min, Wang Yan-Zhao, Su Xin-Ning, Wang Yong-Jia, Cai Ling-

Zhi, Zhu Tian-Bao, Hu Bi-Tao, Zuo Wei, and Li Jun-Qing. Theoretical analysis and new formulae for half-lives of proton emission. *Chinese Physics Letters*, 26(7):072301, 2009.

[18] J.M. Dong, H.F. Zhang, and Guy Royer. Proton radioactivity within a generalized liquid drop model. *Physical Review C*, 79(5):054330, 2009.

[19] Sven Aberg, B. Semmes, Paul, and Witold Nazarewicz. Spherical proton emitters. *Physical Review C*, 56(4):1762, 1997.

[20] D.S. Delion, Ramon Wyss, Daniel Karlgren, and R.J. Liotta. Proton emission from triaxial nuclei. *Physical Review C*, 70(6):061301, 2004.

[21] J.S. Al-Khalili, A.J. Cannon, and P.D. Stevenson. The two-potential approach to one-proton emission. In *AIP Conference Proceedings*, volume 961, pages 66–71. American Institute of Physics, 2007.

[22] V.P. Bugrov and S.G. Kadmenskii. Proton decay of deformed nuclei. *Soviet Journal of Nuclear Physics (English Translation);(USA)*, 49(6), 1989.

[23] S.G. Kadmensky and V.P. Bugrov. Proton decay and shapes of neutron-deficient nuclei. *Physics of Atomic Nuclei*, 59(3):399–402, 1996.

[24] E. Maglione, L.S. Ferreira, and R.J. Liotta. Proton emission from deformed nuclei. *Physical Review C*, 59(2):R589, 1999.

[25] M. Del Santo, Z. Meisel, Dominique Bazin, A. Becerril, B.A. Brown, H. Crawford, R. Cyburt, S. George, G.F. Grinyer, G. Lorusso, et al. β-delayed proton emission of 69kr and the 68se rp-process waiting point. *Physics Letters B*, 738:453–456, 2014.

[26] S.A. Alavi, V. Dehghani, and M. Sayahi. Calculation of proton radioactivity half-lives. *Nuclear Physics A*, 977:49–59, 2018.

[27] D. Baye and E.M. Tursunov. β delayed emission of a proton by a one-neutron halo nucleus. *Physics Letters B*, 696(5):464–467, 2011.

[28] W.F. Feix and E.R. Hilf. Nuclear proton emission predictions. *Physics Letters B*, 120(1-3):14–18, 1983.

[29] C. Giusti and F.D. Pacati. Two-proton emission induced by electron scattering. *Nuclear Physics A*, 535(3-4):573–591, 1991.

[30] P. Arumugam, L.S. Ferreira, and E. Maglione. Proton emission, gamma deformation, and the spin of the isomeric state of 141ho. *Physics Letters B*, 680(5):443–447, 2009.

[31] S.B. DUARTE, O.A.P. TAVARES, F. GUZMÁN, A. DIMARCO, F. GARCÍA, O. RODRÍGUEZ, and M. GONÇALVES. Half-lives for proton emission, alpha decay, cluster radioactivity, and cold fission processes calculated in a unified theoretical framework. *Atomic Data and Nuclear Data Tables*, 80(2):235–299, 2002.

[32] L.S. Ferreira, E. Maglione, and P. Ring. Self-consistent description of proton radioactivity. *Physics Letters B*, 701(4):508–511, 2011.

[33] E. Maglione and L.S. Ferreira. Fine structure in proton emission from deformed 131 eu. *Physical Review C*, 61(4):047307, 2000.

[34] K.P. Santhosh and Indu Sukumaran. Description of proton radioactivity using the coulomb and proximity potential model for deformed nuclei. *Physical Review C*, 96(3):034619, 2017.

[35] Bertram Blank and M.J.G. Borge. Nuclear structure at the proton drip line: Advances with nuclear decay studies. *Progress in Particle and Nuclear Physics*, 60(2):403–483, 2008.

[36] H.C. Manjunatha, B.M. Chandrika, and L. Seenappa. Empirical formula for mass excess of heavy and superheavy nuclei. *Modern Physics Letters A*, 31(28):1650162, 2016.

[37] Borut Bajc, Junji Hisano, Takumi Kuwahara, and Yuji Omura. Threshold corrections to dimension-six proton decay operators in non-minimal susy su (5) guts. *Nuclear Physics B*, 910:1–22, 2016.

[38] Ivan Mukha, E. Roeckl, J. Doring, L. Batist, A. Blazhev, H. Grawe, C.R. Hoffman, Marc Huyse, Z. Janas, R. Kirchner, et al. Observation of proton radioactivity of the (21+) high-spin isomer in ag 94. *Physical review letters*, 95(2):022501, 2005.

[39] K.P. Rykaczewski. New experimental results in proton radioactivity. *The European Physical Journal A*, 15(1):81–84, 2002.

[40] V. Yu. Denisov and A.A. Khudenko. α-decay half-lives: Empirical relations. *Physical Review C*, 79(5):054614, 2009.

[41] Chang Xu, Zhongzhou Ren, and Yanqing Guo. Competition between α decay and spontaneous fission for heavy and superheavy nuclei. *Physical Review C*, 78(4):044329, 2008.

[42] Yibin Qian, Zhongzhou Ren, and Dongdong Ni. Attempt to probe nuclear charge radii by cluster and proton emissions. *Physical Review C*, 87(5):054323, 2013.

[43] Dongdong Ni, Zhongzhou Ren, Tiekuang Dong, and Chang Xu. Unified formula of half-lives for α decay and cluster radioactivity. *Physical Review C*, 78(4):044310, 2008.

[44] Doru S. Delion. Heavy cluster decays. In *Theory of Particle and Cluster Emission*, pages 259–268. Springer, 2010.

[45] R. Budaca and A.I. Budaca. Proton emission with a screened electrostatic barrier. *The European Physical Journal A*, 53(8):1–8, 2017.

[46] Gerald Gilbert. Wormhole-induced proton decay. *Nuclear Physics B*, 328(1):159–170, 1989.

[47] J. Uusitalo, C. N. Davids, P. J. Woods, D. Seweryniak, A. A. Sonzogni, J. C. Batchelder, C. R. Bingham, T. Davinson, J. deBoer, D. J. Henderson, H. J. Maier, J. J. Ressler, R. Slinger, and W. B. Walters. Proton emission from the closed neutron shell nucleus ^{155}Ta. *Phys. Rev. C*, 59:R2975–R2978, Jun 1999.

[48] K. Livingston, P.J. Woods, T. Davinson, N.J. Davis, S. Hofmann, A.N. James, R.D. Page, P.J. Sellin, and A.C. Shotter. Proton radioactivity from 146tm. the completion of a sequence of four odd-odd proton emitters. *Physics Letters B*, 312(1):46–48, 1993.

[49] A. A. Sonzogni, C. N. Davids, P. J. Woods, D. Seweryniak, M. P. Carpenter, J. J. Ressler, J. Schwartz, J. Uusitalo, and W. B. Walters. Fine structure in the decay of the highly deformed proton emitter ^{131}eu. *Phys. Rev. Lett.*, 83:1116–1118, Aug 1999.

[50] V. Dehghani and S. A. Alavi. Empirical formulas for proton decay half-lives: Role of nuclear deformation and q-value. *Chinese Physics C*, 42(10):104101, sep 2018.

[51] J. Rotureau, J. Okołowicz, and M. Ploszajczak. Microscopic theory of the two-proton radioactivity. *Phys. Rev. Lett.*, 95:042503, Jul 2005.

[52] D.D. Bogdanov, V.P. Bugrov, and S.G. Kadmenskij. Proton decay of the nuclei 121 pr and 117 la. *Yadernaya Fizika*, 52(2):358–363, 1990.

[53] J. Honkanen, M.D. Cable, R.F. Parry, S.H. Zhou, Z.Y. Zhou, and Joseph Cerny. Beta-delayed two-proton decay of 26p. *Physics Letters B*, 133(3):146–148, 1983.

[54] Fengzhu Xing, Jianpo Cui, Yanzhao Wang, and Jianzhong Gu. Two-proton radioactivity of

ground and excited states within a unified fission model. *Chinese Physics C*, 45(12):124105, 2021.

[55] M. Balasubramaniam and N. Arunachalam. Proton and α-radioactivity of spherical proton emitters. *Physical Review C*, 71(1):014603, 2005.

[56] M.R. Oudih, M. Fellah, and N.H. Allal. Theoretical study of proton radioactivity. *Bulletin of the Russian Academy of Sciences: Physics*, 84(8):1022–1026, 2020.

[57] V.A. Rubakov. Monopole catalysis of proton decay. *Reports on Progress in Physics*, 51(2):189, 1988.

[58] Y. Ayyad, B. Olaizola, W. Mittig, G. Potel, V. Zelevinsky, M. Horoi, S. Beceiro-Novo, M. Alcorta, C. Andreoiu, T. Ahn, et al. Direct observation of proton emission in be 11. *Physical Review Letters*, 123(8):082501, 2019.

[59] D.S. Delion, J. Liotta, Roberto, and Ramon Wyss. Simple approach to two-proton emission. *Physical Review C*, 87(3):034328, 2013.

[60] T.N. Ginter, J.C. Batchelder, C.R. Bingham, C.J. Gross, R. Grzywacz, J.H. Hamilton, Z. Janas, M. Karny, S.H. Kim, J.F. Mas, et al. Proton emission from 150 lu. *Physical Review C*, 61(1):014308, 1999.

[61] M.G. Procter, D.M. Cullen, M.J. Taylor, G.A. Alharshan, L.S. Ferreira, E. Maglione, K. Auranen, T. Grahn, P.T. Greenlees, U. Jakobsson, et al. Proton emission from an oblate nucleus 151lu. *Physics Letters B*, 725(1-3):79–84, 2013.

[62] C.R. Bain, P.J. Woods, R. Coszach, T. Davinson, P. Decrock, M. Gaelens, W. Galster, Marc Huyse, R.J. Irvine, Pierre Leleux, et al. Two proton emission induced via a resonance reaction. *Physics Letters B*, 373(1-3):35–39, 1996.

[63] Bertram Blank, A. Bey, G. Canchel, C. Dossat, A. Fleury, J. Giovinazzo, I. Matea, N. Adimi, F. De Oliveira, I. Stefan, et al. First observation of zn 54 and its decay by two-proton emission. *Physical review letters*, 94(23):232501, 2005.

[64] M.V. Lund, A. Andreyev, M.J.G. Borge, J. Cederkall, Hilde De Witte, L.M. Fraile, H.O.U. Fynbo, P.T. Greenlees, L.J. Harkness-Brennan, A.M. Howard, et al. Beta-delayed proton emission from mg-20. *EUROPEAN PHYSICAL JOURNAL A*, 52(10), 2016.

[65] J. Uusitalo, C.N. Davids, P.J. Woods, D. Seweryniak, A.A. Sonzogni, J.C. Batchelder, C.R. Bingham, T. Davinson, J. DeBoer, D.J. Henderson, et al. Proton emission from the closed neutron shell nucleus 155 ta. *Physical Review C*, 59(6):R2975, 1999.

[66] G. Canchel, L. Achouri, J. Aysto, R. Béraud, Bertram Blank, E. Chabanat, S. Czajkowski, P. Dendooven, A. Emsallem, J. Giovinazzo, et al. The β-delayed one-and two-proton emission of 27s. *The European Physical Journal A-Hadrons and Nuclei*, 12(4):377–380, 2001.

[67] J. Giovinazzo, Bertram Blank, M. Chartier, S. Czajkowski, Agnès Fleury, M. J. Lopez Jimenez, M. S. Pravikoff, J.C. Thomas, Francois de Oliveira Santos, M. Lewitowicz, et al. Two-proton radioactivity of ^{45}Fe. *Physical review letters*, 89(10):102501, 2002.

[68] Bertram Blank and Marek Ploszajczak. Two-proton radioactivity. *Reports on Progress in Physics*, 71(4):046301, 2008.

[69] Chong Qi, S. Delion, Doru, J. Liotta, Roberto, and Ramon Wyss. Effects of formation properties in one-proton radioactivity. *Physical Review C*, 85(1):011303, 2012.

[70] G. Raciti, M. De Napoli, G. Cardella, E. Rapisarda, F. Amorini, and C. Sfienti. Two-proton correlated emission from 18ne excited states. *Nuclear Physics A*, 834(1-4):464c–466c, 2010.

[71] R. Coniglione, P. Sapienza, E. Migneco, C. Agodi, R. Alba, G. Bellia, A. Del Zoppo, P. Finocchiaro, K. Loukachine, C. Maiolino, et al. High energy proton emission in heavy ion reactions close to the fermi energy. *Physics Letters B*, 471(4):339–345, 2000.

[72] B. Ludewigt, R. Glasow, H. Lohner, and R. Santo. Proton emission in α-induced reactions at 43 mevnucleon. *Nuclear Physics A*, 408(2):359–371, 1983.

[73] K. Riisager et al. $^{11}Be(\beta p)$, a quasi-free neutron decay? *Phys. Lett. B*, 732:305–308, 2014.

[74] G.Z. Shi, J.J. Liu, Z.Y. Lin, H.F. Zhu, X.X. Xu, L.J. Sun, P.F. Liang, C.J. Lin, J. Lee, C.X. Yuan, et al. β-delayed two-proton decay of s 27 at the proton-drip line. *Physical Review C*, 103(6):L061301, 2021.

[75] A. P. Robinson, C. N. Davids, G. Mukherjee, D. Seweryniak, S. Sinha, P. Wilt, and P. J. Woods. Proton decay study of $^{150}\mathrm{Lu}$ and $^{150}\mathrm{lu}^{m}$. *Phys. Rev. C*, 68:054301, Nov 2003.

[76] J. C. Batchelder, C. R. Bingham, K. Rykaczewski, K. S. Toth, T. Davinson, J. A. McKenzie, P. J. Woods, T. N. Ginter, C. J. Gross, J. W. McConnell, E. F. Zganjar, J. H. Hamilton, W. B. Walters, C. Baktash, J. Greene, J. F. Mas, W. T. Milner, S. D. Paul, D. Shapira, X. J. Xu, and C. H. Yu. Observation of the exotic nucleus $^{145}\mathrm{Tm}$ via its direct proton decay. *Phys. Rev. C*, 57:R1042–R1046, Mar 1998.

[77] A.A. Lis, C. Mazzocchi, W. Dominik, Z. Janas, M. Pfutzner, M. Pomorski, L. Acosta, S. Baraeva, E. Casarejos, J Duénas-Díaz, et al. β-delayed three-proton decay of ar 31. *Physical Review C*, 91(6):064309, 2015.

[78] L. Faux, M. S. Pravikoff, S. Andriamonje, B. Blank, R. Del Moral, J.-P. Dufour, A. Fleury, C. Marchand, K.-H. Schmidt, K. Sümmerer, T. Brohm, H.-G. Clerc, A. Grewe, E. Hanelt,

B. Voss, and C. Ziegler. First observation of the β-delayed proton decay of ^{52}Ni. *Phys. Rev. C*, 49:2440–2443, May 1994.

[79] M. D. Cable, J. Honkanen, E. C. Schloemer, M. Ahmed, J. E. Reiff, Z. Y. Zhou, and Joseph Cerny. Beta-delayed two-proton decays of ^{22}Al and ^{26}P. *Phys. Rev. C*, 30:1276–1285, Oct 1984.

[80] Li-Jie Sun, Cheng-Jian Lin, Xin-Xing Xu, Jian-Song Wang, Hui-Ming Jia, Feng Yang, Yan-Yun Yang, Lei Yang, Peng-Fei Bao, Huan-Qiao Zhang, Shi-Lun Jin, Zhen-Dong Wu, Ning-Tao Zhang, Si-Ze Chen, Jun-Bing Ma, Peng Ma, Nan-Ru Ma, and Zu-Hua Liu. Experimental study of beta-delayed proton emission of ca-36 , ca-37. *Chinese Physics Letters*, 32(1):012301, jan 2015.

[81] R. D. Page, P. J. Woods, R. A. Cunningham, T. Davinson, N. J. Davis, S. Hofmann, A. N. James, K. Livingston, P. J. Sellin, and A. C. Shotter. Discovery of new proton emitters ^{160}Re and ^{156}Ta. *Phys. Rev. Lett.*, 68:1287–1290, Mar 1992.

[82] P. Ascher, L. Audirac, N. Adimi, B. Blank, C. Borcea, B. A. Brown, I. Companis, F. Delalee, C. E. Demonchy, F. de Oliveira Santos, J. Giovinazzo, S. Grévy, L. V. Grigorenko, T. Kurtukian-Nieto, S. Leblanc, J.-L. Pedroza, L. Perrot, J. Pibernat, L. Serani, P. C. Srivastava, and J.-C. Thomas. Direct observation of two protons in the decay of ^{54}Zn. *Phys. Rev. Lett.*, 107:102502, Sep 2011.

[83] M. Pomorski, M. Pfutzner, W. Dominik, R. Grzywacz, T. Baumann, J.S. Berryman, H. Czyrkowski, R. Dkabrowski, T. Ginter, J. Johnson, et al. First observation of two-proton radioactivity in ni 48. *Physical Review C*, 83(6):061303, 2011.

[84] A. Azhari, T. Baumann, J.A. Brown, M. Hellstrom, J.H. Kelley, R.A. Kryger, D.J. Millener,

H. Madani, E. Ramakrishnan, D.E. Russ, et al. Proton decay of states in 11 n. *Physical Review C*, 57(2):628, 1998.

[85] VI Goldansky. On neutron-deficient isotopes of light nuclei and the phenomena of proton and two-proton radioactivity. *Nuclear Physics*, 19:482–495, 1960.

[86] K. P. Jackson, C. U. Cardinal, H. C. Evans, N. A. Jelley, and Joseph Cerny. 53com: A proton-unstable isomer. *Physics Letters B*, 33(4):281–283, 1970.

[87] Joseph Cerny, E. Esterl, John, A. Gough, Richard, and G. Sextro, Richard. Confirmed proton radioactivity of 53com. *Physics Letters B*, 33(4):284–286, 1970.

[88] D. N. Poenaru, R. A. Gherghescu, and W. Greiner. Heavy-particle radioactivity of superheavy nuclei. *Phys. Rev. Lett.*, 107:062503, Aug 2011.

[89] D. N. Poenaru, R. A. Gherghescu, and W. Greiner. Heavy-particle radioactivity. In *Journal of Physics: Conference Series*, volume 436, page 012056. IOP Publishing, 2013.

[90] A. M. Nagaraja, H. C. Manjunatha, N. Sowmya, L. Seenappa, P. S .Damodara Gupta, N. Manjunatha, and S. Alfred Cecil Raj. Heavy particle radioactivity of superheavy element z= 126. *Nuclear Physics A*, 1015:122306, 2021.

[91] M. Pfutzner, E. Badura, C. Bingham, Bertram Blank, M. Chartier, H. Geissel, J. Giovinazzo, L.V. Grigorenko, R. Grzywacz, M. Hellstrom, et al. First evidence for the two-proton decay of 45 fe. *The European Physical Journal A-Hadrons and Nuclei*, 14(3):279–285, 2002.

[92] J. Giovinazzo, B. Blank, M. Chartier, S. Czajkowski, A. Fleury, M. J. Lopez Jimenez, M. S. Pravikoff, J.-C. Thomas, F. de Oliveira Santos, M. Lewitowicz, V. Maslov, M. Stanoiu,

R. Grzywacz, M. Pfützner, C. Borcea, and B. A. Brown. Two-proton radioactivity of ^{45}Fe. *Phys. Rev. Lett.*, 89:102501, Aug 2002.

[93] Jun-Hao Cheng, Jiu-Long Chen, Jun-Gang Deng, Xiao-Hua Li, Zhen Zhang, and Peng-Cheng Chu. Systematic study of proton emission half-lives within the two-potential approach with skyrme-hartree-fock. *Nuclear Physics A*, 997:121717, 2020.

[94] Madhubrata Bhattacharya and G. Gangopadhyay. Microscopic calculation of half lives of spherical proton emitters. *Physics Letters B*, 651(2-3):263–267, 2007.

[95] J.P. Jeukenne, A. Lejeune, and C. Mahaux. Optical-model potential in nuclear matter from reid's hard core interaction. *Phys. Rev. C*, 10:1391–1401, Oct 1974.

[96] D. N. Basu, P. Roy Chowdhury, and C. Samanta. Folding model analysis of proton radioactivity of spherical proton emitters. *Phys. Rev. C*, 72:051601, Nov 2005.

[97] Bidhubhusan Sahu, S. K. Agarwalla, and S. K. Patra. Half-lives of proton emitters using relativistic mean field theory. *Phys. Rev. C*, 84:054604, Nov 2011.

[98] S. Hofmann, F.P. Heßberger, D. Ackermann, S. Antalic, P. Cagarda, S. Cwiok, B. Kindler, J. Kojouharova, B Lommel, R Mann, et al. The new isotope 270 110 and its decay products 266 hs and 262 sg. *The European Physical Journal A-Hadrons and Nuclei*, 10(1):5–10, 2001.

[99] Nithu Ashok, Deepthy Maria Joseph, and Antony Joseph. Cluster decay in osmium isotopes using hartree–fock–bogoliubov theory. *Modern Physics Letters A*, 31(07):1650045, 2016.

[100] Qiang Zhao, Jian Min Dong, Jun Ling Song, and Wen Hui Long. Proton radioactivity described by covariant density functional theory with the similarity renormalization group method. *Phys. Rev. C*, 90:054326, Nov 2014.

[101] BirBikram Singh, S. K. Patra, and Raj K. Gupta. Cluster radioactive decay within the preformed cluster model using relativistic mean-field theory densities. *Phys. Rev. C*, 82:014607, Jul 2010.

[102] Dong Jian-Min, Zhang Hong-Fei, Zuo Wei, and Li Jun-Qing. Unified fission model for proton emission. *Chinese Physics C*, 34(2):182, 2010.

[103] G. R. Sridhara, H. C. Manjunatha, N. Sowmya, and P. S. Damodara Gupta. A study of alpha-decay using effective liquid drop model. *International Journal of Modern Physics E*, page 2150094, 2021.

[104] K. P. Santhosh, B. Priyanka, and M. S. Unnikrishnan. Cluster decay half-lives of trans-lead nuclei within the coulomb and proximity potential model. *Nuclear Physics A*, 889:29–50, 2012.

[105] H. C. Manjunatha. Alpha decay properties of superheavy nuclei z= 126. *Nuclear Physics A*, 945:42–57, 2016.

[106] H. C. Manjunatha. Comparison of alpha decay with fission for isotopes of superheavy nuclei z= 1 2 4. *International Journal of Modern Physics E*, 25(09):1650074, 2016.

[107] M. G. Srinivas, H. C. Manjunatha, K. N. Sridhar, N. Sowmya, and Alfred Cecil Raj. Proton decay of actinide nuclei. *Nuclear Physics A*, 995:121689, 2020.

[108] H. C. Manjunatha, N. Sowmya, K. N. Sridhar, and L. Seenappa. A study of probable alpha-ternary fission fragments of 257 fm. *Journal of Radioanalytical and Nuclear Chemistry*, 314(2):991–999, 2017.

[109] Jiu-Long Chen, Jun-Yao Xu, Jun-Gang Deng, Xiao-Hua Li, Biao He, and Peng-Cheng

Chu. New geiger-nuttall law for proton radioactivity. *The European Physical Journal A*, 55(11):1–8, 2019.

[110] N. Sowmya and H. C. Manjunatha. Investigations on different decay modes of darmstadtium. *Physics of Particles and Nuclei Letters*, 17(3):370–378, 2020.

[111] N. Sowmya and H. C. Manjunatha. Competition between different decay modes of superheavy element z= 116 and synthesis of possible isotopes. *Brazilian Journal of Physics*, 49(6):874–886, 2019.

[112] T .R. Routray, S. K. Tripathy, B. B. Dash, B. Behera, and D. N. Basu. Proton radioactivity with a yukawa effective interaction. *The European Physical Journal A*, 47(8):1–9, 2011.

[113] T. R. Routray, Abhishek Mishra, S. K. Tripathy, B. Behera, and D .N. Basu. Proton radioactivity half-lives with skyrme interactions. *The European Physical Journal A*, 48(6):1–10, 2012.

[114] Yu-Qi Xin, Jun-Gang Deng, and Hong-Fei Zhang. Proton radioactivity within the generalized liquid drop model with various versions of proximity potentials. *Communications in Theoretical Physics*, 73(6):065301, 2021.

[115] S. Hofmann, W. Reisdorf, G. Munzenberg, F. P. Hessberger, J.R.H. Schneider, and P. Armbruster. Proton radioactivity of 151 lu. *Zeitschrift für Physik A Atoms and Nuclei*, 305(2):111–123, 1982.

[116] Chong Qi, S. Delion, Doru, J. Liotta, Roberto, and Ramon Wyss. Effects of formation properties in one-proton radioactivity. *Phys. Rev. C*, 85:011303, Jan 2012.

[117] T. Faestermann, A. Gillitzer, K. Hartel, P. Kienle, and E. Nolte. Evidence for proton radioactivity of 113cs and 109i. *Physics Letters B*, 137(1-2):23–26, 1984.

[118] I. Mukha, E. Roeckl, J. Döring, L. Batist, A. Blazhev, H. Grawe, C. R. Hoffman, M. Huyse, Z. Janas, R. Kirchner, M. La Commara, C. Mazzocchi, C. Plettner, S. L. Tabor, P. Van Duppen, and M. Wiedeking. Observation of proton radioactivity of the (21^+) high-spin isomer in ^{94}Ag. *Phys. Rev. Lett.*, 95:022501, Jul 2005.

[119] Mamta Aggarwal. Proton radioactivity at non-collective prolate shape in high spin state of 94ag. *Physics Letters B*, 693(4):489–493, 2010.

[120] E. Roeckl, Ivan Mukha, L. Batist, A. Blazhev, J. Doering, H. Grawe, L. Grigorenkof, Marc Huyse, Z. Janas, R. Kirchner, et al. One-proton and two-proton radioactivity of the (21+) isomer in 94 ag. *Acta Physica Polonica B*, 38(4), 2007.

[121] Joseph Cerny, R.A. Gough, R.G. Sextro, and E. Esterl, John. Further results on the proton radioactivity of 53mco. *Nuclear Physics A*, 188(3):666–672, 1972.

[122] E.L. Medeiros, M.M.N. Rodrigues, S.B. Duarte, and O.A.P. Tavares. Systematics of half-lives for proton radioactivity. *The European Physical Journal A*, 34(4):417–427, 2007.

[123] G. L. Poli, C. N. Davids, P. J. Woods, D. Seweryniak, M. P. Carpenter, J. A. Cizewski, T. Davinson, A. Heinz, R. V. F. Janssens, C. J. Lister, J. J. Ressler, A. A. Sonzogni, J. Uusitalo, and W. B. Walters. Proton and α radioactivity of ^{185}Bi. *Phys. Rev. C*, 63:044304, Mar 2001.

[124] L. S. Ferreira, E. Maglione, and P. Ring. Covariant density functional theory for decay of deformed proton emitters: A self-consistent approach. *Physics Letters B*, 753:237–241, 2016.

[125] G. A. Lalazissis. Covariant density functional theory: Description of rare nuclei. In *Collec-*

tive Motion And Phase Transitions In Nuclear Systems, pages 287–318. World Scientific, 2007.

[126] H.C. Manjunatha, M.G. Srinivas, N. Sowmya, P.S. Damodara Gupta, and Alfred Cecil Raj. Proton radioactivity of heavy nuclei of atomic number range 72¡ z¡ 88. *Physics of Particles and Nuclei Letters*, 17(7):909–915, 2020.

[127] M.G. Srinivas, H.C. Manjunatha, K.N. Sridhar, N. Sowmya, and Alfred Cecil Raj. Proton radioactivity of 241-251db. In *Proceedings of the DAE Symp. on Nucl. Phys*, volume 64, page 417, 2019.

[128] M.G. Srinivas, H.C. Manjunatha, N. Sowmya, P.S. Damodara Gupta, S. Alfred, and Cecil Raj. Competition between different decay modes in bismuth. In *Proceedings of the DAE Symp. on Nucl. Phys*, volume 65, page 164, 2021.

[129] M.G Srinivas, H.C. Manjunatha, N. Sowmya, Damodara P.S. Gupta, and Alfred Cecil Raj. Systematics of proton decay of actinides. *Indian journal of pure and applied physics*, 58:255–262, 2020.

[130] Bertram Blank, P. Ascher, . Audirac, J. Giovinazzo, N. Adimi, G. Canchel, F. Delalee, C. E. Demonchy, C. Dossat, S. Grevy, et al. Two-proton radioactivity as a tool for nuclear structure. In *Nuclear Structure Problems*, pages 130–135. World Scientific, 2013.

[131] Marta Anguiano, Giampaolo Co', and Antonio M. Lallena. Photo-emission of two protons from nuclei. *Nuclear Physics A*, 744:168–191, 2004.

[132] G. Raciti, M. De Napoli, G. Cardella, E. Rapisarda, F. Amorini, and C. Sfienti. Two-proton correlated emission from 18ne excited states. *Nuclear Physics A*, 834(1):464c–466c, 2010. The 10th International Conference on Nucleus-Nucleus Collisions (NN2009).

[133] V.I. Goldansky. On neutron-deficient isotopes of light nuclei and the phenomena of proton and two-proton radioactivity. *Nuclear Physics*, 19:482–495, 1960.

[134] Ivan Mukha, Ernst Roeckl, Leonid Batist, Andrey Blazhev, Joachim Doring, Hubert Grawe, Leonid Grigorenko, Mark Huyse, Zenon Janas, Reinhard Kirchner, et al. Proton–proton correlations observed in two-proton radioactivity of 94 ag. *Nature*, 439(7074):298–302, 2006.

[135] J. Giovinazzo, Bertram Blank, C. Borcea, G. Canchel, J.C. Dalouzy, C.E. Demonchy, F. de Oliveira Santos, C. Dossat, S. Grevy, L. Hay, et al. First direct observation of two protons in the decay of fe 45 with a time-projection chamber. *Physical review letters*, 99(10):102501, 2007.

[136] P. Ascher, L. Audirac, N. Adimi, Bertram Blank, C. Borcea, B. A. Brown, F. Companis, I.and Delalee, C.E. Demonchy, Francois de Oliveira Santos, et al. Direct observation of two protons in the decay of zn 54. *Physical review letters*, 107(10):102502, 2011.

[137] I. Mukha, K. Summerer, L. Acosta, M.A.G. Alvarez, E. Casarejos, A. Chatillon, D. Cortina-Gil, J. Espino, A. Fomichev, J.E. Garcia-Ramos, et al. Observation of two-proton radioactivity of mg 19 by tracking the decay products. *Physical review letters*, 99(18):182501, 2007.

[138] I. Mukha, L. Grigorenko, K. Summerer, L. Acosta, M.A.G. Alvarez, E Casarejos, A Chatillon, D Cortina-Gil, J M Espino, A Fomichev, et al. Proton-proton correlations observed in two-proton decay of mg 19 and ne 16. *Physical Review C*, 77(6):061303, 2008.

[139] C. N. Davids, P. J. Woods, D. Seweryniak, A. A. Sonzogni, J. C Batchelder, C R Bingham, T Davinson, D .J. Henderson, R. J. Irvine, G. L. Poli, et al. Proton radioactivity from highly deformed nuclei. *Physical review letters*, 80(9):1849, 1998.

[140] T. Goigoux, P. Ascher, Bertram Blank, M. Gerbaux, J. Giovinazzo, S. Grevy, T. Kurtukian Nieto, C. Magron, P. Doornenbal, G.G. Kiss, et al. Two-proton radioactivity of kr 67. *Physical review letters*, 117(16):162501, 2016.

[141] I. Mukha, L. Grigorenko, K. Summerer, L. Acosta, M. A. G. Alvarez, E. Casarejos, A. Chatillon, D. Cortina-Gil, J. M. Espino, A. Fomichev, J. E. Garcia-Ramos, H. Geissel, J. Gomez-Camacho, J. Hofmann, O. Kiselev, A. Korsheninnikov, N. Kurz, Yu. Litvinov, I. Martel, C. Nociforo, W. Ott, M. Pfutzner, C. Rodriguez-Tajes, E. Roeckl, M. Stanoiu, H. Weick, and P. J. Woods. Proton-proton correlations observed in two-proton decay of $^{19}\mathrm{Mg}$ and $^{16}\mathrm{Ne}$. *Phys. Rev. C*, 77:061303, Jun 2008.

[142] M. Pomorski, M. Pfutzner, W. Dominik, R. Grzywacz, T. Baumann, J. S. Berryman, H. Czyrkowski, R. Dkabrowski, T. Ginter, J. Johnson, G. Kaminski, A. Kuzniak, N. Larson, S. N. Liddick, M. Madurga, C. Mazzocchi, S. Mianowski, K. Miernik, D. Miller, S. Paulauskas, J. Pereira, K. P. Rykaczewski, A. Stolz, and S. Suchyta. First observation of two-proton radioactivity in $^{48}\mathrm{Ni}$. *Phys. Rev. C*, 83:061303, Jun 2011.

[143] C. Giusti and F.D. Pacati. Two-proton emission induced by electron scattering. *Nuclear Physics A*, 535(3):573–591, 1991.

[144] O. A. P. Tavares and E. L. Medeiros. A calculation model to half-life estimate of two-proton radioactive decay process. *The European Physical Journal A*, 54(4):65, 2018.

[145] M. Gonçalves, N. Teruya, O.A.P. Tavares, and S.B. Duarte. Two-proton emission half-lives in the effective liquid drop model. *Physics Letters B*, 774:14–19, 2017.

[146] C. Dossat, A. Bey, Bertram Blank, G. Canchel, Agnes Fleury, J. Giovinazzo, I. Matea, Francois de Oliveira Santos, S. Georgiev, G .and Grevy, et al. Two-proton radioactivity studies with fe 45 and ni 48. *Physical Review C*, 72(5):054315, 2005.

[147] J. P. Cui, Y. H. Gao, Y. Z. Wang, J. Z. Gu, et al. Two-proton radioactivity within a generalized liquid drop model. *Physical Review C*, 101(1):014301, 2020.

[148] L. V. Grigorenko, R. C. Johnson, I. J. Mukha, I. G .and Thompson, and M. V. Zhukov. Theory of two-proton radioactivity with application to 19 mg and 48 ni. *Physical review letters*, 85(1):22, 2000.

[149] Qian Yi-Bin, Ren Zhong-Zhou, and Ni Dong-Dong. Theoretical calculation for half-lives of spherical proton emitters. *Chinese Physics Letters*, 27(7):072301, 2010.

[150] D. N. Basu, P. Roy Chowdhury, and C. Samanta. Folding model analysis of proton radioactivity of spherical proton emitters. *Physical Review C*, 72(5):051601, 2005.

[151] Yibin Qian and Zhongzhou Ren. Calculations on decay rates of various proton emissions. *The European Physical Journal A*, 52(3):1–7, 2016.

[152] Qian Yi-Bin, Ren Zhong-Zhou, Ni Dong-Dong, and Sheng Zong-Qiang. Half-lives of proton emitters with a deformed density-dependent model. *Chinese Physics Letters*, 27(11):112301, 2010.

[153] Qiang Zhao, Jian Min Dong, Jun Ling Song, Wen Hui Long, et al. Proton radioactivity described by covariant density functional theory with the similarity renormalization group method. *Physical Review C*, 90(5):054326, 2014.

[154] Zhi-Xing Zhang and Jian-Min Dong. A formula for half-life of proton radioactivity. *Chinese Physics C*, 42(1):014104, 2018.

[155] E. Maglione, L. S. Ferreira, and R. J. Liotta. Nucleon decay from deformed nuclei. *Physical review letters*, 81(3):538, 1998.

[156] B. Alex Brown. Diproton decay of nuclei on the proton drip line. *Physical Review C*, 43(4):R1513, 1991.

[157] W. Nazarewicz, J. Dobaczewski, J. A. Werner, T. R .and Maruhn, P.G. Reinhard, K. Rutz, C. R. Chinn, A. S. Umar, and M. R. Strayer. Structure of proton drip-line nuclei around doubly magic ni 48. *Physical Review C*, 53(2):740, 1996.

[158] B. J. Cole. Stability of proton-rich nuclei in the upper sd shell and lower pf shell. *Physical Review C*, 54(3):1240, 1996.

[159] W. E. Ormand. Mapping the proton drip line up to a= 70. *Physical Review C*, 55(5):2407, 1997.

[160] Erik Olsen, M. PfUtzner, N. Birge, M. Brown, Witold Nazarewicz, and A. Perhac. Landscape of two-proton radioactivity. *Physical review letters*, 110(22):222501, 2013.

[161] H. C. Manjunatha and N. Sowmya. Competition between spontaneous fission ternary fission cluster decay and alpha decay in the super heavy nuclei of z= 126. *Nuclear Physics A*, 969:68–82, 2018.

[162] N. Sowmya, H .C. Manjunatha, and A .M. Dhananjaya, N .and Nagaraja. Competition between binary fission, ternary fission, cluster radioactivity and alpha decay of ^{281}ds. *Journal of Radioanalytical and Nuclear Chemistry*, 323(3):1347–1351, 2020.

[163] G. R. Sridhar, H. C. Manjunatha, N. Sowmya, P. S. Damodara Gupta, and H. B. Ramalingam. Atlas of cluster radioactivity in actinide nuclei. *The European Physical Journal Plus*, 135(3):1–28, 2020.

[164] H. C. Manjunatha and N. Sridhar, K. N .and Sowmya. Investigations of the synthesis of the superheavy element z= 122. *Physical Review C*, 98(2):024308, 2018.

[165] H. C. Manjunatha and N. Sowmya. Decay modes of superheavy nuclei z= 1 2 4. *International Journal of Modern Physics E*, 27(05):1850041, 2018.

[166] N. Sowmya and H. C. Manjunatha. Investigations on different decay modes of darmstadtium. *Physics of Particles and Nuclei Letters*, 17(3):370–378, 2020.

[167] N. Sowmya and H. C. Manjunatha. Competition between different decay modes of superheavy element z= 116 and synthesis of possible isotopes. *Brazilian Journal of Physics*, 49(6):874–886, 2019.

[168] N. Sowmya, H. C. Manjunatha, and P. S. Damodara Gupta. Competition between decay modes of superheavy nuclei 281-310og. *International Journal of Modern Physics E*, 2020.

[169] K. N. Sridhar, H. C. Manjunatha, and H. B. Ramalingam. Search for possible fusion reactions to synthesize the superheavy element z= 121. *Physical Review C*, 98(6):064605, 2018.

[170] G. Royer and R. Moustabchir. Light nucleus emission within a generalized liquid-drop model and quasimolecular shapes. *Nuclear Physics A*, 683(1-4):182–206, 2001.

[171] G. Royer and B. Remaud. Fission processes through compact and creviced shapes. *Journal of Physics G: Nuclear Physics*, 10(8):1057, 1984.

[172] A. M. Nagaraja, H. C. Manjunatha, N. Sowmya, N. Manjunath, and S. Alfred Cecil Raj. Cluster radioactivity of superheavy nuclei 290–310 120 using different proximity functions. *The European Physical Journal Plus*, 135(10):1–16, 2020.

[173] H. C. Manjunatha, G. R. Sridhar, N. Sowmya, P. S. Damodara Gupta, and H. B. Ramalingam. A systematic study of alpha decay in actinide nuclei using modified generalized liquid drop model. *International Journal of Modern Physics E*, page 2150013, 2021.

[174] N. Sowmya, H. C. Manjunatha, P.S. Damodara Gupta, and N. Dhananjaya. Competition between cluster and alpha decay in odd z superheavy nuclei $111 \leq z \leq 125$. *Brazilian Journal of Physics*, pages 1–37, 2020.

[175] M. Goncalves and S. B. Duarte. Effective liquid drop description for the exotic decay of nuclei. *Physical Review C*, 48(5):2409, 1993.

[176] M. Goncalves, S. B. Duarte, F. Garcia, and O. Rodriguez. Prescold: Calculation of the half-life for alpha decay, cluster radioactivity and cold fission processes. *Computer physics communications*, 107(1-3):246–252, 1997.

[177] O. A. P. Tavares, S. B. Duarte, O. Rodriguez, F. Guzman, M. Goncalves, and F. Garcia. Effective liquid drop description for alpha decay of atomic nuclei. *Journal of Physics G Nuclear and Particle Physics*, 24(9):1757, 1998.

[178] J. P. Cui, Y. L. Zhang, S. Zhang, Y. Z. Wang, et al. α-decay half-lives of superheavy nuclei. *Physical Review C*, 97(1):014316, 2018.

[179] Y. Z. Wang, S. J. Wang, Z. Y. Hou, J. Z. Gu, et al. Systematic study of α-decay energies and half-lives of superheavy nuclei. *Physical Review C*, 92(6):064301, 2015.

[180] Sheng Zong-Qiang, Shu Liang-Ping, Fan Guang-Wei, Meng Ying, and Qian Jian-Fa. Investigation of proton radioactivity with the effective liquid drop model. *Chinese Physics C*, 39(2):024102, 2015.

[181] A. M. Nagaraja, H. C. Manjunatha, N. Sowmya, and S. Raj. Cluster radioactivity in superheavy nuclei 299-302 120. *Indian journal of pure and applied physics*, 58:207–212, 2020.

[182] H. Mahmud, Cary N. Davids, P. J. Woods, T. Davinson, A. Heinz, G. L. Poli, J. J. Ressler, K. Schmidt, D. Seweryniak, M. B. Smith, et al. Proton radioactivity of ^{117}La. *Physical Review C*, 64(3):031303, 2001.

[183] Carolyn J. Anderson and Riccardo Ferdani. Copper-64 radiopharmaceuticals for pet imaging of cancer: advances in preclinical and clinical research. *Cancer Biotherapy and Radiopharmaceuticals*, 24(4):379–393, 2009.

[184] V. A. Karnaukhov, G. M. Ter-Akopian, and V. G. Subbotin. Search for proton emitters among the products of heavy ion induced reactions. In *Proceedings of the Third Conference on Reactions Between Complex Nuclei: Held at Asilomar (Pacific Grove, California) April 14-18, 1963*, page 434. University of California Press, 1963.

[185] Zhongzhou Ren, Chang Xu, and Zaijun Wang. New perspective on complex cluster radioactivity of heavy nuclei. *Physical Review C*, 70(3):034304, 2004.

[186] E. M.. Kozulin, G. N. Knyazheva, I. M. Itkis, M. G. Itkis, A. A. Bogachev, E. V. Chernysheva, L. Krupa, Francis Hanappe, O. Dorvaux, Louise Stuttge, et al. Fusion-fission and quasifission of superheavy systems with z= 110–116 formed in ca 48-induced reactions. *Physical Review C*, 90(5):054608, 2014.

[187] Tiekuang Dong and Zhongzhou Ren. New calculations of α-decay half-lives by the viola-seaborg formula. *The European Physical Journal A-Hadrons and Nuclei*, 26(1):69–72, 2005.

[188] K. P. Santhosh and C. Nithya. α-decay chains of the superheavy nuclei rg 255–350. *Physical Review C*, 95(5):054621, 2017.

[189] Elsje Alessandra Quadrelli. Lanthanide contraction over the 4f series follows a quadratic decay. *Inorganic chemistry*, 41(2):167–169, 2002.

[190] J. M. Nitschke, P. A. Wilmarth, J. Gilat, P. Moller, and K. S. Toth. Beta-delayed proton decay in the lanthanide region. In *AIP Conference Proceedings*, volume 164, pages 697–707. American Institute of Physics, 1987.

[191] Y. J. Yao, G. L. Zhang, W. W. Qu, and J. Q. Qian. Comparative studies for different proximity potentials applied to α decay. *The European Physical Journal A*, 51(9):122, 2015.

[192] Dong Bai and Zhongzhou Ren. α-cluster structures above double shell closures via double-folding potentials from chiral effective field theory. *Phys. Rev. C*, 103:044316, Apr 2021.

[193] V. Zanganeh, R. Gharaei, and A. M. Izadpanah. Comparative study for different nuclear proximity potentials applied to quasi-elastic scattering and fusion reactions. *Nuclear Physics A*, 992:121637, 2019.

[194] K. P. Santhosh and Antony Joseph. Effect of parent and daughter deformation on half-life time in exotic decay. *Pramana*, 59(4):679–684, 2002.

[195] Ishwar Dutt and Rajeev K. Puri. Comparison of different proximity potentials for asymmetric colliding nuclei. *Physical Review C*, 81(6):064609, 2010.

[196] M. Pfützner, M. Karny, L. V. Grigorenko, and K. Riisager. Radioactive decays at limits of nuclear stability. *Rev. Mod. Phys.*, 84:567–619, Apr 2012.

[197] Lídia S Ferreira, Miguel Costa Lopes, and Enrico Maglione. Decays of drip line nuclei. *Progress in Particle and Nuclear Physics*, 59(1):418–424, 2007.

[198] A.A. Sonzogni. Proton radioactivity in z¿ 50 nuclides. *Nuclear Data Sheets*, 95(1):1–48, 2002.

[199] A. T. Kruppa and W. Nazarewicz. Gamow and r-matrix approach to proton emitting nuclei. *Phys. Rev. C*, 69:054311, May 2004.

[200] P Belli, R Bernabei, F Cappella, R Cerulli, FA Danevich, ML Di Vacri, A Incicchitti, M Laubenstein, SS Nagorny, S Nisi, et al. First search for double β decay of dysprosium. *Nuclear Physics A*, 859(1):126–139, 2011.

[201] D Schardt, PO Larsson, R Kirchner, O Klepper, VT Koslowsky, E Roeckl, K Rykaczewski, P Kleinheinz, and K Zuber. Beta-delayed proton emission of dysprosium and erbium precursors. 1984.

[202] VV Mazepus. Spectra of rotational bands for odd dysprosium isotopes in the non-adiabatic particle+ rotor model. *Yadernaya Fizika*, 42(1):117–124, 1985.

[203] VA Kuz'min and VG Solov'ev. Effect of interaction in particle-particle channel on gamow-teller β+ decay in spherical nuclei. *Pis' ma v Zhurnal Ehksperimental'noj i Teoreticheskoj Fiziki*, 47(2):68–69, 1988.

[204] GD Alkhazov, AA Bykov, VD Wittmann, FV Morozov, SY Orlov, VE Starodubskii, and VK Tarasov. Quenching of spin-isospin excitations in. beta./sup+/decay. *Sov. J. Nucl. Phys.(Engl. Transl.);(United States)*, 42(6), 1985.

[205] HC Manjunatha, N Sowmya, and PS Gupta. Competition between different decay modes in the isotopes of actinide nuclei. *Iranian Journal of Science and Technology, Transactions A: Science*, 45(6):2201–2217, 2021.

[206] HC Manjunatha, N Sowmya, N Manjunath, and L Seenappa. Investigations on the superheavy nuclei with magic number of neutrons and protons. *International Journal of Modern Physics E*, 29(05):2050028, 2020.

[207] N. Sowmya, H. C. Manjunatha, and P. S. Damodara Gupta. Competition between decay modes of superheavy nuclei 281-310og. *International Journal of Modern Physics E*, 2020.

[208] Marta Anguiano, Antonio M. Lallena, et al. Photo-emission of two protons from nuclei. *Nuclear Physics A*, 744:168–191, 2004.

[209] Enrico Maglione and Lidia S. Ferreira. Proton emission from pm 125 could be observed. *Physical Review C*, 94(4):044317, 2016.

[210] H.C. Manjunatha, K.N. Sridhar, and N. Sowmya. Investigations on ni64+ zana$\rightarrow$ z= 104–123 (shn) a= 250–310 reactions. *Nuclear Physics A*, 987:382–395, 2019.

[211] H.C. Manjunatha and K.N. Sridhar. Projectile target combination to synthesis superheavy nuclei z= 126. *Nuclear Physics A*, 962:7–23, 2017.

[212] H.C. Manjunatha and K.N. Sridhar. Investigation to synthesis more isotopes of superheavy nuclei z= 118. *Nuclear Physics A*, 975:136–153, 2018.

[213] N. Sowmya and H.C. Manjunatha. A study of binary fission and ternary fission. *Bulg. J. Phys*, 46:16–27, 2019.

[214] N. Sowmya and H.C. Manjunatha. Investigations on the synthesis and decay properties of roentgenium. *Brazilian Journal of Physics*, 50(3):317–330, 2020.

[215] N. Sowmya and H.C. Manjunatha. Investigations on different decay modes of darmstadtium. *Physics of Particles and Nuclei Letters*, 17(3):370–378, 2020.

[216] O. Klepper, T. Batsch, S. Hofmann, R. Kirchner, W. Kurcewicz, W. Reisdorf, E. Roeckl, D. Schardt, and G. Nyman. Direct and beta-delayed proton decay of very neutron-deficient rare-earth isotopes produced in the reaction58ni+ 92mo. *Zeitschrift für Physik A Atoms and Nuclei*, 305(2):125–130, 1982.

[217] AP Robinson, CN Davids, G Mukherjee, D Seweryniak, S Sinha, P Wilt, and PJ Woods. Proton decay study of lu 150 and lu m 150. *Physical Review C*, 68(5):054301, 2003.

[218] Borut Bajc, Pavel Fileviez Perez, and Goran Senjanović. Proton decay in minimal supersymmetric su (5). *Physical Review D*, 66(7):075005, 2002.

[219] T.J. Goldman and D.A. Ross. A new estimate of the proton lifetime. *Physics Letters B*, 84(2):208–210, 1979.

[220] LV Grigorenko, TD Wiser, K Miernik, RJ Charity, M Pfützner, A Banu, CR Bingham, M Ćwiok, IG Darby, W Dominik, et al. Complete correlation studies of two-proton decays: 6be and 45fe. *Physics Letters B*, 677(1-2):30–35, 2009.

[221] Jun-Gang Deng, Xiao-Hua Li, Jiu-Long Chen, Jun-Hao Cheng, and Xi-Jun Wu. Systematic study of proton radioactivity of spherical proton emitters within various versions of proximity potential formalisms. *The European Physical Journal A*, 55(4):1–10, 2019.

[222] P. J. Woods, P. Munro, D. Seweryniak, C. N. Davids, T. Davinson, A. Heinz, H. Mahmud, F. Sarazin, J. Shergur, W. B. Walters, et al. Proton decay of the highly deformed nucleus tb 135. *Physical Review C*, 69(5):051302, 2004.

[223] E. Maglione and Lidia S. Ferreira. New developments in the theory of proton radioactivity. In *Exotic Nuclei and Atomic Masses*, pages 135–138. Springer, 2003.

[224] Sowmya Nagaraj, H.C. Manjunatha, P. Gupta, and Narayanappa Dhananjaya. Competition between cluster and alpha decay in odd z superheavy nuclei 111 $\pm$z $\pm$125. *Brazilian Journal of Physics*, 51, 11 2020.

[225] Yibin Qian, Zhongzhou Ren, and Dongdong Ni. Calculations of α-decay half-lives for heavy and superheavy nuclei. *Physical Review C*, 83(4):044317, 2011.

[226] Wenjin Tan, Dongdong Ni, and Zhongzhou Ren. Calculations of the β-decay half-lives of neutron-deficient nuclei. *Chinese Physics C*, 41(5):054103, 2017.

[227] J. Giovinazzo, T. Goigoux, B. Blank, P. Ascher, M. Gerbaux, S. Grevy, T. Kurtukian-Nieto, C. Magron, P. Doornenbal, N. Fukuda, et al. Two-proton radioactivity: the interesting case of ^{67}Kr and further studies. In *36th Mazurian Lakes Conference on Physics*, volume 51, page 577, 2019.

[228] J. Giovinazzo, P. Ascher, L. Audirac, Bertram Blank, C. Borcea, G. Canchel, C.E. Demonchy, C. Dossat, S. Grvy, S. Leblanc, et al. Two-proton radioactivity: 10 years of experimental progresses. In *Journal of Physics: Conference Series*, volume 436, page 012057. IOP Publishing, 2013.

[229] Philip J Woods. Proton radioactivity. In *AIP Conference Proceedings*, volume 481, pages 207–215. American Institute of Physics, 1999.

[230] S. Hofmann, G. Munzenberg, F.P. Hesseberger, and H.J. Schott. Detector system for investigation of proton radioactivity and new elements at ship. *Nuclear Instruments and Methods in Physics Research*, 223(2-3):312–318, 1984.

[231] K. Auranen, D. Seweryniak, M. Albers, A.D. Ayangeakaa, S. Bottoni, M.P. Carpenter, C.J.

Chiara, P. Copp, H.M. David, D.T. Doherty, et al. Proton decay of 108i and its significance for the termination of the astrophysical rp-process. *Physics Letters B*, 792:187–192, 2019.

[232] J. Dobaczewski and W. Nazarewicz. Limits of proton stability near sn 100. *Physical Review C*, 51(3):R1070, 1995.

[233] E. Olsen, M. Pfutzner, N. Birge, M. Brown, W. Nazarewicz, and A. Perhac. Erratum: landscape of two-proton radioactivity [phys. rev. lett. 110, 222501 (2013)]. *Physical Review Letters*, 111(13):139903, 2013.

[234] M Pfutzner, M Karny, LV Grigorenko, and K Riisager. Radioactive decays at limits of nuclear stability. *Reviews of modern physics*, 84(2):567, 2012.

[235] Swati Modi, M. Patial, Paramasivan Arumugam, E. Maglione, and L.S. Ferreira. Triaxiality in the proton emitter i 109. *Physical Review C*, 95(5):054323, 2017.

[236] Indira Mehrotra and Shweta Prakash. Proton radioactivity with analytically solvable potential. *Pramana*, 70(1):101–111, 2008.

[237] Enrico Maglione et al. Theoretical description of proton radioactivity. *Progress of Theoretical Physics Supplement*, 154:154–160, 2004.

[238] N. Teruya, S.B. Duarte, and M.M.N. Rodrigues. Nonlocality effect in the tunneling of one-proton radioactivity. *Physical Review C*, 93(2):024606, 2016.

[239] O.A.P. Tavares and E.L. Medeiros. Proton radioactivity: the case for 53mco proton-emitter isomer. *The European Physical Journal A*, 45(1):57–60, 2010.

[240] Claude Detraz and David J Vieira. Exotic light nuclei. *Annual Review of Nuclear and Particle Science*, 39(1):407–465, 1989.

[241] Joachim Janecke. The emission of protons from light neutron-deficient nuclei. *Nuclear Physics*, 61(2):326–341, 1965.

[242] N. Poenaru, Dorin, W. Greiner, and R Gherghescu. New island of cluster emitters. *Physical Review C*, 47(5):2030, 1993.

[243] Hongfei Zhang, Junqing Li, Wei Zuo, Zhongyu Ma, Baoqiu Chen, and Soojae Im. Properties of the superheavy element 287 115 and its α-decay time. *Physical Review C*, 71(5):054312, 2005.

[244] G.A. Lalazissis and S. Raman. Proton drip-line nuclei in relativistic mean-field theory. *Physical Review C*, 58(3):1467, 1998.

[245] N. Sowmya and H.C. Manjunatha. Proc. dae symp. nucl. *Phys.*, 63:200–201, 2018.

[246] P.J. Sellin, P.J. Woods, T. Davinson, N.J. Davis, K. Livingston, R.D. Page, A.C. Shotter, S. Hofmann, and A.N. James. Proton spectroscopy beyond the drip line near a= 150. *Physical Review C*, 47(5):1933, 1993.

[247] P.J. Page, R.D.and Woods, R.A. Cunningham, T. Davinson, N.J. Davis, A.N. James, K. Livingston, P.J. Sellin, and A.C. Shotter. Decays of odd-odd n-z= 2 nuclei above sn 100: The observation of proton radioactivity from cs 112. *Physical review letters*, 72(12):1798, 1994.

[248] K. Livingston, P.J. Woods, T. Davinson, N.J. Davis, S. Hofmann, A.N. James, R.D. Page, P.J. Sellin, and A.C. Shotter. Proton radioactivity from 146tm. the completion of a sequence of four odd-odd proton emitters. *Physics Letters B*, 312(1-2):46–48, 1993.

[249] Joachim Gorres, Michael Wiescher, and Friedrich-Karl Thielemann. Bridging the waiting points: The role of two-proton capture reactions in the rp process. *Physical Review C*, 51(1):392, 1995.

[250] L.V. Grigorenko and Mikhail V. Zhukov. Three-body resonant radiative capture reactions in astrophysics. *Physical Review C*, 72(1):015803, 2005.

[251] L.V. Grigorenko, K. Langanke, N.B. Shul'Gina, and Mikhail V. Zhukov. Soft dipole mode in 17ne and the astrophysical 2p capture on 15o. *Physics Letters B*, 641(3-4):254–259, 2006.

[252] D.S. Delion, R.J. Liotta, and R. Wyss. Theories of proton emission. *Physics Reports*, 424(3), 2006.

[253] E. Maglione, L. S. Ferreira, and R. J. Liotta. Proton emission from deformed nuclei. *Phys. Rev. C*, 59, Feb 1999.

[254] M. Del Santo, Z. Meisel, D. Bazin, A. Becerril, B.A. Brown, H. Crawford, R. Cyburt, S. George, G.F. Grinyer, G. Lorusso, P.F. Mantica, F. Montes, J. Pereira, H. Schatz, K. Smith, and M. Wiescher. β-delayed proton emission of 69kr and the 68se rp-process waiting point. *Physics Letters B*, 738, 2014.

[255] S.A. Alavi, V. Dehghani, and M. Sayahi. Calculation of proton radioactivity half-lives. *Nuclear Physics A*, 977, 2018.

[256] D. Baye and E.M. Tursunov. β delayed emission of a proton by a one-neutron halo nucleus. *Physics Letters B*, 696(5), 2011.

[257] W.F. Feix and E.R. Hilf. Nuclear proton emission predictions. *Physics Letters B*, 120(1), 1983.

[258] R. Coniglione, P. Sapienza, E. Migneco, C. Agodi, R. Alba, G. Bellia, A. Del Zoppo, P. Finocchiaro, K. Loukachine, C. Maiolino, P. Piattelli, and D. Santonocito. High energy

proton emission in heavy ion reactions close to the fermi energy1experiment performed at ganil, caen, france.1. *Physics Letters B*, 471(4), 2000.

[259] B. Ludewigt, R. Glasow, H. Löhner, and R. Santo. Proton emission in α-induced reactions at 43 mevnucleon. *Nuclear Physics A*, 408(2), 1983.

[260] F. Guzman, M. Goncalves, O. A. P. Tavares, S. B. Duarte, F. Garcia, and O. Rodriguez. Proton radioactivity from proton-rich nuclei. *Phys. Rev. C*, 59, May 1999.

[261] D. S. Delion, R. J. Liotta, and R. Wyss. Systematics of proton emission. *Phys. Rev. Lett.*, 96, Feb 2006.

[262] Enrico Maglione and S. Ferreira, Lidia. Proton emission from $^{125}\mathrm{Pm}$ could be observed. *Phys. Rev. C*, 94, Oct 2016.

[263] P. Arumugam, L.S. Ferreira, and E. Maglione. Proton emission, gamma deformation, and the spin of the isomeric state of 141ho. *Physics Letters B*, 680(5), 2009.

[264] S.B. DUARTE, O.A.P. TAVARES, F. GUZMÁN, A. DIMARCO, F. GARCÍA, O. RODRÍGUEZ, and M. GONÇALVES. Half-lives for proton emission, alpha decay, cluster radioactivity, and cold fission processes calculated in a unified theoretical framework. *Atomic Data and Nuclear Data Tables*, 80(2), 2002.

[265] L.S. Ferreira, E. Maglione, and P. Ring. Self-consistent description of proton radioactivity. *Physics Letters B*, 701(4), 2011.

[266] H. C. Manjunatha and K. N. Sridhar. Radioactive decay of rutherfordium. *Iranian Journal of Science and Technology, Transactions A: Science*, 44(4), 2020.

[267] H. C. Manjunatha, G. R. Sridhar, P. S. Gupta, K. N. Sridhar, M. G. Srinivas, and H. B.

Ramalingam. Decay modes of uranium in the range $203 < a < 299$. *Indian journal of Pure and Applied Physics*, 58, 2020.

[268] H. C. Manjunatha, G. R. Sridhar, P. S. Damodara Gupta, H. B. Ramalingam, and V. H. Doddamani. Pocket formula for alpha decay energies and half-lives of actinide nuclei. *Zeitschrift für Naturforschung A*, 75(6), 2020.

[269] G. R. Sridhara, H. C. Manjunatha, K. N. Sridhar, and H.B. Ramalingam. Systematic study of the alpha decay properties of actinides. *Pramana*, 93(5), 2019.

[270] H.C. Manjunatha and N. Sowmya. Pocket formula for mass excess of nuclei in the range 57¡ z¡ 103. *Modern Physics Letters A*, 34(15):1950112, 2019.

[271] Meng Wang, WJ Huang, G. Kondev, Filip, Georges Audi, and Sarah Naimi. The ame 2020 atomic mass evaluation (ii). tables, graphs and references. *Chinese Physics C*, 45(3):030003, 2021.

[272] M. Balasubramaniam and N. Arunachalam. Proton and α-radioactivity of spherical proton emitters. *Phys. Rev. C*, 71:014603, Jan 2005.

[273] K.P. Santhosh and Tinu Ann Jose. Cluster decay half-lives using modified generalized liquid drop model (mgldm) with different pre-formation factors. *Indian Journal of Physics*, 95(1):121–131, 2021.

[274] Dashty T. Akrawy, K. P. Santhosh, and H. Hassanabadi. α-decay half-lives of some superheavy nuclei within a modified generalized liquid drop model. *Phys. Rev. C*, 100:034608, Sep 2019.

[275] Hans Geiger and J. M. Nuttall. Lvii. the ranges of the α particles from various radioactive substances and a relation between range and period of transformation. *The London,*

Edinburgh, and Dublin Philosophical Magazine and Journal of Science, 22(130):613–621, 1911.

[276] M.G. Srinivas, H.C. Manjunatha, K.N. Sridhar, N. Sowmya, and Alfred Cecil Raj. Proton decay of actinide nuclei. *Nuclear Physics A*, 995:121689, 2020.

[277] V. Dehghani and S.A. Alavi. Empirical formulas for proton decay half-lives: Role of nuclear deformation and q-value. *Chinese Physics C*, 42(10):104101, 2018.

[278] J. Blocki, J. Randrup, W .J. Swiatecki, and C. F. Tsang. Proximity forces. *Annals of Physics*, 105(2):427–462, 1977.

[279] G.L. Zhang, Y.J. Yao, M.F. Guo, M. Pan, G.X. Zhang, and X.X. Liu. Comparative studies for different proximity potentials applied to large cluster radioactivity of nuclei. *Nuclear Physics A*, 951:86–96, 2016.

[280] Reference input parameter library (ripl-3). `https://www-nds.iaea.org/RIPL-3.html`.

[281] W. E. Ormand. Properties of proton drip-line nuclei at the sd-fp-shell interface. *Physical Review C*, 53(1):214, 1996.

[282] N.S. Rajeswari and M. Balasubramaniam. Exotic decay modes of odd-z (105–119) super-heavy nuclei. *The European Physical Journal A*, 50(6):1–8, 2014.

[283] N.S. Rajeswari, I. Sreeja, and M. Balasubramaniam. Two proton radioactivity in 45 fe and 48 ni. In *Proceedings of the DAE-BRNS Symp. on Nucl. Phys*, volume 61, page 422, 2016.

[284] M.M.N. Rodrigues, N. Teruya, and S. B. Duarte. Half-lives of proton emitters in the region of intermediate mass and heavy nuclei. In *AIP Conference Proceedings*, volume 1529, pages 174–177. American Institute of Physics, 2013.

[285] Jun-Gang Deng, Hong-Fei Zhang, G. Royer, et al. Improved empirical formula for α-decay half-lives. *Physical Review C*, 101(3):034307, 2020.

[286] HENG Zong-Qiang, Shu Liang-Ping, Meng Ying, Hu Ji-Gang, and Qian Jian-Fa. Competition between α-decay and β-decay for heavy andsuperheavy nuclei. *Chinese Physics C*, 38(12):124101–124101, 2014.

[287] Zhongzhou Ren and Chang Xu. Spontaneous fission half-lives of heavy nuclei in ground state and in isomeric state. *Nuclear Physics A*, 759(1-2):64–78, 2005.

[288] Meng Wang, WJ Huang, Filip G Kondev, Georges Audi, and Sarah Naimi. The ame 2020 atomic mass evaluation (ii). tables, graphs and references. *Chinese Physics C*, 45(3):030003, 2021.

[289] *https://www-nds.iaea.org/RIPL-3/masses.*

[290] P. Moller, Arnold John Sierk, Takatoshi Ichikawa, and Hiroyuki Sagawa. Nuclear ground-state masses and deformations: Frdm (2012). *Atomic Data and Nuclear Data Tables*, 109:1–204, 2016.

[291] G. Audi, M. Wang, A.H. Wapstra, F.G. Kondev, M. MacCormick, and X. Xu. The 2012 atomic mass evaluation and the mass tables. *Nuclear Data Sheets*, 120:1–5, 2014.

[292] Zhi-Hui Li and Jing-Yu Tang. A cw superconducting linac as the proton driver for a medium baseline neutrino beam in china. *Chinese Physics C*, 38(12):127001, 2014.

[293] Xiaoping Zhang, Zhongzhou Ren, Qijun Zhi, and Qiang Zheng. Systematics of β–decay half-lives of nuclei far from the β-stable line. *Journal of Physics G: Nuclear and Particle Physics*, 34(12):2611, 2007.

[294] Yuichi Hatsukawa, Hiromichi Nakahara, and Darleane C. Hoffman. Systematics of alpha decay half-lives. *Physical Review C*, 42(2):674, 1990.

[295] XJ Bao, SQ Guo, HF Zhang, YZ Xing, JM Dong, and JQ Li. Competition between α-decay and spontaneous fission for superheavy nuclei. *Journal of Physics G: Nuclear and Particle Physics*, 42(8):085101, 2015.

[296] R.J. Tighe, Dennis M. Moltz, J.C. Batchelder, T.J. Ognibene, M.W. Rowe, and Joseph Cerny. Evidence for the ground-state proton decay of sb 105. *Physical Review C*, 49(6):R2871, 1994.

[297] A. Gillitzer, T. Faestermann, K. Hartel, P. Kienle, and E. Nolte. Groundstate proton radioactivity of nuclei in the tin region. *Zeitschrift für Physik A Atomic Nuclei*, 326(1):107–119, 1987.

[298] K.S. Toth, D.C. Sousa, P.A. Wilmarth, J.M. Nitschke, and K.S. Vierinen. Electron capture and β+ decay of tm 147. *Physical Review C*, 47(4):1804, 1993.

[299] PJ Woods, T Davinson, NJ Davis, S Hofmann, AN James, and K Livingston. R. d. page, p.j. sellin, and a.c. shotter. *Nucl. Phys. A*, 553:485c, 1993.

[300] R.D. Page, P.J. Woods, R.A. Cunningham, T. Davinson, N.J. Davis, S. Hofmann, A.N. James, K. Livingston, P.J. Sellin, and A.C. Shotter. Discovery of new proton emitters re 160 and ta 156. *Physical review letters*, 68(9):1287, 1992.

[301] R.J. Irvine, C.N. Davids, P.J. Woods, D.J. Blumenthal, L.T. Brown, L.F. Conticchio, T. Davinson, D.J. Henderson, J.A. Mackenzie, H.T Penttila, et al. Proton emission from drip-line nuclei 157 ta and 161 re. *Physical Review C*, 55(4):R1621, 1997.

[302] C.N Davids, P.J. Woods, J.C. Batchelder, C.R. Bingham, D.J. Blumenthal, L.T. Brown, B.C. Busse, L.F. Conticchio, T. Davinson, S.J. Freeman, et al. New proton radioactivities 1 6 5, 1 6 6, 1 6 7 ir and 171 au. *Physical Review C*, 55(5):2255, 1997.

[303] C.N. Davids, P.J. Woods, H.T. Penttila, J.C. Batchelder, C.R. Bingham, D.J. Blumenthal, L.T. Brown, B.C. Busse, L..F Conticchio, T. Davinson, et al. Proton decay of an intruder state in b 185 i. *Physical review letters*, 76(4):592, 1996.

[304] Guy Royer. Alpha emission and spontaneous fission through quasi-molecular shapes. *Journal of Physics G: Nuclear and Particle Physics*, 26(8):1149, 2000.

[305] D.N. Poenaru, R.A. Gherghescu, and W. Greiner. Single universal curve for cluster radioactivities and α decay. *Physical Review C*, 83(1):014601, 2011.

[306] *RIPL-3: Reference Input Parameter Library*, https://www-nds.iaea.org/RIPL-3/, 2013.

[307] M. Kowal, P. Jachimowicz, and J. Skalski. Ground state and saddle point: masses and deformations for even-even superheavy nuclei with $98 < z < 126$ and $134 < n < 192$. *arXiv:1203.5013*, 2012.

[308] G Royer. Alpha emission and spontaneous fission through quasi-molecular shapes. *Journal of Physics G: Nuclear and Particle Physics*, 26(8), jun 2000.

[309] D. N. Poenaru, R. A. Gherghescu, and W. Greiner. Single universal curve for cluster radioactivities and α decay. *Phys. Rev. C*, 83, Jan 2011.

[310] Dongdong Ni, Zhongzhou Ren, Tiekuang Dong, and Chang Xu. Unified formula of half-lives for α decay and cluster radioactivity. *Phys. Rev. C*, 78, Oct 2008.

[311] V. Yu. Denisov and A. A. Khudenko. α-decay half-lives: Empirical relations. *Phys. Rev. C*, 79, May 2009.

[312] Chang Xu, Zhongzhou Ren, and Yanqing Guo. Competition between α decay and spontaneous fission for heavy and superheavy nuclei. *Phys. Rev. C*, 78, Oct 2008.

[313] Yibin Qian, Zhongzhou Ren, and Dongdong Ni. Attempt to probe nuclear charge radii by cluster and proton emissions. *Phys. Rev. C*, 87, May 2013.

[314] K. P. Santhosh and Indu Sukumaran. Description of proton radioactivity using the coulomb and proximity potential model for deformed nuclei. *Phys. Rev. C*, 96:034619, Sep 2017.

[315] K. Pomorski and J. Dudek. Nuclear liquid-drop model and surface-curvature effects. *Phys. Rev. C*, 67:044316, Apr 2003.

[316] P Moller et al. At. data nucl. tables 39 (1988) 225; p. moeller, jr nix, wd myers and wj swiatecki. *At. Data Nucl. Data Tables*, 59:185, 1995.

[317] W.D. Myers and W.J. Swiatecki. Nuclear properties according to the thomas-fermi model. *Nuclear Physics A*, 601(2):141–167, 1996.

[318] S. Goriely, N. Chamel, and J. M. Pearson. Further explorations of skyrme-hartree-fock-bogoliubov mass formulas. xii. stiffness and stability of neutron-star matter. *Phys. Rev. C*, 82:035804, Sep 2010.

[319] Stanislas Goriely, Stephane Hilaire, Michel Girod, and S. Peru. First gogny-hartree-fock-bogoliubov nuclear mass model. *Physical review letters*, 102(24):242501, 2009.

[320] J. Duflo and A.P. Zuker. Microscopic mass formulas. *Phys. Rev. C*, 52:R23–R27, Jul 1995.

[321] Hiroyuki Koura, Takahiro Tachibana, Masahiro Uno, and Masami Yamada. Nuclidic mass formula on a spherical basis with an improved even-odd term. *Progress of theoretical physics*, 113(2):305–325, 2005.

[322] R.C. Nayak and L. Satpathy At. Data and nucl. *Data Tables*, 98:616–719, 2012.

[323] Ning Wang and Min Liu. Nuclear mass predictions with a radial basis function approach. *Phys. Rev. C*, 84:051303, Nov 2011.

[324] A. Sobiczewski, Yu. A. Litvinov, and M. Palczewski. Detailed illustration of the accuracy of currently used nuclear-mass models. *Atomic Data and Nuclear Data Tables*, 119:1–32, 2018.

[325] Georges Audi, F.G. Kondev, Meng Wang, W.J. Huang, and S Naimi. The nubase2016 evaluation of nuclear properties. *Chin. Phys. C*, 41(3):030001, 2017.

[326] Z. Liu, P. J. Woods, K. Schmidt, H. Mahmud, P. S. L. Munro, A. Blazhev, J. Doring, H. Grawe, M. Hellstrom, R. Kirchner, Z. K. Li, C. Mazzocchi, I. Mukha, C. Plettner, E. Roeckl, and M. La Commara. Reinvestigation of direct proton decay of $^{105}\mathrm{Sb}$. *Phys. Rev. C*, 72:047301, Oct 2005.

[327] C. Mazzocchi, R. Grzywacz, S. N. Liddick, K. P. Rykaczewski, H. Schatz, J. C. Batchelder, C. R. Bingham, C. J. Gross, J. H. Hamilton, J. K. Hwang, S. Ilyushkin, A. Korgul, W. Królas, K. Li, R. D. Page, D. Simpson, and J. A. Winger. α decay of $^{109}\mathrm{I}$ and its implications for the proton decay of $^{105}\mathrm{Sb}$ and the astrophysical rapid proton-capture process. *Phys. Rev. Lett.*, 98:212501, May 2007.

[328] *https:// www-nds.iaea.org/ relnsd/ vcharthtml/ VChartHTML.html*.

[329] JP Cui, YH Gao, YZ Wang, JZ Gu, et al. Two-proton radioactivity within a generalized liquid drop model. *Physical Review C*, 101(1):014301, 2020.

[330] Mohsen Mashayekhi, Ali Asghar Mowlavi, and Sayyed Bijan Jia. Simulation of positron

emitters for monitoring of dose distribution in proton therapy. *Reports of Practical Oncology and Radiotherapy*, 22(1):52–57, 2017.

[331] Alexandru Dasu, Anna M Flejmer, Anneli Edvardsson, and Petra Witt Nystrom. Normal tissue sparing potential of scanned proton beams with and without respiratory gating for the treatment of internal mammary nodes in breast cancer radiotherapy. *Physica Medica*, 52:81–85, 2018.

[332] Kavita K. Mishra and Inder K. Daftari. Proton therapy for the management of uveal melanoma and other ocular tumors. *Chin Clin Oncol*, 5(4):50, 2016.

[333] Keith J. Stelzer. Acute and long-term complications of therapeutic radiation for skull base tumors. *Neurosurgery Clinics*, 11(4):597–604, 2000.

[334] Jack Phan, Terence T. Sio, Theresa P. Nguyen, Vinita Takiar, G. Brandon Gunn, Adam S. Garden, David I. Rosenthal, Clifton D. Fuller, William H. Morrison, Beth Beadle, et al. Reirradiation of head and neck cancers with proton therapy: outcomes and analyses. *International Journal of Radiation Oncology* Biology* Physics*, 96(1):30–41, 2016.

[335] Shinji Sugahara, Yoshiko Oshiro, Hidetsugu Nakayama, Kuniaki Fukuda, Masashi Mizumoto, Masato Abei, Junichi Shoda, Yasushi Matsuzaki, Eriko Thono, Mari Tokita, et al. Proton beam therapy for large hepatocellular carcinoma. *International Journal of Radiation Oncology* Biology* Physics*, 76(2):460–466, 2010.

[336] Julie Constanzo, Marie Vanstalle, Christian Finck, David Brasse, and Marc Rousseau. Dosimetry and characterization of a 25-mev proton beam line for preclinical radiobiology research. *Medical physics*, 46(5):2356–2362, 2019.

[337] Frank Rosch. Radiolanthanides in endoradiotherapy: an overview. *Radiochimica Acta*, 95(6):303–311, 2007.

LIST OF PUBLICATIONS

Journal publications

[1] M.G.Srinivas, H.C.Manjunatha, K.N.Sridhar, N.Sowmya and Alfred Cecilraj. Proton decay of actinide nuclei. ***Nuclear physics A*** 995(2020)121689. ISSN : 0375-9474.

[2] M.G.Srinivas, H.C.Manjunatha, N.Sowmya, Damodara Gupta and Alfred Cecil Raj. Systematics of proton decay of actinides. ***Indian Journal of Pure and Applied Physics*** Vol.58, April 2020,pp.255-262. ISSN : 0975-1041.

[3] H.C.Manjunatha, M.G.Srinivas, N.Sowmya, Damodara Gupta and Alfred Cecil Raj. Proton radioactivity of heavy nuclei of atomic number range $72 < Z < 88$. ***Physics of Particles and Nuclei Letters***, 2020,vol 17,No,7,pp.909-915 ISSN : 1547-4771.

[4] M.G.Srinivas, H.C. Manjunatha , Y.S.Vidya , P.S.Damodara Gupta , and Alfred Cecil Raj. Exploring new proton emitting isotopes of Lanthanides. ***Indian Journal of Physics*** (2022)pp1-10 ISSN: 0973-1458.

[5] M.G.Srinivas, N.Sowmya, H.C. Manjunatha , N.Manjunatha , S.Alfred Cecil Ra. Proton Radioactivity of Tantalum. ***Journal of Advanced Scientific Research***, icitnas;2021:250-254 ISSN 0976-9595.

[6] M.G. Srinivas, N. Sowmya, H.C. Manjunatha, P.S. Damodara Gupta and R. Munirathnam and N.Manjunatha Proton Radioactivity of Dysprosium, DOI-10.1142 / S0218301322500434.

Int. mod. phys. E 2022.

[7] M.G.Srinivas, H.C.Manjunatha, K.N.Sridhar, and Alfred Cecil Raj. A Systematic study of proton decay in super heavy elements. (accepted in Ukranian Journal of Physics)

[8] M.G.Srinivas, H.C. Manjunatha, N.Sowmya, N.Manjunatha, and S.Alfred Cecil Raj. Semi-empirical formulae for one and two proton radioactivity. (Communicated to Indian Journal of Physics.)

[9] M.G. Srinivas , R. Munirathnam, N. Sowmya, H.C. Manjunatha, and S.Alfred Cecil Raj. Predictive power of macroscopic and microscopic models for proton decay. (Communicated to European Physical Journal plus).

Full papers in conference proceedings

1. M.G.Srinivas, H.C.Manjunatha, K.N.Sridhar, N.Sowmya, Alfred Cecilraj. Proton radioactivity of $^{241-251}$Db. ***Proceedings of the DAE Symposium on Nuclear Physics***. 64(2019). ISBN : 818372083-8.

2. H.C.Manjunatha, M.G.Srinivas, N.Sowmya, P.S.Damodara Gupta and S.Alfred Cecil Raj. Competition between different decay modes in Bismuth. Proceedings of the ***Proceedings of the DAE Symposium on Nuclear Physics***. 65(2021) ISBN : 818372084-6.

3. M.G.Srinivas, H.C.Manjunatha, K.N.Sridhar and Alfred Cecilraj. Proton emission from superheavy element Z=121, ***Proceedings of NCEMIAM–2019***. ISBN- 978-93-88680-09-7.

Available online at www.sciencedirect.com

ScienceDirect

Nuclear Physics A 995 (2020) 121689

NUCLEAR PHYSICS A

www.elsevier.com/locate/nuclphysa

Proton decay of actinide nuclei

M.G. Srinivas [a], H.C. Manjunatha [b,*], K.N. Sridhar [c], N. Sowmya [b], Alfred Cecil Raj [d]

[a] *Department of Physics, Government First Grade College, Mulbagal-563131 Karnataka, India*
[b] *Department of Physics, Government College for Women, Kolar-563101 Karnataka, India*
[c] *Department of Physics, Government First Grade College, Kolar-563101 Karnataka, India*
[d] *Department of Physics, St. Joseph's college (autonomous), Thiruchirapalli, Tamilnadu, India*

Received 16 September 2019; accepted 17 December 2019
Available online 27 December 2019

Abstract

The half-lives of one-proton emitters in the actinide region are presented using the coulomb and proximity potential method. The studied proton decay half-lives are compared with that of other decay modes such as alpha decay, spontaneous fission and beta decay. We have identified proton emitters in the actinide region and also it is the competing decay mode for all the observed proton emitters. We have included the effects of deformations in the present study. One-proton decay half-lives of present study have shown good agreement with the available experimental values.

Keywords: Actinides; Half-lives; Branching ratio

1. Introduction

The phenomenon of proton emission from nuclear ground states limits the possibilities of creation of more exotic proton rich nuclei which are generally produced by fusion-evaporation nuclear reactions. In the energy domain of radioactivity, proton can be considered as a point charge having highest probability of being present in the parent nucleus. In the early 60s, Goldanskii [1] experimentally proposed one and two proton radioactivity for both odd and even atomic

* Corresponding author.
E-mail address: manjunathhc@rediffmail.com (H.C. Manjunatha).

https://doi.org/10.1016/j.nuclphysa.2019.121689

number. Mukha et al. [2,3] observed one and two-proton radioactivity of more than 21 high-spin isomers in ^{94}Ag. Routray et al. [4] estimated the half-lives of proton radioactivity with Yukawa effective interaction. Deng et al. [5] used different proximity potentials to study the proton activity, α decay and heavy particle radioactivity. In 2015 previous researchers [6] measured the proton activity in ^{67}Kr at the RIKEN Nishina Center. Using silicon detectors Giovinazzo et al. [7] experimentally studied two-proton activity in ^{45}Fe. Previous workers [8,9] experimentally studied one and two proton radioactivity of ^{45}Fe and ^{54}Zn. Theoretical models of proton radioactivity from spherical nuclei can predict the systematics of proton decay and spectroscopic factors [10]. Santhosh et al. [11] described proton activity of nuclei with $Z > 50$ using CPPMDN model. The researchers identified proton active nucleus beyond proton drip line using the new detector system designed at SHIP [12]. Auranen et al. [13] experimentally observed the proton decay of ^{108}I. Alavi et al. [14] evaluated the proton decay half-lives using WKB method. Earlier workers [15–17] theoretically studied proton decay emission in alkaline metals and actinides. Pfutzner et al. [18] studied the proton emission phenomenon of odd Z nuclei yielding detailed structural information. The experiments are intended at finding exotic decay, are normally based on establishment of the radioactive atoms and subsequent decay of the radioactive atoms. The two-proton radioactivity was experimentally observed in ^{45}Fe [19,20], and later in ^{19}Mg [21,22], ^{48}Ni [23], and ^{54}Zn [24]. In the year 1970, the proton radioactivity was experimentally confirmed by Jackson [25] by detecting emission of proton from the ^{53}Co to the ground state of ^{52}Fe.

Subsequently many theoretical models were put forward to study half-lives of spherical and deformed nuclei [26–33]. Earlier workers [34–38] also attended to study half-lives of superheavy nuclei using different proximity potentials. Examination for proton emitting nuclei

will results in determining nuclear stability in proton rich nuclei. Although the proton emission is difficult process, the simplified method of the one-proton penetrating the coulomb barrier will explain the process with great extent. Compared to all other decay modes, proton emissions are categorised with lowest coulomb potential and less reduced mass. From the literature, it is clearly observed that a systematic study of one-proton decay half-lives are required in the actinide region. The main objective of our work is to study proton decay half-lives in the actinide region. The coulomb and proximity potential model, which have been applied for alpha and cluster decay over many years were used to study proton radioactivity. It is predicted from the study that the proton unstable nuclei near or outside the proton drip line will be discovered in the future experiments. We have predicted the half-lives of proton emitters in the actinide region, which have not been detected experimentally. The present work is organised in the following order. Section 2 explains the theoretical framework, detailed results and discussion in section 3 and conclusion in section 4.

2. Theoretical framework

2.1. Proton decay

The proton emission half-life in the actinide region is given by

$$T_{1/2} = \frac{\ln(2)}{\nu P} \tag{1}$$

where ν is the assault frequency of proton against the potential energy barrier and P is penetration probability. The assault frequency approximation is given by the harmonic oscillator frequency using Nilson's potential and it is given by [39],

$$\nu = \frac{41}{hA^{1/3}}\text{MeV} \tag{2}$$

where h is the planks constant and A is Proton mass number. Similar to spontaneous fission, ternary fission, alpha and cluster decay, and proton emission can be expressed in terms of quantum tunnelling through one dimensional barrier. Penetration probability P is calculated using WKB approximation [40].

$$P = \exp\left[-\frac{2}{\hbar}\int_{Rin}^{Rout}\sqrt{2\mu(V-Q)}dr\right] \tag{3}$$

Where μ is reduced mass of emitted proton, $\mu = (m_P m_{A-1}/m_P + m_{A-1}) = 938.3(A-1)/A$ MeV/C^2 and Q is the energy released. R_{in} and R_{out} are the classical inner and outer turning points. The inner turning point is equal to the radius of the spherical square well in which the proton is trapped before emission and it is given by

$$R_{in} = r_0\left(A_1^{1/3} + A_2^{1/3}\right) \tag{4}$$

Where $A_1 = 1$ and $A_2 = A-1$ for proton emission. R_{out} is determined by the condition $V = Q$. The proton–nucleus potential should consist of a Coulomb potential V_C and Proximity potential V_P.

$$V = V_C + V_P. \tag{5}$$

Where V_c Coulomb interaction potential, V_p is the proximity potential. The coulomb interaction potential is given by,

$$V_c = \frac{Z_1 Z_2 e^2}{r}\left[1 + \frac{3R^2}{5r^2}\beta_2 Y_{20}(\theta) + \frac{3R^4}{9r^4}\beta_4 Y_{40}\right] \tag{6}$$

Where Z_1 and Z_2 are the atomic numbers of proton and daughter nuclei respectively, and 'r' is the distance between fragment centres. R, β, Y_{20} (θ) is the radius of the nuclei, quadrupole deformation parameter and spherical harmonic function respectively. Proximity potential consists of two parts, one depends on shape and geometry of the nuclei and the other is the universal function which depends on distance between two nuclei. Proximity potential given by [41,42],

$$V_P = 4\pi\gamma b\left[\frac{C_1 C_2}{C_1 + C_2}\right]\phi \tag{7}$$

where $b = 0.99$ fm is the width of the nuclear surface, ϕ is the universal function, C_1 and C_2 are the Susmann central radii and γ is the nuclear surface tension coefficient and it is given by

$$\gamma = \gamma_0\left[1 - K_S\left(\frac{N-Z}{A}\right)^2\right]\text{MeV/fm}^2 \tag{8}$$

N, A and Z are neutron, mass and proton number of the parent nuclei respectively. Where $\gamma_0 = 1.460734$ MeV/fm^2 and $K_s = 4.0$ [43]. Susmann central radii C_1 and C_2 are obtained by using equation,

$$C_i = R_i - \left(\frac{b^2}{R_i}\right) \quad \text{for } i = 1, 2 \tag{9}$$

Where sharp radii R_i can be obtained by

$$R_i = 1.28A_i^{1/3} - 0.76 + 0.8A_i^{-1/3} \quad \text{for } i = 1, 2 \tag{10}$$

ϕ represents the universal proximity potential given as [16]

$$\Phi(z) = \begin{cases} -4.41\exp(\frac{-z}{0.7176}) & \text{for } \varepsilon \geq 1.9475 \\ -1.7817 + 0.9270z + 0.0169z^2 - 0.05148z^3 & \text{for } 0 \leq \varepsilon \leq 1.9475 \end{cases} \tag{11}$$

2.2. Alpha decay

In the present work, we have evaluated alpha decay half-lives using the semi empirical models such as Royer formula [44], UNIV [45], NRDX [46] and Denisov Khudenko [47].

2.2.1. Royer formula (Royer)

Royer [44] proposed the semi-empirical formula for alpha decay half-lives using potential energy within a liquid drop model including proximity effects between the alpha particle and the daughter nucleus. The alpha decay half-lives depends on the decay energy, atomic number (Z_P), and mass number of parent nuclei (A_P) respectively.

$$\log T_{1/2}^R = aZQ^{-1/2} + bA^{1/6}Z^{1/2} + c \tag{12}$$

where a, b and c are adjustable parameters and are depend on parity of the parent nucleus combination (Z_p, N_p). The fitting parameters are $a_{e-e} = 1.5864$, $a_{e-o} = 1.5848$, $a_{o-e} = 1.592$, $a_{o-o} = 1.6971$, $b_{e-e} = -1.1629$, $b_{e-o} = -1.0859$, $b_{o-e} = -1.1423$, $b_{o-o} = -1.113$, $c_{e-e} = -25.31$, $c_{e-o} = -26.65$, $c_{o-o} = -29.48$, $c_{o-e} = -25.68$.

2.2.2. UNIV formula

Poenaru et al. [45] derived universal (UNIV) curve for α decay and cluster radio activities by plotting the sum of the decimal logarithm of the half-life and cluster preformation probability versus the decimal logarithm of the penetrability of external barrier. The alpha decay half-lives is given as,

$$\log T_{1/2}^{UNIV} = -\log P_S - 22.169 + 0.598(A_e - 1) \tag{13}$$

A_e is the mass number of emitted particle and

$$\text{where } -\log P_S = c_{AZ}\left(\arccos\sqrt{r} - \sqrt{r(1-r)}\right) \tag{14}$$

$$\text{with } c_{AZ} = 0.22873(\mu_A Z_d Z_e R_b)^{1/2} \tag{15}$$

where Z_d, $Z_e R_b$ are the atomic number of daughter, emitted cluster and classical turning point respectively and $r = R_t/R_b$, $R_t = 1.2249(A_d^{1/3} + A_e^{1/3})$, $R_b = 1.43998Z_dZ_e/Q$ and $\mu_A = A_dA_e/A$ A_d, A_e are the mass number of daughter and emitted particle respectively, $R_t = R_a$ is the first turning point and Q is the amount of energy released during the decay process.

2.2.3. NRDX formula

Ni et al. [46] proposed semi-empirical formula for alpha decay and cluster decay half-lives derived from the WKB barrier penetration probability and it is given by

$$\log T_{1/2}^{NRDX} = a\sqrt{\mu}Z_\alpha Z_d Q^{-1/2} + b\sqrt{\mu}(Z_\alpha Z_d)^{1/2} + c \tag{16}$$

where a, b, and c are fitting coefficients and the corresponding values are 6.8, 6.9 and -22.4 respectively.

2.2.4. Denisov Khudenko formula

Denisov and Khudenko [47] constructed the empirical formula for alpha decay half-lives by including terms related to the orbital moment, parity of alpha transition and electron screening effect. The semi empirical formula for the evaluation of alpha decay in even–even, even–odd, odd–even and odd–odd are as follows;

$$\log T_{1/2}^{e-e} = -26.1779 - 1.1521\frac{A^{1/6}Z^{1/2}}{\mu} + \frac{1.6068Z}{\sqrt{Q}} \tag{17}$$

$$\log T_{1/2}^{e-o} = -30.3391 - 1.0785\frac{A^{1/6}Z^{1/2}}{\mu} + \frac{1.6068Z}{\sqrt{Q}} + \frac{0.2688\sqrt{\ell(\ell+1)}}{QA^{-1/6}} - 0.6784\big((-1)^{\ell}-1\big) \tag{18}$$

$$\log T_{1/2}^{o-e} = -30.2138 - 1.0841\frac{A^{1/6}Z^{1/2}}{\mu} + \frac{1.6949Z}{\sqrt{Q}} + \frac{0.1302\sqrt{\ell(\ell+1)}}{QA^{-1/6}} - 0.5972\big((-1)^{\ell}-1\big) \tag{19}$$

$$\log T_{1/2}^{o-o} = -30.3526 - 1.0149\frac{A^{1/6}Z^{1/2}}{\mu} + \frac{1.6609Z}{\sqrt{Q}} + \frac{0.2762\sqrt{\ell(\ell+1)}}{QA^{-1/6}} - 0.2209\big((-1)^{\ell}-1\big) \tag{20}$$

where A and Z are the mass number and atomic number of parent nuclei. Q and ℓ are the amount of energy released during the reaction and orbital angular momentum of the emitted alpha particle respectively. The reduced mass is given by $\mu = (A/A-4)^{1/6}$.

2.3. Spontaneous fission

In the present work, we have evaluated spontaneous fission half-lives using the semi empirical models such as Bao et al. [49] and Ren et al. [51].

2.3.1. Bao et al. [49] formula

In the year 1955 Swiatecki [48] proposed the significance of shell structure in the spontaneous fission process. He explained the irregularities observed if the fission half-lives with respect to Z^2/A. Bao et al. [49] used the modified Swiatecki's formula by considering the shell effects and observed systematic variation for spontaneous fission half-lives. The modified formula for spontaneous fission half-lives by considering shell correction and isospin effect is as follows,

$$\log_{10}\big[T_{1/2}(yr)\big] = c_1 + c_2\left(\frac{Z^2}{(1-kI^2)A}\right) + c_3\left(\frac{Z^2}{(1-kI^2)A}\right)^2 + c_4E_{sh} + h_i. \tag{21}$$

Where $Z^2/(1-kI^2)A$ is the fissionability parameter which includes isospin effect and the constants are $c_1 = 1174.353441$, $c_2 = -47.666855$, $c_3 = 0.471307$, $c_4 = 3.378848$. The constant $k = 2.6$ [50]. The "h_i" is the blocking factor of unpaired nucleon. The values of $h_{e-o} = 2.609374$ for the odd-N nuclei and $h_{o-e} = 2.619768$ for the odd-Z nuclei.

2.3.2. Ren et al. [51] formula

The generalised spontaneous fission including pairing, shell model calculations and valence nucleons, Ren et al. [51] constructed a semi-empirical formula for spontaneous fission half-lives is as follows;

$$\log_{10}\left[T_{1/2}(yr)\right] = 21.08 + c_1\frac{Z-90-\upsilon}{A} + c_2\frac{(Z-90-\upsilon)^2}{A} + c_3\frac{(Z-90-\upsilon)^3}{A} + c_4\frac{(Z-90-\upsilon)}{A}(N-Z-52)^2 \quad (22)$$

where $c_1 = -548.825021$, $c_2 = -5.359139$, $c_3 = 0.767379$, $c_4 = -4,28222$ and $\upsilon = 0$ for even–even nuclei and $\upsilon = 2$ for odd-A nuclei.

2.4. β^- decay formula

β^- decay process occurs in proton rich nuclei. Zhang et al. [52] constructed a semi-empirical formula for β^- decay half-lives and it is expressed as,

$$\log_{10} T_{1/2} = (c_1 Z + c_2)N + c_3 Z + c_4 + shell(Z,N) \quad (23)$$

where shell correction term is expressed as;

$$shell(Z,N) = c_5\left(e^{-(N-29)^2/15} + e^{-(N-50)^2/37} + e^{-(N-85)^2/9} + e^{-(N-131)^2/3}\right) + c_6 e^{-[(Z-51.5)^2+(N-80.5)^2]/1.9} \quad (24)$$

Z and N are the proton and neutron number of the parent nuclei respectively. $T_{1/2}$ is the half-life of β^- decay. The parameters are $c_1 = 3.37 \times 10^{-4}$, $c_2 = -0.2558$, $c_3 = 0.4028$, $c_4 = -1.01$, $c_5 = 0.9039$, and $c_6 = 7.7139$.

2.5. β^+ decay formula

Zhang et al. [53] proposed semi empirical formula for β^+ decay and it is expressed as;

$$\log_{10} T_{1/2} = (c_1 Z + c_2)N + c_3 Z + c_4 \quad (25)$$

Z and N are the proton and neutron number respectively. The parameters c_1, c_2, c_3 and c_4 are different for different order. The first and second forbidden transition for β^+ decay and the different parameters are in detail explained in [53]. The effect of even–odd effects are also considered in the above equation.

3. Results and discussions

Using coulomb and proximity potential model, we have studied proton decay from the proton rich emitters in the actinide region. The proton emission is energetically possible only when the amount energy released is positive and it is given by;

$$Q = \delta M_p - (\delta M_d + \delta M_z) + k\left(Z_P^{\varepsilon} - Z_d^{\varepsilon}\right) \quad (26)$$

where δM_P, δM_d, and δM_z are the mass excess values of parent, daughter and emitted proton respectively. The term $kZ_{p(d)}^{\varepsilon}$ is the total binding energy of electrons in the parent or daughter nuclei, where $k = 8.7$ eV and $\varepsilon = 2.517$ for the nuclei $Z > 60$. The value of $k = 13.6$ eV and $\varepsilon = 2.408$ for the nuclei $Z \leq 60$ [54]. The experimental mass excess values are extracted from [55]. Wherever experimental mass excess values are not available, we have used the theoretical mass excess values available in the literature [56–59]. We have calculated penetration probability and proton decay half-lives in the actinide region. We have also studied logarithmic half-lives of

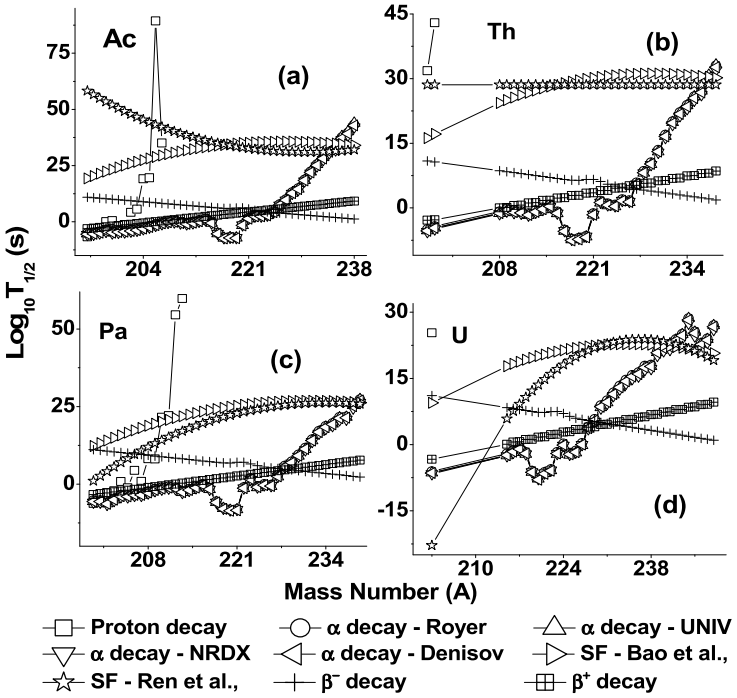

Fig. 1. Variation of $\log(T_{1/2})$ of proton activity, alpha decay, spontaneous fission and beta decay as a function of mass number of the parent nuclei (A).

alpha decay, spontaneous fission half-lives, β^- decay and β^+ decay half-lives as explained in section 2.

The comparison of $log(T_{1/2})$ of proton emission with that of alpha decay, spontaneous fission and beta decay as a function of mass number of parent nuclei is as presented in figures. From the Fig. 1(a) it is observed that proton decay for Actinium (Ac) is energetically possible for the mass number of $195 < A < 207$. The Fig. 1(a) gives the comparison of proton decay with that of alpha decay, spontaneous fission and beta decay. Similarly from the Fig. 1(b) for Th, proton decay is energetically possible in the mass number region $195 < A < 207$. From the Fig. 1(c) for Pa, it is observed that the proton decay is energetically possible in the mass number region $200 < A < 209$ and $212 < A < 213$. From the Fig. 1(d) for U, proton decay is energetically possible for ^{203}U. Similarly the Figure 2–4 gives the comparison of proton decay with that of alpha decay, spontaneous fission and beta decay in the actinide region $Z = 93 - 103$. The energetically favour proton emission is tabulated in Table 1.

For better understanding of predictable decay modes, a graph is plotted with the logarithmic half-lives of different decay modes such as proton decay, spontaneous fission, alpha decay and beta decay half-lives and it is presented in Fig. 5. From the Fig. 5(a) it is observed that the ^{194}Ac is a proton emitter, alpha decay mode is observed in the mass number of range $^{195–209}$Ac and $^{211–224}$Ac, β^+ decay and β^- decay is energetically possible in the nuclei ^{210}Ac and $^{225–239}$Ac respectively. Similarly the decay modes for actinide nuclei with $Z = 90 - 103$ (Th-Lr) are shown in the Fig. 5. We have predicted the energy released during proton decay, penetration probability and half-lives for $Z = 89 - 103$ and the results are tabulated in Table 2. In order to predict the

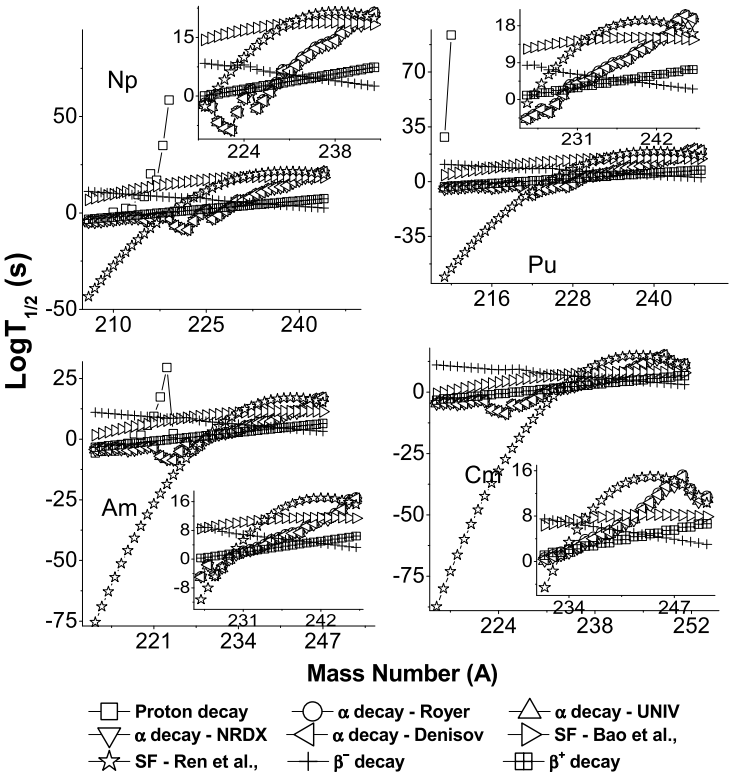

Fig. 2. Variation of $\log(T_{1/2})$ of proton activity, alpha decay, spontaneous fission and beta decay as a function of mass number of the parent nuclei (A).

dominant decay mode in the atomic number range $Z = 89 - 103$, we have calculated branching ratios. The branching ratio of proton decay to alpha decay is defined as,

$$BR = \frac{\lambda_P}{\lambda_{\alpha/SF/\beta^+/\beta^-}}. \tag{27}$$

Where λ_P is the decay constant corresponding to proton emission and $\lambda_{\alpha/SF/\beta^+/\beta^-}$ is the decay constant corresponds to alpha decay, spontaneous fission, β^+ decay and β^- decay respectively. The variation of branching ratios of proton decay with respect to the alpha decay, SF, β^- and β^+ decay as a function mass number of the nuclei is as shown in Fig. 6. From the Fig. 6(a) it observed that the branching ratio of $\lambda_P/\lambda_{\alpha/\beta^+}$ values are higher in the mass number range $^{194–197}$Ac and gradually decreases with increase in mass number above $^{197–207}$Ac. The branching ratio of $\lambda_P/\lambda_{SF/\beta^-}$ values are higher in the mass number range $^{194–203}$Ac and decreases with increase in mass number range $^{204–207}$Ac. Similarly from the Fig. 6(b) to 6(h) it is observed that the values of branching ratios gradually decreases with increase in mass number. The Fig. 7 denotes the variation of calculated logarithmic half-lives with the available experimental values [60–78]. The continuous line represents the calculated half-lives of proton emitters and dotted line represents the experimental logarithmic half-lives values. Table 3 also lists the experimental half-live values, proton energy released during the proton decay and calculated half-lives. From the Fig. 7 and Table 3 it is observed that our results are good agreement with the experimental

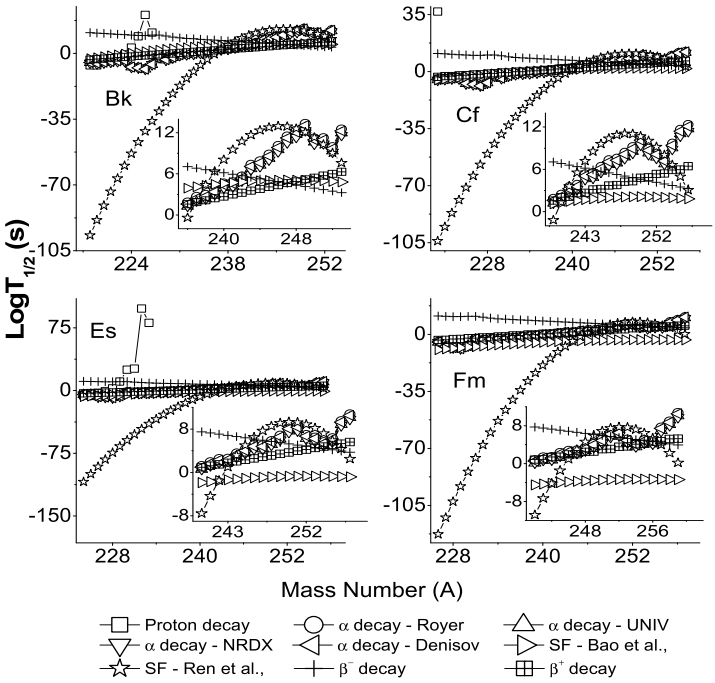

Fig. 3. Variation of $\log(T_{1/2})$ of proton activity, alpha decay, spontaneous fission and beta decay as a function of mass number of the parent nuclei (A).

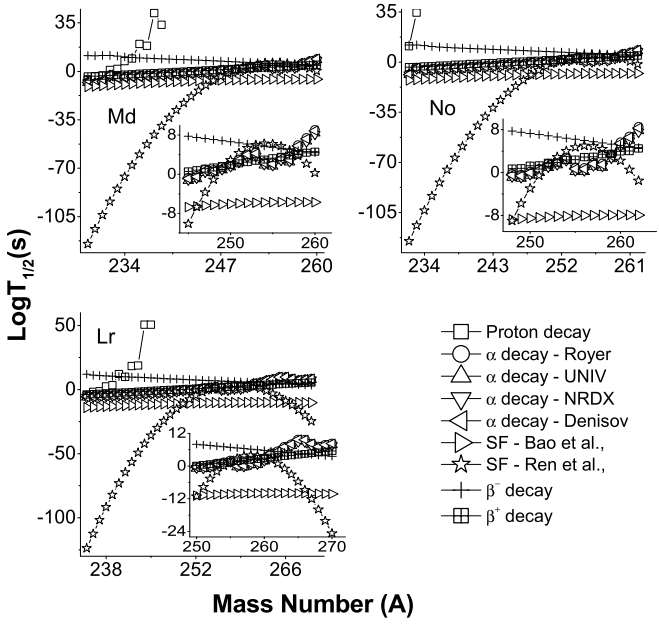

Fig. 4. Variation of $\log(T_{1/2})$ of proton activity, alpha decay, spontaneous fission and beta decay as a function of mass number of the parent nuclei (A).

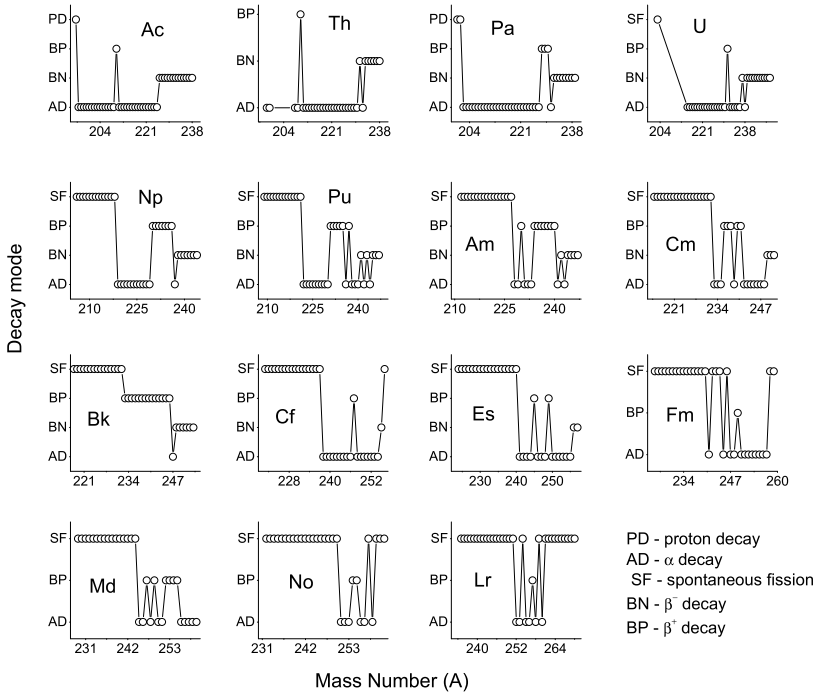

Fig. 5. Variation of decay modes such as proton activity, alpha decay, spontaneous fission, beta plus decay and beta minus decay as a function of mass number of the parent nuclei (A).

Table 1
List of studied actinide nuclei for proton decay.

Z	Mass number range studied	Mass number range where $Q + V_e$	Mass number range where $Q - V_e$
89	195–293	195–207	208–293
90	198–296	198–199	200–296
91	200–300	200–209, 212–213	210–211, 214–300
92	203–303	203	204–303
93	206–306	206–217	218–306
94	209–309	209	210–309
95	212–313	212–224	225–313
96	215–316	215	216–316
97	218–319	218–227	228–319
98	221–322	221	222–322
99	224–326	224–231	232–326
100	226–329	–	226–329
101	229–332	229–239	240–332
102	232–335	232–233	234–335
103	235–339	235–243	244–339

values [60–78]. We also studied standard deviation of calculated proton decay with the experimental values. The standard deviation of present work with the experimental is presented in

Table 2
Energy released, penetration factor and logarithmic half-lives for proton decay in actinide nuclei.

Nuclei	Q	P	T	Nuclei	Q	P	T
^{195}Ac	2.161	2.142×10^{-15}	1.892×10^{-7}	^{224}Am	1.181	2.105×10^{-26}	2.016×10^{4}
^{196}Ac	1.591	1.396×10^{-19}	2.907×10^{-3}	^{215}Cm	0.221	8.665×10^{-78}	4.832×10^{55}
^{197}Ac	1.591	1.391×10^{-19}	2.923×10^{-3}	^{218}Bk	2.241	1.015×10^{-16}	4.142×10^{-6}
^{198}Ac	1.321	1.775×10^{-22}	2.294	^{219}Bk	2.231	8.983×10^{-17}	4.690×10^{6}
^{199}Ac	1.331	2.277×10^{-22}	1.791	^{220}Bk	1.841	1.507×10^{19}	2.799×10^{-3}
^{200}Ac	1.441	4.324×10^{-21}	9.452×10^{-2}	^{221}Bk	1.871	2.730×10^{-19}	1.547×10^{-3}
^{201}Ac	1.371	6.726×10^{-22}	6.087×10^{-1}	^{222}Bk	1.611	1.288×10^{-21}	3.283×10^{-1}
^{202}Ac	0.971	6.033×10^{-28}	6.797×10^{5}	^{223}Bk	1.461	2.993×10^{-23}	1.416×10^{1}
^{203}Ac	1.018	4.688×10^{-27}	8.762×10^{4}	^{224}Bk	1.171	3.263×10^{-27}	1.300×105
^{204}Ac	0.595	1.424×10^{-38}	2.889×10^{16}	^{225}Bk	0.841	4.615×10^{-34}	9.210×10^{11}
^{205}Ac	0.707	1.575×10^{-34}	2.616×10^{12}	^{226}Bk	0.501	1.852×10^{-47}	2.298×10^{25}
^{206}Ac	0.383	5.019×10^{-51}	8.225×10^{28}	^{227}Bk	0.771	4.652×10^{-36}	9.165×10^{13}
^{207}Ac	0.277	4.149×10^{-62}	9.965×10^{39}	^{221}Cf	0.281	6.088×10^{-69}	6.941×10^{46}
^{198}Th	0.291	2.163×10^{-56}	1.883×10^{34}	^{224}Es	2.181	1.426×10^{-17}	2.976×10^{-5}
^{199}Th	0.201	1.218×10^{-76}	3.350×10^{54}	^{225}Es	2.181	1.419×10^{-17}	2.995×10^{-5}
^{200}Pa	2.111	3.807×10^{-16}	1.073×10^{-6}	^{226}Es	1.771	1.186×10^{-20}	3.589×10^{-2}
^{201}Pa	2.091	2.964×10^{-16}	1.381×10^{-6}	^{227}Es	1.541	6.434×10^{-23}	6.626
^{202}Pa	1.751	1.028×10^{-18}	3.988×10^{-4}	^{228}Es	1.251	1.236×10^{-26}	3.454×10^{4}
^{203}Pa	1.491	3.735×10^{-21}	1.099×10^{-1}	^{229}Es	0.821	2.005×10^{-35}	2.132×10^{13}
^{204}Pa	1.221	1.868×10^{-24}	2.202×10^{2}	^{230}Es	0.441	1.030×10^{-52}	4.157×10^{30}
^{205}Pa	1.391	2.895×10^{-22}	1.423	^{231}Es	0.421	2.493×10^{-54}	1.719×10^{32}
^{206}Pa	0.981	1.738×10^{-28}	2.375×10^{6}	^{229}Md	2.251	1.482×10^{-17}	2.883×10^{-5}
^{207}Pa	1.221	1.842×10^{-24}	2.244×10^{2}	^{230}Md	1.921	6.453×10^{-20}	6.636×10^{-3}
^{208}Pa	0.801	1.222×10^{-32}	3.388×10^{10}	^{231}Md	1.871	2.514×10^{-20}	1.705×10^{-2}
^{209}Pa	0.801	1.215×10^{-32}	3.412×10^{10}	^{232}Md	1.441	1.172×10^{-24}	3.662×10^{2}
^{212}Pa	0.42	3.479×10^{-49}	1.197×10^{27}	^{233}Md	1.381	1.935×10^{-25}	2.222×10^{3}
^{213}Pa	0.283	4.874×10^{-14}	8.563×10^{-9}	^{234}Md	1.001	8.656×10^{-32}	4.975×10^{9}
^{203}U	0.381	3.469×10^{-53}	1.184×10^{31}	^{236}Md	0.911	7.300×10^{-34}	5.909×10^{11}
^{206}Np	1.911	5.525×10^{-18}	7.471×10^{-5}	^{237}Md	0.561	2.862×10^{-46}	1.509×10^{24}
^{207}Np	1.881	3.226×10^{-18}	1.281×10^{-4}	^{238}Md	0.591	9.869×10^{-45}	4.383×10^{22}
^{208}Np	1.751	3.040×10^{-19}	1.362×10^{-3}	^{239}Md	0.251	2.607×10^{-76}	1.661×10^{54}
^{209}Np	1.691	8.868×10^{-20}	4.677×10^{-3}	^{232}No	0.831	2.217×10^{-36}	1.936×10^{14}
^{210}Np	1.301	5.444×10^{-24}	7.631×10^{1}	^{233}No	0.331	6.422×10^{-65}	6.697×10^{42}
^{211}Np	1.561	5.185×10^{-21}	8.025×10^{-2}	^{235}Lr	2.161	1.317×10^{-18}	3.273×10^{-4}
^{212}Np	1.151	3.491×10^{-26}	1.193×10^{4}	^{236}Lr	1.781	1.250×10^{-21}	3.455×10^{-1}
^{213}Np	1.181	1.025×10^{-25}	4.072×10^{3}	^{237}Lr	1.731	4.252×10^{-22}	1.017
^{214}Np	0.771	2.498×10^{-34}	1.673×10^{12}	^{238}Lr	1.361	2.602×10^{-26}	1.66×10^{4}
^{215}Np	0.811	3.254×10^{-33}	1.286×10^{11}	^{239}Lr	1.281	1.766×10^{-27}	2.455×10^{5}
^{216}Np	0.471	4.977×10^{-47}	8.426×10^{24}	^{240}Lr	0.811	2.142×10^{-37}	2.027×10^{15}
^{217}Np	0.541	4.641×10^{-43}	9.050×10^{20}	^{241}Lr	0.901	6.580×10^{-35}	6.610×10^{12}
^{209}Pu	0.351	2.896×10^{-57}	1.432×10^{35}	^{242}Lr	0.611	8.460×10^{-45}	5.149×10^{22}
^{212}Am	2.051	1.838×10^{-17}	2.267×10^{-5}	^{243}Lr	0.601	2.884×10^{-45}	1.51235×10^{23}
^{213}Am	1.951	3.465×10^{-18}	1.204×10^{-4}	^{232}No	0.831	2.217×10^{-36}	1.936×10^{14}
^{214}Am	1.911	1.705×10^{-18}	2.451×10^{-4}	^{233}No	0.331	6.422×10^{-65}	6.697×10^{42}
^{215}Am	1.931	2.449×10^{-18}	1.709×10^{-4}	^{235}Lr	2.161	1.317×10^{-18}	3.273×10^{-4}
^{216}Am	1.601	3.564×10^{-21}	1.176×10^{-1}	^{236}Lr	1.781	1.250×10^{-21}	3.455×10^{-1}
^{217}Am	1.531	6.843×10^{-22}	6.138×10^{-1}	^{237}Lr	1.731	4.252×10^{-22}	1.017
^{218}Am	1.191	3.191×10^{-26}	1.318×10^{4}	^{238}Lr	1.361	2.602×10^{-26}	1.66×10^{4}

(*continued on next page*)

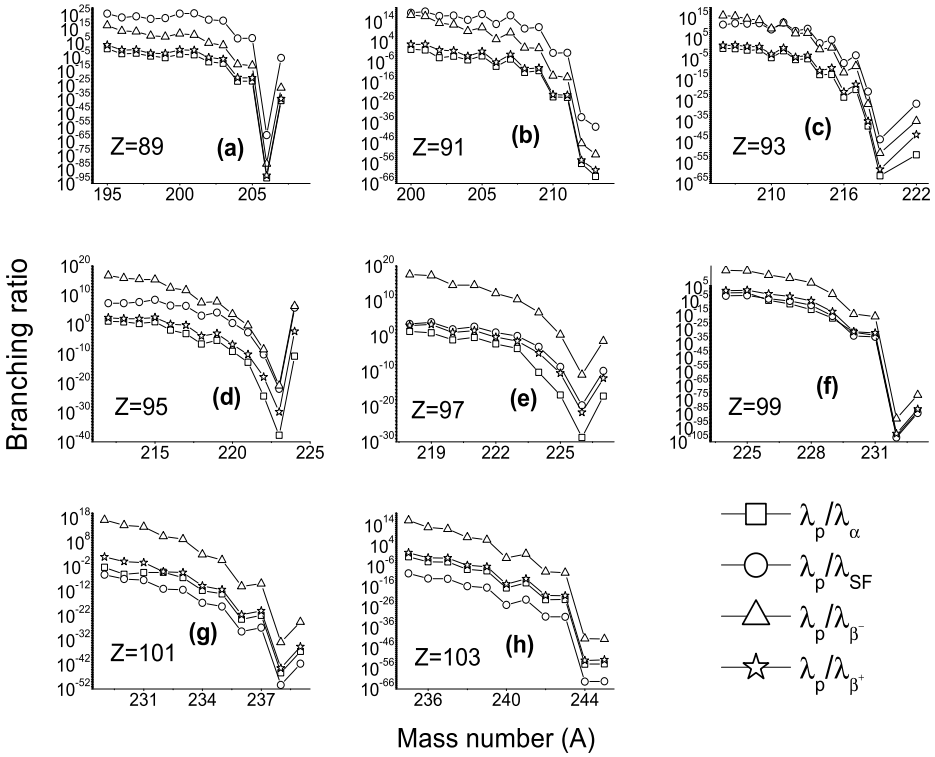

Fig. 6. A variation of branching ratios of proton decay to the alpha decay (NRDX), SF (Bao et al. [49]), beta (minus) decay and beta (plus) decay as a function mass number of the nuclei.

Table 2 (*continued*)

Nuclei	Q	P	T	Nuclei	Q	P	T
^{219}Am	1.231	1.290×10^{-25}	3.264×10^{3}	^{239}Lr	1.281	1.766×10^{-27}	2.455×10^{5}
^{220}Am	0.971	3.403×10^{-30}	1.240×10^{8}	^{240}Lr	0.811	2.142×10^{-37}	2.027×10^{15}
^{221}Am	0.801	2.486×10^{-34}	$1.700 \times 10^{+12}$	^{241}Lr	0.901	6.580×10^{-35}	6.610×10^{12}
^{222}Am	0.551	1.326×10^{-43}	3.189×10^{21}	^{242}Lr	0.611	8.460×10^{-45}	5.149×10^{22}
^{223}Am	0.341	5.349×10^{-59}	7.923×10^{36}	^{243}Lr	0.601	2.884×10^{-45}	1.51235×10^{23}

Fig. 8. The standard root mean square deviation of calculated logarithmic half-lives are calculated using following equation;

$$\sigma = \left\{ \sum_{i=1}^{n} \left[\log_{10}(T_{cal}/T_{\exp}) \right]^2 / (n-1) \right\}^{1/2}. \tag{28}$$

The overall standard deviation of proton decay half-lives in the odd–odd nuclei are observed to be 1.09065 and for odd–even were observed to be 0.879551 and are tabulated in Table 4. From the predictions of proton decay in the atomic nuclei range $Z = 51 - 83$, it is observed that our calculations are good agreement with the experimental values. Hence forth, we have predicted half-lives of proton decay in the actinide region.

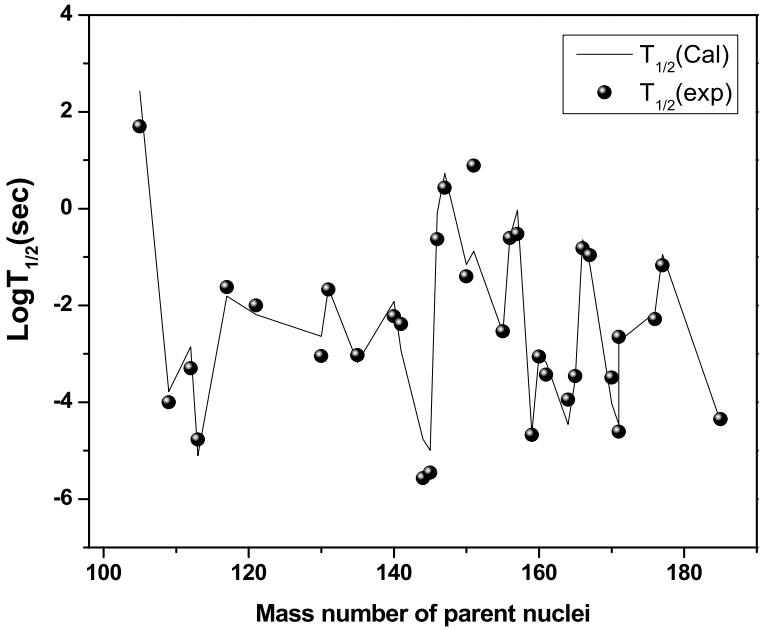

Fig. 7. The variation of calculated logarithmic half-lives of proton decay of different mass number of proton emitters with the available experimental values.

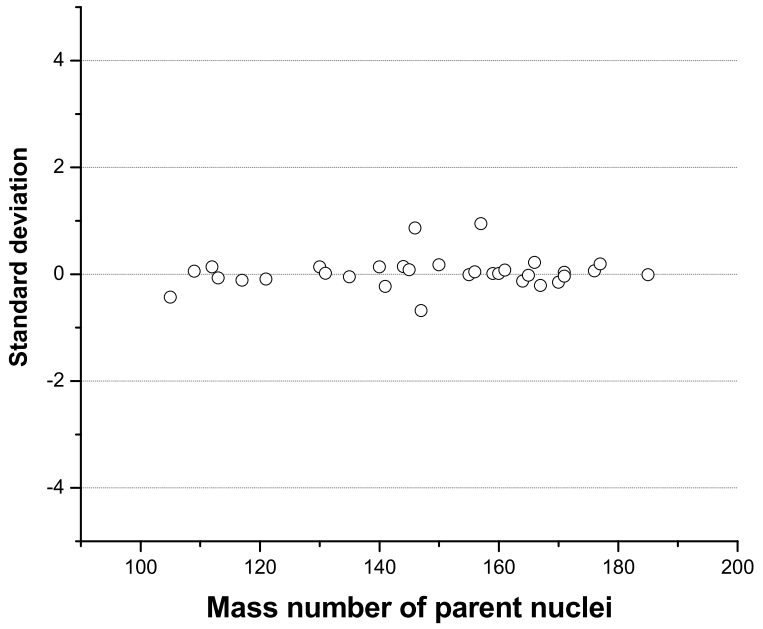

Fig. 8. A standard deviation of proton decay from the experimental values with that of mass number of parent nuclei.

Table 3
The comparison of calculated half-lives are compared with the experimental values [60,62,62–78].

Isotopes	Q_P	β_2	β_4	l	log T	log $T_{1/2}$ exp	Ref.
^{105}Sb	0.48	0.081	0.051	2	2.430	1.7	[60]
^{109}I	0.82	0.16	0.06	2	−3.779	−4	[61–63]
^{112}Cs	0.81	0.208	0.067	2	−2.856	−3.3	[64]
^{113}Cs	0.98	0.207	0.052	2	−5.100	−4.77	[61,64]
^{117}La	0.814	0.29	0.1	2	−1.812	−1.623	[74–78]
^{121}Pr	0.9	0.318	0.075	2	−2.188	−2	[74–78]
^{130}Eu	1.039	0.331	0	2	−2.637	−3.046	[74–78]
^{131}Eu	0.959	0.331	0	2	−1.639	−1.67	[74–78]
^{135}Tb	1.2	0.325	−0.046	3	−3.178	−3.027	[74–78]
^{140}Ho	1.106	0.297	−0.07	3	−1.920	−2.222	[74–78]
^{141}Ho	1.19	0.286	−0.063	3	−2.941	−2.387	[74–78]
^{144}Tm	1.725	0.258	−0.077	5	−4.767	−5.569	[74–78]
^{145}Tm	1.753	0.249	−0.078	5	−4.996	−5.456	[74–78]
^{146}Tm	1.13	−0.199	−0.038	5	−0.086	−0.63	[65]
^{147}Tm	1.06	−0.19	−0.04	5	0.723	0.43	[63,66,67]
^{150}Lu	1.27	−0.164	−0.05	5	−1.153	−1.4	[63,68]
^{151}Lu	1.24	−0.156	−0.045	5	−0.876	0.89	[63,69]
^{155}Ta	1.468	0.008	0	5	−2.563	−2.538	[74–78]
^{156}Ta	1.03	−0.053	0.001	2	−0.584	−0.609	[74–78]
^{157}Ta	0.947	0.045	0.001	0	−0.030	−0.523	[74–78]
^{159}Re	1.816	0.053	−0.007	5	−4.636	−4.678	[74–78]
^{160}Re	1.28	0.08	0.002	2	−3.026	−3.06	[70]
^{161}Re	1.36	0.08	−0.006	3	−3.171	−3.43	[71]
^{164}Ir	1.844	0.089	−0.006	5	−4.459	−3.947	[74–78]
^{165}Ir	1.7	0.099	−0.012	5	−3.529	−3.46	[72]
^{166}Ir	1.12	0.107	−0.004	2	−0.642	−0.82	[72]
^{167}Ir	1.11	0.116	−0.011	0	−1.163	−0.96	[72]
^{170}Au	1.488	−0.096	−0.012	2	−4.027	−3.493	[74–78]
^{171}Au	1.464	−0.105	−0.011	0	−4.458	−4.611	[74–78]
^{171}Au	1.51	−0.105	−0.011	4	−2.745	−2.65	[72]
^{176}Tl	1.282	−0.053	−0.007	0	−2.148	−2.284	[74–78]
^{177}Tl	1.18	−0.053	−0.007	0	−0.947	−1.174	[74–78]
^{185}Bi	1.56	−0.052	0.016	0	−4.402	−4.35	[73]

Table 4
Standard deviation of proton decay half-lives in the nuclei region $Z = 51 - 83$.

n	Parent	σ
21	o–o	1.09065
12	o–e	0.879551

4. Conclusions

In summary, we have theoretically studied the one-proton emission in the actinide region from $Z = 89 - 103$. We have also compared one-proton decay half-lives with alpha decay, spontaneous fission and beta decay. In the present work the calculated one-proton decay half-live values compare fairly well with the available experimental values. The standard deviation for

odd–odd nuclei is found to 1.09065 and for odd–even nuclei the deviation is 0.879551. We have also identified proton emitters in the actinide region and also it is the competing decay mode for all observed proton emitters. The prediction of the new proton emitters in the actinide region are having measurable half-lives can be retrieved in future with developing experimental techniques.

References

[1] V.I. Goldanskii, Nucl. Phys. 19 (1960) 482.
[2] I. Mukha, E. Roeckl, J. Döring, L. Batist, et al., Phys. Rev. Lett. 95 (2) (2005) 022501.
[3] I. Mukha, E. Roeckl, L. Batist, A. Blazhev, et al., Nature 439 (2006) 298–302.
[4] T.R. Routray, S.K. Tripathy, B.B. Dash, B. Behera, D.N. Basu, Eur. Phys. J. A 47 (2011) 92.
[5] J.G. Deng, X.H. Li, J.L. Chen, J.H. Cheng, et al., Eur. Phys. J. A 55 (2019) 58.
[6] T. Goigoux, P. Ascher, B. Blank, M. Gerbaux, et al., Acta Phys. Pol. B 50 (2019) 3.
[7] J. Giovinazzo, P. Ascher, L. Audirac, B. Blank, et al., J. Phys. Conf. Ser. 436 (2013) 012057.
[8] J. Giovinazzo, et al., Phys. Rev. Lett. 99 (2007) 102501.
[9] P. Ascher, et al., Phys. Rev. Lett. 107 (2011) 102502.
[10] Philip J. Woods, AIP Conf. Proc. 481 (1999) 207.
[11] K.P. Santhosh, I. Sukumaran, Phys. Rev. C 96 (2017) 034619.
[12] S. Hofmann, G. Munzenberg, et al., Nucl. Instrum. Methods Phys. Res. 223 (2–3) (1984) 312–318.
[13] K. Auranen, D. Seweryniak, M. Albers, A.D. Ayangeakaa, S. Bottoni, et al., Phys. Lett. B 792 (2019) 187–192.
[14] S.A. Alavi, V. Dehghani, M. Sayahi, Nucl. Phys. A 977 (2018) 49–59.
[15] J. Dobaczewski, W. Nazarewicz, Phys. Rev. C 51 (1995) R1070(R).
[16] E. Olsen, M. Pfützner, N. Birge, et al., Phys. Rev. Lett. 110 (2013) 222501.
[17] E. Olsen, M. Pfützner, N. Birge, M. Brown, et al., Phys. Rev. Lett. 111 (2013) 139903.
[18] M. Pfutzner, M. Karny, L. Grigorenko, K. Riisager, Rev. Mod. Phys. 84 (2012) 567.
[19] M. Pfützner, et al., Eur. Phys. J. A 14 (2002) 279.
[20] J. Giovinazzo, et al., Phys. Rev. Lett. 89 (2002) 102501.
[21] I. Mukha, K. Summerer, L. Acosta, M.A.G. Alvarez, et al., Phys. Rev. Lett. 99 (2007) 182501.
[22] I. Mukha, L. Grigorenko, K. Summerer, L. Acosta, et al., Phys. Rev. C 77 (2008) 061303(R).
[23] M. Pomorski, et al., Phys. Rev. C 83 (2011) 061303.
[24] B. Blank, et al., Phys. Rev. Lett. 94 (2005) 232501;
P. Ascher, et al., Phys. Rev. Lett. 107 (2011) 102502.
[25] K.P. Jackson, C.U. Cardinal, H.C. Evans, N.A. Jelley, J. Cerny, Phys. Lett. B 33 (1970) 281.
[26] S. Modi, M. Patial, P. Arumugam, E. Maglione, L.S. Ferreira, Phys. Rev. C 95 (2017) 054323.
[27] C. Qi, D.S. Delion, R.J. Liotta, R. Wyss, Phys. Rev. C 85 (2012) 011303(R).
[28] I. Mehrotra, S. Prakash, Pramana 70 (2008) 101.
[29] E. Maglione, L.S. Ferreira, Eur. Phys. J. A 15 (2002) 89.
[30] E. Maglione, L.S. Ferreira, Prog. Theor. Phys. 154 (2004) 154.
[31] N. Teruya, S.B. Duarte, M.M.N. Rodrigues, Phys. Rev. C 93 (2016) 024606.
[32] E.L. Medeiros, M.M.N. Rodrigues, S.B. Duarte, O.A.P. Tavares, Eur. Phys. J. A 34 (2007) 417.
[33] O.A.P. Tavares, E.L. Medeiros, Eur. Phys. J. A 45 (2010) 57.
[34] H.C. Manjunatha, N. Sowmya, K.N. Sridhar, L. Seenappa, J. Radioanal. Nucl. Chem. 314 (2) (2017) 991–999.
[35] H.C. Manjunatha, N. Sowmya, Nucl. Phys. A 969 (2018) 68–82.
[36] H.C. Manjunatha, N. Sowmya, Int. J. Mod. Phys. E 27 (5) (2018) 1850041.
[37] H.C. Manjunatha, K.N. Sridhar, N. Sowmya, Phys. Rev. C 98 (2018) 024308.
[38] K.N. Sridhar, H.C. Manjunatha, H.B. Ramalingam, Phys. Rev. C 98 (2018) 064605.
[39] S.G. Nilsson, Mat.-Fys. Medd. 29 (1955) 16.
[40] A. Zdeb, M. Warda, C.M. Petrache, K. Pomorski, Eur. Phys. J. A 52 (2016) 323.
[41] J. Blocki, W.J. swiatecki, Ann. Phys. (N. Y.) 132 (1981) 53.
[42] J. Blocki, J. Randrup, W.J. swiatecki, C.F. Tsang, Ann. Phys. (N. Y.) 105 (1977) 427.
[43] I. Dutt, R.K. Puri, Phys. Rev. C 81 (2010) 047601.
[44] G. Royer, J. Phys. G, Nucl. Part. Phys. 26 (2000) 1149.
[45] D.N. Poenaru, R.A. Gherghescu, W. Greiner, Phys. Rev. C 83 (2011) 014601.
[46] D. Ni, Z. Ren, T. Dong, C. Xu, Phys. Rev. C 78 (2008) 044310.
[47] V.Yu. Denisov, A.A. Khudenko, Phys. Rev. C 79 (2009) 054614.

[48] W. Swiatecki, Phys. Rev. 100 (1955) 937.
[49] X.J. Bao, S.Q. Guo, H.F. Zhang, et al., J. Phys. G, Nucl. Part. Phys. 42 (2015) 085101.
[50] G. Royer, J. Phys. G, Nucl. Part. Phys. 26 (2000) 1149.
[51] Z. Ren, C. Xu, Nucl. Phys. A 759 (2005) 64.
[52] S.Z. Qiang, S.L. Ping, M. Ying, H.J. Gang, et al., Chin. Phys. C 38 (12) (2014) 124101.
[53] X.P. Zhang, Z.Z. Ren, Q.J. Zhi, et al., J. Phys. G, Nucl. Part. Phys. 34 (2007) 2611.
[54] K.N. Huang, M. Aoyagi, et al., At. Data Nucl. Data Tables 18 (243) (1976) 054614.
[55] https://www-nds.iaea.org/RIPL-3.
[56] P. Möller, A.J. Sierk, T. Ichikawa, H. Sagawa, At. Data Nucl. Data Tables 109 (2016) 1.
[57] H.C. Manjunatha, B.M. Chandrika, L. Seenappa, Mod. Phys. Lett. A 31 (28) (2016) 1650162.
[58] M. Wang, G. Audi, A.H. Wapstra, et al., Chin. Phys. C 36 (2012) 1603.
[59] H.C. Manjunatha, N. Sowmya, Mod. Phys. Lett. A 34 (15) (2019) 1950112.
[60] R.J. Tighe, D.M. Moltz, J.C. Batchelder, T.J. Ognibene, et al., Phys. Rev. C 49 (1994) R2871.
[61] A. Gillitzer, T. Faestermann, K. Hartel, P. Kienle, E. Noite, Z. Phys. A 326 (1987) 107.
[62] T. Faestermann, A. Gillitzer, K. Hartel, et al., Phys. Lett. B 137 (1984) 23.
[63] P.J. Sellin, P.J. Woods, T. Davinson, N.J. Davis, et al., Phys. Rev. C 47 (1993) 1933.
[64] R.D. Page, P.J. Woods, R.A. Cunningham, et al., Phys. Rev. Lett. 72 (1994) 1798.
[65] K. Livingston, P.J. Woods, T. Davinson, et al., Phys. Lett. B 312 (1993) 46.
[66] K.S. Toth, D.C. Sousa, P.A. Wilmarth, et al., Phys. Rev. C 47 (1993) 1804.
[67] O. Klepper, T. Batsch, S. Hofmann, R. Kirchner, et al., Z. Phys. A 305 (1982) 125.
[68] P.J. Woods, T. Davinson, N.J. Davis, S. Hofmann, et al., Nucl. Phys. A 553 (1993) 485c.
[69] S. Hofmann, W. Reisdorf, G. Miinzenberg, et al., Z. Phys. A 305 (1982) 111.
[70] R.D. Page, P.J. Woods, R.A. Cunningham, et al., Phys. Rev. Lett. 68 (1992) 1287.
[71] R.J. Irvine, C.N. Davids, P.J. Woods, et al., Phys. Rev. C 55 (1997) R1621.
[72] C.N. Davids, P.J. Woods, J.C. Batchelder, et al., Phys. Rev. C 55 (1997) 2255.
[73] C.N. Davids, P.J. Woods, H.T. Penttilá, et al., Phys. Rev. Lett. 76 (1996) 592.
[74] M. Pfutzner, M. Karny, L.V. Grigorenko, K. Riisager, Rev. Mod. Phys. 84 (2012) 567.
[75] K.P. Santhosh, Indu Sukumaran, Phys. Rev. C 96 (2017) 034619.
[76] A.A. Sonzogni, Nucl. Data Sheets 95 (2002) 1.
[77] D.S. Delion, R.J. Liotta, R. Wyss, Phys. Rev. Lett. 96 (2006) 072501.
[78] B. Blank, M.J.G. Borge, Prog. Part. Nucl. Phys. 60 (2008) 403.

Indian Journal of Pure & Applied Physics
Vol. 58, April 2020, pp. 255-262

Systematics of proton decay of actinides

M G Srinivas[a], H C Manjunatha[b*], N Sowmya[b], Damodara Gupta P S[c] & Alfred Cecil Raj[d]

[a]Department of Physics, Government First Grade College, Mulbagal 563 131, India
[b]Department of Physics, Government College for Women, Kolar 563 101, India
[c]Department of Physics, Government First Grade College, Hoskote 562 114, India
[d]Department of Physics, St. Joseph's college, Thiruchirapalli 620 002, India

Received 17 February 2020

The phenomenon of proton emission from nuclear ground states limits the possibilities of the creation of more exotic proton rich nuclei that are usually produced by fusion-evaporation nuclear reactions. In the energy domain of radioactivity, proton can be considered as a point charge having highest probability of being present in the parent nucleus. Conclaves *et al*.[1] studied the two-proton radioactivity of nuclei of mass number A<70 using the effective liquid drop model. Delion *et al*.[2] reviewed the theories of proton emission to analyse the properties of nuclear matter. Maglione *et al*.[3] analysed the proton emission from the some deformed nuclei. We have studied proton decay in almost all actinide nuclei. We have calculated the energy released during the proton decay (Q_P), penetration factor (P), and half-lives of proton decay. Proton decay half-lives are also longer than that of other decay modes such as alpha decay and spontaneous fission. To check the Geiger-Nuttal law for proton decay in actinide nuclei, we have plotted the logarithmic proton decay half-lives versus 1/sqrt(Q). The competition of proton decay with different decay modes such as alpha decay and spontaneous fission are also studied. We have also highlighted possible proton emitters with the corresponding energies and half-lives in the actinide region.

Keywords: Proton decay, Half-lives, Probability, Geiger-Nuttal law

1 Introduction

The nuclei beyond the proton drip line with the $Qp > 0$ are the one with proton unstable and also exhibit exotic decay modes. The understanding of the proton decay is important to study the nuclear structure. The exotic nuclei exists away from the stability. The binding energy of protons above the drip line gradually decreases and hence one-proton and two proton decay is predicted. Brown[4] studied two proton decay in Z=22-28 in the ground state. Goldanskii[5] for the first time studied the one proton and two proton decay for odd and even atomic number. Janecke[6] studied the emission of protons from the light nuclei ^{12,13}O, ^{21}Mg and $^{24,\ 32}$Si. The spherical proton and deformed proton emitters were investigated in lanthanides and transaction metals. Previous workers[7-18] experimentally observed one and two proton decay in proton rich nuclei. They are several theoretical models[19-21], studied one proton and two proton activity in light nuclei. Using different proximity potentials previous workers[22-24] studied proton activity in the light nuclei. The emission of heavy particles such as one proton, one neutron, two protons, 2 neutrons and alpha particle emission takes place when the nuclei are proton rich, neutron rich and very heavy nuclei. Successively many theoretical models[25-32] were presented to study the half-lives of spherical and deformed nuclei. Dobaczewski and Nazarewicz[33] studied two-proton stability in doubly magic nuclei ^{100}Sn using self-consistent Skyrme-Hartree-Fock-Bogoliubov theory. Olsen *et al.*[34-35] investigated two-proton decay in even-even nuclei and also studied competition between proton decay and alpha decay. Poenaru *et al.*[36] measured half-lives and branching ratios for ^{12}C, ^{16}O and ^{28}Si and proton and neutron rich nuclei with Z=56-64.

The observations of the proton decay is quite recent, they are several approaches to study this proton decay process, such as distorted-wave Born approximation[37], the study of effective interaction by the density dependent M3Y (DDM3Y)[38,39]. The construction of proton nucleus potential by Jeukenne, Lejeune and Mahaux (JLM) applied to finite nuclei in the Local Density Approximation[40], the unified fission model[2], the coupled-channels approach[41] and also generalized liquid drop models[42-44]. Earlier workers[45-53] studied half-lives of spontaneous fission, ternary fission, cluster decay and alpha decay in the

*Corresponding author (E-mail: manjunathhc@rediffmail.com)

superhaevy region using different proximity potentials. Faestermann[54] experimentally observed proton decay half-lives and proton energies in ^{113}Cs and ^{109}I. Sellin[55] experimentally measured proton decay half-lives in ^{150}Lu, ^{151}Lu and ^{147}Tm. Page *et al.*[56] reported proton emitter ^{112}Cs with the half-life of 500±100μs. Livingston[57] experimentally observed proton emission from the ^{146}Tm. The two proton radioactivity[58-63] was experimentally observed ^{45}Fe, ^{19}Mg, ^{48}Ni and ^{54}Zn. In the year 1970, Jackson[64] confirmed the proton radioactivity form the proton emitter ^{53}Co.

The proton radioactivity is applied for nuclear astrophysics. In the nuclear astrophysics, the process of two-proton radiation capture process is considered, which is important for extremely high densities and temperatures. The example of such an astrophysical environment is the sources of gamma bursts related with the explosive burning of deposited hydrogen on the surface of neutron stars. Previous workers[65-67] explained the astrophysical applications of the two-proton radioactivity.

From the available literature, the study on one proton emission in the actinide region is required. The study on the proton decay not only provides information about the drip line, but also provides spectroscopic information on the unpaired proton not substantial in its orbit. Hence, in the present work we want to emphasize on the possible proton emitters in the actinide region and also prediction of half-lives in the same region. The main objective is to systematically study the one proton decay half-lives of spherical and deformed nuclei in the actinide region.

2 Theoretical Framework

2.1 Proton emission half-lives

The reaction of nuclear one proton decay can be written as:

$$ {}^{A}_{Z}(X)_N \rightarrow {}^{A-1}_{Z-1}(Y)_N + {}^{1}_{1}(H) + Q_P \quad \text{... (1)} $$

where Q_P is the amount of energy released during proton decay. To study the proton decay, we have used preformed cluster model[68,69]. The decay constant and half-lives is defined as

$$ \lambda = \nu\, PP_0 \quad \text{… (2)} $$

$$ T_{1/2} = \frac{\ln 2}{\lambda} \quad \text{… (3)} $$

where ν, P and P_0 are the assault frequency[79] with which proton hits the barrier, probability of penetration barrier and preformation probability respectively. In the present work we have selected P_0=1 for the emitted proton. The penetration probability is solved numerically using WKB approximation[71].

$$ P = \exp\left[-\frac{2}{\hbar} \int_{Rin}^{Rout} \sqrt{2\mu(V - Q_P)}\, dr \right] \quad \text{… (4)} $$

where μ is reduced mass of proton decay, Q_P is the energy released during proton decay. R_{in} and R_{out} are the inner and outer turning points. The inner turning point is given by:

$$ R_{in} = r_0 (A_1^{1/3} + A_2^{1/3}) \quad \text{… (5)} $$

where A_1=1 and A_2=A-1 for proton emission. R_{out} is determined by the condition V=Q. The r_0 is the effective nuclear constant. The total interacting potential is defined by:

$$ V = V_C + V_P + V_l \quad \text{… (6)} $$

where V_c Coulomb interaction potential[72], Vp is the proximity potential and V_l is the angular potential. Proximity potential[73-74] given by:

$$ V_P = 4\pi\gamma b \left[\frac{C_1 C_2}{C_1 + C_2} \right] \phi \quad \text{… (7)} $$

where $b \approx 1$ fm is the width of the nuclear surface, ϕ is the universal function[34], C_1 and C_2 are the Susmann central radii and γ is the nuclear surface tension coefficient it is given by:

$$ \gamma = \gamma_0 \left[1 - K_S \left(\frac{N - Z}{A} \right)^2 \right] \text{MeV/fm}^2 \quad \text{… (8)} $$

neutron mass (N), atomic mass (A) and proton number (Z) of the parent nuclei. Where γ_0 = 1.460734 MeV/fm^2 and Ks=4.0[75]. C1 and C2 are the Susmann central radii, R_i is the sharp radii[74] of the daughter nuclei.

3 Results and Discussion

The proton decay rates are sensitive to amount of energy released (Q_P) and the orbital angular momentum of the emitted proton. The proton emission is energetically possible when Q_P is positive and it is given by:

$$Q_P = \Delta M(A,Z) - \sum_i^n \Delta M(A_i, Z_i) \quad \ldots (9)$$

where $\Delta M(A, Z)$ and $\Delta M(A_i, Z_i)$ are mass excess of the parent and emitted daughter and proton nuclei, respectively. We have selected experimental and theoretical values in case of non-availability of experimental values available in the literature[76-80]. We have studied total interacting potential which is a sum of coulomb, proximity and angular potential as explained in the theory. During the proton emission, the ground state to ground state transactions has zero angular momentum $\ell = 0$. Thus we neglect the effects of angular potential in case of proton emission and we have also considered deformed nuclei in the present work. We have evaluated penetration probability using WKB approximation and studied logarithmic half-lives of proton decay in the actinide region. The amount of energy released during proton decay as function of mass number of parent nuclei in the actinide region as shown in Fig. 1. From the figure it is observed that the amount of energy released during proton decay gradually decreases with the increase in mass number of parent nuclei.

The studied logarithmic half-lives of proton decay in the actinide region is plotted as function of the mass number of parent nuclei is presented in Fig. 2. The figure indicates that the logarithmic half-lives increases with increase in mass number of parent nuclei. The half-lives values are of the order of 10^{-6} to 10^{-4} S for the actinides ^{195}Ac, ^{200}Pa, ^{206}Np, ^{212}Am, ^{218}Bk, ^{224}Es, ^{229}Md and ^{235}Lr and the corresponding values of Q(MeV), penetration factor and half-lives are tabulated in Table 1. Hence proton decay is favourably observed in the actinides such as ^{195}Ac, ^{200}Pa, ^{206}Np, ^{212}Am, ^{218}Bk, ^{224}Es, ^{229}Md and ^{235}Lr. Then we have also plotted logarithmic half-lives of proton decay with the product of $Z_d Q^{-1/2}$ in the actinide region and is as shown in Fig. 3. From the

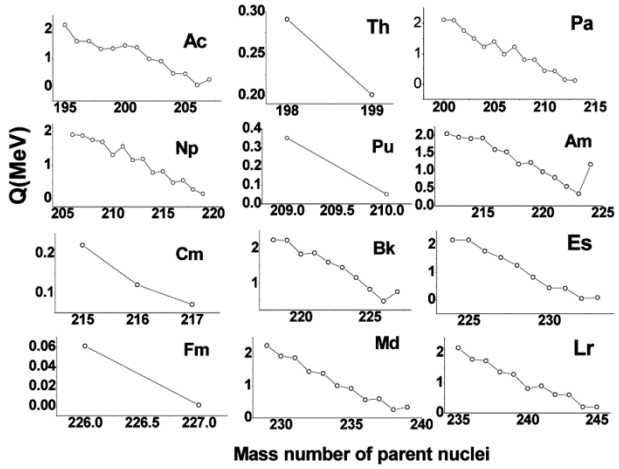

Fig. 1 — The variation of amount of energy released during proton decay with the mass number of parent nuclei in the actinide region.

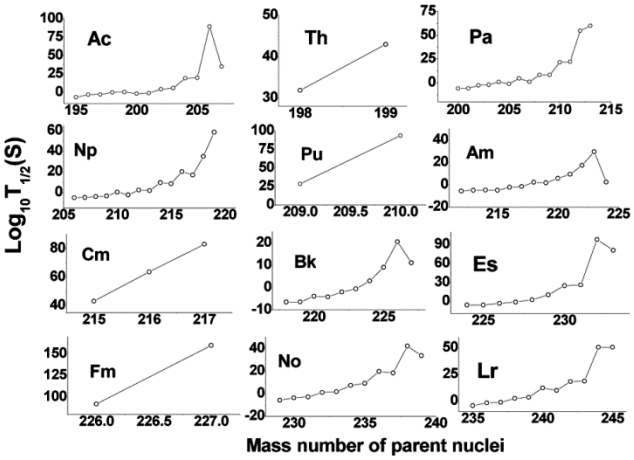

Fig. 2 — The variation of logarithmic half-lives of proton decay with the mass number of parent nuclei in the actinide region.

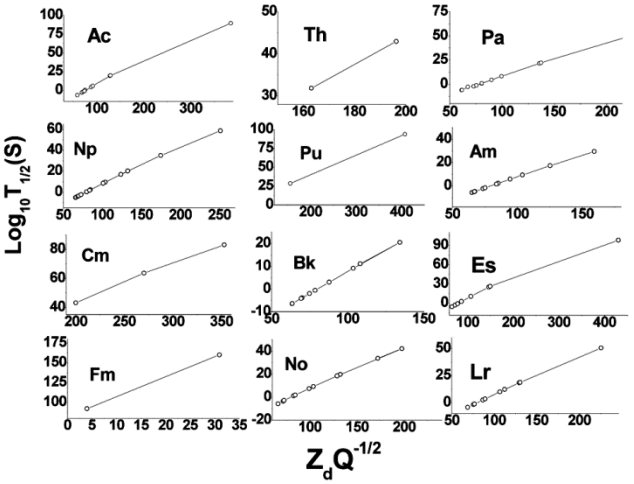

Fig. 3 — Variation of logarithmic half-lives of proton decay with the product of $Z_d Q^{-1/2}$ in the actinide region.

Table 1 — Proton decay half-lives, penetration factor and amount of energy released during proton decay in actinides.

Nuclei	Q(MeV)	Penetration factor	$\text{Log}T_{1/2}$
^{195}Ac	2.161	$2.142\text{x}10^{-15}$	$1.892\text{x}10^{-7}$
^{200}Pa	2.111	$3.807\text{x}10^{-16}$	$1.073\text{x}10^{-6}$
^{206}Np	1.911	$5.525\text{x}10^{-18}$	$7.471\text{x}10^{-5}$
^{212}Am	2.051	$1.838\text{x}10^{-17}$	$2.267\text{x}10^{-5}$
^{218}Bk	2.241	$1.015\text{x}10^{-16}$	$4.142\text{x}10^{-6}$
^{224}Es	2.181	$1.426\text{x}10^{-17}$	$2.976\text{x}10^{-5}$
^{229}Md	2.251	$1.482\text{x}10^{-17}$	$2.883\text{x}10^{-5}$
^{235}Lr	2.161	$1.317\text{x}10^{-18}$	$3.273\text{x}10^{-4}$

Table 2 — A comparison of logarithmic half-lives of proton decay with Royer, Univ, NRDX, Denisov and Bao.

		$LogT_{1/2}(S)$						Decay mode
Z_P	A_P	Proton	Royer(α)	UNIV(α)	NRDX(α)	Denisov(α)	Bao(SF)	
89	195	-6.7230	1.9019	1.3890	1.0527	1.4794	19.2850	Proton decay
89	196	-2.5360	4.1825	3.6576	3.2810	3.7588	20.3250	Proton decay
89	197	-2.5300	4.1610	3.6370	3.2830	3.7390	21.3300	Proton decay
89	198	0.3608	5.3396	4.8169	4.4464	4.9171	22.3023	Proton decay
89	199	0.2533	5.2725	4.7510	4.4043	4.8513	23.2399	Proton decay
89	200	-1.0245	4.7543	4.2340	3.9256	4.3348	24.1421	Proton decay
89	201	-0.2156	5.0479	4.5289	4.2323	4.6293	25.0094	Proton decay
89	202	5.8323	6.9328	6.4209	6.0791	6.5134	25.8415	Proton decay
89	203	4.9426	6.6779	6.1659	5.8550	6.2600	26.6385	Proton decay
89	204	16.461	8.8704	8.3763	7.9999	8.4513	27.4004	α decay
89	205	12.42	8.2391	7.7403	7.4114	7.8219	28.1272	α decay
89	206	28.92	10.038	9.5593	9.1753	9.6197	28.8189	α decay
89	207	39.985	10.65	10.180	9.7900	10.2318	29.4757	α decay
90	198	34.275	11.31	10.813	10.10	10.8917	16.1819	α decay
90	199	54.525	11.845	11.357	10.641	11.4272	17.1443	α decay
91	200	-5.9691	2.9029	2.3410	1.9651	2.5071	12.2615	Proton decay
91	201	-5.8597	2.9600	2.3991	2.0424	2.5654	13.1791	Proton decay
91	202	-3.3992	4.3279	3.7624	3.3775	3.9330	14.0680	Proton decay
91	203	-0.9587	5.4434	4.8786	4.4705	5.0485	14.9279	Proton decay
91	204	2.3428	6.6790	6.1190	5.6790	6.2840	15.7583	Proton decay
91	205	0.1534	5.8572	5.2957	4.9125	5.4643	16.5588	Proton decay
91	206	6.3757	7.8264	7.2758	6.8254	7.4327	17.3293	Proton decay
91	207	2.3511	6.6162	6.0597	5.6857	6.2249	18.0696	Proton decay
91	208	10.530	8.7260	8.1856	7.7340	8.3337	18.7794	α decay
91	209	10.533	8.7054	8.1659	7.7364	8.3143	19.4586	α decay
91	212	27.078	10.794	10.281	9.8076	10.4027	21.3128	α decay
91	213	-8.0673	11.60	11.10	10.61	11.2130	21.8698	α decay
92	203	31.073	11.764	11.23	10.42	11.3731	9.4360	α decay
93	206	-4.1266	4.5136	3.9048	3.4685	4.1449	6.7169	Proton decay
93	207	-3.8922	4.6184	4.0107	3.5904	4.2508	7.4948	Proton decay
93	208	-2.8658	5.1529	4.5460	4.1214	4.7860	8.2485	Proton decay
93	209	-2.3300	5.3939	4.7883	4.3730	5.0279	8.9775	Proton decay
93	210	1.8826	7.1678	6.5688	6.0847	6.8012	9.6813	Proton decay
93	211	-1.0955	5.9324	5.3299	4.9296	5.5683	10.3596	Proton decay
93	212	4.0769	7.8628	7.2705	6.7906	7.4977	11.0122	Proton decay
93	213	3.6098	7.6927	7.1005	6.6504	7.3291	11.6388	Proton decay
93	214	12.224	9.8169	9.2454	8.6965	9.4522	12.2391	α decay
93	215	11.11	9.5771	9.0040	8.4897	9.2138	12.8132	α decay
93	216	24.926	11.5	10.95	10.34	11.1356	13.3607	α decay
93	217	20.957	11.065	10.516	9.9510	10.7020	13.8818	α decay
94	209	35.156	12.929	12.374	11.439	12.5655	4.1089	α decay
95	212	-4.6445	4.7376	4.0882	3.6407	4.3973	1.6163	Proton decay
95	213	-3.9192	5.1358	4.4870	4.0386	4.7962	2.2689	Proton decay
95	214	-3.6105	5.2852	4.6376	4.2014	4.9467	2.9012	Proton decay
95	215	-3.7671	5.1793	4.5329	4.1226	4.8422	3.5128	Proton decay
95	216	-0.9294	6.6160	5.9729	5.5024	6.2785	4.1033	Proton decay
95	217	-0.2120	6.9190	6.2783	5.8103	6.5824	4.6721	Proton decay
95	218	4.1200	8.5489	7.9199	7.3731	8.2118	5.2192	Proton decay
95	219	3.5138	8.3273	7.6976	7.1848	7.9916	5.7441	Proton decay
95	220	8.0934	9.6523	9.0362	8.4594	9.3163	6.2466	Proton decay
95	221	12.231	10.5613	9.9572	9.3406	10.2256	6.7266	SF
95	222	21.504	11.9864	11.4037	10.7102	11.6503	7.1840	SF
95	223	36.899	13.2599	12.6999	11.9365	12.9237	7.6186	SF

(*Contd.*)

Table 2 — A comparison of logarithmic half-lives of proton decay with Royer, Univ, NRDX, Denisov and Bao. (*Contd.*)

		$LogT_{1/2}(S)$						Decay mode
Z_P	A_P	Proton	Royer(α)	UNIV(α)	NRDX(α)	Denisov(α)	Bao(SF)	
95	224	4.3046	8.4788	7.8558	7.4335	8.1488	8.0304	Proton decay
96	215	55.684	14.7612	14.1951	13.0602	14.4243	-0.7570	SF
97	218	-5.3828	4.7539	4.0643	3.6171	4.4420	-3.0072	Proton decay
97	219	-5.3288	4.7740	4.0855	3.6571	4.4633	-2.4670	Proton decay
97	220	-2.5529	6.4100	5.7228	5.2133	6.0987	-1.9435	Proton decay
97	221	-2.8104	6.2571	5.5707	5.0908	5.9472	-1.4371	Proton decay
97	222	-0.4836	7.4155	6.7345	6.1991	7.1056	-0.9482	SF
97	223	1.1511	8.1082	7.4325	6.8702	7.7987	-0.4774	SF
97	224	5.1142	9.5409	8.8787	8.2362	9.2310	-0.0248	SF
97	225	11.964	11.3070	10.6676	9.9153	10.9964	0.4093	SF
97	226	25.362	13.2970	12.6906	11.8050	12.9856	0.8245	SF
97	227	13.962	11.6660	11.0339	10.2944	11.3574	1.2206	SF
98	221	46.841	15.3640	14.7670	13.5179	15.0549	-5.1307	SF
99	224	-4.5262	5.7952	5.0641	4.5505	5.5104	-7.1242	SF
99	225	-4.5235	5.7749	5.0449	4.5523	5.4914	-6.6849	SF
99	226	-1.4450	7.5555	6.8314	6.2318	7.2712	-6.2589	SF
99	227	0.8213	8.6204	7.9043	7.2448	8.3362	-5.8467	SF
99	228	4.5384	10.0548	9.3534	8.6021	9.7703	-5.4488	SF
99	229	13.329	12.3930	11.7244	10.8019	12.1071	-5.0656	SF
99	230	30.619	14.6914	14.0653	12.9649	14.4042	-4.6974	SF
99	231	32.236	14.8004	14.1776	13.0875	14.5144	-4.3445	SF
101	229	-4.5400	6.3166	5.5442	4.9712	6.0582	-11.0676	SF
101	230	-2.1781	7.7399	6.9732	6.3081	7.4812	-10.7089	SF
101	231	-1.7682	7.9478	7.1833	6.5207	7.6900	-10.3599	SF
101	232	2.5638	9.9984	9.2518	8.4382	9.7396	-10.0213	SF
101	233	3.3468	10.2843	9.5419	8.7231	10.0264	-9.6935	SF
101	234	9.6969	12.3090	11.5948	10.6168	12.0501	-9.3769	SF
101	235	11.772	12.8028	12.0975	11.0941	12.5445	-9.0719	SF
101	236	24.179	14.9003	14.2344	13.0556	14.6409	-8.7790	SF
101	237	22.642	14.6912	14.0222	12.8826	14.4333	-8.4983	SF
101	238	54.221	16.9150	16.2950	14.9613	16.6559	-8.2302	SF
101	239	42.18	16.3479	18.4435	21.3829	16.0906	-7.9750	SF
102	232	14.287	13.8567	13.1417	11.8994	13.6041	-12.6100	SF
102	233	42.826	17.0247	16.3769	14.8403	16.7700	-12.2943	SF
103	235	-3.4850	7.5036	6.6935	6.0196	7.2718	-14.0132	SF
103	236	-0.4616	9.2220	8.4237	7.6179	8.9895	-13.7382	SF
103	237	0.0075	9.4420	8.6467	7.8401	9.2105	-13.4702	SF
103	238	4.2212	11.2859	10.5120	9.5541	11.0536	-13.2097	SF
103	239	5.3901	11.6911	10.9237	9.9465	11.4596	-12.9572	SF
103	240	15.307	14.3468	13.6242	12.4066	14.1136	-12.7131	SF
103	241	12.82	13.7897	13.0578	11.9148	13.5583	-12.4779	SF
103	242	22.712	15.5493	14.8527	13.5519	15.3172	-12.2519	SF
103	243	23.179	15.5979	14.8991	13.6128	15.3628	-12.0354	SF

figure we have observed that there is a linear variation half-lives with the product of $Z_d Q^{-1/2}$. We have also compared logarithmic half-lives of proton decay with that of alpha decay (Royer[81], Univ[82], NRDX[83], Denisov[84])and spontaneous fission (Bao[85]) and are tabulated in Table 2. From the table it is clear that the predicted isotopes such as $^{195\text{-}203}$Ac, $^{200\text{-}207}$Pa, $^{212\text{-}220,224}$Am, and $^{218\text{-}221}$Bk are having less half-lives compared to alpha decay and spontaneous fission decay mode. We have also identified and specified the dominant decay mode in the actinide region Z=89-103 in the corresponding table. Due to non-availability of experimental values in the actinide region, the predictive power is tested by comparing the available experimental values with the present work and it is tabulated in Table 3. From the table it is observed that studied values obtained from the present work agrees well with the available experimental values.

Table 3 — The comparison of calculated half-lives with the experimental values [54-56,87-102].

Isotopes	Z_d	A_d	l	logT (present work)	$logT_{1/2}$ (experimental)	Ref.
^{105}Sb	49	101	2	2.430	1.7	87
^{109}I	51	105	2	-3.779	-4	88,54-55
^{112}Cs	53	108	2	-2.856	-3.3	56
^{113}Cs	53	109	2	-5.100	-4.77	88, 56
^{117}La	55	113	2	-1.812	-1.623	98-102
^{121}Pr	57	117	2	-2.188	-2	98-102
^{130}Eu	61	126	2	-2.637	-3.046	98-102
^{131}Eu	61	127	2	-1.639	-1.67	98-102
^{135}Tb	63	131	3	-3.178	-3.027	98-102
^{140}Ho	65	136	3	-1.920	-2.222	98-102
^{141}Ho	65	137	3	-2.941	-2.387	98-102
^{144}Tm	67	140	5	-4.767	-5.569	98-102
^{145}Tm	67	141	5	-4.996	-5.456	98-102
^{146}Tm	67	142	5	-0.086	-0.63	89
^{147}Tm	67	143	5	0.723	0.43	55,87-88
^{150}Lu	69	146	5	-1.153	-1.4	55,92
^{151}Lu	69	147	5	-0.876	0.89	55,92
^{155}Ta	71	151	5	-2.563	-2.538	98-102
^{156}Ta	71	152	2	-0.584	-0.609	98-102
^{157}Ta	71	153	0	-0.030	-0.523	98-102
^{159}Re	73	155	5	-4.636	-4.678	98-102
^{160}Re	73	156	2	-3.026	-3.06	94
^{161}Re	73	157	3	-3.171	-3.43	95
^{164}Ir	75	160	5	-4.459	-3.947	98-102
^{165}Ir	75	161	5	-3.529	-3.46	96
^{166}Ir	75	162	2	-0.642	-0.82	96
^{167}Ir	75	163	0	-1.163	-0.96	96
^{170}Au	77	166	2	-4.027	-3.493	98-102
^{171}Au	77	167	0	-4.458	-4.611	98-102
^{171}Au	77	167	4	-2.745	-2.65	96
^{176}Tl	79	172	0	-2.148	-2.284	98-102
^{177}Tl	79	173	0	-0.947	-1.174	98-102
^{185}Bi	81	181	0	-4.402	-4.35	97

4 Conclusions

We have studied one proton decay in the actinide region through the study of energy released, penetration probability and logarithmic half-lives in the actinide region. The studied half-lives of present work is compared with the different decay modes such as alpha decay and spontaneous fission. We have identified the possible proton emitters with the corresponding energies and half-lives in the actinide region. The possible proton emitters in the actinide region are $^{195\text{-}203}$Ac, $^{200\text{-}207}$Pa, $^{212\text{-}220,224}$Am, and $^{218\text{-}221}$Bk. We have identified the proton emitters in the unexplored isotopes of actinide region which is not specified in the nuclear chart[86].

References

1 Gonçalves M, Teruya N, Tavares O A P & Duarte S B, *Phys Lett*, 774 (2017) 14.

2 Delion D S, Liotta R J & Wyss R, *Phys Rep*, 424 (2006) 113.

3 Maglione E, Ferreira L S & Liotta R, *J Phys Rev C*, 59 (1999) 589.

4 Detraz C V, *Ann Rev Nucl Part Sci*, 39 (1989) 407.

5 Goldansky V I, *Nucl Phys*, 19 (1960) 482.

6 Janecke J, *Nucl Phys*, 61 (1965) 326.

7 Goigoux T, Ascher P, Blank B & Gerbaux M, *Acta Phys Polo B*, 50 (2019) 3.

8 Giovinazzo J, Ascher P, Audirac L, Blank B & Borcea C, *J Phys Conf Ser*, 436 (2013) 012057.

9 Giovinazzo J, Blank B, Borcea C & Canchel G, *Phys Rev Lett*, 99 (2007) 102501.

10 Ascher P, Audirac L, Adimi N, Blank B & C Borcea C, *Phys Rev Lett,* 107 (2011) 102502.

11 Auranen K, Seweryniak D, Albers V, Ayangeakaa A D & Bottoni S, *Phys Lett B*, 792 (2019) 187.

12 Pfutzner M, Badura E, Bingham C & Blank B *Eur Phys J A*, 14 (2002) 279.

13 Giovinazzo J, Blank B, Chartier M & Czajkowski S *Phys Rev Lett*, 89 (2002) 102501.

14 Mukha I, Summerer K, Acosta L & Alvarez M A G, *Phys Rev Lett*, 99 (2007) 182501.

15 Mukha I, Grigorenko L, Summerer K & Acosta L, *Phys Rev C*, 77 (2008) 061303.
16 Pomorski M, Pfützner M, Dominik W & Grzywacz R, *Phys Rev C*, 83 (2011) 061303.
17 Blank B, Bey A, Canchel G, Dossat C & Fleury A, *Phys Rev Lett*, 94 (2005) 232501.
18 Jackson K P, Cardinal C U, Evans H C, Jelley N A & Cerny J, *Phys Lett B*, 33 (1970) 281.
19 Mukha I, Roeckl E, Döring J & Batist L, *Phys Rev Lett*, 95 (2005) 022501.
20 Mukha I, Roeckl E, Batist L & Blazhev A, *Nature,* 439 (2006) 298.
21 Routray T R, Tripathy S K, Dash B B, Behera B & Basu D N, *Euro Phys J A*, 47 (2011) 92.
22 Deng J G, Li X H, Chen J L, & Cheng J H, *Eur Phys J A*, 55 (2019) 58.
23 Philip J, *AIP Conf Proc*, 481 (1999) 207.
24 Santhosh K P & Sukumaran I, *Phys Rev C*, 96 (2017) 034619.
25 Modi S, Patial M, Arumugam P, Maglione E & Ferreira L S, *Phys Rev C*, 95 (2017) 054323.
26 Qi C, Delion D S, Liotta R J & Wyss R, *Phys Rev C*, 85 (2012) 011303.
27 Mehrotra I & Prakash S, *Pramana*, 70 (2008) 101.
28 Maglione E & Ferreira L S, *Eur Phys J A*, 15 (2002) 89.
29 Maglione E & Ferreira L S, *Prog Theor Phys*, 154 (2004) 154.
30 Teruya N, Duarte S B & Rodrigues M M N, *Phys Rev C*, 93 (2016) 024606.
31 Medeiros E L, Rodrigues M M N, Duarte S B & Tavares O A P, *Eur Phys J A*, 34 (2007) 417.
32 Tavares O A P & Medeiros E L, *Eur Phys J A*, 45 (2010) 57.
33 Dobaczewski J & Nazarewicz W, *Phys Rev C*, 51 (1995) 1070.
34 Olsen E, Pfützner M, Birge N, Brown M, Nazarewicz W & Perhac A *Phys Rev Lett*, 110 (2013) 222501.
35 Olsen E, Pfützner M, Birge N, Brown M, Nazarewicz W & Perhac A *Phys Rev Lett*, 111 (2013) 139903.
36 Poenaru D N, Greiner W & Gherghescu R A, *Phys Rev C*, 47 (1993) 2030.
37 Aberg S, Semmes P B & Nazarewicz W, *Phys Rev C*, 56 (1997) 1762.
38 Basu D N, Chowdhury P R & Samanta C, *Phys Rev C*, 72 (2005) 051601.
39 Bhattacharya M & Gangopadhyay G, *Phys Lett B*, 651 (2007) 263.
40 Balasubramaniam M & Arunachalam N, *Phys Rev C*, 71 (2005) 014603.
41 Guzman F, Gonçalves M, Tavares O A P, Duarte S B, García F & Rodríguez O, *Phys Rev C*, 59 (1999) R2339.
42 Dong J M, Zhang H F & Royer G, *Phys Rev C*, 79 (2009) 054330.
43 Zhang H, Li J, Zuo W, et al., *Phys Rev C*, 71 (2005) 054312.
44 Lalazissis G A & Raman S, *Phys Rev C*, 58 (1998) 1467.
45 Manjunatha H C, Sowmya N, Sridhar K N & Seenappa L, *J Radio Anal Nucl Chem*, 314 (2017) 991.
46 Manjunatha H C & Sowmya N, *Nucl Phys A*, 969 (2018) 68.
47 Manjunatha H C & Sowmya N, *Int J Mod Phys E*, 27 (2018) 1850041.
48 Manjunatha H C, Sridhar K N & Sowmya N, *Phys Rev C*, 98 (2018) 024308.
49 Sridhar K N, Manjunatha H C & Ramalingam H B, *Phys Rev C*, 98 (2018) 064605.
50 Manjunatha H C, Sridhar K N & Sowmya N, *Nucl Phys A*, 987 (2019) 382.
51 Sowmya N & Manjunatha H C, *Bulg J Phys*, 46 (2019) 16.
52 Sowmya N & Manjunatha H C, *Proc DAE Symp Nucl Phys*, 63 (2018) 200.
53 Sowmya N & Manjunatha H C, *Braz J Phys*, 49 (2019) 874.
54 Faestermann T, Gillitzer A, Hartel K, Kienle P & Nolte E, *Phys Lett B*, 137 (1984) 23.
55 Sellin P J, Woods P J, Davinson T, Davis N J & Livingston K *Phys Rev C*, 47 (1993) 1933.
56 Page R D, Woods P J, Cunningham R A & Davinson T, *Phys Rev Lett*, 72 (1994) 1798.
57 Livingston K, Woods P J, Davinson T, Davis N J & Hofmann S *Phys Lett B*, 312 (1993) 46.
58 Pfutzner M, Badura E, Bingham C, Blank B & Chartier M, *Eur Phys J A*, 14 (2002) 279.
59 Giovinazzo J, Blank B, Chartier M, Czajkowski S & Fleury A, *Phys Rev Lett*, 89 (2002) 102501.
60 Mukha I, Summerer K, Acosta L, Alvarez M A G, Casarejos. E & Chatillon A*, Phys Rev Lett*, 99 (2007) 182501.
61 Mukha I, Grigorenko L, Summerer K, Acosta L & Alvarez M A G *Phys Rev C*, 77 (2008) 061303.
62 Pomorski, Pfützner M, Dominik W, Grzywacz R, Baumann T & Berryman J S, *Phys Rev C*, 83 (2011) 061303.
63 Blank B, Bey A, Canchel G, Dossat C & Fleury A, *Phys Rev Lett*, 94 (2005) 232501;
64 Jackson K P, Cardinal C U, Evans H C, Jelley N A & Cerny J, *Phys Lett B*, 33 (1970) 281.
65 Görres J, Wiescher M & Thielemann F K, *Phys Rev C*, 51 (1995) 392.
66 Grigorenko L V & Zhukov M V, *Phys Rev C*, 72, (2005) 015803.
67 Grigorenko L V, Langanke K, Shulgina N B & Zhukov M V, *Phys Lett B*, 641 (2006) 254.
68 Malik S S & Gupta R K*, Phys Rev C*, 39 (1989) 1992.
69 Balasubramaniam M & Gupta R K, *Phys Rev C*, 60 (1999) 064316.
70 Nilsson S G, *Dan Mat Fys Med*, 29 (1955) 16.
71 Zdeb A, Warda M, Petrache C M & Pomorski K, *Eur Phys J A*, 52 (2016) 323.
72 Denisov V Y & Ikezoe H, *Phy Rev C*, 72 (2005) 064613.
73 Blocki J & Swiatecki W J, *Ann Phys(N Y)*, 132 (1981) 53.
74 Blocki J, Randrup J, Swiatecki W J & Tsang C F, *Ann Phys (N Y)*, 105 (1977) 427.
75 Dutt I & Puri R K, *Phys Rev C*, 81 (2010) 047601.
76 https://www-nds.iaea.org/RIPL-3.
77 Möller P, Sierk A J, Ichikawa T & Sagawa H, *At Data Nucl Data Tables*, 109 (2016) 1.
78 Manjunatha H C, Chandrika B M & Seenappa L, *Mod Phys Lett A*, 31 (2016) 1650162.
79 Wang M, Audi G, Wapstra A H, et al., *Chin Phys C*, 36 (2012) 1603.
80 Manjunatha H C & Sowmya N, *Mod Phys Lett A*, 34 (15) (2019) 1950112.
81 Royer G, *J Phys G: Nucl Part Phys*, 26 (2000) 1149.
82 Poenaru D N, Gherghescu R A & Greiner W, *Phys Rev C*, 83 (2011) 014601.
83 Ni D, Ren Z, Dong T & Xu C, *Phys Rev C*, 78 (2008) 044310.

84 Denisov V Y & Khudenko A A, *Phys Rev C*, 79 (2009) 054614.
85 Bao X J, Guo S Q, Zhang H F, et al., *J Phys G Nucl Part Phys*, 42 (2015) 085101.
86 https://www-nds.iaea.org/relnsd/vcharthtml/VChartHTML.html
87 Tighe R J, Moltz D M, Batchelder J C, Ognibene T J, et al., *Phys Rev C*, 49 (1994) R2871.
88 Gillitzer A, Faestermann T, Hartel K, P Kienle & Noite E, *Z Phys A*, 326 (1987) 107.
89 Livingston K, Woods P J, Davinson T, et al., *Phys Lett B*, 312 (1993) 46.
90 Toth K S, Sousa D C, Wilmarth P A, et al., *Phys Rev C*, 47 (1993) 1804.
91 Klepper O, Batsch T, Hofmann S, Kirchner R, et al., *Z Phys A*, 305 (1982) 125.
92 Woods P J, Davinson T, Davis N J, Hofmann S, et al., *Nucl Phys A*, 553 (1993) 485.
93 Hofmann S, Reisdorf W, Miinzenberg G, et al., *Z Phys A*, 305 (1982) 111.
94 Page R D, Woods P J, Cunningham R A, et al., *Phys Rev Lett*, 68 (1992) 1287.
95 Irvine R J, Davids C N, Woods P J, et al., *Phys Rev C*, 55 (1997) R1621.
96 Davids C N, Woods P J, J Batchelder C, et al., *Phys Rev C*, 55 (1997) 2255.
97 Davids C N, Woods P J, Penttilá H T, et al., *Phys Rev Lett*, 76 (1996) 592.
98 Pfutzner M, Karny M, Grigorenko L V & Riisager K, *Rev Mod Phys*, 84 (2012) 567.
99 Santhosh K P & Sukumaran I, Phys Rev C, 96 (2017) 034619.
100 Sonzogni A A, *Nucl Data Sheets*, 95(2002) 1.
101 Delion D S, Liotta R J & Wyss R, *Phys Rev Lett*, 96 (2006) 072501.
102 Blank B & Borge M J G, *Prog Part Nucl Phys*, 60 (2008) 403.

ISSN 1547-4771, Physics of Particles and Nuclei Letters, 2020, Vol. 17, No. 7, pp. 909–915. © Pleiades Publishing, Ltd., 2020.

PHYSICS OF ELEMENTARY PARTICLES AND ATOMIC NUCLEI. THEORY

Proton Radioactivity of Heavy Nuclei of Atomic Number Range 72 < Z < 88

H. C. Manjunatha[a, *], M. G. Srinivas[b, c], N. Sowmya[a], P. S. Damodara Gupta[d], and Alfred Cecil Raj[c]

[a] *Department of Physics, Government College for Women, Kolar, Karnataka, 563101 India*
[b] *Department of Physics, Government First Grade College, Mulbagal, Karnataka, 563131 India*
[c] *Department of Physics, St. Joseph's college (autonomous), Tiruchirapalli, Tamil Nadu, 620002 India*
[d] *Department of Physics, Government First Grade College, Kolar, Karnataka, 563101 India*
**e-mail: manjunathhc@rediffmail.com*

Received June 4, 2020; revised June 8, 2020; accepted June 18, 2020

Abstract—We have studied proton radioactivity of heavy nuclei of atomic number range $72 < Z < 88$. We have calculated the energy released during the proton decay (Q_P) and half-lives of proton decay. To study the competition between different decay modes, we have compared the proton decay half lives with that of the decay modes such as alpha decay, beta decay, cluster decay and spontaneous fission. To check the Geiger–Nuttall law for proton decay, we have plotted the logarithmic proton decay half-lives versus 1/sqrt(Q). We have also highlighted possible proton emitters with the corresponding energies and half-lives in the atomic number range $72 < Z < 88$.

DOI: 10.1134/S1547477120070043

1. INTRODUCTION

In the energy domain of radioactivity, proton can be considered as a point charge having highest probability of being present in the parent nucleus. Conclaves et al. [1] studied the two-proton radioactivity of nuclei of mass number $A < 70$ using the effective liquid drop model. Delion et al. [2] reviewed the theories of proton emission to analyse the properties of nuclear matter. Maglione et al. [3] analysed the proton emission half–lives from the deformed nuclei $^{109}_{53}$I, $^{131}_{63}$Eu and $^{141}_{67}$Ho. Delsanto et al. [4] investigated the β-delayed proton emission of ^{69}Kr and ^{68}Se and extracted their proton separation energies, half-lives and excitation energies. Alavi et al. [5] calculated the proton radioactivity half–lives of 45 proton emitters by WKB Method and observed the decrease in values of calculated half-lives using the orientation angle dependent formalism. Raciti et al. [6] measured the emission of two protons from the decay of ^{18}Ne. Baye et al. [7] evaluated the decay probability per second for ^{11}Be, ^{19}C and ^{31}Ne one-neutron halo nuclei. Feix et al. [8] computed the decay widths of nuclear proton emission for $Z = 51$ to 71 nuclei using Droplet Model. Anguiano et al. [9] investigated the photo-emission of two protons from the ^{12}C, ^{16}O and ^{40}Ca nuclei for the study of short range correlations. Coniglione et al. [10] explored high energy proton emission in heavy ion reactions close to the Fermi energy by investigating the production mechanism of energetic protons in an experiment performed with the MEDEA detector. Giusti et al. [11] developed the theoretical frame work of emission of two protons in electron induced reactions. Ludewigt et al. [12] studied the proton emission in α-induced reactions at 43 MeV nucleon. Guzman et al. [13] analysed the proton emission from proton-rich nuclei and calculated the half-lives using the effective liquid drop model. Delion et al. [14] proposed semi empirical formula for logarithmic half-lives of proton decay. Dong et al. [15] theoretically calculated the half-lives of proton emitters using generalized liquid drop model (GLDM) and WKB approximation. Maglione et al. [16] studied the proton emission from ^{125}Pm and the behaviour of the half-lives were discussed as a function of deformation, spin of the decaying state, and energy of the emitted protons. Arumugam et al. [17] investigated the proton emission, gamma deformation, and the spin of the isomeric state of ^{141}Ho and revealed that proton deformations and other structural properties of exotic nuclei beyond the proton drip-line. Duarte et al. [18] explored the half-lives for proton emission, alpha decay, cluster radioactivity, and cold fission processes theoretically. Ferreira et al. [19] planned to study the proton radioactivity from spherical nuclei theoretically based on relativistic density functional derived from meson exchange and point coupling models. Ginter et al. [20] studied the proton emission from ^{150}Lu and new proton emitting state was

observed. Delion et al. [21] investigated proton decay from tri-axially deformed nuclei ^{161}Re and ^{185}Bi and studied the dependence of angular distribution of decaying particle on triaxial deformation parameters. Earlier workers [22–24] studied one and two proton decay half-lives of ^{131}Eu, ^{45}Fe and also studied proton emission from the deformed nuclei. In the literature, different theoretical approaches are available [25–41] to study different decay modes including proton decay. Aim of the present work is to study the proton radioactivity of heavy nuclei in the atomic number range $72 < Z < 88$.

2. THEORY

The proton emission half–life in the region $72 < Z < 88$ is given by

$$T_{1/2} = \frac{\ln(2)}{\nu_0 P}, \tag{1}$$

where ν_0 is the assault frequency, which is related to oscillator frequency related to ω;

$$\nu_0 = \frac{\omega}{2\pi} = \frac{\left(2n_r + \ell + \frac{3}{2}\right)}{2\pi\mu R_n^2} = \frac{\left(G + \frac{3}{2}\right)}{1.2\mu R_0^2}, \tag{2}$$

where $R_n^2 = \frac{3}{5}R_0^2$ and $R_0 = 1.14$ fm is used here. $G = 2n_r + \ell$ is the principal quantum number. For the proton radioactivity, we have selected $G = 4$ or 5 corresponding to the $4\hbar\omega$ or $5\hbar\omega$ oscillator shell depending on the individual nucleus. The penetration probability P is evaluated using WKB approximation [42].

$$P = \exp\left[-\frac{2}{\hbar}\int_{\text{Rin}}^{\text{Rout}}\sqrt{2\mu(V-Q)}dr\right], \tag{3}$$

where μ is reduced mass of emitted proton, $\mu = \left(m_P m_{A-1}/m_P + m_{A-1}\right) = 938.3(A-1)/\text{A MeV}/c^2$ and Q is the amount of energy released. R_{in} and R_{out} are the classical inner and outer turning points. The inner turning point is given by;

$$R_{\text{in}} = r_0(A_1^{1/3} + A_2^{1/3}), \tag{4}$$

where $A_1 = 1$ and $A_2 = A - 1$ for proton emission. R_{out} is determined by the condition $V = Q$. The total potential is given as;

$$V = V_{\text{C}} + V_{\text{P}} + V_\ell, \tag{5}$$

where V_{C} Coulomb interaction potential, V_{P} is the proximity potential and V_ℓ is the centrifugal potential. The V_{C} is given by,

$$V_{\text{C}} = \frac{Z_1 Z_2 e^2}{r}\left[1 + \frac{3R^2}{5r^2}\beta_2 Y_{20}(\theta) + \frac{3R^4}{9r^4}\beta_4 Y_{40}\right], \tag{6}$$

where Z_1 and Z_2 are the atomic numbers of proton and daughter nuclei respectively, and "r" is the distance between fragment centres. R, β, $Y_{20}(\theta)$ is the radius of the nuclei, quadrupole deformation parameter and spherical harmonic function respectively. Proximity potential given by [43, 44],

$$V_{\text{P}}(Z) = 4\pi\gamma\bar{R}\Phi(s). \tag{7}$$

Φ is the universal proximity potential which is independent of the shapes of nuclei or the geometry of the nuclear system, but depends on the minimum separation distance $s = z/b$. z is the distance between the near surfaces of the fragments and $b = 0.99$ is the nuclear surface thickness. In Eq. (7), $\bar{R}$ is the mean curvature radius and it is expressed as;

$$\bar{R} = \frac{C_1 C_2}{C_1 + C_2}. \tag{8}$$

The C_i is the Sussmann central radii of the fragments related to sharp radii R_i is expressed as;

$$C_i = R_i - \left(\frac{b^2}{R_i}\right). \tag{9}$$

For sharp radii R_i,

$$R_i = 1.28A_i^{1/3} - 0.76 + 0.8A_i^{-1/3}. \tag{10}$$

In Eq. (7), γ is given as;

$$\gamma = \gamma_0\left[1 - K_s\left(\frac{N-Z}{A}\right)^2\right]\text{MeV}/\text{fm}^2 \tag{11}$$

$\gamma_0 = 1.460734$ MeV/fm^2 and $K_s = 4.0$ [26].

Universal proximity potential is given by [26]

$$\Phi(\varepsilon) = \begin{cases} -4.41\exp\left(\dfrac{-\varepsilon}{0.7176}\right) & \text{for} \quad 0 \geq \varepsilon \geq 1.9475 \\ -1.7817 + 0.9270\varepsilon + 0.0169\varepsilon^2 - 0.05148\varepsilon^3 & \text{for} \quad 0 \leq \varepsilon \leq 1.9475 \end{cases}. \tag{12}$$

The centrifugal potential V_ℓ is expressed as

$$V_\ell(r) = \frac{\hbar^2}{2\mu}\frac{\ell(\ell+1)}{r^2}, \tag{13}$$

where μ, ℓ and r are the reduced mass, the angular momentum and the distance between the mass centre's respectively.

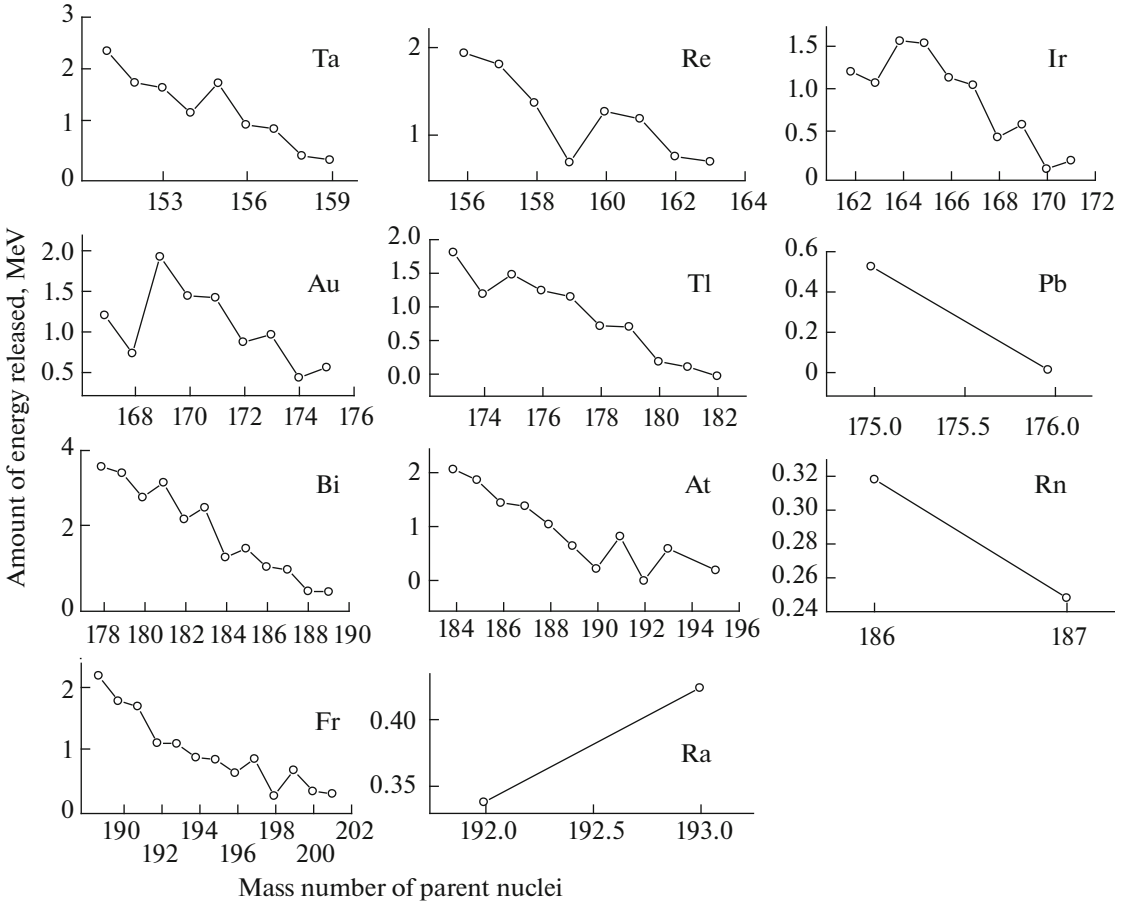

Fig. 1. A variation of amount of energy released during the proton emission in the nuclei region $72 < Z < 88$ with the mass number of parent nuclei.

3. RESULTS AND DISCUSSIONS

The amount of energy released during proton decay are studied using mass excess values available in [45–49]. We have studied driving potential, penetration factor and half-lives of proton emission in the nuclei region $72 < Z < 88$ as explained in the theory section. The variation of amount of energy released during proton decay with the mass number of parent nuclei is as shown in Fig. 1. From the figure we have observed that as the mass number of the parent nuclei increases the energy released decreases. The variation of logarithmic half-lives for the proton emission with the mass number of parent nuclei is as shown in Fig. 2. From the figure it depicts that the logarithmic half-lives for the proton emission increases with the mass number of parent nuclei. To check the Geiger–Nuttal law for proton decay, we have plotted the logarithmic proton decay half-lives versus 1/sqrt(Q) and it is as shown in Fig. 3. From the figure we have observed linear variation of logarithmic half-lives with the $Z_d Q^{-1/2}$. We have also studied the competition between different decay modes such as alpha decay, β^+-decay, β^--decay and proton decay. The half-lives corresponding to β^+-decay and β^--decay are evaluated using the semi empirical formula available in the literature [53, 54]. Alpha decay half–lives are evaluated using the procedure explained in the previous work [24]. The plot of different decay modes are as shown in Fig. 4 and also highlighted possible proton emitters with the corresponding energies and half-lives in the atomic number range $72 < Z < 88$. To validate the present work, The proton emission half-lives produced by the present work is compared with that of experiments and available semi empirical formulae such as Hatsukawa et al. [55] and Gamow [42] it is tabulated in Table 1. We have also compared the proton radioactivity logarithmic half-lives of present work with that of available experimental values and it is depicted in Fig. 5. From Fig. 5 and Table 1, it is clearly observed that the present work is in close agreement with the experimental values.

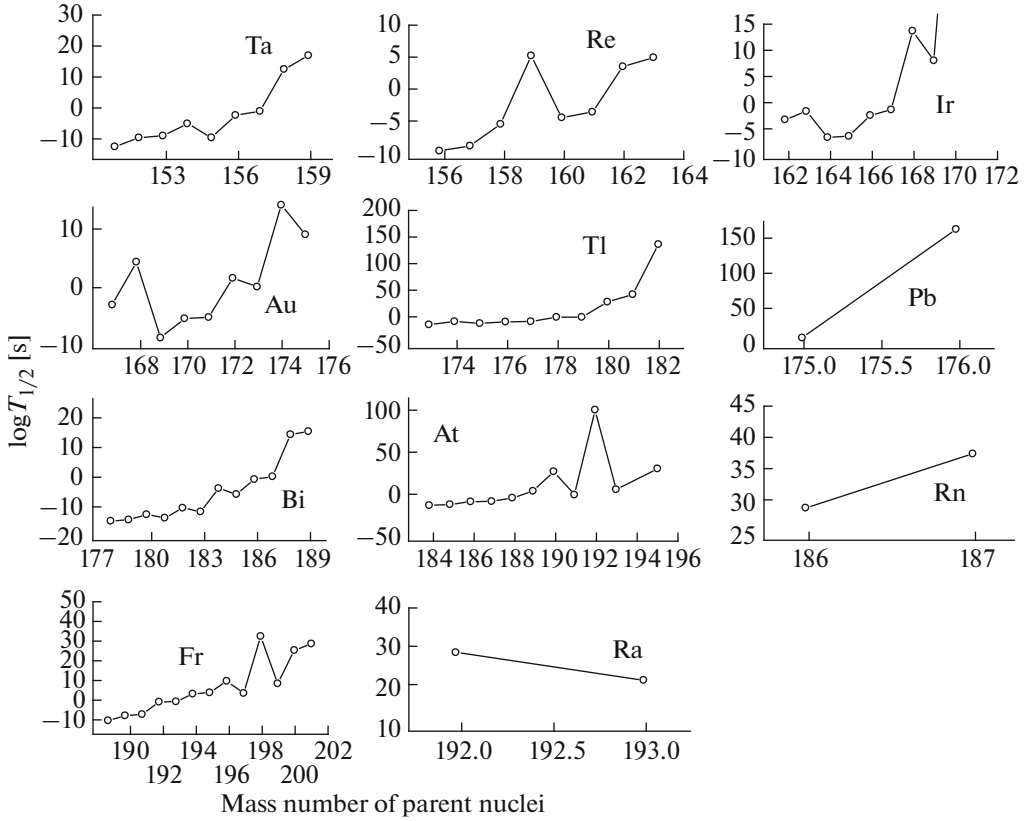

Fig. 2. A variation of logarithmic half-lives for the proton emission in the nuclei region $72 < Z < 88$ with the mass number of cluster.

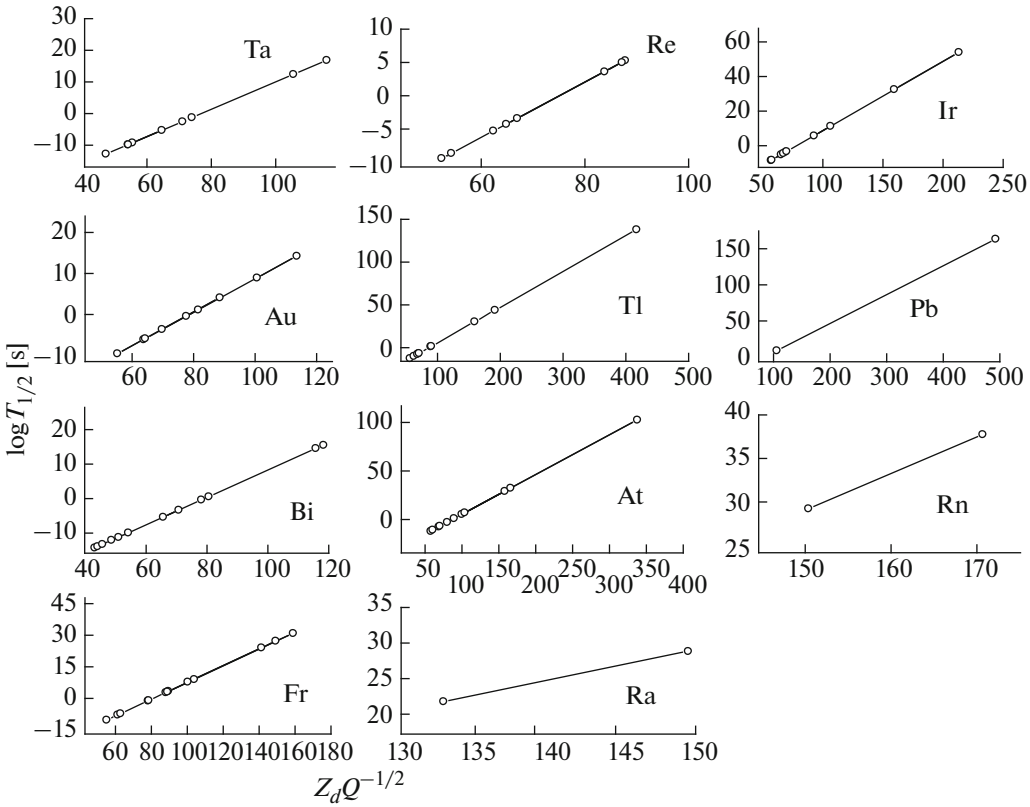

Fig. 3. A variation of logarithmic half-lives for the proton emission in the nuclei region $72 < Z < 88$ with the product of atomic number of daughter and amount of energy released during proton emission ($Z_dQ^{-1/2}$).

Table 1. Comparison of present work with experiments [2, 50–52] and other models

Parent nuclei	Q [Expt.], MeV	$\log T_{1/2}$ Expt. [2, 50–52]	Q (present work), MeV	ℓ	$\log T_{1/2}$				
					present work	CPPMDN [51]	CPPM [51]	Hatsukawa et al. [55]	Gamow [42]
^{155}Ta	1.453	−2.538	1.789	5	−2.836	−3.302	−3.218	−5.998	−5.490
^{156}Ta	1.020	−0.609	1.027	2	−0.618	−0.854	−0.620	−1.221	−0.716
^{160}Re	1.267	−3.060	1.292	2	−2.292	−2.339	−1.986	−3.732	−3.231
^{161}Re	1.197	−3.357	1.211	0	−3.614	−1.981	−1.603	−2.955	−2.454
^{164}Ir	1.540	−3.947	1.584	5	−3.599	−3.601	−3.182	−5.904	−5.406
^{166}Ir	1.152	−0.818	1.166	2	−0.874	−0.542	−0.097	−1.887	−1.392
^{167}Ir	1.070	−0.959	1.084	0	−1.016	0.298	0.752	−0.673	−0.179
^{170}Au	1.472	−3.493	1.489	2	−3.503	−3.054	−2.959	−4.643	−4.152
^{171}Au	1.447	−4.611	1.467	0	−4.593	−3.331	−3.102	−4.393	−3.903
^{176}Tl	1.265	−2.284	1.265	0	−2.362	−0.739	−0.501	−1.883	−1.399
^{177}Tl	1.159	−1.174	1.177	0	−1.184	0.633	0.878	−0.545	−0.063
^{185}Bi	1.526	−4.237	1.559	4	−4.119	−5.268	−3.507	−4.769	−4.293

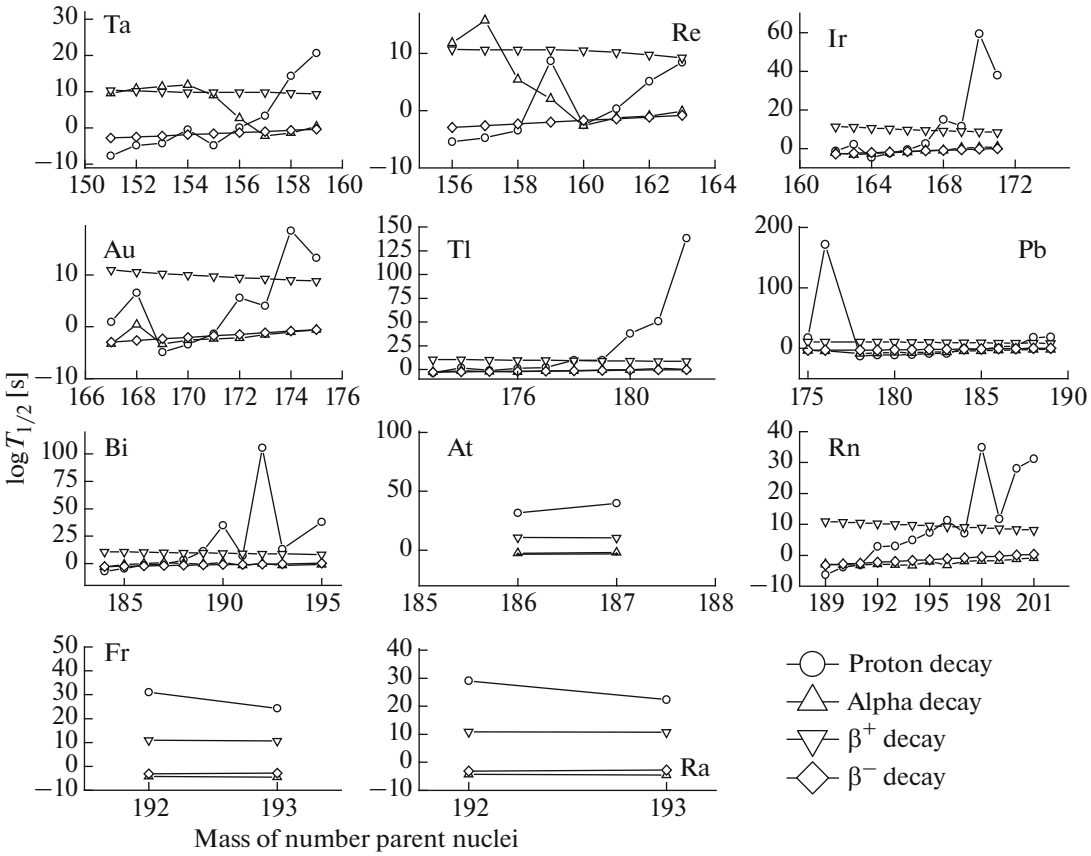

Fig. 4. Variation of $\log(T_{1/2})$ of proton activity, alpha decay, β^+ and β^- decay as a function of mass number of the parent nuclei (A).

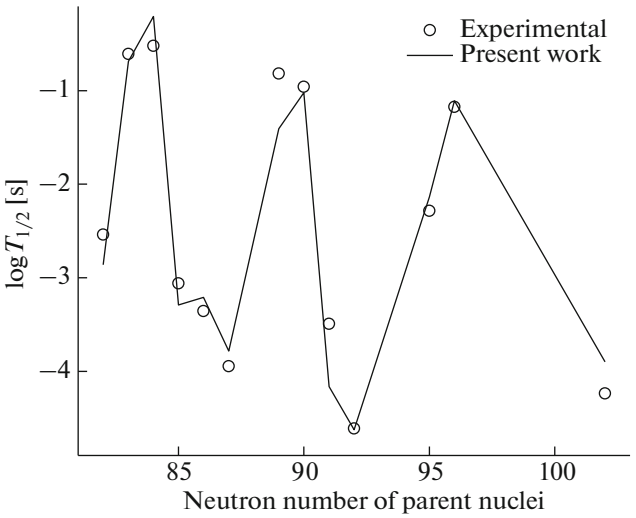

Fig. 5. A comparison of logarithmic half-lives of proton radioactivity of present work with that of available experimental values.

4. CONCLUSIONS

We have studied the amount of energy released during the proton decay (Q_P) and and half-lives of proton decay. We have studied the competition between different decay modes by comparing the proton decay half-lives with that of the other decay modes such as alpha decay, β^+ and β^- decay. We have also checked the Geiger–Nuttal law for proton decay by plotting the logarithmic proton decay half-lives versus 1/sqrt(Q). We have highlighted possible proton emitters with the corresponding energies and half-lives in the atomic number range $72 < Z < 88$.

REFERENCES

1. M. Gonclaves, N. Teruya, O. A. P. Tavares, and S. B. Duarte, Phys. Lett. B **774**, 14–19 (2017).
2. D. S. Delion, R. J. Liotta, and R. Wyss, Phys. Rep. **424**, 113–174 (2006).
3. E. Maglione, L. S. Ferreira, and R. J. Liotta, Phys. Rev. C **59**, 589 (1999).
4. M. Delsanto et al., Phys. Lett. B **738**, 453 (2014).
5. S. A. Alavi, V. Dehghani, and M. Sayahi, Nucl. Phys. A **977**, 49–59 (2018).
6. G. Raciti, M. de Napoli, et al., Nucl. Phys. A **834**, 464c–466c (2010).
7. D. Baye and E. M. Tursunov, Phys. Lett. B **696**, 464–467 (2011).
8. W. F. Feix and E. R. Hilf, Phys. Lett. B **120**, 14–18 (1983).
9. M. Anguiano, G. Co, and A. M. Lallena, Nucl. Phys. A **744**, 168–191 (2004).
10. R. Coniglione, P. Sapienza, E. Migneco, C. Agodi, et al., Phys. Lett. B **471**, 339–345 (2000).
11. C. Giusti and F. D. Pacati, Nucl. Phys. A **535**, 573–591 (1991).
12. B. Ludewigt, R. Glasow, H. Lohner, and R. Santo, Nucl. Phys. A **408**, 359–371 (1983).
13. F. Guzman, M. Goncalves, O. A. P. Tavares, et al., Phys. Rev. C **59**, 2339 (1999).
14. D. S. Delion, R. J. Liotta, and R. Wyss, Phys. Rev. Lett. **96**, 772501 (2006).
15. J. M. Dong, H. F. Zhang, and G. Royer, Phys. Rev. C **79**, 054330 (2009).
16. E. Maglione, S. Lidia, and S. Ferreira, Phys. Rev. C **94**, 044317 (2016).
17. P. Arumugam, S. Ferreira, and E. Maglione, Phys. Lett. B **680**, 443–447 (2009).
18. S. B. Duarte, O. A. P. Tavares, F. Guzman, et al., At. Data Nucl. Data Tabl. **80**, 235–299 (2002).
19. L. S. Ferreira, E. Maglione, and P. Ring, Phys. Lett. B **701**, 508–511 (2011).
20. T. N. Ginter, J. C. Batchelder, C. R. Bingham, C. J. Gross, et al., Phys. Rev. C **61**, 014308 (1999).
21. D. S. Delion, R. Wyss, D. Karlgren, and R. J. Liotta, Phys. Rev. C **70**, 061301 (2004).
22. E. Maglione and L. S. Ferreira, Phys. Rev. C **61**, 047307 (2000).
23. J. Giovinazzo, B. Blank, M. Chartier, et al., Phys. Rev. Lett. **89**, 102501 (2002).
24. L. S. Ferreira, E. Maglione, and D. E. P. Fernandes, Phys. Rev. C **65**, 024323 (2002).
25. H. C. Manjunatha, Nucl. Phys. A **945**, 42–57 (2016).
26. H. C. Manjunatha and N. Sowmya, Nucl. Phys. A **969**, 68-82 (2018).
27. H. C. Manjunatha, K. N. Sridhar, and N. Sowmya, Nucl. Phys. A **987**, 382–395 (2019).
28. H. C. Manjunatha and K. N. Sridhar, Nucl. Phys. A **962**, 7–23 (2017).
29. N. Sowmya and H. C. Manjunatha, Braz. J. Phys. **49**, 874 (2019).
30. H. C. Manjunatha, K. N. Sridhar, and N. Sowmya, Phys. Rev. C **98**, 024308 (2018).
31. K. N. Sridhar, H. C. Manjunatha, and H. B. Ramalingam, Phys. Rev. C **98**, 064605 (2018).
32. H. C. Manjunatha, K. N. Sridhar, and N. Sowmya, Nucl. Phys. A **987**, 382–395 (2019).
33. N. Sowmya and H. C. Manjunatha, Bulg. J. Phys. **46**, 16–27 (2019).
34. H. C. Manjunatha, Int. J. Mod. Phys. E **25**, 1650074 (2016).
35. H. C. Manjunatha and N. Sowmya, J. Radioanal. Nucl. Chem. **314**, 991–999 (2017).
36. H. C. Manjunatha and N. Sowmya, Int. J. Mod. Phys. E **27**, 1850041 (2018).
37. M. G. Srinivas, H. C. Manjunatha, K. N. Sridhar, N. Sowmya, and A. C. Raj, Nucl. Phys. A **995**, 1216 (2020).
38. N. Sowmya, H. C. Manjunatha, and N. Dhananjaya, J. Radioanal. Nucl. Chem. **323**, 1347–1351 (2020).
39. G. R. Sridhar, H. C. Manjunatha, N. Sowmya, P. S. Damodara Gupta, and H. B. Ramalingam, Eur. Phys. J. Plus **135**, 291 (2020)
40. N. Sowmya and H. C. Manjunatha, Braz. J. Phys. **50**, 317–330 (2020).

41. N. Sowmya and H. C. Manjunatha, Phys. Part. Nucl. Lett. **17**, 370–378 (2020).
42. A. Zdeb, M. Warda, C. M. Petrache, and K. Pomorski, Eur. Phys. J. A **52**, 23 (2016).
43. J. Blocki and W. J. Swiatecki, Ann. Phys. (N.Y.) **132**, 53 (1981)
44. J. Blocki, J. Randrup, W. J. Swiatecki, and C. F. Tsang, Ann. Phys. (N.Y.) **105**, 427 (1977).
45. https://www-nds.iaea.org/RIPL-3/masses.
46. P. Möller, A. J. Sierk, T. Ichikawa, and H. Sagawa, At. Data Nucl. Data Tables **109**, 1 (2016).
47. H. C. Manjunatha, B. M. Chandrika, and L. Seenappa, Mod. Phys. Lett. A **31**, 1650162 (2016).
48. M. Wang, G. Audi, A. H. Wapstra, F. G. Kondev, et al., Chin. Phys. C **36**, 1603 (2012)
49. H. C. Manjunatha and N. Sowmya, Mod. Phys. Lett. A **34**, 1950112 (2019).
50. P. Futzner, M. Karny, M. Grigorenko, and L. V. Riisager, Rev. Mod. Phys. **84**, 567 (2012).
51. K. P. Santhosh and I. Sukumaran, Phys. Rev. C **96**, 034619 (2017).
52. B. Blank and M. J. G. Borge, Nucl. Phys. **60**, 403 (2008).
53. S. Z. Qiang et al., Chin. Phys. C **38**, 12 (2014).
54. X. P. Zhang et al., J. Phys. G: Nucl. Part. Phys. **34**, 2611 (2007).
55. Y. Hatsukawa, H. Nakahara, and D. C. Hoffman, Phys. Rev. C **42**, 674 (1990).

Indian J Phys
https://doi.org/10.1007/s12648-021-02273-0

ORIGINAL PAPER

Exploring new proton emitting isotopes of Lanthanides

M G Srinivas[1,2], H C Manjunatha[3]*, Y S Vidya[4]*, P S Damodara Gupta[3] and S Alfred Cecil Raj[2]

[1]Department of Physics, Government First Grade College, Mulbagal, Karnataka 563131, India

[2]Department of Physics, St. Joseph's College (Autonomous), Affiliated to Bharathidasan University, Tiruchirapalli, Tamilnadu, India

[3]Department of Physics, Government College for women, Kolar, Karnataka 563101, India

[4]Department of Physics, Lal Bahadur Shastri Government First Grade College, RT Nagar, Bangalore, Karnataka 560032, India

Received: 11 April 2021 / Accepted: 23 December 2021

Abstract: Present work explores the 24 new proton decay emitters in the Lanthanide region by studying the competition between the different possible decay modes such as proton decay, alpha decay, beta decay and spontaneous fission. The proton emission half-lives of different lanthanide isotopes have been studied using different proximity functions such as Prox. 13, Prox. 77, MP 77, Ng 80 and Bass 80. Though the experimental values are found to be in good agreement with the proximity function of Ng 80, we have developed an empirical formula to calculate the half-lives of such proton-emitting lanthanides. The half-life values produced by the present formula are compared with that of NG 80. The present formula produces the half lives with simple inputs of Z_d and Q values, and hence, we may call this as pocket formula. Newly identified proton emitters are presented in a nuclide chart. The identified proton emitters may find applications in radiation therapy.

1. Introduction

Light and medium nuclei mostly show proton decay, whereas lanthanides show the proton and β decay. Furthermore, heavy nuclei ($Z = 72$–88) show β^+ and β^- decay, actinides ($Z = 89$–103) and superheavy nuclei or transactinides decay through α particles. It is also predicted that nuclei with $Z \geq 126$ may undergo cluster decay/exotic decay [1]. The competition between decay modes depends sensitively on the Coulomb and centrifugal barriers. Proton radioactivity studies provide a unique insight into the structure of nuclei beyond the drip line limit [2]. Proton emission from long-lived excited states has been investigated since the 1970s in ^{53m}Co [3]. Subsequent discoveries of proton decay from ^{151}Lu [4], ^{113}Cs, ^{109}I [5] and eventually other exotic heavy isotopes like ^{117}La [6] and ^{135}Tb [7] have motivated additional measurements.

The Lanthanide series includes 14 elements having atomic numbers from 58 to 71. The lanthanides and their analogs finds importance in radiotherapy due to their physical properties physical half-life, type(s) of decay emission(s), energy of the emission, cost and availability, and specific activity [8]. Few studies have been devoted toward the different decay modes of actinides, lanthanides and transactinides [9–14]. Sridhar et al. [15] studied the cluster radioactivity in actinide nuclei. Quadrelli et al. [16] analyzed the quadratic decay observed for Ln(III) ionic radii and calculated bond distances and lanthanide atomic orbital expectation values. Nitscke et al. [17] identified a total of 24 new β-delayed proton precursors and several new decay branches in the region of $56 < Z < 72$ and $N < 82$ using OASIS online mass separator facility. Davids et al. [18] identified proton decay from ^{141}Ho and ^{131}Eu. Sowmya et al. [19] studied the competition between different decay modes such as binary, ternary, cluster radioactivity and alpha decay of Darmstadtium. Although different decay modes are explained for few series of actinide and the heavy elements, the lanthanide series yet to be explored.

The presence of high coulomb barrier for heavy nuclei ($Z > 52$), reduces the proton barrier penetration probability to the extent that proton decay taking place from

*Corresponding author, E-mail: manjunathhc@rediffmail.com; vidyays.phy@gmail.com

Published online: 29 January 2022

the ground states of nuclei have measurable long half lives [13]. There are various methods to investigate the proton radioactivity such as the density-dependent M3Y effective interaction [20, 21], the Jeukenne-Lejeune-Mahaux (JLM) interaction [20], the unified fission model [22, 23], the generalized liquid drop model [24], the cluster model [25], the deformed density model [26], the coulomb and proximity potential model [27], the covariant density functional theory [28]. These nuclear proximity potentials provide the phenomenological potentials for nuclear reaction and structure including nuclear decay [29]. Santhosh et al. [27] explained the half life predictions for the proton emitters with $Z > 50$ in the ground state and isomeric state using coulomb and proximity potential model for the deformed nuclei Dong et al. [30]. The α-decay was studied using double-folding potentials from chiral effective field theory for the nuclei ^{104}Te.

The coulomb and nuclear proximity potential provides another simple and practical formalism to estimate the strength of the nuclear interactions during collision of heavy-ions. When two surfaces are approaching each other, approximately at a distance of 2–3 fm, an additional force due to the proximity of surfaces will appear which is called proximity potential [31]. There are adjustable parameters in various parts of the proximity formalism such as the radius parameter R, the surface energy coefficient and the universal function which lead to introduce different versions of the proximity potentials. Santhosh et al. [32] studied the coulomb and proximity potential as interacting barrier for post-scission region and calculated half-life time for different modes of exotic decay treating parent and fragments as spheres and these values are compared with experimental data. Dutta et al. [33] performed a detailed comparative study of fusion barriers for asymmetric colliding nuclei using the different versions of phenomenological proximity potential as well as other parameterizations within the proximity concept.

From the detailed analysis of the literature, it is found that, there is no systematic study of proton decay in the lanthanide region. The aim of the study is to predict the unexplored proton emitters in the lanthanide region. Experimentally, only 11 proton emitters were identified in the lanthanide region. From the present study, it is of first kind where we systematically explored the unexplored 24 proton decay emitters in the lanthanide region. This article is organized into four sections. The second section explains the theory used for the study. Results and discussion are presented in the third section, whereas fourth section concentrates on the summary of the present work.

2. Theory

The macroscopic modified generalized liquid drop energy between the two nuclei is given by [1]

$$E = E_V + E_S + E_C + E_{\text{prox.}} + E_\ell \tag{1}$$

E_V, E_S, E_C, $E_{\text{prox.}}$ and E_ℓ be the volume, surface, Coulomb, proximity and centrifugal energies, respectively. The centrifugal energies depend on the angular momentum. The selection rule for proton decay is as follows;

$$J_i = J_f + J_{p_i} \tag{2}$$

where $p_i = 1, 2$ for one and two proton decay, respectively. The conservation of parity is expressed as;

$$\pi_i = \pi_f \pi_{p_i} (-1)^\ell \tag{3}$$

where i and f are the initial and final states in the proton decay. ℓ is the angular momentum at the proton transition and p_i is nonzero and zero for both one and two proton, respectively. The selection rules for the minimum angular momentum are expressed as;

$$\ell_{\min} = \begin{cases} \Delta_j \quad \text{for even} \quad \Delta_j \quad \text{and} \quad \pi_p = \pi_d \\ \Delta_j + 1 \quad \text{for even} \quad \Delta_j \quad \text{and} \quad \pi_p \neq \pi_d \\ \Delta_j \quad \text{for odd} \quad \Delta_j \quad \text{and} \quad \pi_p \neq \pi_d \\ \Delta_j + 1 \quad \text{for odd} \quad \Delta_j \quad \text{and} \quad \pi_p = \pi_d \end{cases} \tag{4}$$

where $\Delta_j = |J_p - J_d - J_{p_i}|$.

The term $E_{\text{prox.}}$ is used to calculate nuclear part of the potential. It is very difficult to calculate the nuclear potential part. Many models such as double-folding, proximity potential, liquid drop model have been used. Among these, the proximity model has been easily and successfully used to calculate the nuclear interaction between two nuclei. It is mainly composed of two parts. One depends on the shape and geometry of two nuclei, and the other is the universal function $\Phi(s_0)$ only related to the short separation distance between two nuclei. The proximity energy is defined as.

$$E_{\text{prox.}}(Z) = 4\pi\gamma\bar{R}\Phi\left(\frac{z}{b}\right) \tag{5}$$

Here Φ is universal proximity potential function, and z is distance between the near surfaces of the fragments, respectively. $b \approx 0.99$ is the nuclear surface thickness. In the above Eq. (5) $\bar{R}$ is the mean curvature radius and γ is the surface energy co-efficient [1]. To Evaluate $E_{\text{prox.}}$ we have used following five different proximity functions.

2.1. Prox 13(Prox. 13)

The idea of the universal function is the fundamental advantage of the proximity potential model. Because of the

unique nature of the nucleus where the density distribution is different for different nucleus. Double-folding model (DFM) with the density-dependent nucleon-nucleon interaction gives the average results of the effective nucleon–nucleon interaction at all nuclear densities. The microscopic double-folding potential is proved more potential in studying the nuclear structural information, such as nuclear deformation parameters, charge root mean square radius and alpha-preformation factors [34–41]. Zhang et al. [42] used the density-dependent nucleon–nucleon interaction to calculate the nuclear potential and then deduced the universal function. This is termed as "Prox.2013" and the proposed universal function can be expressed as;

$$\Phi(\epsilon) = \frac{p_1}{1+\exp\left(\frac{s_0+p_2}{p_3}\right)} \qquad (6)$$
$$\text{With } s_0 = \frac{R-R_1-R_2}{b}$$

Here p_1, p_2 and p_3 are -7.65, 1.02 and 0.89, respectively. Previous researchers [43] also used this proximity potential to study the proton radio activities of some nuclei and compared with that experiments.

2.2. Prox 1977 (Prox. 77)

Blocki et al. [44] suggested a generalized proximity theorem that leads to the formula for the interaction potential between the two nuclei and a function of simple geometrical factor and universal separation function. This theorem is important for discussing the interaction between types of surfaces for which the curvatures at the point of least separation are no longer small compared to the diffuseness of the surface region. Proximity function based on this proximity theorem is called prox 77 and it is expressed as;

$$\phi(s) = \begin{cases} -0.5(S-2.54)^2 - \\ 0.0852(S-2.54)^3 & S<1.2511 \\ -3.437\exp(-S/0.75) & S>1.2511 \end{cases}$$

With $S = (r - C_1 - C_2)/b$ and $b \approx 1$. This proximity function was successfully applied in studying potential energy surfaces (PES) in the ground-state decay [45], quasielastic scattering [46] and barrier distribution [31].

2.3. Modified Prox 1977 (MP77)

The original form of the proximity potential 1977 overestimates the experimental data by 4% for fusion barrier heights [47]. Several improvements/modifications were made over the original proximity potential 1977 to remove the discrepancy between theory and data. It included either the better form of the surface energy coefficient [48] or universal function and/or nuclear radius [47]. Later, Ishwar Dutt [49] modified the original proximity potential 77 which includes the reactions with combine mass between $A = 19$ and $A = 294$ units, totally 390 reactions were experimentally studied by considering symmetric as well as asymmetric colliding partners. The modified form of Prox 1977 [44] is expressed as [49];

$$\phi(S) = \begin{cases} -1.7817 + 0.9827S + 0.143S^2 \\ \quad -0.09S^3 & S<0 \\ -1.7817 + 0.01696S^2 \\ \quad -0.05148S^3 & 0<S<1.9475 \\ -4.41\exp(-S/0.7176) & S>1.9475 \end{cases} \qquad (7)$$

with $S = (r - C_1 - C_2)/b$ and b is the surface width, $b = (\pi/\sqrt{3})a$ with $a = 55$ fm and it is nearly equal to unity. Furthermore, This modified proximity potential has been successfully used for the prediction of different decay modes of superheavy elements α decays of the yet-to-be-discovered superheavy element $Z = 119$ in the mass range of $A = 274$–313 [50–53].

2.4. Prox Ngo 1980 (Ng80)

In 1980 Ngo [54] proposed a proximity function based on the calculated interaction potential between two nuclei using the energy density formalism and Fermi distributions for the nuclear densities. The proposed proximity function is expressed as;

$$\phi(S) = \begin{cases} -33 + 5.4(S-S_0)^2 & \text{for } S<S_0 \\ -33\exp\left[-\frac{1}{5}\right](S-S_0)^2 & \text{for } S\geq S_0 \end{cases} \qquad (8)$$

where $S_0 = -1.6$ fm. Furthermore, this proximity function was used by the previous researchers [55] along with the dynamical Cluster decay Model to produce the alpha decay half-lives. This proximity function was also employed in the study of nucleus-nucleus interactions such as fusion [56].

2.5. Bass Model 1980 (Bass 80)

Bass in 1977 [57] derived a universal nucleus–nucleus potential from a classical analysis of experimental fusion cross sections. The deduced potential is consistent with the liquid-drop model at small separation, and with quantum analyses of elastic scattering at large separation. Bass potentials do not have a repulsive core at shorter distance. A newer version of the Bass potential referred as "Bass 80" [48] shows slight improvement over Bass 77 and Bass 80 reproduce the experimental data within 1.5%. The proposed proximity function is given by

$$\Phi(S) = [0.033\exp(S/3.5) + B\exp(S/0.65)]^{-1} \qquad (9)$$

This proximity potential was also employed in the elastic scattering cross section [58, 59]. This proximity function was also successfully used in the study of decay process such as alpha decay and cluster decay [29, 60–62].

3. Method of calculation of half-life

According to WKB approximation (Wentzel–Kramers–Brillouin) of the penetration probability P through the potential barrier was studied for the cluster and alpha decay by the following equation;

$$P = \exp\left\{-\frac{2}{\hbar}\int_{R_a}^{R_b}\sqrt{2\mu(E-Q}dr\right\} \tag{10}$$

where the total energy is evaluated using Eq. (1) by using different proximity functions, where μ is the reduced mass of proton decay system, R_a and R_b are the inner and outer turning points and these turning points were evaluated using following conditions;

$$V_T(R_a) = Q = V_T(R_b) \tag{11}$$

The alpha decay half-life is studied using following equation;

$$T_{1/2} = \frac{\ln 2}{\lambda} = \frac{\ln 2}{\nu P S_p} \tag{12}$$

where λ is decay constant and ν is the assault frequency. S_p is the spectroscopic factor and it is model dependent and very sensitive to decay energy. The accurate consideration decay energies in the calculation results half-lives close to experiment and spectroscopic factors close to one. It is also evident from the literature [63, 64] that the spectroscopic factors are assumed as one in proton decay half-life calculation while using the WKB approximation. In the present work, we have used WKB approximation and accurate recent mass excess values in the calculation of decay energies. Thus the spectroscopic factors are assumed to be one. E_v is the empirical vibration energy and it is evaluated using the following equations;

$$\nu = \frac{\omega}{2\pi} = \frac{2E_v}{h} \tag{13}$$

$$E_v = Q\left\{0.056 + 0.039\exp\left[\frac{4-A_2}{2.5}\right]\right\} for A_2 \geq 4 \tag{14}$$

4. Present formula

The variation of experimental $\log(T_{1/2})$ of proton decay in the lanthanide region as a function of $Z_d/\sqrt{Q}$ is shown in Fig. 1. We have fitted empirical relation for experimental

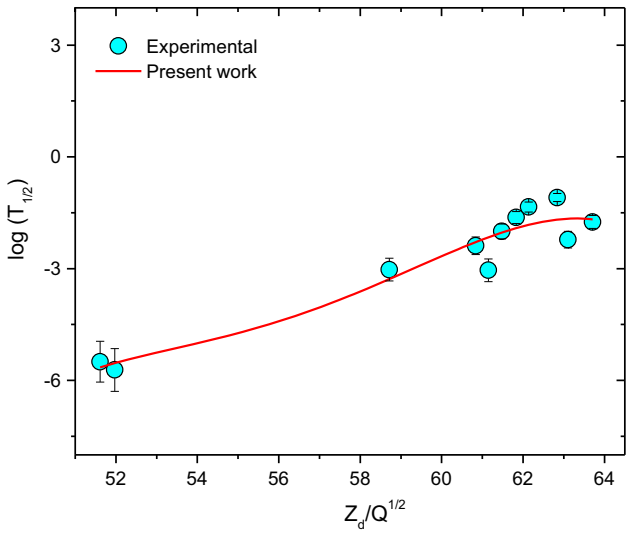

Fig. 1 Variation of experimental and present formula produced proton decay half lives as a function of $Z_d/\sqrt{Q}$

$\log(T_{1/2})$ such a way that it should have maximum R^2 and minimum residual sum of squares. Hence, proposed empirical formula for $\log(T_{1/2})$ of proton decay is given below; the half-lives for proton decay in the lanthanide region as a function of fissility parameter $Z_d/\sqrt{Q}$ is given by:

$$\log(T_{1/2}) = \sum_{i=0}^{i=4} A_i\left(\frac{Z_d}{\sqrt{Q}}\right)^i \tag{15}$$

where Z_d is the atomic number of the daughter nuclei and Q is the decay energy. The fitting parameters A_0, A_1, A_2, A_3 and A_4 are having the values -1.61, -20.82×10^{-2}, 71×10^{-4}, -8.18×10^{-5} and -3.11×10^{-7} $\mathrm{MeV}^{1/2}\mathrm{s}$, respectively.

5. Results and discussion

The phenomenon of proton decay is treated as the transmission of the proton across a potential barrier developed due to combined effect of coulombic and nuclear potential [65]. Experimentally there are 11 proton emitters were identified in the lanthanide region. We have studied the proton decay for lanthanide nuclei in which its decay energy (Q_p) is positive. In the present work, it is of first kind where we systematically explored the unexplored 24 proton decay emitters in the lanthanide region. These proton emitters having half-lives in terms of $1\,\mathrm{s} - 1\,\mu\mathrm{s}$. Generally, the half-lives of proton emitters nuclei have been determined by quantum-mechanical tunneling calculation through a potential barrier [66].

The universal function proposed by five different versions of coulomb and nuclear proximity potentials such as Prox. 13, Prox. 77, MP 77, Ng 80 and Bass 80 are used to calculate the half lives of proton emitters in the lanthanide region for different isotopes of lanthanides. Table 1 gives the range of studied lanthanide isotopes having positive proton decay energy.

In order to study whether the shape of the potential leads to different half-lives, the different proximity potentials are plotted as a function of R as shown in Fig. 2. X-axis corresponds to the distance between interacting nuclei, and Y-axis corresponds to interacting potential. The area under the potential curve is directly proportional to the penetration probability. If the area under the potential curve is more, the probability of penetration is more which clearly indicates the short half-life of the decay particle and vice versa. In the present study, from Fig. 2, it is observed that, the area under the curve is found to be maximum for Bass 80 and then follows the order Prox. 13, Mod. Prox. 77, Prox. 77 and Ng 80.

The calculated proton decay half lives are compared with the experiments. The calculated Mean square error of different proximity functions with respect to experiments is shown in Table 3. The sum of the squared residuals between the $\log(T_{1/2})$ of experimental and different proximity potentials ($\mathrm{SSR} = \sum_{i=1}^{n} e_i^2$), where e_i is the ith residual or difference and n is the number of data points. Mean square error with respect to experiments for different proximity functions and proposed present formula ($\sigma_\epsilon^2 = \frac{SSR}{n-2}$) are shown in Table 3. From Table 3, it is

Table 1 The range of lanthanide isotopes having positive proton decay energy

Z	Range of mass number studied
57	$110 \leq A \leq 119$
58	$113 \leq A \leq 115$
59	$115 \leq A \leq 123$
60	$118 \leq A \leq 119$
61	$120 \leq A \leq 128$
62	$123 \leq A \leq 125$
63	$125 \leq A \leq 135$
64	$128 \leq A \leq 130$
65	$130 \leq A \leq 139$
66	$133 \leq A \leq 135$
67	$136 \leq A \leq 143$
68	$138 \leq A \leq 139$
69	$141 \leq A \leq 149$
70	$143 \leq A \leq 147$
71	$146 \leq A \leq 155$

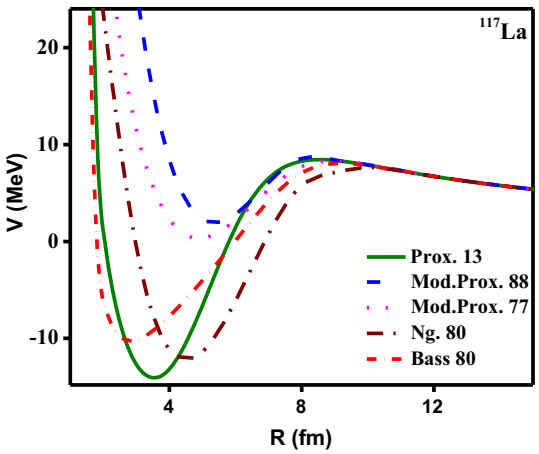

Fig. 2 Variation of potential energy as a function of R for different proximity potentials

observed that the mean square error was found to be less for Ng 80 compared to other proximity potentials. The experimental values are found to be agree well with Ng 80 among the studied proximity functions. Thus, Ng 80 proximity potential was used to study the competition between different decay modes in the lanthanide region.

We have constructed new simple empirical relation to calculate the half life of proton emitters in the lanthanide region for different isotopes of lanthanides other than the above-mentioned models. The constructed empirical formula is given in Eq. 15. The half-lives values produced with proximity function NG80 is close to the experiment. From the comparison of mean square error it shows that MP88 is better than the present empirical formula. Mean square error difference between Mp88 and Present Formula is 0.08, and it is almost negligible means both methods used to calculate half lives will produce the almost same deviation. But, to calculate half lives using the MP88 proximity function involves many physical quantities. Whereas, the present formula produces the half lives with simple inputs of Zd and Q values and this we may call pocket formula. So that the present formula is more advantageous than the MP88. The evaluated proton decay half-lives using present formula and different proximity functions along with the experiments are presented in Table 2. From this table, it is found that the present formula produces proton decay half lives close to the experiments. Proton decay energies are also presented in this Table 2.

Dominant decay mode can be identified by studying the competition between the different possible decay modes such as alpha, β^+, β^-, Spontaneous fission (SF) and proton decay. We have also calculated the half lives of possible decay modes using the well established formulae available in the literature [alpha [67], β^+ [68], β^- [68] and SF [69]].

Table 2 Comparison of evaluated proton decay half-lives using different proximity functions with that of the experiments

Proton emitter	Q_p MeV	$\log T_{1/2}$(s)						
		Expt	Ng. 80	Mp. 88	Mp. 77	Bass. 80	Prox. 13	Present formula
^{111}La $\rightarrow^{110}$ Ba	4.321	–	−3.80	−6.96	−6.82	−17.94	−17.76	−3.51
^{112}La $\rightarrow^{111}$ Ba	3.791	–	−3.62	−6.62	−6.46	−17.18	−17.03	−3.45
^{113}La $\rightarrow^{112}$ Ba	3.071	–	−3.38	−5.85	−5.67	−15.86	−15.51	−3.35
^{114}La $\rightarrow^{113}$ Ba	1.891	–	−3.13	−4.25	−4.00	−12.21	−12.07	−2.98
^{115}La $\rightarrow^{114}$ Ba	2.517	–	−3.01	−5.19	−4.99	−14.51	−14.13	−3.21
^{116}La $\rightarrow^{115}$ Ba	1.206	–	−2.77	−2.18	−1.89	−7.89	−7.76	−2.51
^{117}La $\rightarrow^{116}$ Ba	0.803	−1.63	−2.58	−2.11	−2.43	−2.99	−2.92	−2.12
^{118}La $\rightarrow^{117}$ Ba	0.378	–	−2.36	−2.33	−3.68	−2.00	−6.22	−2.13
^{113}Ce $\rightarrow^{112}$ La	1.971	–	−3.45	−4.15	−3.88	−12.32	−11.94	−2.98
^{114}Ce $\rightarrow^{113}$ La	1.491	–	−3.26	−2.91	−2.61	−9.76	−9.37	−2.71
^{115}Ce $\rightarrow^{114}$ La	0.891	–	−3.06	−0.15	−0.79	−3.94	−3.55	−2.17
^{115}Pr $\rightarrow^{114}$ Ce	3.861	–	−3.44	−6.58	−6.41	−17.03	−16.91	−3.43
^{117}Pr $\rightarrow^{116}$ Ce	2.811	–	−3.00	−5.43	−5.24	−14.95	−14.61	−3.25
^{119}Pr $\rightarrow^{118}$ Ce	1.411	–	−2.59	−2.74	−2.43	−8.98	−8.88	−2.61
^{121}Pr $\rightarrow^{120}$ Ce	0.837	−2	−2.24	0.37	0.02	−2.80	−2.43	−2.11
^{122}Pr $\rightarrow^{121}$ Ce	0.526	–	−2.05	3.44	3.79	1.11	4.00	−2.01
^{123}Pr $\rightarrow^{123}$ Ce	0.209	–	−0.56	7.73	7.58	3.93	9.76	−0.46
^{118}Nd $\rightarrow^{117}$ Pr	1.131	–	−2.89	−1.44	−1.11	−6.21	−6.15	−2.33
^{119}Nd $\rightarrow^{118}$ Pr	0.741	–	−2.71	1.36	0.50	−0.93	−0.31	−2.01
^{121}Pm $\rightarrow^{120}$ Nd	3.301	–	−2.70	−6.01	−5.82	−15.77	−15.69	−3.31
^{123}Pm $\rightarrow^{122}$ Nd	1.981	–	−2.28	−4.09	−3.81	−11.78	−11.44	−2.89
^{125}Pm $\rightarrow^{124}$ Nd	0.438	–	−1.85	5.48	6.15	2.47	6.45	−2.16
^{127}Pm $\rightarrow^{126}$ Nd	0.545	–	−1.56	3.58	3.94	1.44	4.63	−2.01
^{124}Sm $\rightarrow^{123}$ Pm	0.481	–	−2.16	5.08	5.12	2.35	6.02	−2.11
^{129}Eu $\rightarrow^{128}$ Sm	1.459	–	−1.61	−2.47	−2.14	−8.31	−7.98	−2.49
^{130}Eu $\rightarrow^{129}$ Sm	1.028	−3.05	−2.43	−0.31	−1.69	−4.14	−4.15	−2.15
^{131}Eu $\rightarrow^{130}$ Sm	0.939	−1.75	−1.28	0.04	0.40	−2.94	−2.64	−2.10
^{133}Eu $\rightarrow^{132}$ Sm	0.675	–	−0.96	2.53	3.81	0.63	1.84	−1.98
^{135}Tb $\rightarrow^{134}$ Gd	0.524	−3.03	−2.91	−4.75	5.18	2.66	6.43	−2.11
^{140}Ho $\rightarrow^{139}$ Dy	1.094	−2.23	−2.50	−0.36	0.06	−3.69	−3.44	−2.11
^{141}Ho $\rightarrow^{140}$ Dy	1.176	−2.39	−2.35	−0.61	−2.01	−4.65	−4.72	−2.16
^{144}Tm $\rightarrow^{143}$ Er	1.712	−5.73	−4.12	−6.34	−6.83	−4.11	−8.66	−5.53
^{145}Tm $\rightarrow^{144}$ Er	1.736	−5.49	−5.07	−2.59	−1.24	−8.79	−8.84	−5.63
^{150}Lu $\rightarrow^{149}$ Yb	1.27	−1.35	−1.10	−0.58	−2.28	−4.49	−4.61	−2.13
^{151}Lu $\rightarrow^{150}$ Yb	1.241	−1.09	−1.78	−0.64	−0.22	−4.19	−3.99	−2.11

Table 3 Mean square error with respect to experiments for different proximity functions and proposed present formula

Proximity function	Ng. 80	MP. 88	MP. 77	Bass. 80	Prox. 13	Present formula
σ	1.23	1.52	1.64	1.82	2.12	1.60

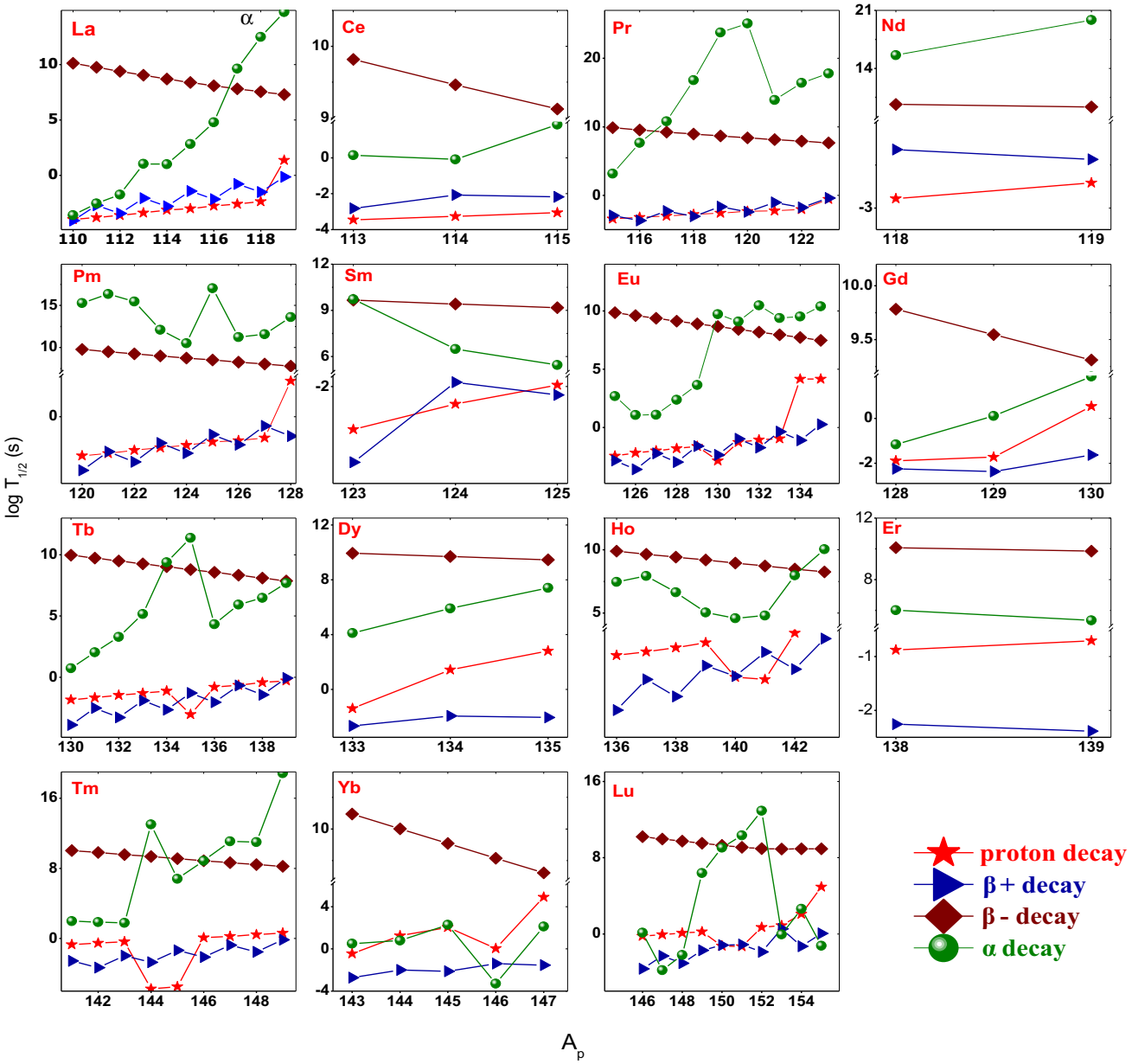

Fig. 3 Competition between different decay modes for lanthanide nuclei

The competition between different decay modes in the studied lanthanide region is shown in Fig. 3. The decay mode which is having shorter half life among the possible decay modes will be identified as the dominant decay mode. The observation of Fig. 3 clearly indicates that some isotopes of lanthanides with atomic number ranging between 57 and 63 (La, Ce, Pr, Nd, Pm, Sm and Eu) are newly identified as proton emitters in the lanthanide region, whereas the Gadollinium, Dysprosium and Erbium show $\beta+$ decay as a dominant decay mode. In Terbium, Holonium, Thullium, even though maximum isotopes are β^+ decay emitters, few of them are proton decay emitters. In Ytterbium and Lutetium, few isotopes are β^+ decay emitters and few of them are α decay emitters. The newly identified 24 proton emitters in the lanthanide region are ^{111}La, ^{112}La, ^{113}La, ^{114}La, ^{115}La, ^{116}La, ^{118}La, ^{113}Ce, ^{114}Ce, ^{115}Ce, ^{115}Pr, ^{117}Pr, ^{119}Pr, ^{122}Pr, ^{123}Pr, ^{118}Nd, ^{119}Nd, ^{121}Pm, ^{123}Pm, ^{125}Pm, ^{127}Pm, ^{124}Sm, ^{129}Eu, ^{133}Eu. The different α, β^+, existing proton emitters, nuclei with electron capture decay mode and the formula predicted new proton emitters are shown in the Nucleide chart (Fig. 4). The predicted new 24 proton emitters are highlighted in pink color, whereas α, β^+, electron capture and existing proton emitters are highlighted in yellow, green, aqua blue and brick red, respectively.

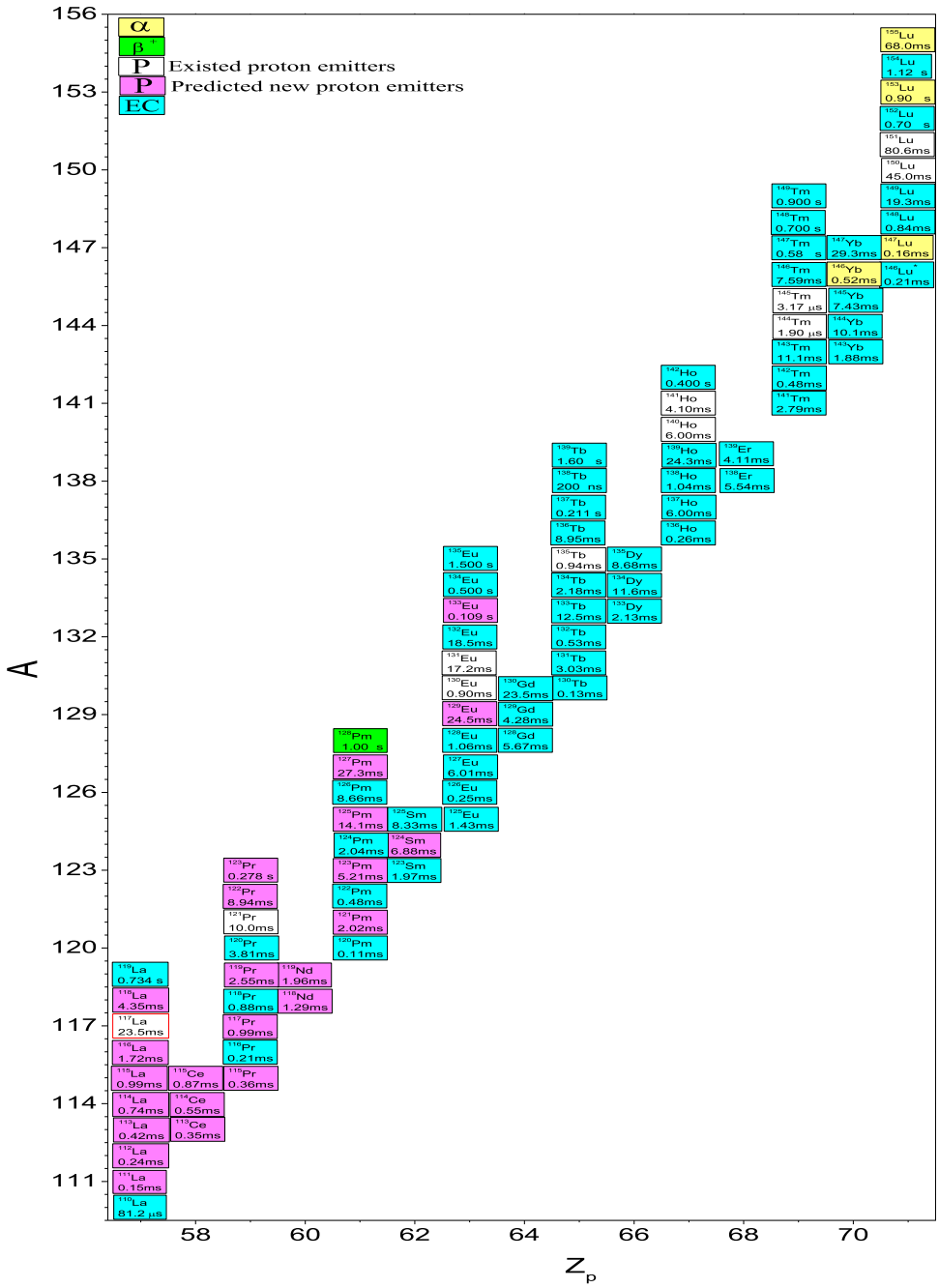

Fig. 4 Nuclide chart of Proton emitters in the lanthanide region

Proton therapy is a type of radiation used to treat cancer, and it sends positively charged atomic particles called protons [70]. This therapy is used to treat breast cancer [71, 72], brain cancer [73], head and neck cancer [74] and hepatocellular carcinoma of a liver tissue [75, 76]. Radio nuclides with different energy ranges up to 5 MeV are used in the radiotherapy [76, 77].The energy of proton is increased using accelerators.The accelerated proton beam is used in the therapy. The identified new proton emitters having decay energy between 0.378 and 4.321 MeV which clearly suggests that the proton emitters identified in the lanthanide region might find application in radiation therapy. There is a need to make progress in preclinical proton radiation biology to give accessible data to medical physicists and practicing radiation oncologists.

6. Conclusions

We have systematically studied proton decay half-lives in the lanthanide region using different proximity functions such as Prox. 13, Prox. 77, MP 77, Ng 80 and Bass 80. The competition between the evaluated proton decay half-lives with other competent decay modes such as alpha, β^+, β^-, spontaneous fission and proton decay are also studied. Eventually, 24 new proton decay emitters in the Lanthanide region are identified. Furthermore, present work also proposed empirical formula to calculate the half lives of proton emitters in the lanthanide region. Newly identified proton emitters may be useful in radiation therapy.

References

[1] A M Nagaraja, H C Manjunatha, N Sowmya, N Manjunath, and S Alfred Cecil Raj. *Eur. Phys. J. Plus* **135** 1 (2020)
[2] K P Rykaczewski. *Eur. Phys. J. A* **15** 81 (2002)
[3] K P Jackson, C U Cardinal, H C Evans, N A Jelley, and J Cerny. *Phys. Lett. B* **33** 281 (1970)
[4] S Hofmann, W Reisdorf, G Münzenberg, F P Heßberger, J R H Schneider, and P Armbruster. *Z. Phys. A Atoms Nuclei* **305** 111 (1982)
[5] T Faestermann, A Gillitzer, K Hartel, P Kienle, and E Nolte. *Phys. Lett. B* **137** 23 (1984)
[6] H Mahmud, Cary N Davids, P J Woods, T Davinson, A Heinz, G L Poli, J J Ressler, K Schmidt, D Seweryniak, M B Smith, *et al. Phys. Rev. C* **64** 031303 (2001)
[7] P J Woods, P Munro, D Seweryniak, C N Davids, T Davinson, A Heinz, H Mahmud, F Sarazin, J Shergur, W B Walters, *et al. Phys. Rev. C* **69** 051302 (2004)
[8] C J Anderson and R Ferdani. *Cancer Biother. Radiopharm.* **24** 379 (2009)
[9] V A Karnaukhov, G M Ter-Akopian, and V G Subbotin. In *Proceedings of the Third Conference on Reactions Between Complex Nuclei: Held at Asilomar (Pacific Grove, California) April 14-18, 1963*, 434. University of California Press (1963)
[10] Z Ren, C Xu, and Z Wang. *Phys. Rev. C* **70** 034304 (2004)
[11] E M Kozulin, G N Knyazheva, I M Itkis, M G Itkis, A A Bogachev, E V Chernysheva, L Krupa, F Hanappe, O Dorvaux, L Stuttgé, *et al. Phys. Rev. C* **90** 054608 (2014)
[12] T Dong and Z Ren. *Eur. Phys. J. A Hadrons Nuclei* **26** 69 (2005)
[13] M G Srinivas, H C Manjunatha, K N Sridhar, N Sowmya, and Alfred Cecil Raj. *Nucl. Phys. A* **995** 121689 (2020)
[14] K P Santhosh and C Nithya. *Phys. Rev. C* **95** 054621 (2017)
[15] G R Sridhar, H C Manjunatha, N Sowmya, P S Damodara Gupta, and H B Ramalingam. *Eur. Phys. J. Plus* **135** 1 (2020)
[16] E A Quadrelli. *Inorg. Chem.* **41** 167 (2002)
[17] J M Nitschke, P A Wilmarth, J Gilat, P Möller, and K S Toth. In *AIP Conference Proceedings*, volume 164 (American Institute of Physics), pp 697–707 (1987)
[18] C N Davids, P J Woods, D Seweryniak, A A Sonzogni, J C Batchelder, C R Bingham, T Davinson, D J Henderson, R J Irvine, G L Poli, *et al. Phys. Rev. Lett.* **80** 1849 (1998)
[19] N Sowmya and H C Manjunatha. *Phys. Particles Nuclei Lett.* **17** 370 (2020)
[20] M Bhattacharya and G Gangopadhyay. *Phys. Lett. B* **651** 263 (2007)
[21] Y-B Qian, Z-Z Ren, D-D Ni, and Z-Q Sheng. *Chin. Phys. Lett.* **27** 112301 (2010)
[22] J-M Dong, H-F Zhang, W Zuo, and J-Q Li. *Chin. Phys. C* **34** 182 (2010)
[23] M Balasubramaniam and N Arunachalam. *Phys. Rev. C* **71** 014603 (2005)
[24] J M Dong, H F Zhang, and G Royer. *Phys. Rev. C* **79** 054330 (2009)
[25] H-F Zhang, J-M Dong, Y-Z Wang, X-N Su, Y-J Wang, L-Z Cai, T-B Zhu, B-T Hu, W Zuo, and J-Q Li. *Chin. Phys. Lett.* **26** 072301 (2009)
[26] A Zdeb, M Warda, C M Petrache, and K Pomorski. *Eur. Phys. J. A* **52** 323 (2016)
[27] K P Santhosh and I Sukumaran. *Phys. Rev. C* **96** 034619 (2017)
[28] Q Zhao, J M Dong, J L Song, W H Long, *et al. Phys. Rev. C* **90** 054326 (2014)
[29] Y J Yao, G L Zhang, W W Qu, and J Q Qian. *Eur. Phys. J. A* **51** 122 (2015)
[30] D Bai and Z Ren. *Phys. Rev. C* **103** 044316 (2021)
[31] V Zanganeh, R Gharaei, and A M Izadpanah. *Nucl. Phys. A* **992** 121637 (2019)
[32] K P Santhosh and A Joseph. *Pramana* **59** 679 (2002)
[33] I Dutt and R K Puri. *Phys. Rev. C* **81** 064609 (2010)
[34] C Xu and Z Ren. *Phys. Rev. C* **74** 014304 (2006)
[35] D Ni and Z Ren. *Phys. Rev. C* **81** 024315 (2010)
[36] C Xu and Z Ren. *Phys. Rev. C* **75** 044301 (2007)
[37] Y Qian and Z Ren. *J. Phys. G: Nucl. Particle Phys.* **39** 115106 (2012)
[38] D Ni, Z Ren, T Dong, and Y Qian. *Phys. Rev. C* **87** 024310 (2013)
[39] Y Qian, Z Ren, and D Ni. *Phys. Rev. C* **89** 024318 (2014)
[40] M Ismail, A Y Ellithi, M M Botros, and A Adel. *Phys. Rev. C* **81** 024602 (2010)
[41] Y Qian and Z Ren. *Sci. China Phys. Mech. Astron.* **56** 1520 (2013)
[42] G L Zhang, H B Zheng, and W W Qu. *Eur. Phys. J. A* **49** 10 (2013)
[43] C L Guo and G L Zhang. *Eur. Phys. J. A* **50** 187 (2014)
[44] J Błocki, J Randrup, W J Światecki, and C F Tsang. *Ann. Phys.* **105** 427 (1977)
[45] K Sharma, G Sawhney, M K Sharma, and R K Gupta. *Eur. Phys. J. A* **55** 1 (2019)
[46] M Aygün. *Turk. J. Phys.* **42** 302 (2018)
[47] W D Myers and W J Światecki. *Phys. Rev. C* **62** 044610 (2000)
[48] W Reisdorf. *J. Phys. G: Nucl. Particle Phys.* **20** 1297 (1994)
[49] I Dutt. *Pramana* **76** 921 (2011)
[50] K P Santhosh and B Priyanka. *Phys. Rev. C* **87** 064611 (2013)
[51] K P Santhosh, J G Joseph, and S Sahadevan. *Phys. Rev. C* **82** 064605 (2010)
[52] K P Santhosh, B Priyanka, J G Joseph, and S Sahadevan. *Phys. Rev. C* **84** 024609 (2011)
[53] K P Santhosh, B Priyanka, and M S Unnikrishnan. *Phys. Rev. C* **85** 034604 (2012)
[54] H Ngô and C H Ngô. *Nucl. Phys. A* **348** 140 (1980)
[55] K Sharma and M K Sharma. *Nucl. Phys. A* **986** 1 (2019)
[56] O K Ganiev and A K Nasirov. *J. Phys. G: Nucl. Particle Phys.* **47** 045115 (2020)
[57] R Bass. *Phys. Rev. Lett.* **39** 265 (1977)
[58] M Aygun. *Rev. Mex. Fís. E* **64** 149 (2018)
[59] N Deb. *J. Appl. Fundam. Sci.* **5** 49 (2020)
[60] G L Zhang, Y J Yao, M F Guo, M Pan, G X Zhang, and X X Liu. *Nucl. Phys. A* **951** 86 (2016)
[61] R Kumar and M K Sharma. *Phys. Rev. C* **85** 054612 (2012)
[62] V Zanganah, D T Akrawy, H Hassanabadi, S S Hosseini, and S Thakur. *Nucl. Phys. A* **997** 121714 (2020)

[63] N S Rajeswari and M Balasubramaniam. *Eur. Phys. J. A* **50** 1 (2014)
[64] N S Rajeswari, I Sreeja, and M Balasubramaniam. In *Proceedings of the DAE-BRNS Symposium on Nucl. Phys*, volume 61, p 422 (2016)
[65] I Mehrotra and S Prakash (2008)
[66] M M N Rodrigues, N Teruya, and S B Duarte. In *AIP Conference Proceedings*, volume 1529 (American Institute of Physics), pp 174–177 (2013)
[67] J-G Deng, H-F Zhang, G Royer, *et al. Phys. Rev. C* **101** 034307 (2020)
[68] Z-Q Sheng, L-P Shu, Y Meng, J-G Hu, and J-F Qian. *Chin. Phys. C* **38** 124101 (2014)
[69] Z Ren and C Xu. *Nucl. Phys. A* **759** 64 (2005)
[70] M Mashayekhi, A A Mowlavi, and S B Jia. *Rep. Pract. Oncol. Radiother.* **22** 52 (2017)
[71] A Dasu, A M Flejmer, A Edvardsson, and P W Nyström. *Phys. Med.* **52** 81 (2018)
[72] K K Mishra and I K Daftari. *Chin. Clin. Oncol.* **5** 50 (2016)
[73] K J Stelzer. *Neurosurg. Clin.* **11** 597 (2000)
[74] J Phan, T T Sio, T P Nguyen, V Takiar, G B Gunn, A S Garden, D I Rosenthal, C D Fuller, W H Morrison, B Beadle, *et al. Int. J. Radiat. Oncol. Biol. Phys.* **96** 30 (2016)
[75] S Sugahara, Y Oshiro, H Nakayama, K Fukuda, M Mizumoto, M Abei, J Shoda, Y Matsuzaki, E Thono, M Tokita, *et al. Int. J. Radiat. Oncol. Biol. Phys.* **76** 460 (2010)
[76] J Constanzo, M Vanstalle, C Finck, D Brasse, and M Rousseau. *Med. Phys.* **46** 2356 (2019)
[77] F Rösch. *Radiochim. Acta* **95** 303 (2007)

ScienSage

Journal of Advanced Scientific Research

Available online through http://www.sciensage.info

ISSN
0976-9595
Research Article

PROTON RADIOACTIVITY OF TANTALUM

M.G. Srinivas[1,3], N. Sowmya[2], H.C.Manjunatha[2], N. Manjunatha*[2], S. Alfred Cecil Raj[3]

[1]*Department of Physics, Government First Grade College, Mulbagal, Karnataka, India*

[2]*Department of Physics, Government College for Women, Kolar, Karnataka, India*

[3]*Department of Physics, St. Joseph's college, Affiliated To Bharathidasan University, Tiruchirappalli, TamilNadu, India*

**Corresponding author: manjunathhc@rediffmail.com, sowmyaprakash8@gmail.com*

ABSTRACT

Using different models such as Coulomb and proximity potential model, effective liquid drop model and modified generalised liquid drop model, we have studied all possible one proton radioactivity tantalum. The calculated half-lives from the present work are compared with the available experiments. One proton decay energy is studied using recent mass excess values [Chinese Physics C Vol. 45, No. 3 (2021) 030003]. The angular momentum dependence of potential have been considered. The penetration probability (P) is studied using WKB integral. The decay constant (λ) and half-lives ($T_{1/2}$) of $^{151\text{-}157}$Ta were predicted. The identified one proton radioactivity of $^{151\text{-}157}$Ta along with half-lives and decay energies plays an important role in the future experiments. Present work may find useful applications in radiotherapy and diagnosis.

Keywords: Proton decay, Half-lives, Penetration probability, Decay constant.

1. INTRODUCTION

Proton decay is one of the key predictions of the various grand unified theories (GUTS) proposed in the1970s, another major one being the existence of magnetic monopoles. Both concepts have been the focus of major experimental physics efforts since the early 1980s. The proton decay hypothesis was first formulated by Andrei Sakharov in 1967 [1]. During the year 1981 at GSI Darmstadt one proton(1P) ground decay was observed [2]. Half-lives of proton emission of nuclei such as ^{151}Lu, ^{53}Co and so on have been studied [3, 4]. A many theoretical models [5-9] have been made used to study 1P-decay. M.Pfutzner et al., [10] observed the decays of fine ^{45}Fe atoms at the fragment separator of GSI. Bajc et al., [11] systematically studied proton decay in the minimal super symmetric SU(5) grand unified theory. Goldman and Ross [12] predicted theoretical upper limit for proton decay. Two proton decay of ^{67}Kr is experimentally observed [13]. The life time of proton has been identified by earlier researchers [14]. Santosh & Indu sukumaran [15] theoretically predicted half-lives of proton emitters with the atomic number of Z>50. The proton radioactivity has been studied using various proximity potentials [16]. Experimental evidence shows proton drip line of ^{45}Fe [17]. After bombardment of ^{92}Mo target nuclei with ^{50}C, Woods et al. [18] observed proton decay [18]. Developmental theories of proton decay has been predicted by Maglione et al., [19]. Detail analysis of proton decay has been by Rykaczewskia et al., [20]. Ferreira et al., [21] based on relativistic density functional theory, the proton radioactivity from spherical nuclei were studied.

Delion et al., [22] examined the characteristics of nuclear matter by reviewing proton emission hypotheses. Recent literature [23-25] also predicts proton emitters in the atomic number range 72<Z<88 and actinides. Many theoretical studies shows the prediction of possible decay mode in the superheavy region [26-38]. Hence, in the present work we made an attempt to study one proton radioactivity of Tantalum using different models such as Coulomb and proximity potential model (CPPM), effective liquid drop model (ELDM) and modified generalised liquid drop model (GLDM).

2. THEORETICAL FRAMEWORK

2.1. Proton emission half-lives

2.1.1. 1P-decay using Coulomb and proximity potential model (CPPM)

The one proton decay is expressed as;

$$ {}^{A}_{Z}(X)_N \rightarrow {}^{A-1}_{Z-1}(Y)_N + {}^{1}_{1}(H) + Q_P \qquad (1) $$

where Q_P is the amount of energy released during 1P decay. The decay constant and half-lives are defined as

$$T_{1/2} = \frac{\ln 2}{\lambda} = \frac{\ln 2}{\nu P P_0} \quad (2)$$

where ν is the assault frequency [39], P is the probability of penetration barrier and P_0 is the preformation probability. In the present work we have selected P_0=1 for one proton decay. The penetration probability using WKB approximation [40] is given by;

$$P = \exp\left[-\frac{2}{\hbar}\int_{Rin}^{Rout}\sqrt{2\mu(V-Q_P)}dr\right] \quad (3)$$

where μ is reduced mass, R_{in} and R_{out} are the inner and outer turning points. The inner turning point R_{in} is expressed as;

$$R_{in} = r_0(A_1^{1/3} + A_2^{1/3}) \quad (4)$$

where A_1=1 and A_2=A-1 for proton emission. R_{out} is determined by the condition $V = Q$. The r_0 is the effective nuclear constant. The total potential is evaluated as explained in [25].

2.1.2. 1P-decay using Effective liquid drop model (ELDM)

$$V_C = \frac{8\pi}{9}a^5\varepsilon(\theta_{2p},\theta_D)\rho_c \quad (5)$$

where ρ_c is the initial charge density, $\varepsilon(\theta_{2p}, \theta_D)$ is a function of the angular variables, and a is the radius of the sharp neck. The surface potential energy is expressed as;

$$V_s = \sigma_{eff}(S_{2P} + S_D) \quad (6)$$

The term effective surface tension σ_{eff} is expressed as;

$$\frac{3}{5}e^2\left[\frac{Z_P^2}{R_p} - \frac{Z_{1p}^2}{\bar{R}_{2P}} - \frac{Z_D^2}{R_D}\right] + 4\pi\sigma_{eff}\left(R_p^2 - \bar{R}_{1p}^2 - \bar{R}_D^2\right) = Q \quad (7)$$

Where Z_p is the atomic number of parent nuclei, Z_{1p} is the atomic number of emitted proton and Z_D is the atomic number of daughter nuclei and other notations are as usual explained in reference [33]. The effect of the centrifugal potential energy is defined as;

$$V_\ell = \frac{\ell(\ell+1)\hbar^2}{2\mu\zeta^2} \quad (8)$$

Here μ represents the reduced mass of the system. Therefore, the effective total potential energy is constructed as;

$$V = V_C + V_s + V_\ell \quad (9)$$

The penetrability factor G is evaluated as explained in reference [33].

2.1.3. 1P-decay using Modified generalised liquid drop model (MGLDM)

The total energy of the system is given by;

$$E = E_V + E_S + E_C + E_{Prox} + E_l \quad (10)$$

The total potential is evaluated is evaluated as explained in reference [33]

The barrier penetration probability is expressed as;

$$P = \exp[-\frac{2}{\hbar}\int_{R_{in}}^{R_{out}}\sqrt{2B(r)(E(r)-E(sphere)]} \quad (11)$$

Where $R_{in} = R_d + R_\alpha$ and $B(r) = \mu$ is the reduced mass and $R_{out} = e^2 Z_d Z_\alpha / Q_\alpha$. The decay half-life is defined as;

$$T_{1/2} = \frac{\ln 2}{\lambda} = \frac{\ln 2}{\nu_0 P} \quad (12)$$

here ν_0 is the assault frequency and whose value is 10^{20} S^{-1} and P is the barrier penetration probability.

3. RESULTS AND DISCUSSIONS

Using three models such as CPPM, ELDM and MGLDM, we have studied proton decay from the proton rich emitter Tantalum. The 1P-decay is energetically possible only when Q-value of the reaction is positive. The decay energy is evaluated using the following equation;

$$Q = \delta M_p - (\delta M_d + \delta M_z) + k(Z_P^\varepsilon - Z_d^\varepsilon) \quad (13)$$

where δM_P is the mass excess of the parent nuclei, δM_d is the mass excess of the daughter nuclei and δM_z is the mass excess of the emitted proton. The term $kZ_{p(d)}^\varepsilon$ is the total binding energy of electrons in the parent or daughter nuclei. The value of k=13.6 eV and ε=2.408 for the nuclei Z≤60 and k=8.7eV and ε=2.517 for the nuclei Z>60 [25]. The recent mass excess values are taken from the reference [42]. Fig. 1 shows a plot of Q-values during 1P-decay with the mass number of parent nuclei. The minimum Q-value is observed in case of ^{157}Ta with 0.941MeV and maximum is observed for ^{151}Ta with 2.361MeV when compared to their neighboring one.

Then, we have calculated total potential using three models in nuclei $^{151\text{-}157}$Ta, the studied potential as function of separation distance is shown in Fig. 2. From the Fig., the minimum potential is observed when the separation energy is 6.5fm. Then the potential gradually increases and area below the curve gives information on penetration probability.

Later, the evaluated penetration probability and 1P-decay half-lives in $^{151-157}$Ta using three models and were tabulated in table 1. The evaluated $\log T_{1/2}$ value varies between -11.21s to -0.35s in case of CPPM. However, in case of ELDM it varies between -10.55s to -0.58s and in case of MGLDM the $\log T_{1/2}$ varies between -10.18s to -0.51s for the nuclei $^{151-157}$Ta. The values obtained using present work is compared with the available experimental value [43]. The studied $\log T_{1/2}$ corresponding to $^{155-157}$Ta shows close agreement with the available experimental values. However, the value obtained using MGLDM produces experimental half-lives more accurately.

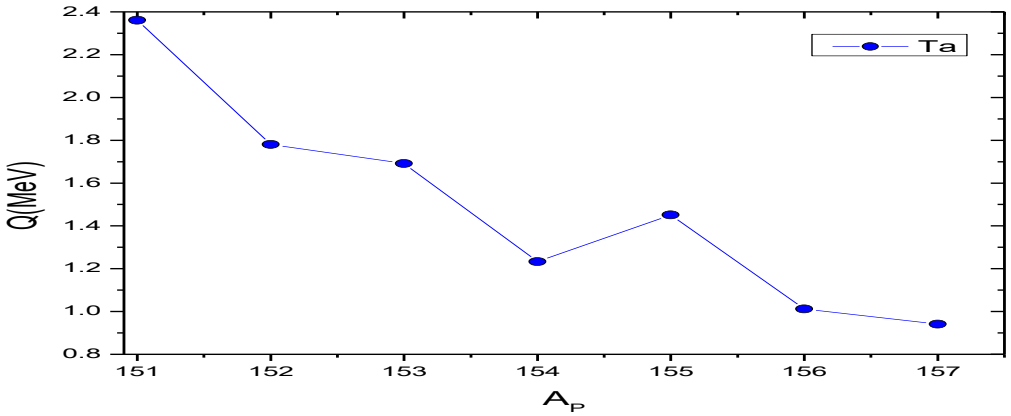

Fig. 1: A plot of Q-values during 1P- decay with the mass number of parent nuclei for the $^{151-157}$Ta nuclei

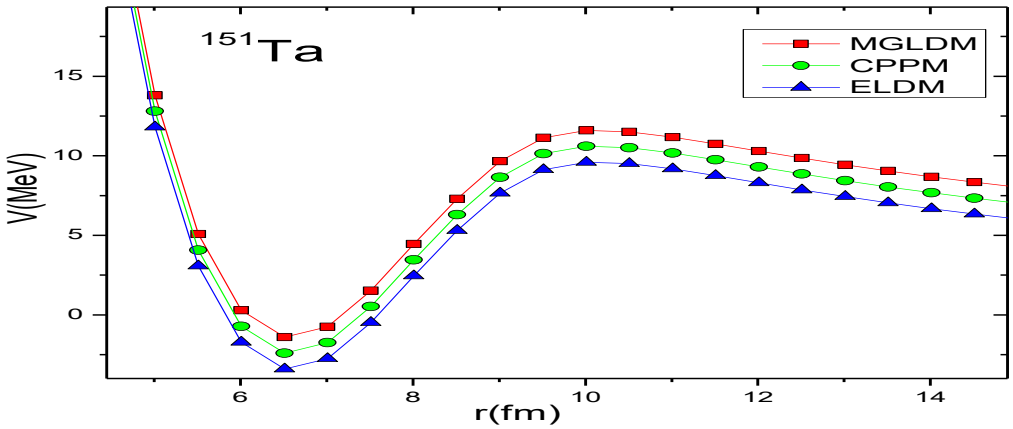

Fig. 2: Variation of total potential using three models such as CPPM, ELDM and MGLDM as function of separation distance in ^{151}Ta nuclei

Table 1: Tabulation of $\log T_{1/2}$ using three different models such as CPPM, ELDM and MGLDM for predicted proton emitters from $^{151-157}$Ta is compared to available experiments.

Parent nuclei	Daughter nuclei	Q(MeV)	ℓ	$\log T_{1/2}$			
				Expt [43]	CPPM	ELDM	MGLDM
^{151}Ta	^{150}Hf	2.361	5	-	-11.21	-10.55	-10.18
^{152}Ta	^{151}Hf	1.781	5	-	-8.67	-7.46	-7.9
^{153}Ta	^{152}Hf	1.691	5	-	-5.6	-5.84	-7.43
^{154}Ta	^{153}Hf	1.233	5	-	-5.28	-4.03	-4.1
^{155}Ta	^{154}Hf	1.451	5	-2.49	-2.68	-2.12	-2.51
^{156}Ta	^{155}Hf	1.012	2	-0.83	-0.55	-0.5	-0.85
^{157}Ta	^{156}Hf	0.941	0	-0.53	-0.35	-0.58	-0.51

4. CONCLUSIONS

Using three different models 1P-radioactivity tantalum is studied. The calculated half-lives from the present work are compared with the available experiments. The decay energy is feasible for the nuclei $^{151-157}$Ta. The angular momentum corresponding to these isotopes varies between 0 to 5 $\hbar$. The evaluated logarithmic half-life value varies between -11.21s to -0.35s in case of CPPM, in case of ELDM it varies between -10.55s to -0.58s and in MGLDM the logarithmic half-lives varies between -10.18s to -0.51s for the nuclei $^{151-157}$Ta. The identified 1P-radioactivity of $^{151-157}$Ta along with half-lives and decay energies plays an important role in the future experiments. The identified proton emitters with typical half-lives and decay energies may find useful applications in radiotherapy and diagnosis.

5. REFERENCES

1. Borut Bajc , Junji Hisano, Takumi Kuwahara , Yuji Omura. *Nuclear Physics B*, 2016; **910:**1-22.
2. Klepper O, Batsch T, Hofmann S, Kirchner R, Kurcewicz W, Reisdorf W et al. *Z Phys A*, 1982; **305**:125-130.
3. Pfutzner M , Karny M , Grigorenko LV, Riisager K. *Rev.Mod.Phys*, 2012; **84**:567-619.
4. Robinson AP, Davids CN, Mukherjee G, Seweryniak D, Sinha S, Wilt P et al. *Phys Rev C*, 2003; **68**:054301.
5. Buck B, Merchant AC, Perez SM. *Phys Rev C*, 1992; **45**:1688.
6. Aberg S, Semmes PB, Nazarewicz W. *Phys Rev C*, 1997; **56**:1762.
7. Guzman F, Goncalves M, Tavares OAP, Duarte SB, Garcia F, Rodriguez O. *Phys Rev C,* 1999; **59**:R2339.
8. Balasubramanyam M, Arunachalam N. *Phys Rev C* , 2005;**71**:014603.
9. Basu DN, Roy Chowdhury P, Samanta C. *Phys Rev C* , 2005;**72**:051601.
10. Pfutzner M, Badura E, Bingham C, Blank B, Chartier M, Geissel H et al. *Eur Phys J A - Hadrons and Nuclei,* 2002;**14:**279-285.
11. Borut Bajc, Pavel Fileviez Perez, Goran Senjanovic. *Phys Rev* D, 2002; **66**:075005.
12. Goldman TJ, Ross DA. *Physics Letters B*, 1979; **84**:208-210.
13. Goigoux T et al. *Phys Rev Lett* , 2016;**117**:162501.
14. Grigorenko LV, Wiser TD, Miernik K, Charity RJ, Pfutzner M, Banu A et al. *Physics Letters B* ,2009; **677**:30-35.
15. Santhosh KP, Indu Sukumaran. *Phys Rev C*, 2017; **96**:034619.
16. Jun Gang Deng, Xiao Hua Li, Jiu Long Chen, Jun Hao Cheng, XiJun Wu. *Eur Phys J A***,** 2019; **55**:58.
17. Giovinazzo J, Blank B, Chartier M, Czajkowski S, Fleury A, Lopez Jimenez MJ et al. *Phys Rev Lett*, 2002; **89**:102501.
18. Woods PJ, Munro P, Seweryniak D, Davids CN, Davinson T, Heinz A et al. *Phys Rev C*, 2004; **69**: 051302.
19. Maglione E, Ferreira LS. *Eur Phys J A* , 2002;**15:**89-92.
20. Rykaczewskia KP. *Eur Phys J A* , 2002;**15**:81-84.
21. Ferreira LS, Maglione E, Ring P. *Physics Letters B*, 2011; **701**:508-511.
22. Delion DS, Liotta RJ, Wyss R. *Physics Reports*, 2006; **424**:113-174.
23. Manjunatha HC, Srinivas MG, Sowmya N, Damodaragupta PS, Alfred Cecil Raj. *Physics of particles and Nuclei Letters*, 2020; **17:**909-915.
24. Srinivas MG, Manjunatha HC, Sowmya N, Damodaragupta PS, Alfred Cecil Raj. *Indian J Pure Appl Phys*, 2020; **58**:255-262.
25. Srinivas MG, Manjunatha HC, Sridhar KN, Sowmya N, Alfred Cecil Raj. *Nuclear Physics A,* 2020; **995**: 121689.
26. Manjunatha HC, Sowmya N. *Nuclear Physics A*, 2018; **969**:68-82.
27. Manjunatha HC, Sowmya N. *Int J Mod Phys E*, 2018; **27**:1850041.
28. Manjunatha HC, Sridhar KN, Sowmya N. *Phys Rev C*, 2018; **98**:024308.
29. Sowmya N, Manjunatha HC. *Bulg J Phys*, 2019; **46**:16-27.
30. Manjunatha HC, Sowmya N, Sridhar KN, Seenappa L. *J Radioanal Nucl Chem*, 2017; **314**:991-999.
31. Sowmya N, Manjunatha HC, Dhananjaya N. *J Radioanal Nucl Chem*, 2020; **323**:1347-1351.
32. Sowmya N, Manjunatha HC, Damodara gupta PS. *Int J Mod Phys E*, 2020; **29**: 10 2050087.
33. Sowmya N, Manjunatha HC. *Braz Jour of Phys,* 2020; **50**:317.
34. Sowmya N, Manjunatha HC. *Braz Jour of Phys,* 2019; **49**:874-886.
35. Sridhar GR, Manjunatha HC, Sowmya N, Gupta PSD, Ramalingam HB. *Eur Phys J Plus*, 2020; **135**:291.
36. Sowmya N, Manjunatha HC. *Phys of Part and Nuclei Lett,* 2020; **17**:370.
37. Manjunatha HC, Seenappa L, Damodara gupta PS, Sridhar KN, Chinappa Reddy B. *Braz Jour of Phys,* 2021; **51**:764-772.
38. Manjunatha HC, Sowmya N, Manjunath N , Seenappa L. *Int J Mod Phys E*, 2020; **29**:2050028.

39. Poenaru DN, Gherghescu RA, Greiner W. *Phys Rev C*, 2011; **83**:014601.
40. Blocki J, Randrup J, Swiatecki WJ, Tsang CF. *Ann Phys,1977;* **105**:427-462.
41. Dutt I, Puri RK. *Phys Rev C*, 2010; **81**:047601.
42. Meng Wang, Huang WJ, Kondev FG, Audi G, Naimi S. *Chinese Phys C* , 2021; **45**:030003.
43. Santhosh KP, Indu Sukumaran. *Eur Phys JA*, 2018; **54**:102.

64th DAE BRNS SYMPOSIUM ON NUCLEAR PHYSICS

Volume 64 (2019)

Department of Physics, University of Lucknow

23rd - 27th December, 2019

Editors

Yogesh K. Gupta, P. C. Rout,
L. M. Pant, B. K. Nayak

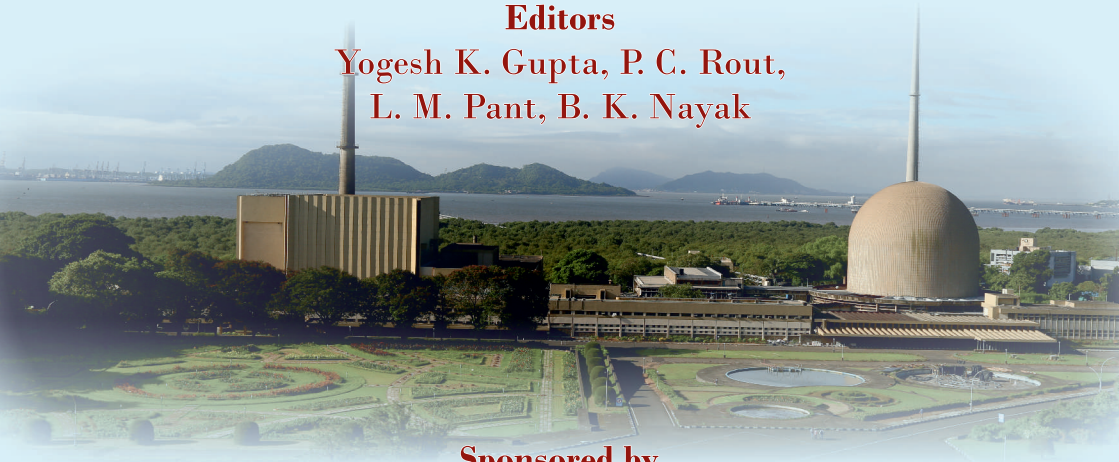

Sponsored by

Board of Research in Nuclear Sciences,
Department of Atomic Energy, Government of India

Proton radioactivity of $^{241\text{-}251}$Db

M.G.Srinivas[1], H.C.Manjunatha[2*], K.N.Sridhar[3], N.Sowmya[2], Alfred Cecil Raj[4]
1Department of Physics, Government First Grade College, Mulbagal-563131 Karnataka, INDIA
2Department of Physics, Government College for Women, Kolar-563101 Karnataka, INDIA
3Department of Physics, Government First Grade College, Kolar-563101 Karnataka, INDIA
4Department of Physics, St.Joseph's college (autonomous), Thiruchirapalli, Tamilnadu, India

Introduction

In the line of stability, the excess protons still adequately bound to the nucleus with the nuclear forces, hence direct emission of proton is not possible. However, while beyond the line of stability the protons are no longer bound by the nuclear forces. In order to study the proton emission beyond the stability line Conclaves et al., [1] studied two-proton radioactivity in the mass number A<70 using liquid drop model. Earlier [2-3] studied proton emission from the deformed nuclei. One proton, two proton, β decay [4-8] were studied using droplet model and WKB approximation. Giusti et al., [9] established theoretical frame work for the emission of two protons in electron induced reactions. Using generalized liquid drop model and WKB approximation, Dong et al., [10] theoretically studied proton decay half-lives of spherical proton emitters.

Previous workers [11-12] theoretically studied half-lives of proton radioactivity. Earlier workers [13-17] were studied ternary fission, binary fission, cluster radioactivity and alpha decay in the superheavy region using different proximity functions. From the available literature, it is essential to study the proton radioactivity in the Dubnium. Hence, in the present work we made a first attempt to study proton radioactivity in the isotopes of Dubnium.

Theory:

The half-lives of proton is studied using the following expression,

$$T_{1/2} = \frac{hLn(2)}{2\pi\Gamma} \qquad (1)$$

here Γ is the decay width and it is calculated using the relation

$$\Gamma = \frac{S\overline{F}h^2\overline{P}}{16\pi^2 m} \qquad (2)$$

here S, F and P are spectroscopic, normalisation and penetration factor respectively and in detail explained in previous work [18].The average normalization factor is expressed as [18]

$$\overline{F} = \frac{2}{\pi}\int_0^{\pi/2} F(\theta)d\theta \qquad (3)$$

where F(ɵ) is angle dependent normalization factor.

$$\overline{P} = \int_0^{\pi/2} P(\theta)\sin(\theta)d\theta \qquad (4)$$

The total potential is the sum of nuclear, coulomb and centrifugal terms [16].

Results and discussions:

The amount of energy released during one-proton radioactivity is studied using the mass excess values available in the literature [16,19]. We have also studied penetration factor (P), normalization factor (F) and logarithmic half-lives for proton decay in the heavy nuclei of $^{241\text{-}251}$Db. We have also studied the spontaneous fission half-lives and alpha decay half-lives of the heavy nuclei of $^{241\text{-}251}$Db. The comparison of the proton decay with the spontaneous fission and alpha decay half-lives are as shown in figure 1. From the figure we have observed that the spontaneous fission half-lives are smaller compared to proton and alpha decay.

The figure 2(a) explains the variation of amount of energy released with the mass number of parent nuclei and it decreases with increase in the mass number of parent nuclei, 2(b), 2(c) represents the penetration probability and normalization factor with the mass number of parent nuclei and both decreases with the increase in mass number of parent nuclei and 2(d) depicts the variation of logarithemic half-

lives with the product of atomic number and energy released during proton decay.

We have studied proton decay in the heavy nuclei $^{241\text{-}251}$Db. From the figure 1 and 2 it is observed that the proton decay half-lives are also longer than that of spontaneous fission and alpha decay. The competition of proton decay with different decay modes such as alpha decay and spontaneous fission reveals that proton decay is not dominant decay mode in the heavy nuclei $^{241\text{-}251}$Db.

Fig. 1: The variation of logarithemic half-lives of the proton decay, spontaneous fission and alpha decay with the mass number of parent nuclei

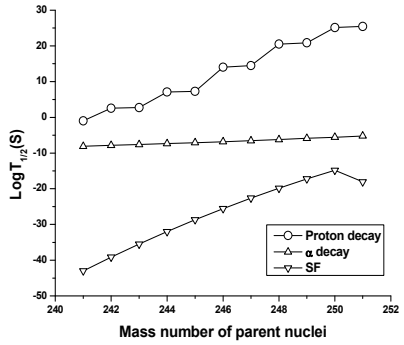

Fig. 2: The variation of amount of energy released, penetration probability and normalization factor with the mass number of parent nuclei and the variation of logarithemic half-lives with the product of atomic number and energy released during proton decay.

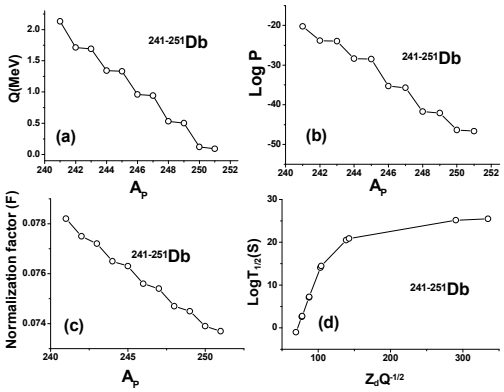

Conclusions:

To summarize the present work, we have studied amount of energy released during the proton decay, penetration probability, normalization factor and logarithemic half-lives in the heavy nuclei of $^{241\text{-}251}$Db. We have also compared present work with the spontaneous fission and alpha decay. From the results we can conclude that the heavy nuclei of $^{241\text{-}251}$Db are having half-lives greater than the spontaneous fission and alpha decay. Hence, the heavy nuclei $^{241\text{-}251}$Db is stable against the proton decay.

References

[1] M.Gonçalves, N.Teruya, Phys. lett.B 774,14(2017)
[2]D.S.Delion,R.J.Liotta,Phys. Reports 424,113(2006)
[3] E.Maglione, L.S.Ferreira, Phys. Rev. C 59, R589(R) (1999)
[4] M.DelSanto,Z.Meisel,Phys. Lett. B 738, 453(2014)
[5] S.A.Alavi, V.Dehghani, Nucl. Phys.A 977,49(2018)
[6] G.Raciti, M.De Napoli, et al., Nucl. Phys.A A83, 4464(2010)
[7] D.Baye, E.M.Tursunov, Physics Letters B 6964642011: 464-467(2011)
[8] W.F.Feix, E.R.Hilf, Physics Letters B 120(1983)14.
[9] C.Giusti, F.D.Pacati,, Nuclear Physics A 535(1991)573.
[10] J. M. Dong, H. F. Zhang, and G. Royer Phys. Rev.C79,054330 (2009).
[11] C.Giusti, F.D.Pacati,, Nuclear Physics A 535(1991)573.
[12] B.Ludewigt, R.Glasow, H.Löhner, R.Santo Nuclear Physics A 408(1983)359.
[13] H.C Manjunatha, N.Sowmya, K.N. Sridhar, L. Seenappa, J. Radioanal Nucl.Chem. 314(2): 991-999(2017).
[14] H.C Manjunatha, N.Sowmya, Nucl Phy A 969:68–82(2018).
[15] H.C Manjunatha, N.Sowmya, Inter Jou of Mod Phy E 27(5), 1850041:1-17, (2018).
[16] H.C Manjunatha, K.N.Sridhar, N. Sowmya Phy Rev C 98: 024308(2018).
[17] K. N. Sridhar, H. C. Manjunatha, H. B. Ramalingam, Phys. Rev. C 98, 064605 (2018).
[18] D.S. Delion, Theory of Particle and Cluster Emission, Springer-Verlag, Berlin Heidelberg, 2010.
[19] https://www-nds.iaea.org/RIPL-3.

Contact : Dr. Yogesh K. Gupta
Dr. P. C. Rout
Dr. L. M. Pant
Dr. B. K. Nayak

Printed by : **Prudent Arts & Fab Pvt. Ltd.**
A-221, TTC Industrial Area,
Opp. Anthony Motors Pvt. Ltd.,
M.I.D.C., Mahape, New Mumbai - 400701
Tel : +91 99302 00043 / 42

ISBN 818372083-A
9 788183 720830

65th DAE BRNS SYMPOSIUM ON NUCLEAR PHYSICS

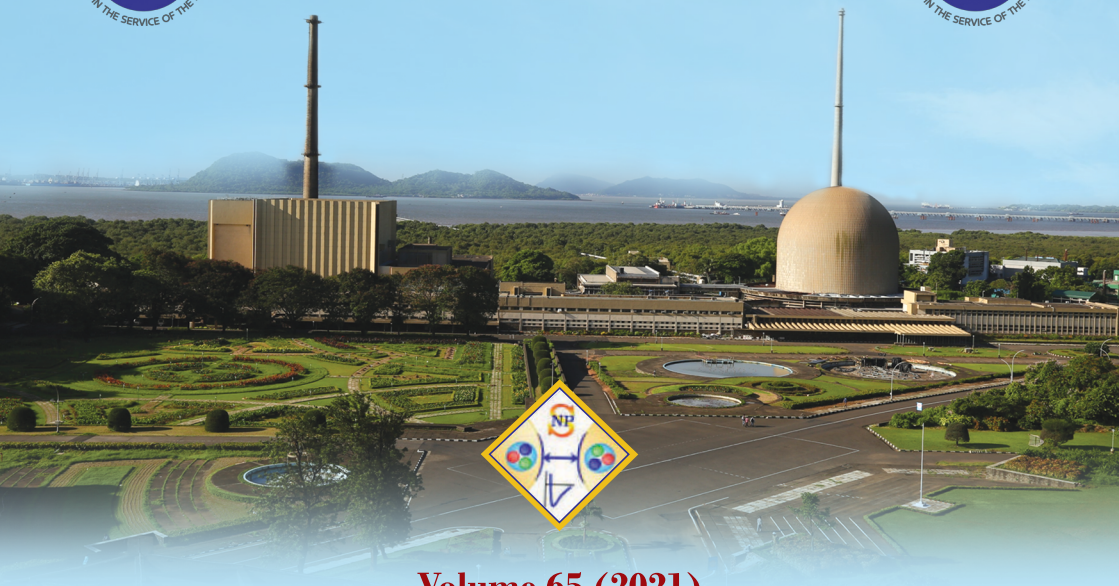

Volume 65 (2021)

DAE Convention Centre Anushaktinagar, Mumbai

December 1 - 5, 2021

Editors

Yogesh K. Gupta, R. R. Sahu,

S. Santra, A. K. Gupta

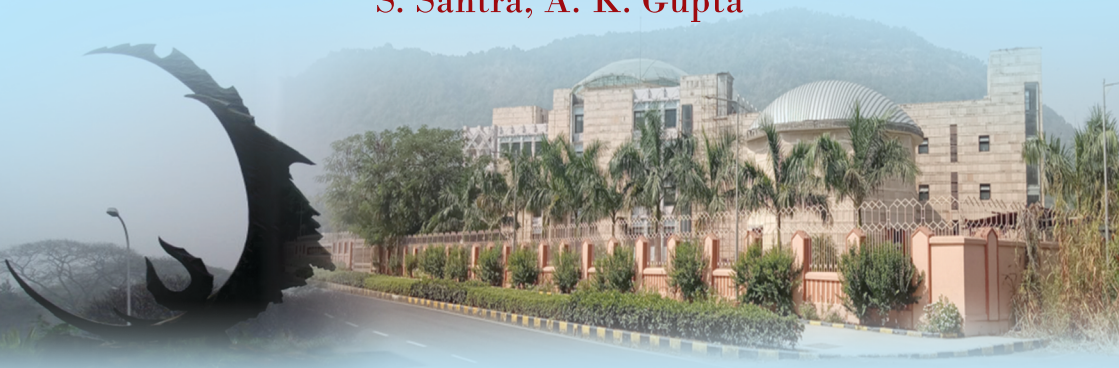

Sponsored by

Board of Research in Nuclear Sciences,

Department of Atomic Energy, Government of India

Competition between different decay modes in Bismuth

M.G.Srinivas[1&3], H.C. Manjunatha[2*], N. Sowmya[2*], P.S.Damodara Gupta[2], S.Alfred Cecil Raj[3]

[1]*Department of Physics, Government First Grade College, Mulbagal, Karnataka, India.*
[2]*Department of Physics, Government College for Women, Kolar, Karnataka, India.*
[3]*Department of Physics, St.Joseph's college, Affiliated to Bharathidasan University, Tiruchirappalli-620002*
Corresponding Author:manjunathhc@rediffmail.com, sowmyaprakash8@gmail.com

Introduction

During the last two decades, significant progress has been made in the experimental investigation of processes leading to super heavy nuclei, their decay properties and structure. The most stable super heavies are anticipated to be positioned along the β-stability line, which is unreachable by fusion reactions with stable beams. The literature studies shows the competition between different decay modes [1-2]. The proton decay half-lives of Lanthanides and actinides were studied[3-6]. Qian et al., [7] systematically studied α-decay half-lives of heavy and super heavy elements. Tan et al.,[8] investigated the β+ decays of some medium-mass nuclei.

Many theoretical models have been proposed to explore the half-lives of spherical and deformed nuclei. Earlier workers [9] have studied different decay modes of super heavy nuclei. Hence, in the present work we have examined possible decay modes such as proton decay using Coulomb and Proximity potential Model (CPPM), $\beta^{\pm}$-decay and an alpha decay are evaluated using semi-empirical relations in the isotopes of Bismuth.

Theoretical Frame work

The proton decay half-lives are evaluated using Coulomb and proximity potential model by including deformation effects and angular momentum. The assault frequency term in half-lives are evaluated using harmonic oscillator frequency is given by [3],

$$\nu = \frac{41}{hA^{1/3}} MeV \qquad (1)$$

The proton-nucleus total potential will consist of Coulomb V_C and Proximity potential V_P is expressed as

$$V = V_C + V_P \qquad (2)$$

The Coulomb interaction (V_C) potential is given by,

$$V_c = \frac{Z_1 Z_2 e^2}{r}\left[1 + \frac{3R^2}{5r^2}\beta_2 Y_{20}(\theta) + \frac{3R^4}{9r^4}\beta_4 Y_{40}\right] \qquad (3)$$

here Z_i is the atomic numbers of proton or daughter nuclei. The term 'r' is the separation distance. R is the radius of the nuclei, β is quadrupole deformation parameter and $Y_{20}(\theta)$ is the spherical hormanic function. Proximity potential is evaluated as follows;

$$V_P = 4\pi\gamma b\left[\frac{C_1 C_2}{C_1 + C_2}\right]\phi \qquad (4)$$

The penetration probability and half-lives are evaluated as explained in detail in literature [3]. The alpha-decay and beta decay half-lives are also evaluated using semi-empirical relations [3].

Results and Discussions:

The proton decay half-lives are studied in the isotopes of heavy nuclei Bismuth (Bi) using CPPM with harmonic oscillator frequency. However, an alpha-decay and $\beta^{\pm}$-decay half-lives are evaluated using semi-empirical relations. If the Q-value of the reaction in proton decay is positive, then the proton radioactivity is energetically feasible [6]. The mass excess values in order to evaluate Q-value of the reaction is taken by recent mass excess data available in literature [10].

The proton decay, an alpha-decay and beta-decay half-lives obtained from the present work are compared with available experiments. The figure 1 shows comparison of proton, an alpha and beta-decay half-lives using CPPM and semi-empirical relations with that of available experiments.

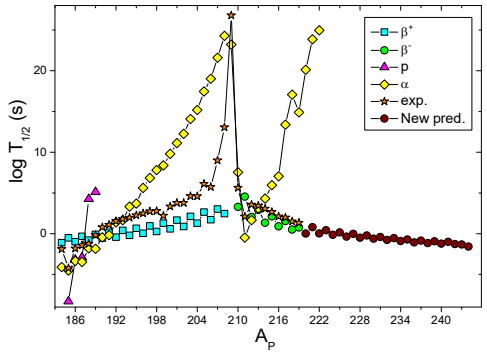

Fig 1: A comparison of proton-decay, an alpha-decay and beta-decay half-lives using CPPM and semi-empirical relations with that of available experiments.

From this comparison it is observed that the nuclei $^{184,186\text{-}189}$Bi and $^{191,209,211\text{-}212}$Bi which possess an alpha decay half-lives are in good agreement with the available experimental alpha decay half-lives. Similarly, the nuclei $^{190,192\text{-}208}$Bi, $^{210,213\text{-}244}$Bi and ^{185}Bi are having β^+ , β^- and proton decay half-lives respectively are in close agreement with the available experimental values.

Table-1: Prediction of logarithmic half-lives of β^--decay in the isotopes of heavy nuclei $^{220\text{-}244}$Bi.

$^{A}_{P}$	$T_{1/2}$	$^{A}_{P}$	$T_{1/2}$	$^{A}_{P}$	$T_{1/2}$
^{220}Bi	0.01	^{229} Bi	-0.22	^{237} Bi	-0.85
^{221} Bi	0.79	^{230} Bi	-0.62	^{238} Bi	-1.16
^{222} Bi	0.04	^{231} Bi	-0.4	^{239} Bi	-0.94
^{223} Bi	0.42	^{232} Bi	-0.77	^{240} Bi	-1.22
^{224} Bi	-0.14	^{233} Bi	-0.55	^{241} Bi	-1.01
^{225} Bi	0.15	^{234} Bi	-0.9	^{242} Bi	-1.28
^{226} Bi	-0.35	^{235} Bi	-0.71	^{243} Bi	-1.33
^{227} Bi	-0.01	^{236} Bi	-1.08	^{244} Bi	-1.59
^{228} Bi	-0.49				

From this comparison it is clear that the values obtained using different decay modes are comparable with the experiments, hence we have extended our studies to isotopes of Bismuth from ^{220}Bi to ^{244}Bi. Then we have studied all possible decay modes such as proton, beta and an alpha decay half-lives. Among all the studied half-lives the β^--decay in the isotopes of heavy nuclei $^{220\text{-}244}$Bi shows shorter half-lives when compared to other decay modes. Hence, the possible decay mode in heavy nuclei $^{220\text{-}244}$Bi is β^--decay only. The table-1 shows the predicted β^--decay half-lives in the heavy nuclei $^{220\text{-}244}$Bi. These predicted half-lives are in seconds to ms.

Conclusions:

The different decay modes such as proton decay, beta-decay and an alpha decay have been evaluated using CPPM and semi-empirical relations in the isotopes of Bismuth. The values obtained from the present work were comparable with the experiments. Around 9 α emitters, one proton emitter, 18 β^+ emitters and 33 β^- emitters were identified. Among the β^- emitters, around 25 new emitters from ^{220}Bi to ^{244}Bi were newly identified. These identified new β^- emitters are useful in the field of radiotherapy.

References

[1] H. C. Manjunatha, L. Seenappa, et al., Brazilian Journal of Physics 51, 764–772 (2021)

[2] H.C.Manjunatha, G.R.Sridhar et al., International Journal of Modern Physics E 30, 2, 2150013, (2021).

[3] M.G.Srinivas, H.C. Manjunatha, et al., Nuclear Physics A 995, 121689 (2020).

[4] H. C. Manjunatha & N.Sowmya: Nuclear Physics A 969, 68-82 (2018).

[5] N. Sowmya & H.C. Manjunatha, Brazilian Journal of Physics 49, 874–886 (2019).

[6] N.Sowmya, H. C. Manjunatha, P.S. Damodaragupta &N. Dhananjaya:, Brazilian Journal of Physics, 51, 99–135 (2021).

[7] Y. Qian, Z. Ren, and D. Ni, Phys. Rev. C 83, 044317 (2011).

[8] W. Tan , D.Ni and Z. Ren, Chinese Phys. C 41 054103(2017).

[9] H.C Manjunatha, K.N.Sridhar, N. Sowmya Phy Rev C 98: 024308(2018).

[10] Meng Wang et al., Chinese Phys. C 45 030003, (2021).

Contact : Yogesh K. Gupta
R. R. Sahu
S. Santra
A. K. Gupta

Printed by : Prudent Arts & Fab Pvt. Ltd.
A-221, TTC Industrial Area,
Opp. Anthony Motors Pvt. Ltd.,
M.I.D.C., Mahape, New Mumbai - 400701
Tel : +91 99302 00043 / 42`

ISBN 818372084-6